Results from ALICE related to collectivity

C.Loizides (LBNL)

The Berkeley School 2014
School of collective dynamics in high energy collisions
June 9-12,2014

http://tbs2014.lbl.gov

Yangshuo river

One of the very interesting interactions with Wit related to hydrodynamics (Nov, 2006)

Outline

- ALICE detector
- The sQGP paradigm at RHIC
- Results related to collective effects in PbPb
- Results related to collective effects in pPb
- Summary/Questions

ALICE detector

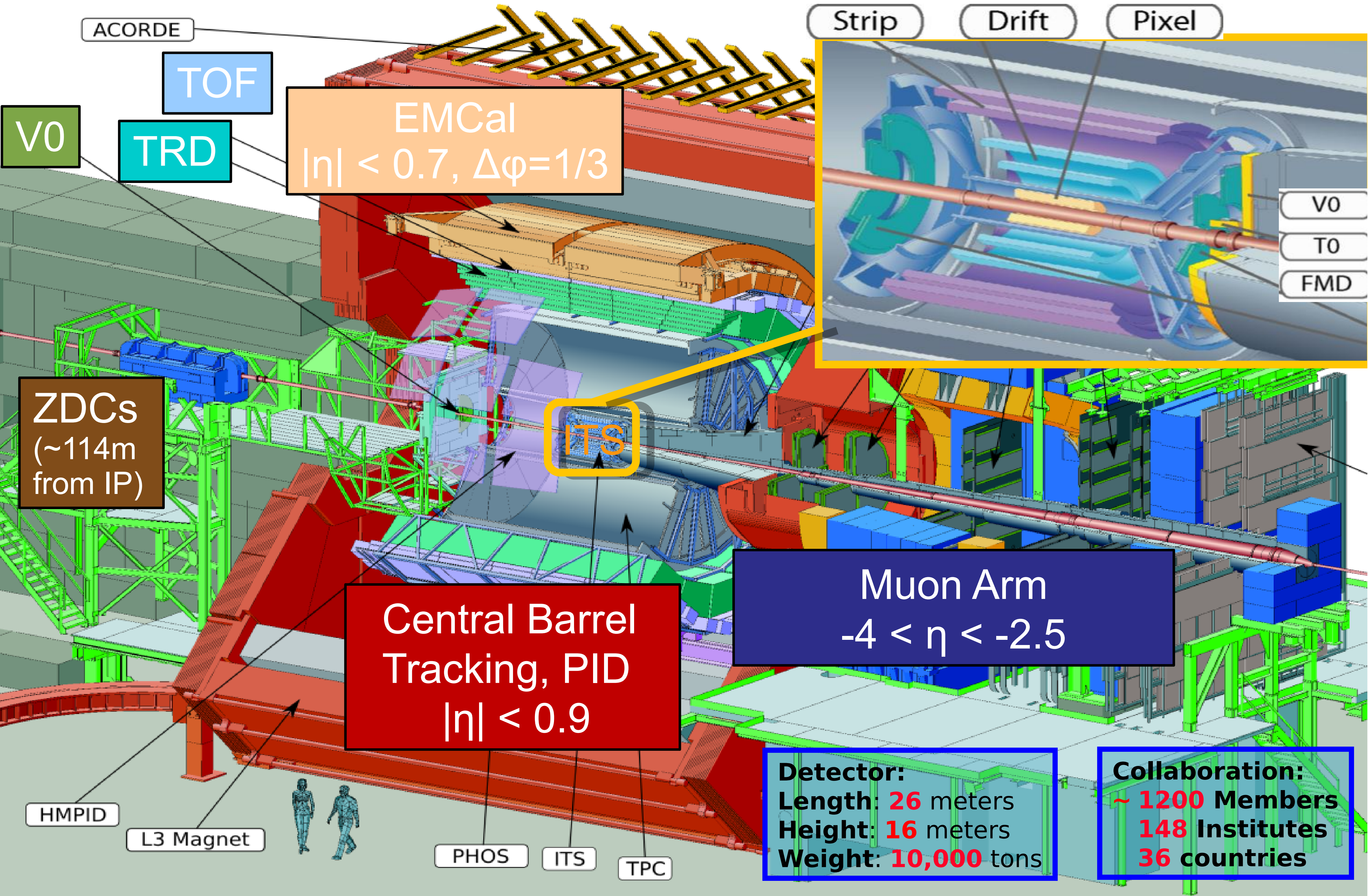

ALICE acceptance

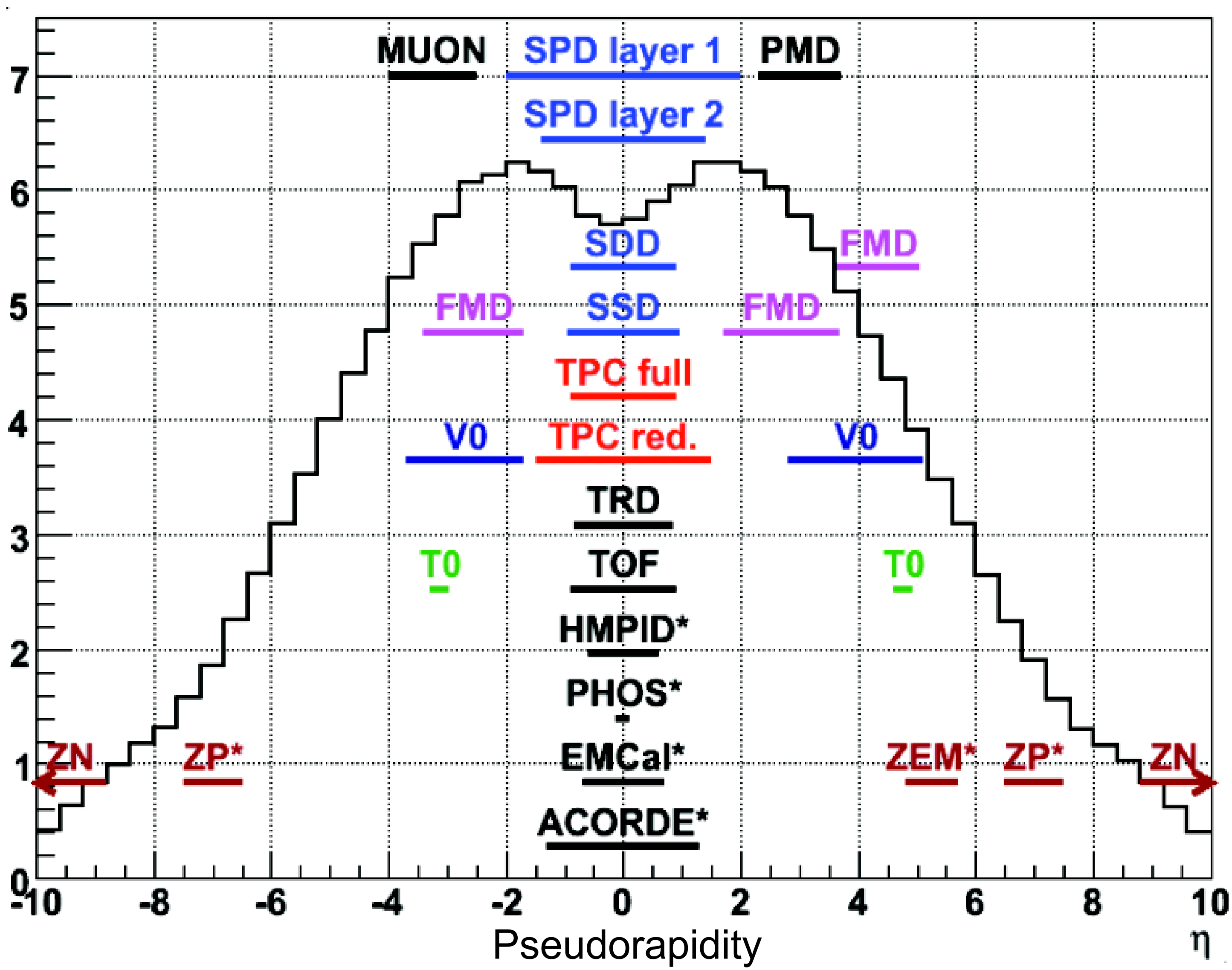

*) Not full 2π

Low material budget for inner barrel

arXiv:1402.4476

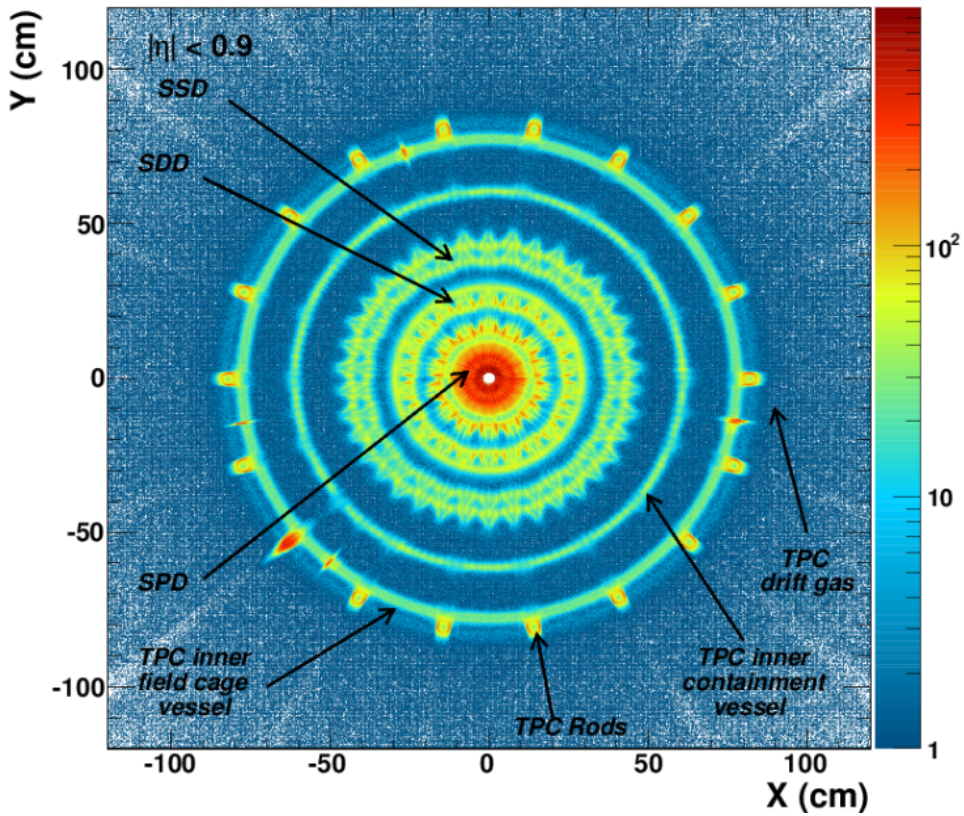

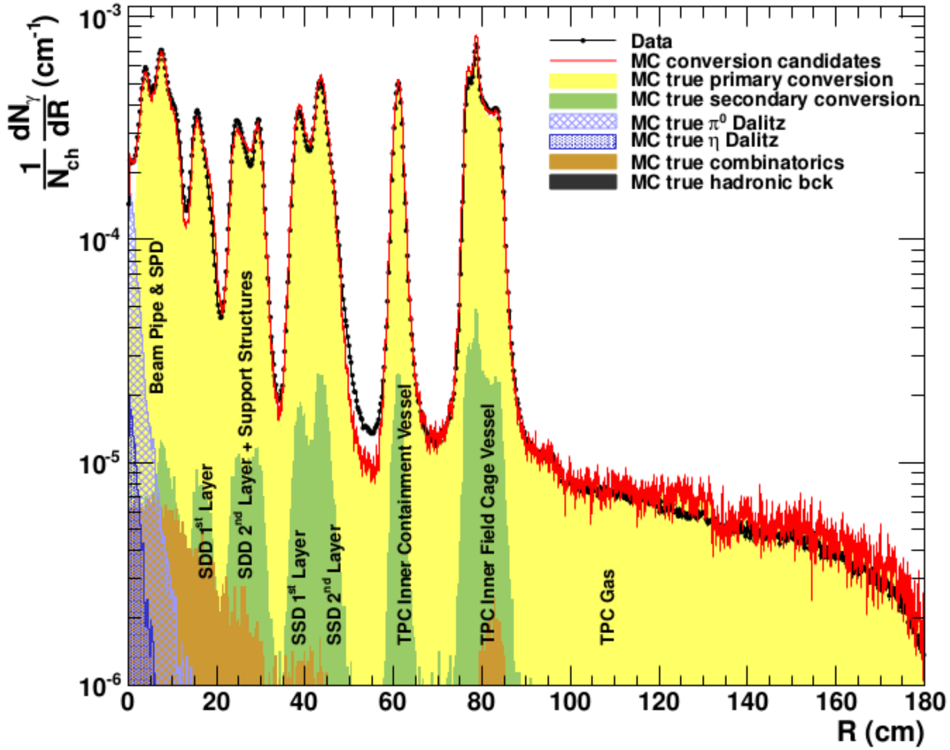

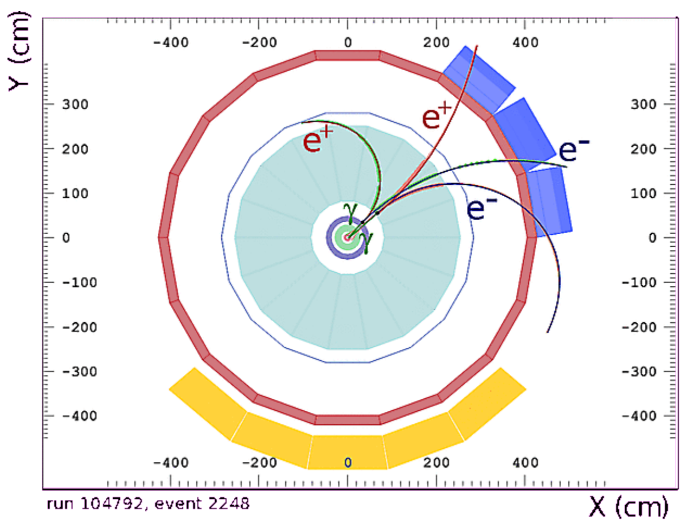

- Tomography for inner barrel using conversions
- Integrated radiation length for R<180cm
  - $11.4 \pm 0.5\%$ X_0 from comparison of MC and data
  - ~5x less than ATLAS/CMS (at |η|<1)
- Work ongoing to further reduce uncertainty and improve understanding for R>180cm and |η|>0.9

Main features and performance

arXiv:1402.4476

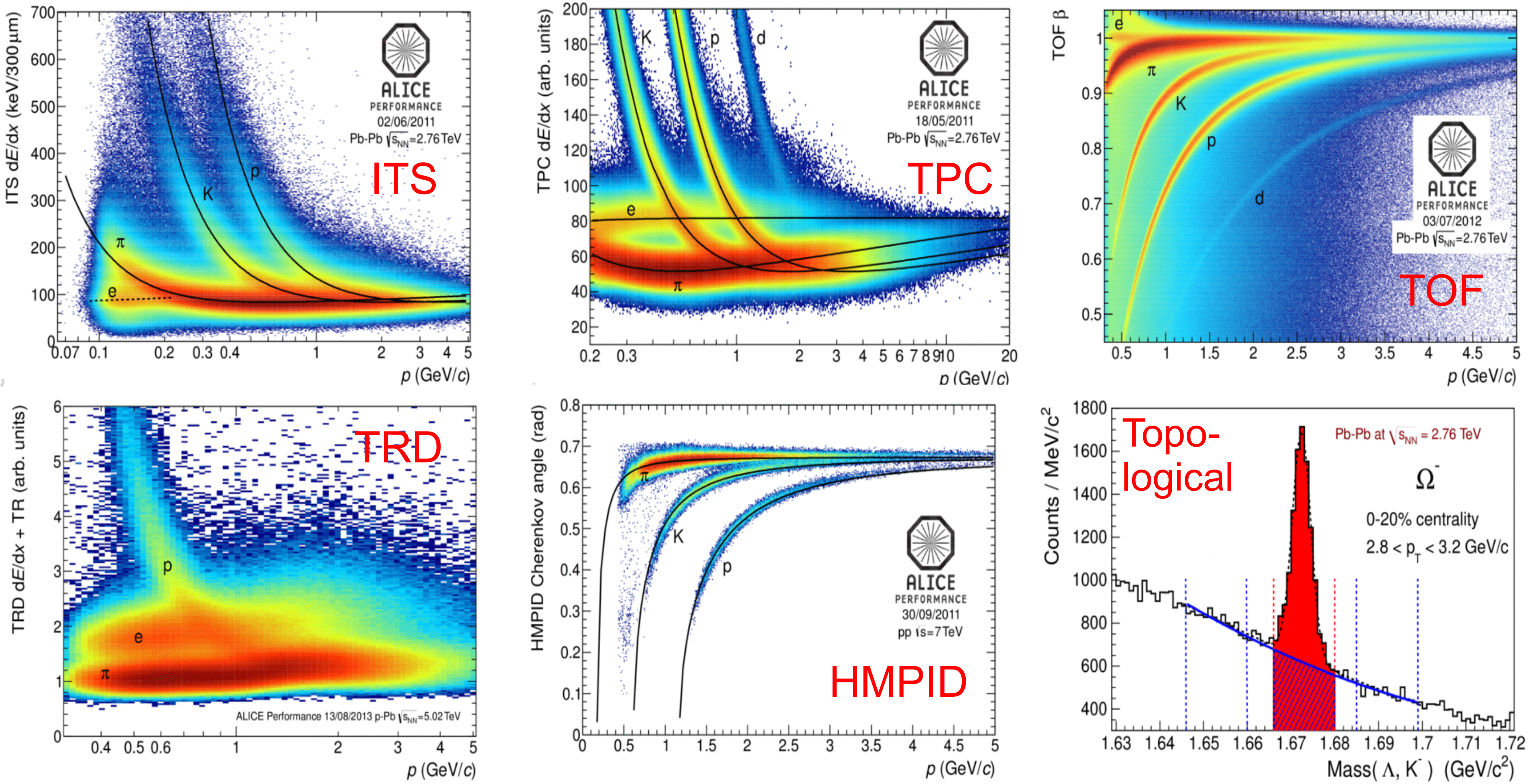

- Excellent+unique PID performance (practically all known techniques)

Main features and performance

arXiv:1402.4476

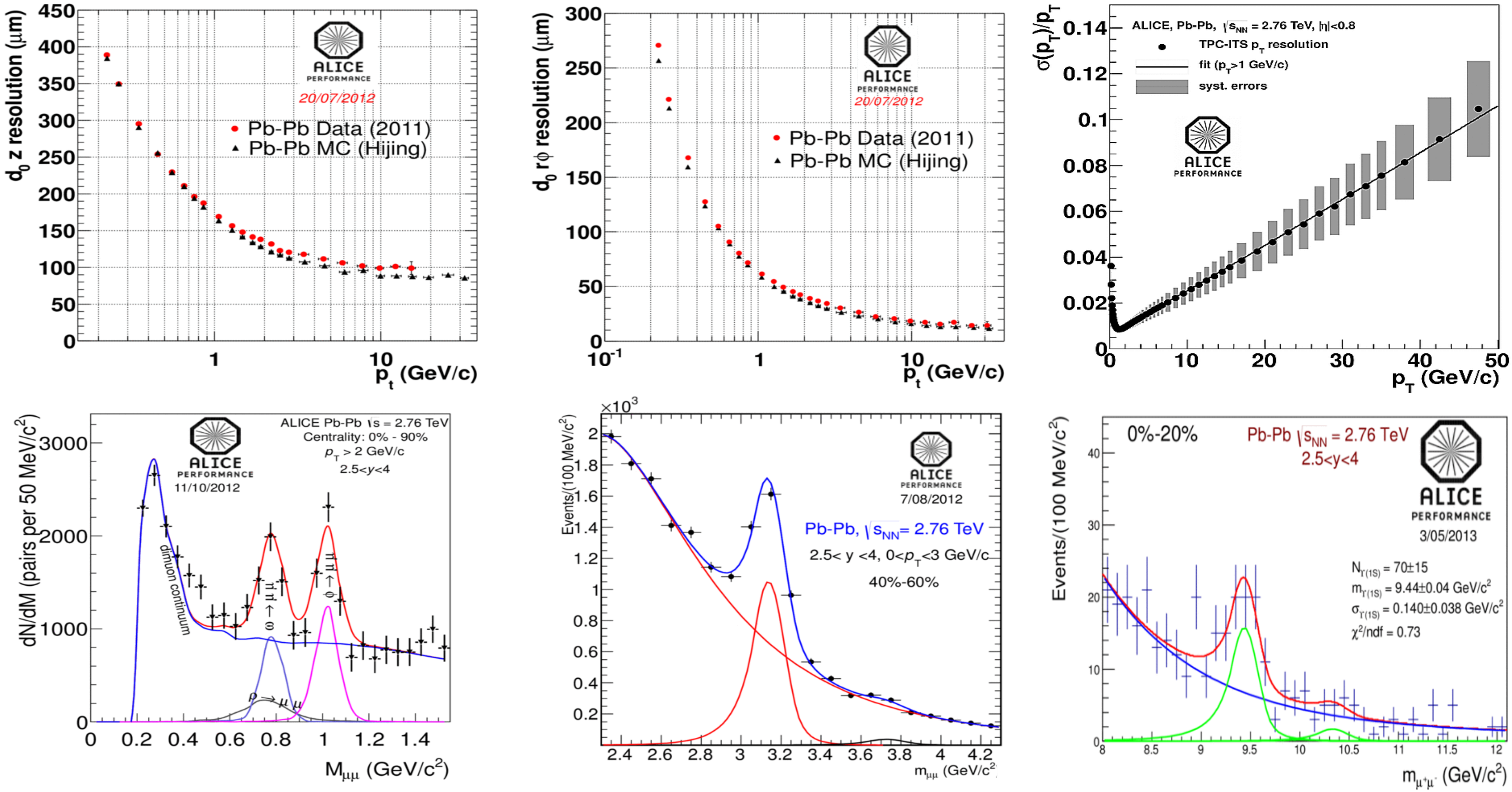

- Excellent+uniquePID performance (practically all known techniques)
- Excellent vertexing and tracking efficiency down to very low p_T
- Quarkonia (mid- and forward rapidity) down to zero p_T

Reminder: Scientific approach

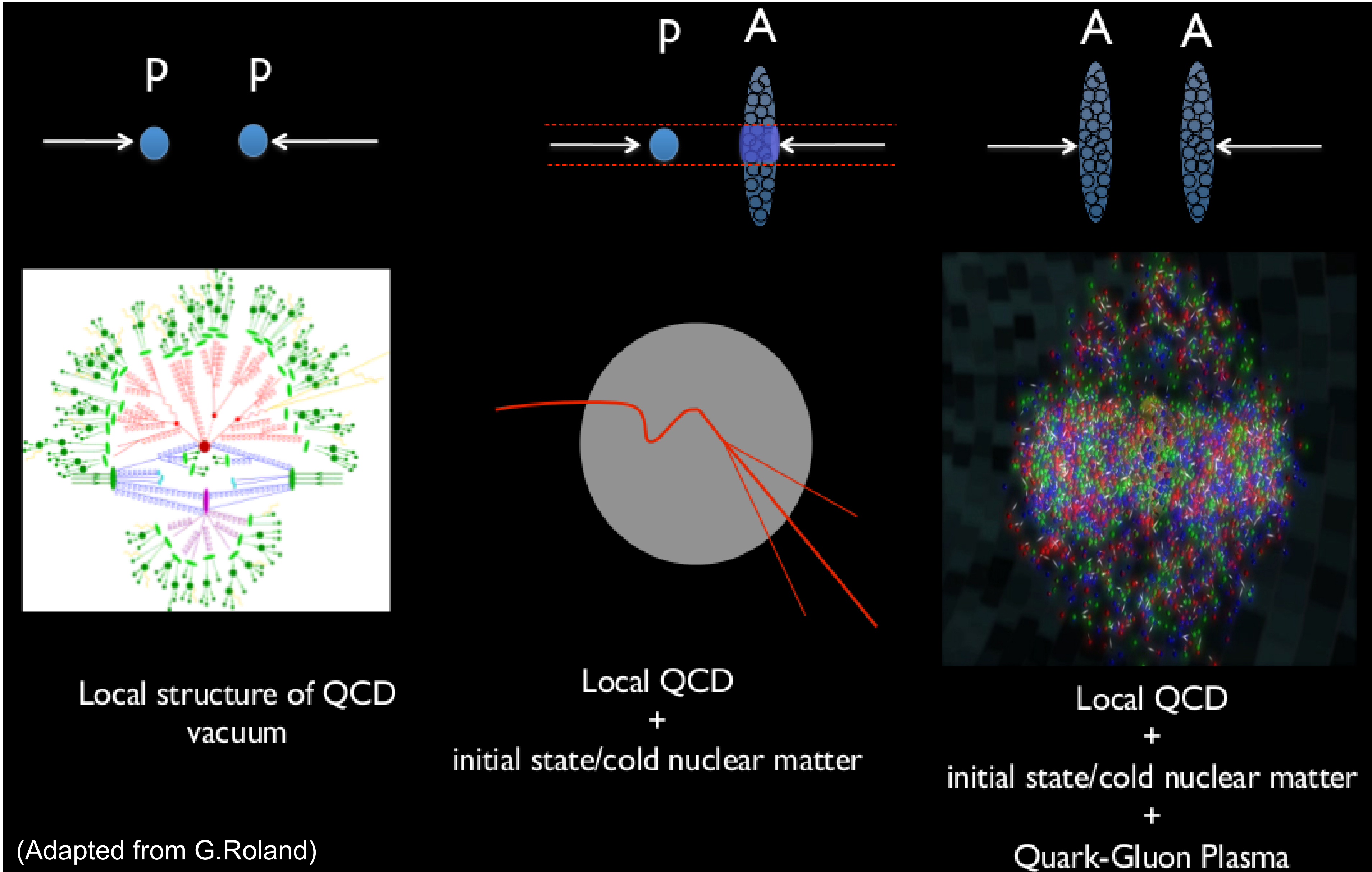

(Adapted from G.Roland)

pA: More than just a control experiment

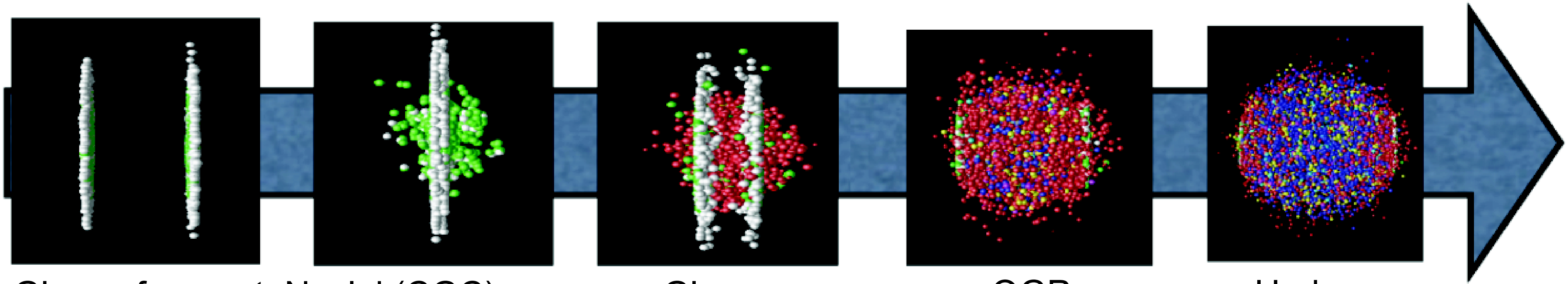

Gluons from sat. Nuclei (CGC) → Glasma → sQGP → Hadrons

- Study pA to benchmark AA
  - Measure properties of hard processes to disentangle initial from final state effects
  - Characterize nuclear PDFs at small-x
- Study high-density QCD in saturation region
  - Saturation scale (Q_s) enhanced in nucleus ($\sim A^{1/3\lambda}$)
  - In perturbative regime at the LHC: Q_s~2-3 GeV/c
  - Qualitatively expect $x \sim 10^{-3}$ at $\eta=0$ (vs 0.01 at RHIC)
- Study interplay of different concepts
  - pA contains elements of pp and AA

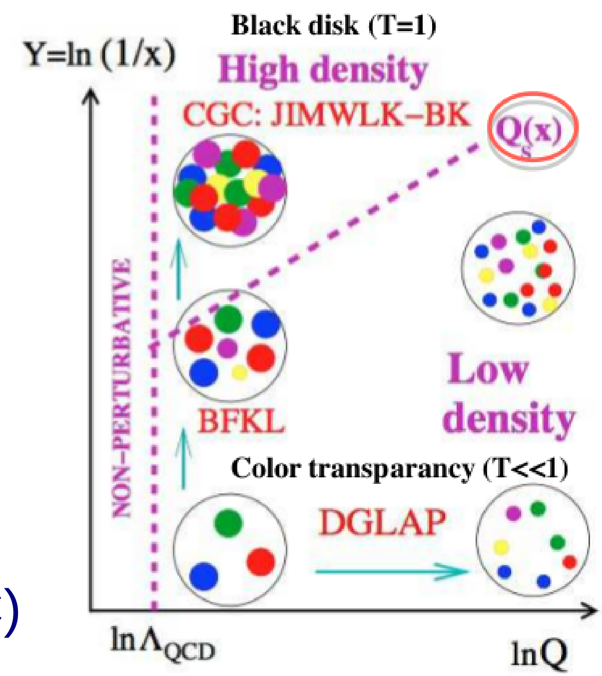

RHIC's major discoveries

STAR, PRL 86 (2001) 402

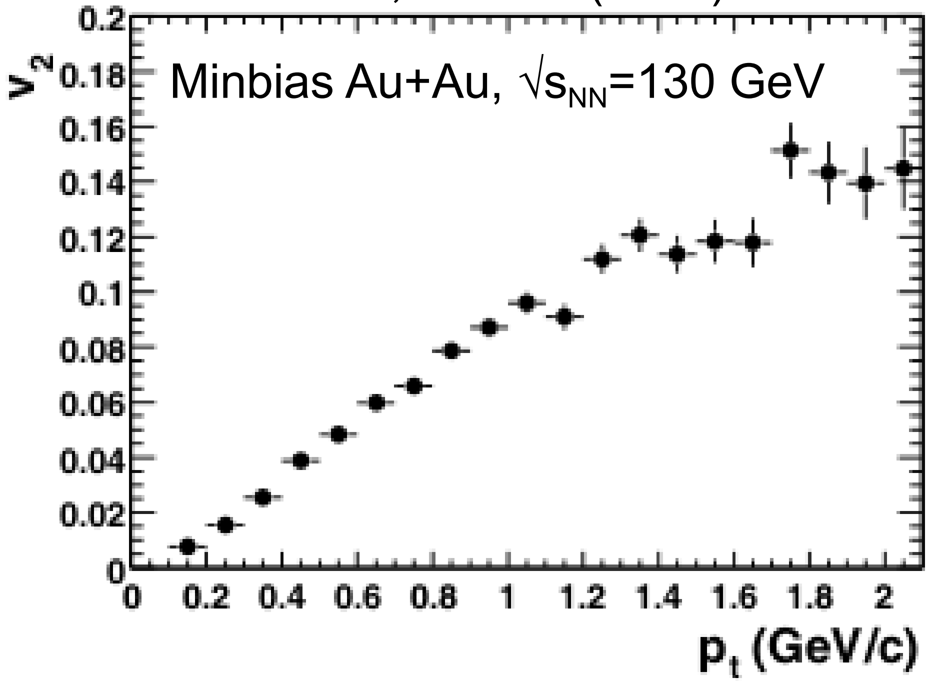

PHENIX, PRL 88 (2001) 022301

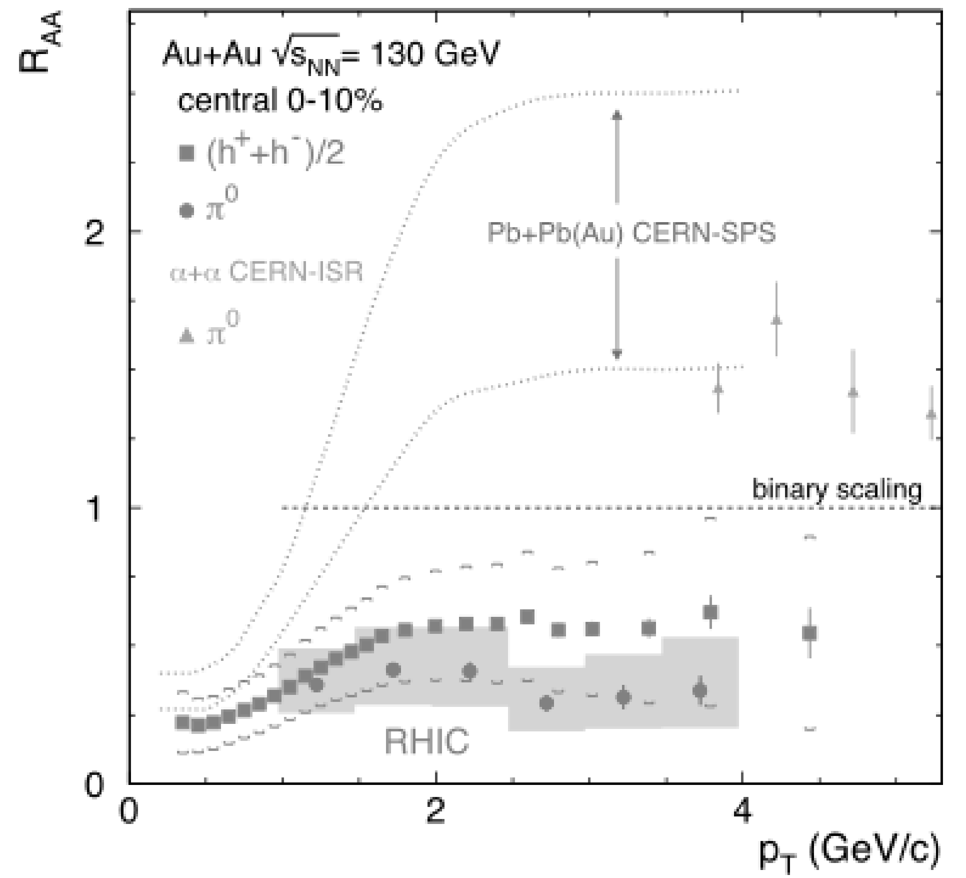

- Discovery of strong elliptic flow
  - Larger than possible from hadron gas models alone
  - Even huge cross sections needed to describe with pQCD $2 \rightarrow 2$ processes
  - Described by (ideal) hydrodynamics using lattice equation of state
- Discovery of strong hadron suppression (jet quenching)
  - Final state effect due to interactions with hot medium?
  - Role of initial state and cold nuclear medium effects?

What's needed partonically to get v_2?

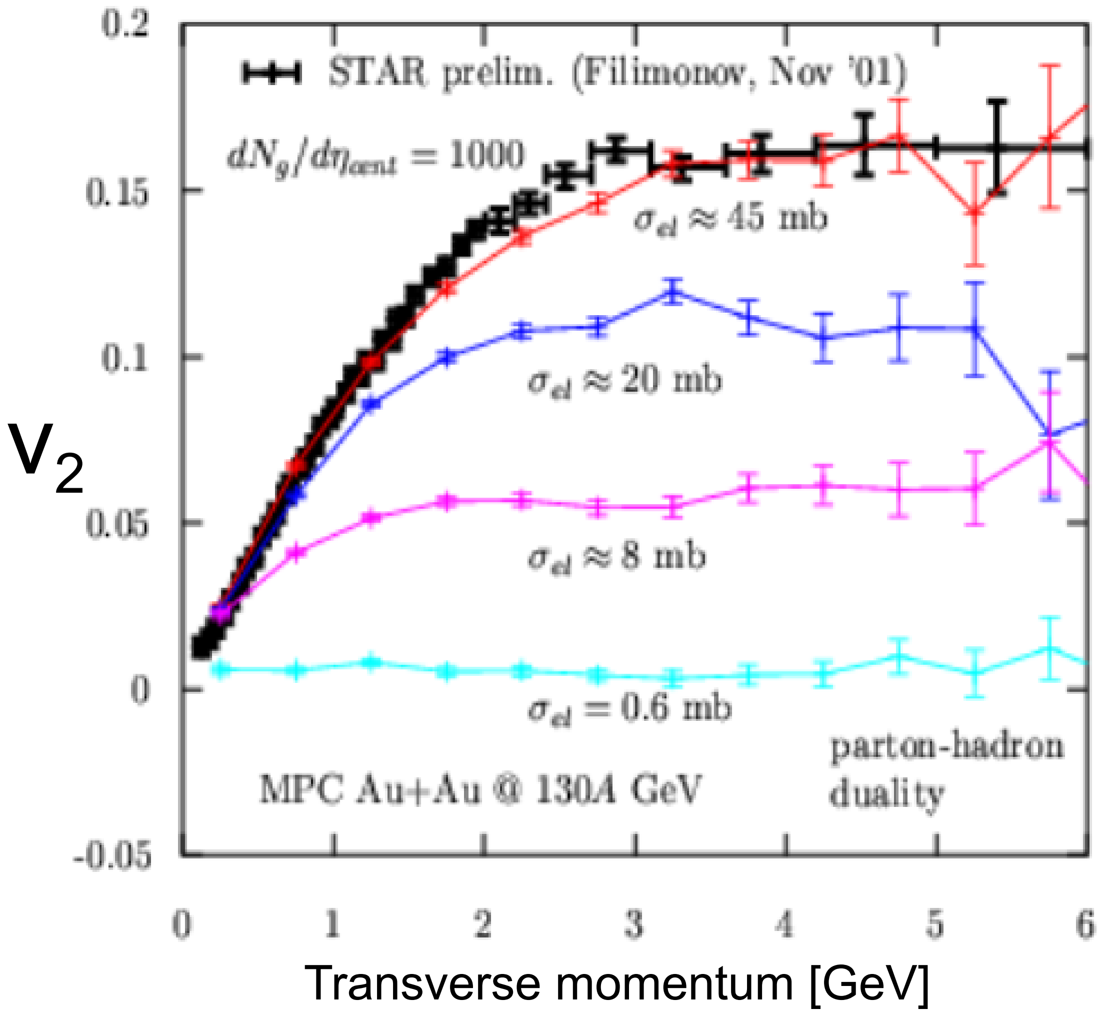

Parton transport model: Bolzmann equation with 2-to-2 gluon processes

D.Molnar, M.Gyulassy
NPA 697 (2002)

HUGE (hadronic!!!) cross sections needed to describe v_2

Need large opacity to describe elliptic flow, ie elastic parton cross sections as large as inelastic the proton cross-section.

Elliptic flow and hydrodynamics

Ideal relativistic hydrodynamics

$$T^{\mu\nu} = (e+p)u^\mu u^\nu - p g^{\mu\nu}$$

$$\delta_\mu T^{\mu\nu} = 0$$

$$\delta_\mu N_i^\mu = 0,\ i = B, S, \ldots$$

$$p = p(e, n)$$ Closure with EoS

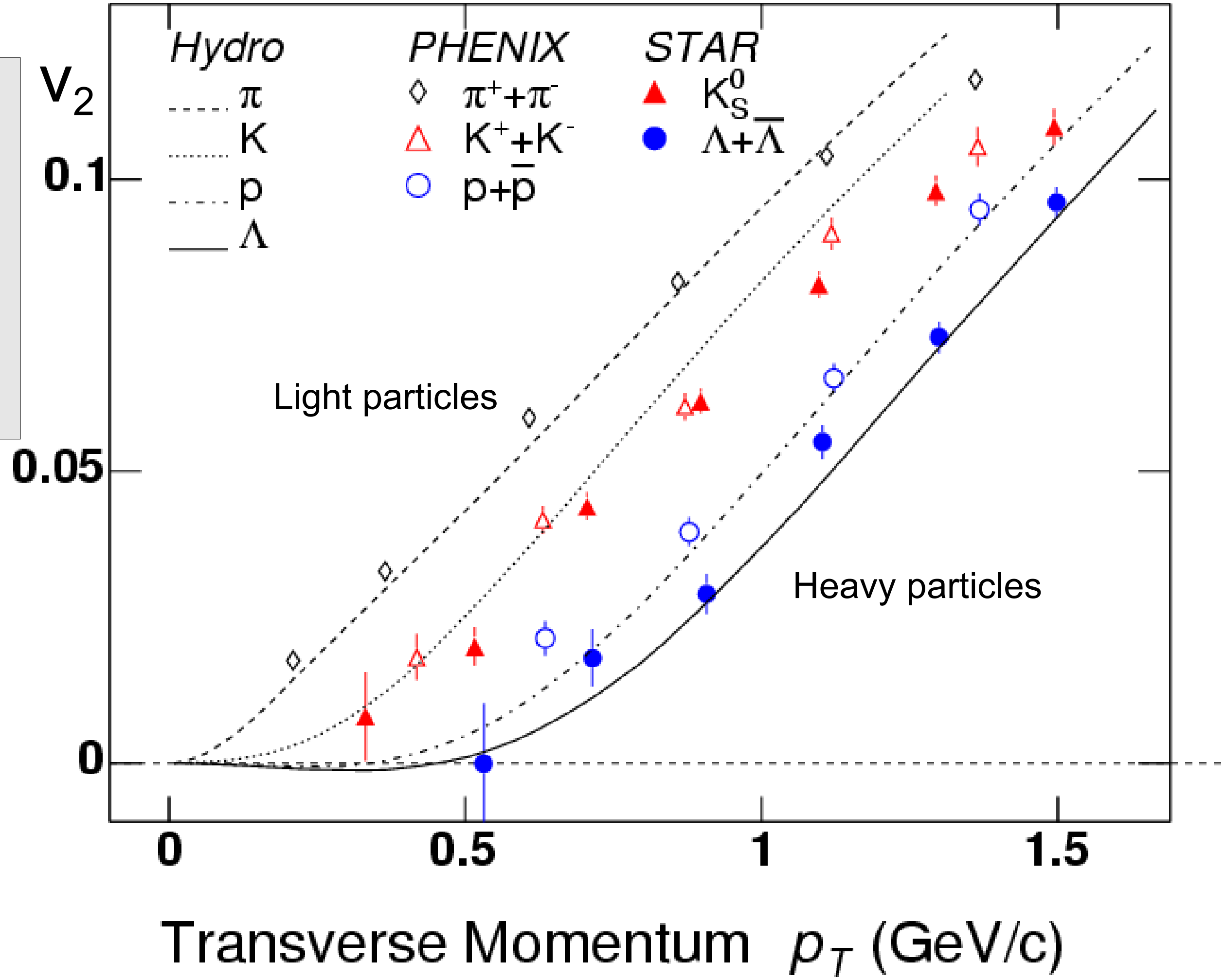

Assumption:
After a thermalization time (≤1fm/c) a system in local equilibrium with zero mean free path and zero viscosity is created

Initial conditions (IC) → Equation of state (EOS) → Freeze-out cond. (FO) → **Hydro** → Observables

Today we use viscous hydro with finite η/s

dAu control experiment at RHIC

PRL 91 (2003) vol 7

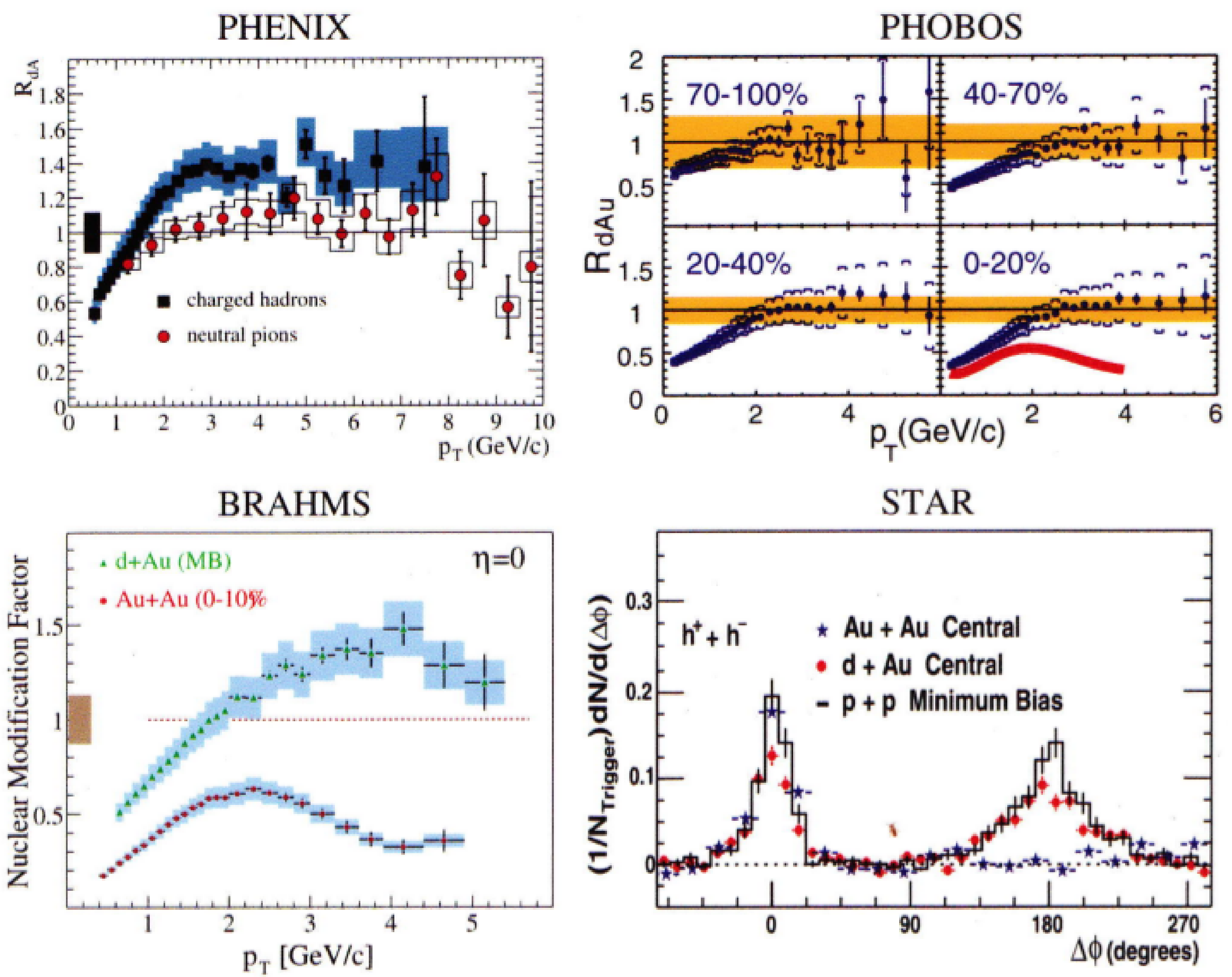

Jet quenching is a final state effect

Eventually lead to a new paradigm

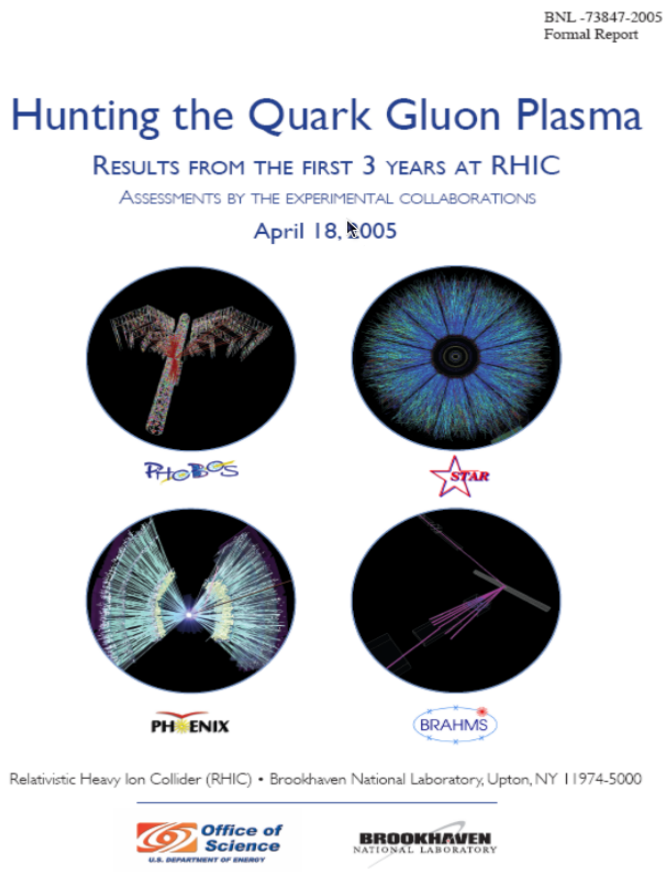

BNL -73847-2005
Formal Report

Hunting the Quark Gluon Plasma

RESULTS FROM THE FIRST 3 YEARS AT RHIC

ASSESSMENTS BY THE EXPERIMENTAL COLLABORATIONS

April 18, 2005

PHOBOS STAR

PHENIX BRAHMS

Relativistic Heavy Ion Collider (RHIC) • Brookhaven National Laboratory, Upton, NY 11974-5000

Office of Science U.S. DEPARTMENT OF ENERGY

BROOKHAVEN NATIONAL LABORATORY

RHIC whitepapers: NPA 757 1-283 (2005)

- Manifestation of strong coupled QGP
- Not freely roaming quarks and gluons
- Instead, strongly coupled reaching almost the minimum value of shear viscosity to entropy density ratio (η/s)

Similar properties at the LHC

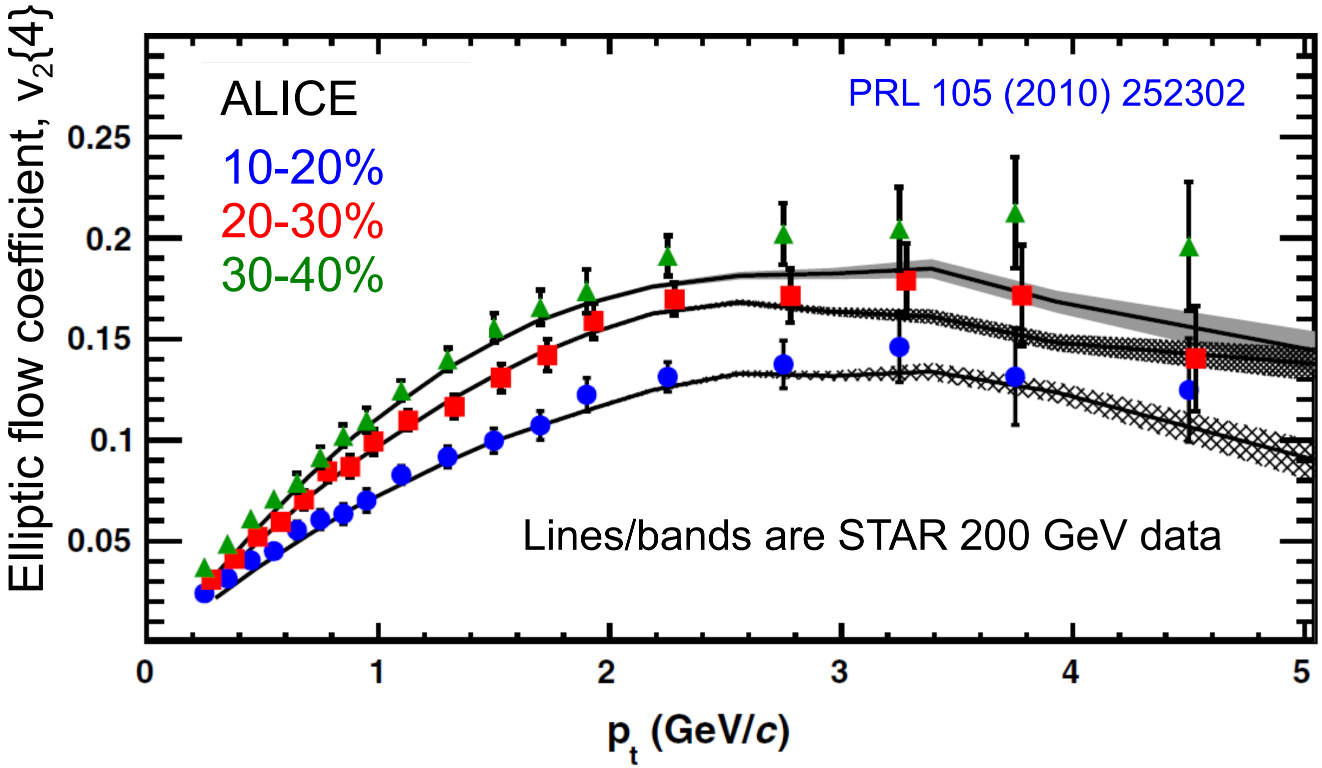

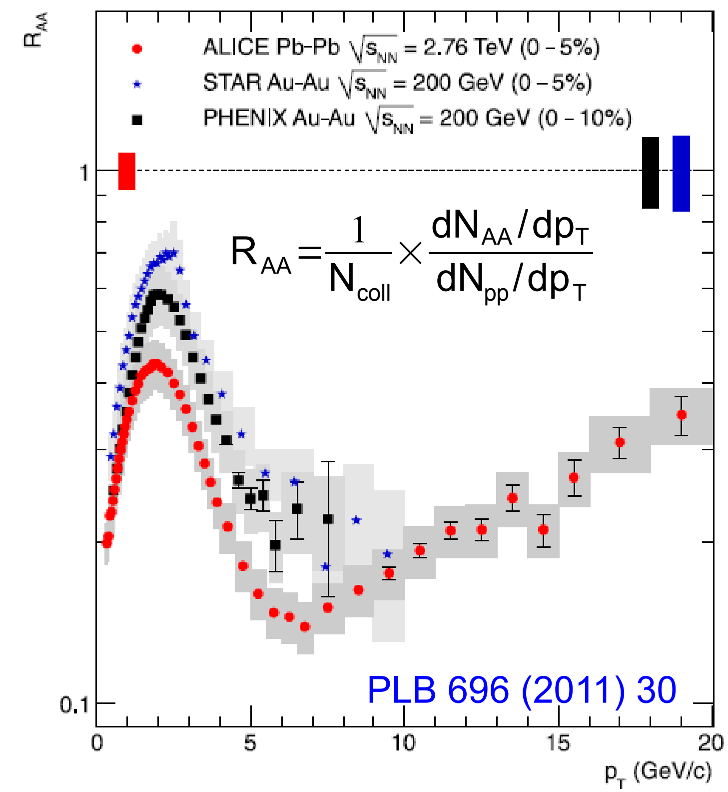

Dijet momentum imbalance

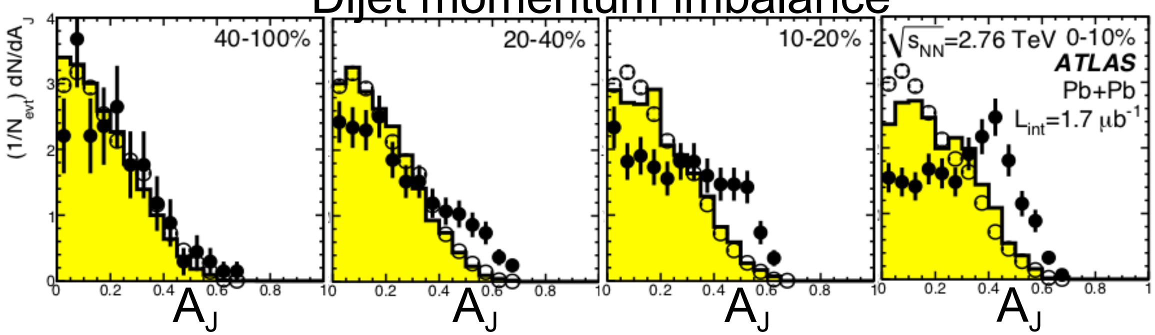

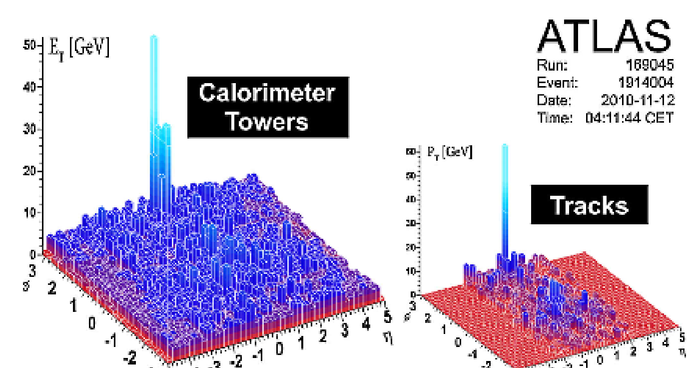

PRL 105 (2010) 252303

Strong elliptic flow and strong (di-)jet quenching

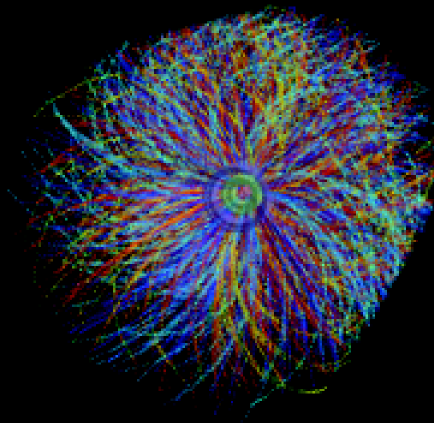

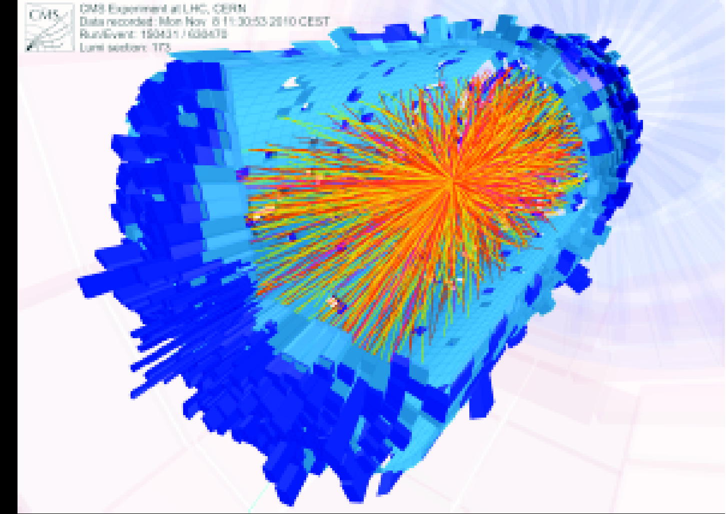

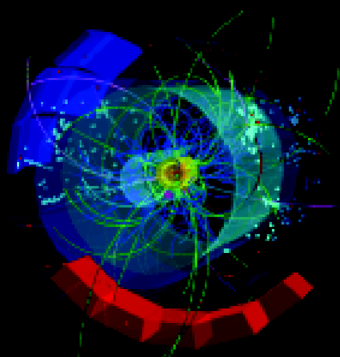

Results related to collectivity from PbPb collisions at the LHC

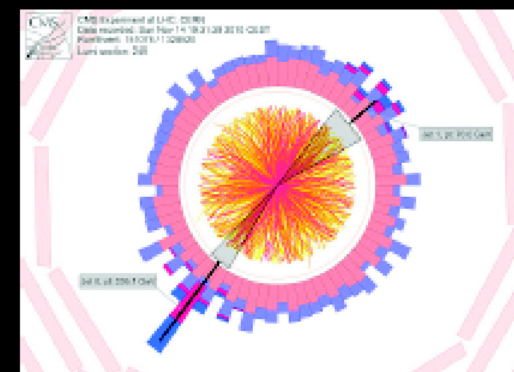

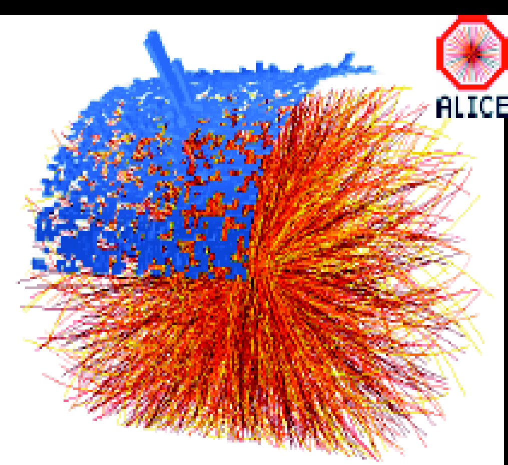

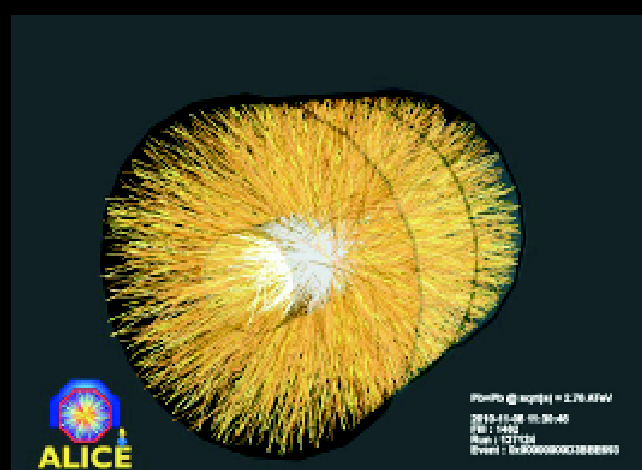

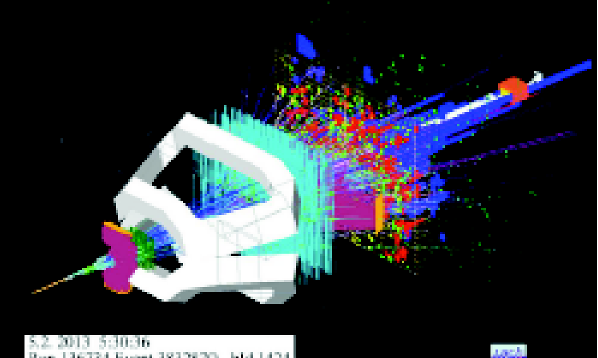

Initial and final state anisotropy

Time →

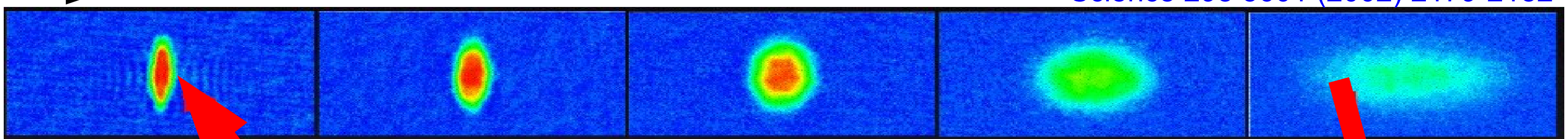

(self quenching)

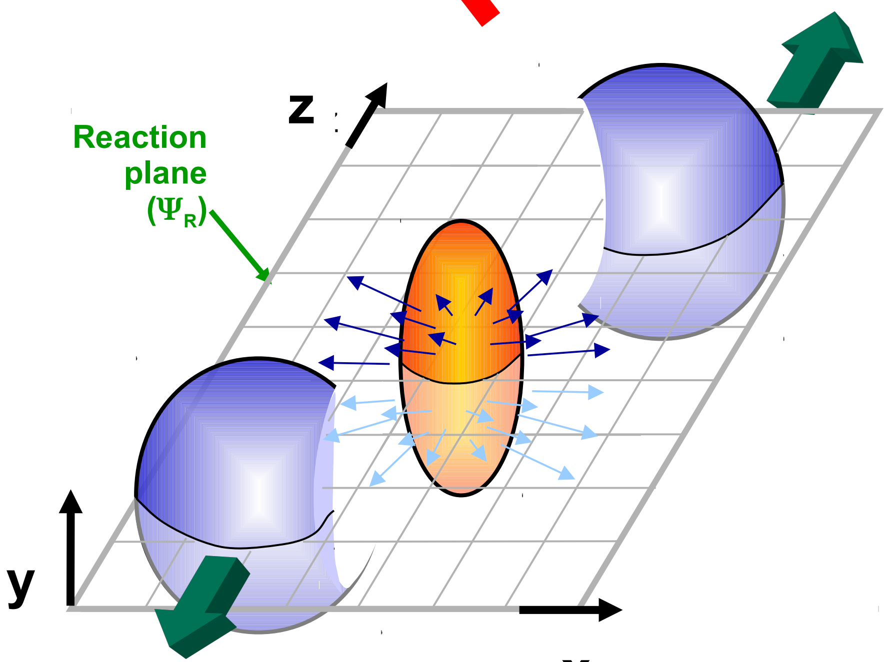

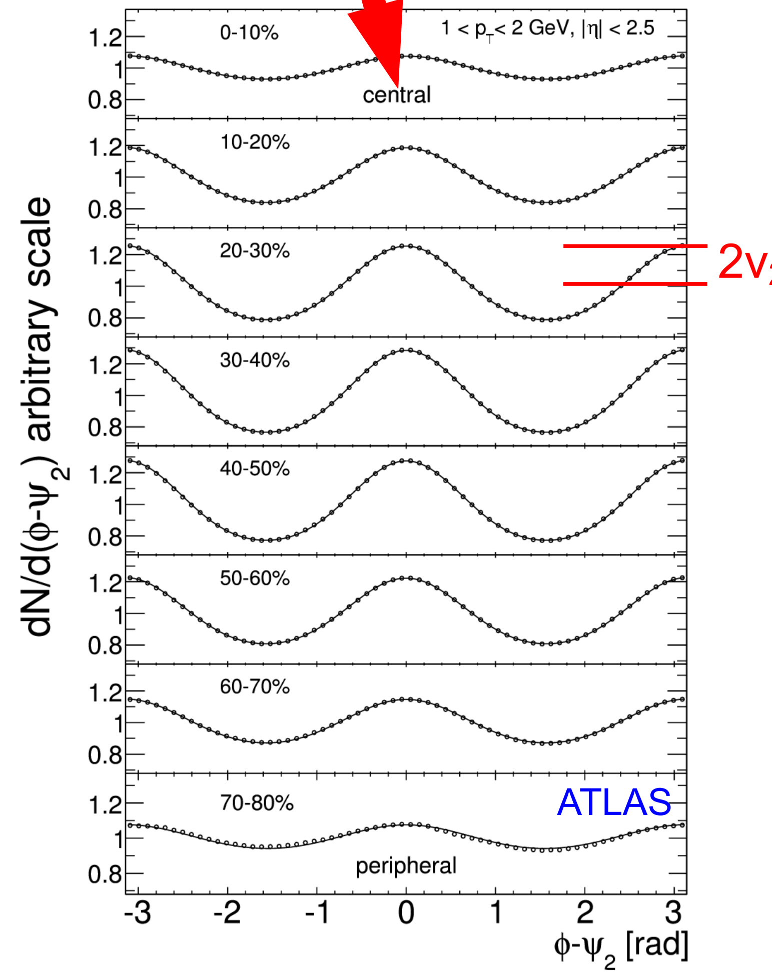

Initial spatial anisotropy: eccentricity ε

→ Interactions present early

Momentum space anisotropy: elliptic flow $v_2 = \langle \cos(2\varphi - 2\Psi_R) \rangle$

Flow methods

$$v_2 = \langle \cos(2\varphi - 2\Psi_R) \rangle$$

Extract from data or use only relative angles

Two-particle cumulant

$$v\{2\} = \sqrt{\langle \cos(2\varphi_1 - 2\varphi_2) \rangle}$$

Can suppress "non-flow" by employing cuts in $|\Delta\eta|$

If p_T cuts are used:

$$v\{2\} = \sqrt{v(p_{T,1})\, v(p_{T,2})}$$

Measures:

$$v\{2\}^2 = \langle v \rangle^2 + \sigma_{v_2}^2 + \delta$$

$$v \gg 1/\sqrt{M}$$

Jet (Near-side region)

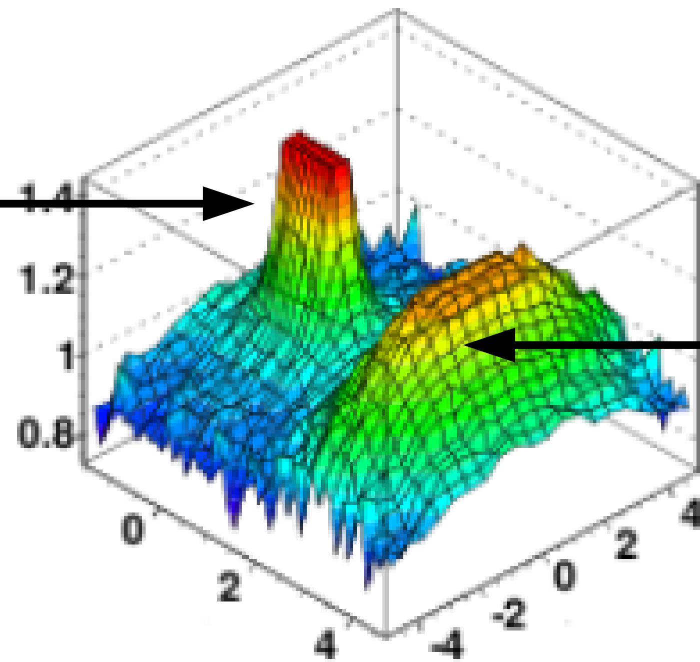

Recoil-jet (Away-side region)

Ollitrault, Poskanzer, Voloshin PRC 80 80 014904 (2009)

Two-particle angular correlations

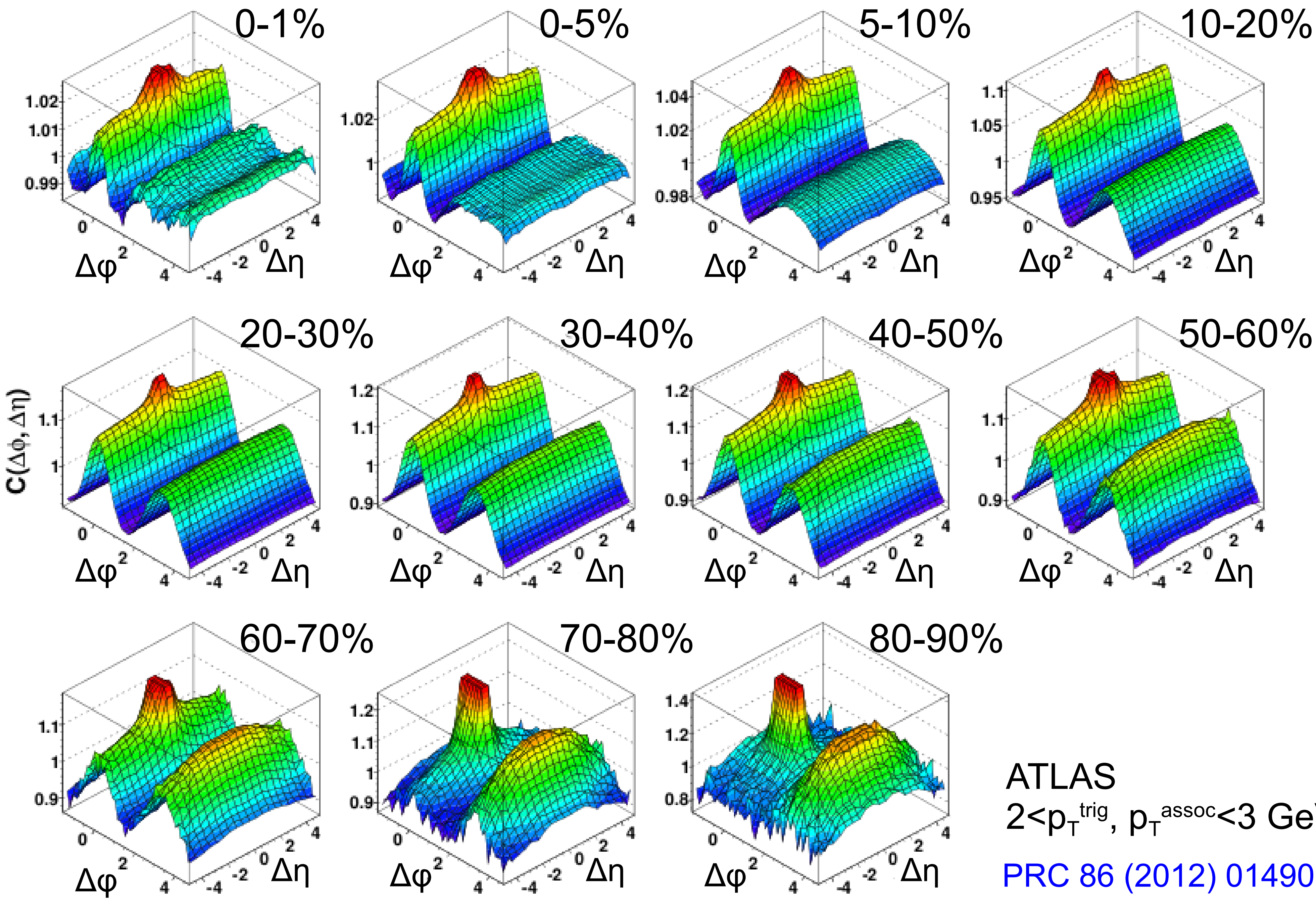

ATLAS

$2<p_T^{trig}, p_T^{assoc}<3$ GeV/c

PRC 86 (2012) 014907

Multi-particle correlations: $v_2\{4\}$ and higher

- Cumulants to extract genuine k-particle correlations excluding those from k-1 particles
- To first order for k=2 and k=4

$$v_2\{2\}^2 = \langle v_2 \rangle^2 + \sigma_{v_2}^2 + \delta_2$$

$$v_2 \gg 1/\sqrt{M}$$

$$v_2\{4\}^2 = \langle v_2 \rangle^2 - \sigma_{v_2}^2$$

$$v_2 \gg 1/M^{3/4}$$

  - eg. M=100, v_2>>0.03
- Care is needed when averaging over M, as cumulants are also sensitive to multiplicity fluctuations

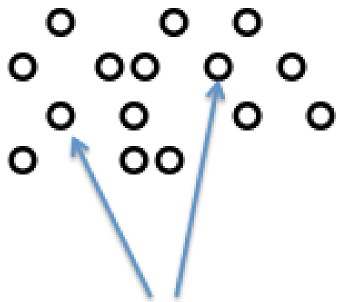

$$\left\langle e^{in(\varphi_1-\varphi_2)} \right\rangle$$

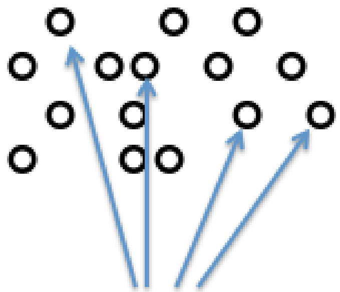

$$\left\langle e^{in(\varphi_1+\varphi_2-\varphi_3-\varphi_4)} \right\rangle$$

Four particle correlations (Q-cumulant method):

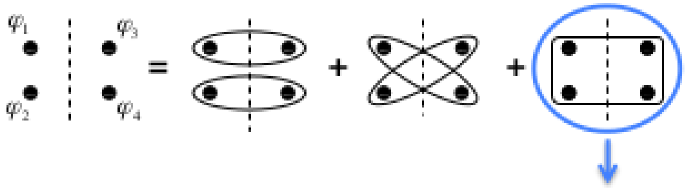

$$c_n\{4\} = \langle\langle 4 \rangle\rangle - 2 \cdot \langle\langle 2 \rangle\rangle^2$$

$$v_2\{4\} = \sqrt[4]{-c_n\{4\}}$$

$$\left\langle e^{in(\varphi_1+\varphi_2-\varphi_3-\varphi_4)} \right\rangle - \left\langle e^{in(\varphi_1-\varphi_3)} \right\rangle \left\langle e^{in(\varphi_2-\varphi_4)} \right\rangle - \left\langle e^{in(\varphi_1-\varphi_4)} \right\rangle \left\langle e^{in(\varphi_2-\varphi_3)} \right\rangle$$

(From S. Tuo)

Multi-particle correlations (cumulant) studies extract the genuine multi-particle correlation

Multi-particle correlations: $v_2\{4\}$ and higher

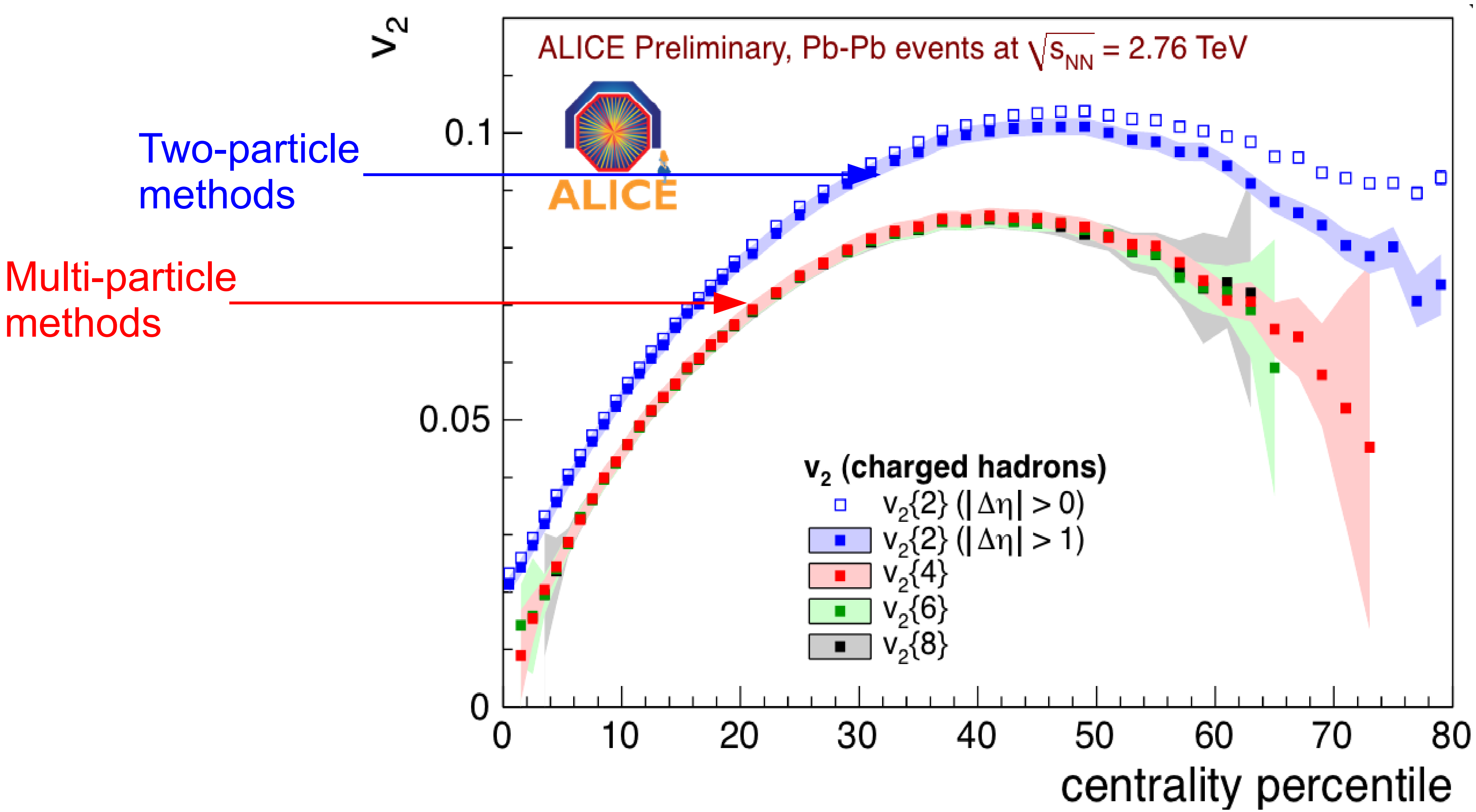

Multi-particle correlation v2{n} results converge for n≥4, indicating that non-flow contribution is negligible for n≥4

Integrated elliptic flow and hydro

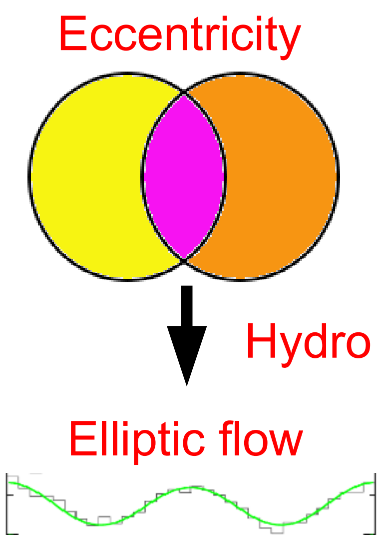

Calculation:
M.Luzum,
arXiv:1011.5173

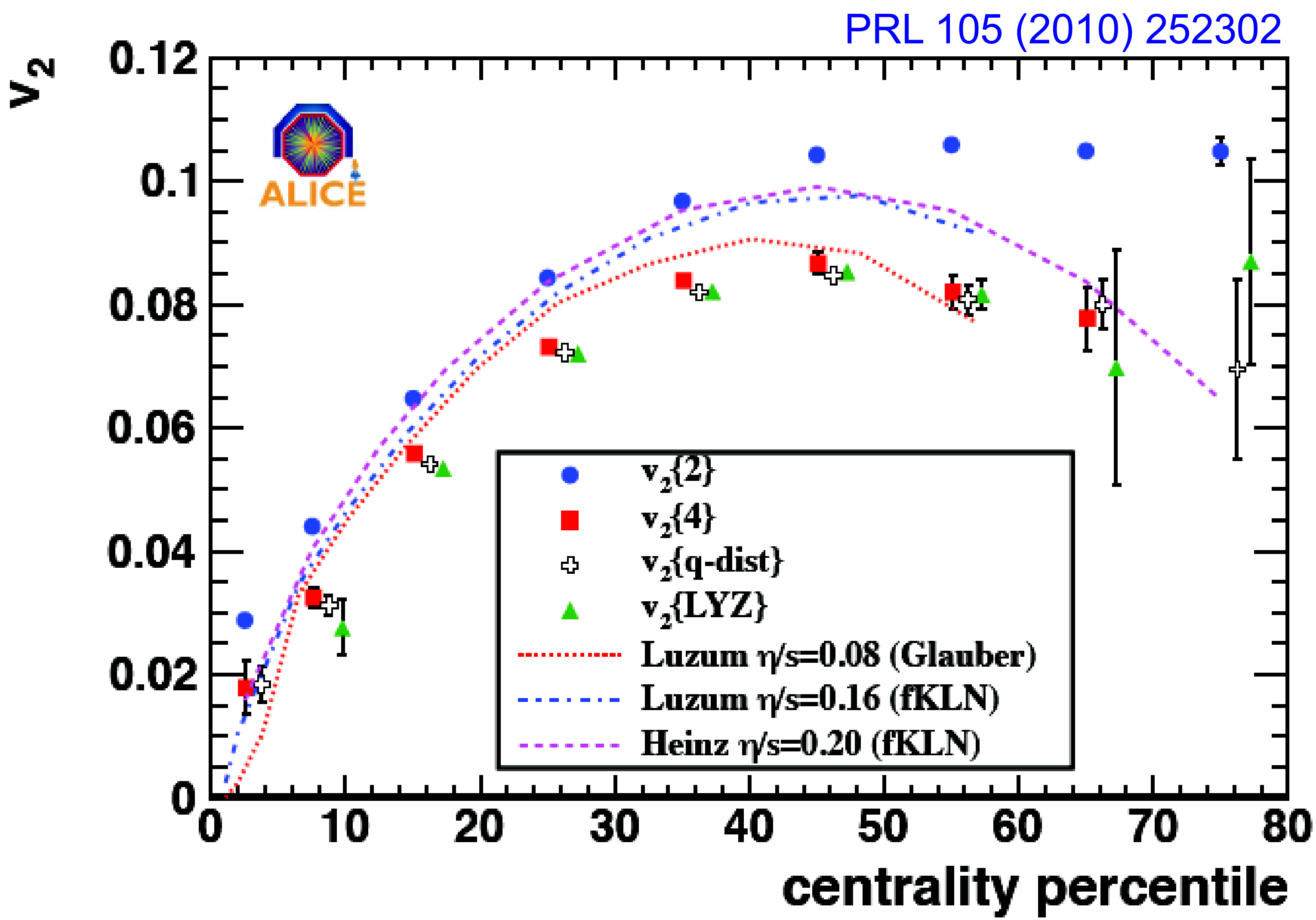

Measured v_2 well within the range of viscous hydro predictions

Radial flow and kinetic freeze-out

- Different shape for particles with different masses indicate radial flow
- Hydro calculations can describe the data
- Blast-wave fits assuming a boosted thermal source with a common temperature and radial velocity

BW model: PRC 48, 2462 (1993)

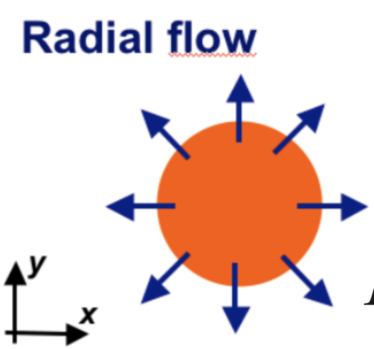

$$p_T^{flow} = p_T + m\beta_T^{flow}\gamma_T^{flow}$$

PRL 109 (2012) 252301

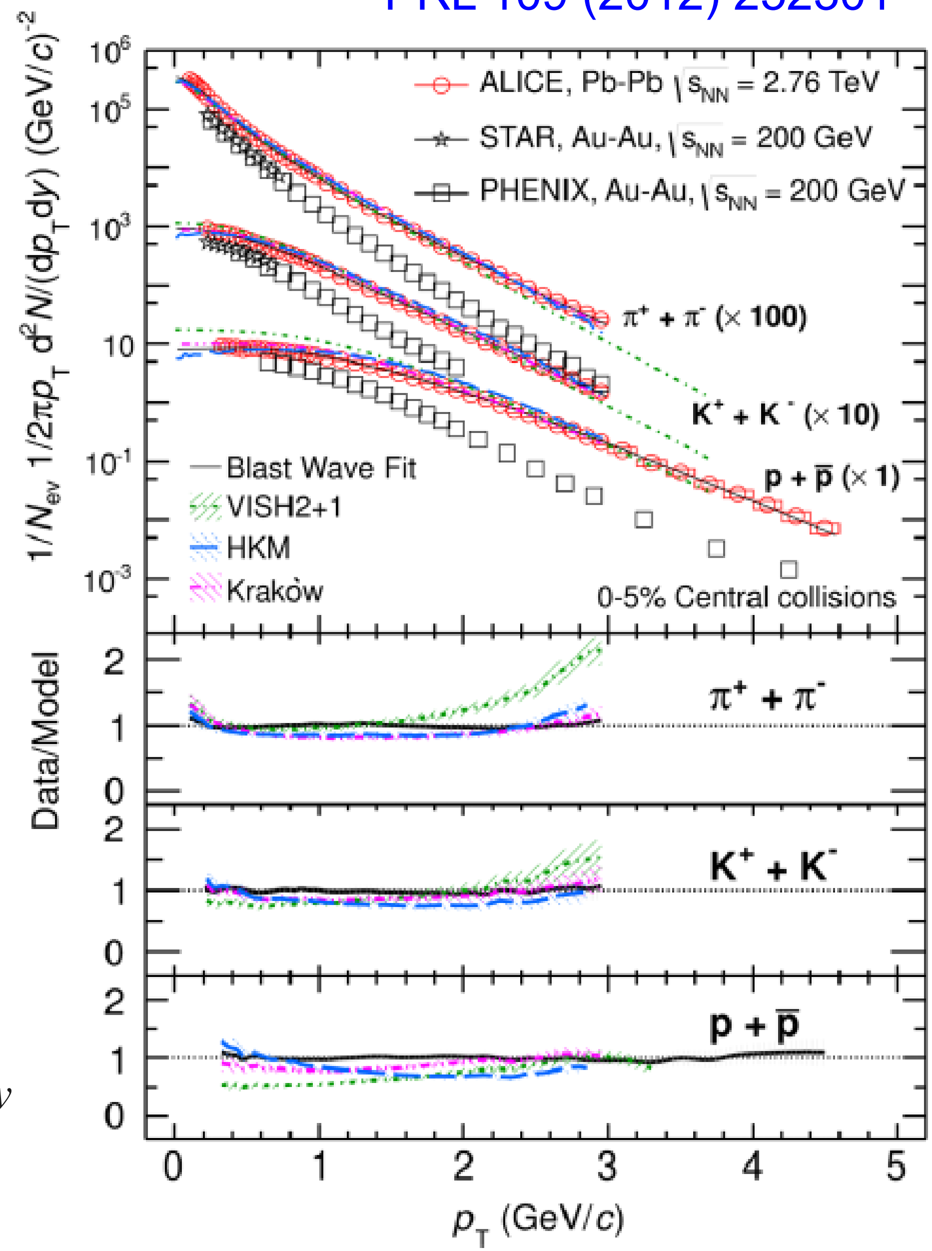

$$E\frac{d^3N}{dp^3} \sim f(p_t) = \int_0^R m_T K_1(m_T\cosh\rho/T_{fo}) I_0(p_T\sinh\rho/T_{fo})\, r\,dr \quad \text{where } m_T = \sqrt{m^2+p_T^2};\ \beta_r(r) = \beta_s\left(\tfrac{r}{R}\right)^n;\ \rho = \tanh^{-1}\beta_r.$$

Radial flow and kinetic freeze-out

- Different shape for particles with different masses indicate radial flow
- Hydro calculations can describe the data
- Blast-wave fits assuming a boosted thermal source with a common temperature and radial velocity

BW model: PRC 48, 2462 (1993)

PRL 109 (2012) 252301

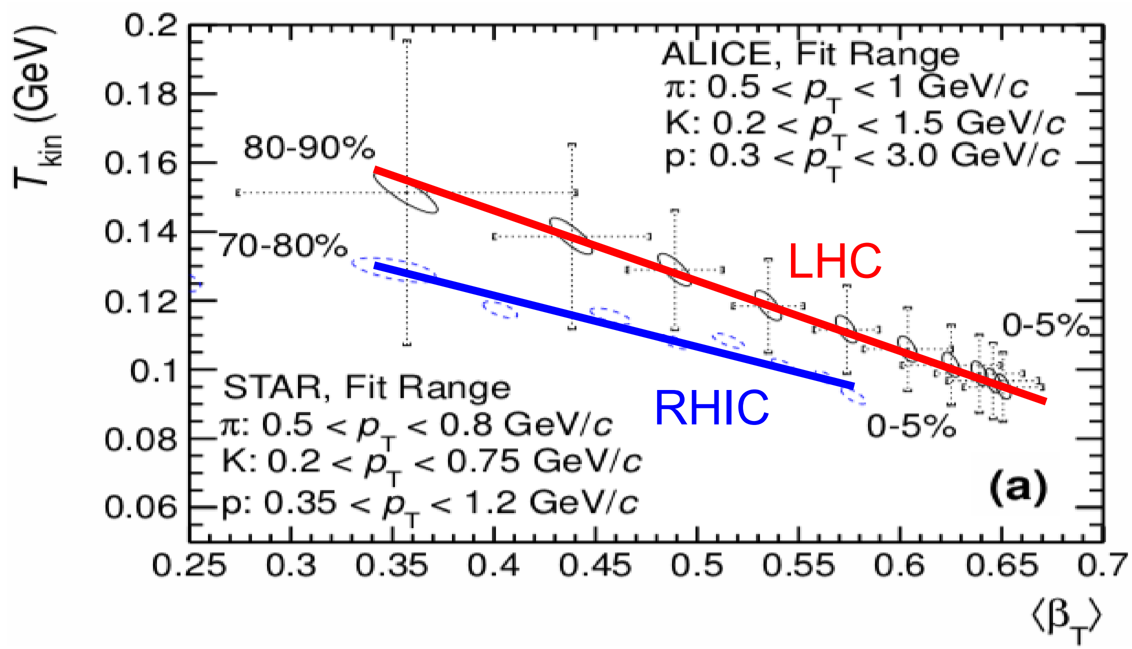

- Strong radial flow up to $\beta_{LHC,central} = 0.65c$
  - $\beta_{LHC,central} = 1.1\ \beta_{RHIC,central}$
- Similar kinetic freeze-out T_{kin}

Radial flow

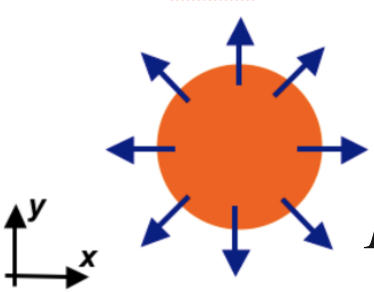

$$p_T^{flow} = p_T + m\beta_T^{flow}\gamma_T^{flow}$$

$$E\frac{d^3N}{dp^3} \sim f(p_t) = \int_0^R m_T K_1(m_T \cosh\rho / T_{fo}) I_0(p_T \sinh\rho / T_{fo}) r dr \quad \text{where } m_T = \sqrt{m^2 + p_T^2};\ \beta_r(r) = \beta_s(\tfrac{r}{R})^n;\ \rho = \tanh^{-1}\beta_r.$$

Identified particle elliptic flow versus p_T

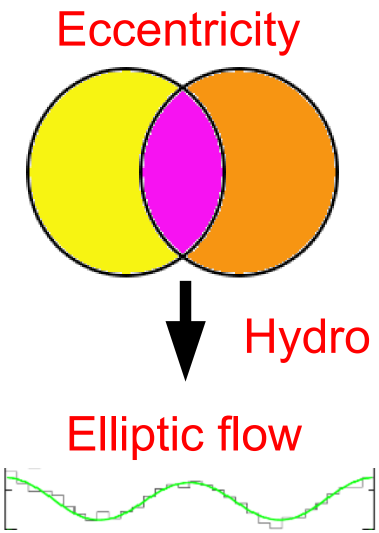

Calculation:
M.Luzum,
arXiv:1011.5173

arXiv:1202.3233

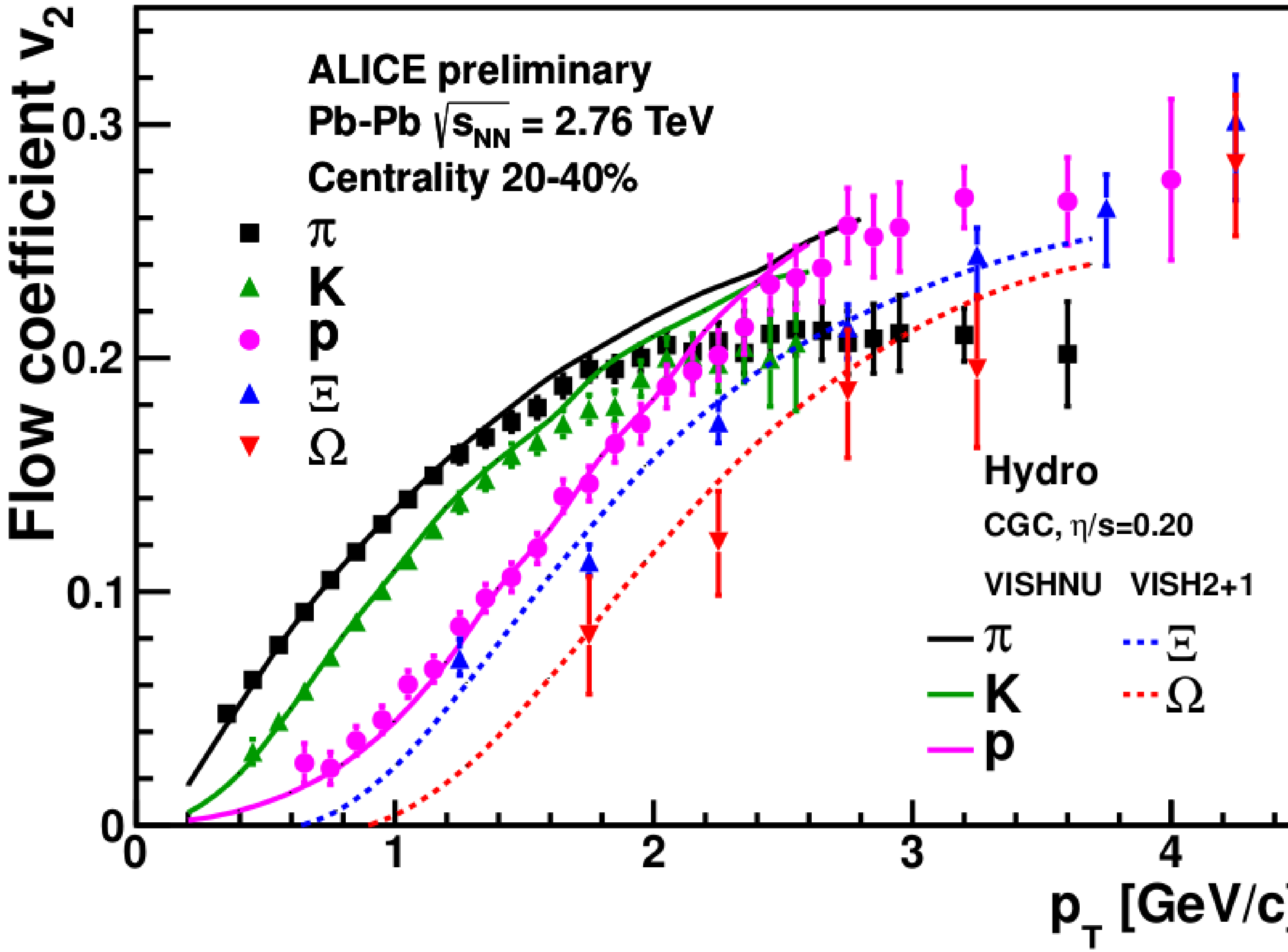

Observed mass ordering in v_2 due to radial flow
can be described by hydrodynamical models

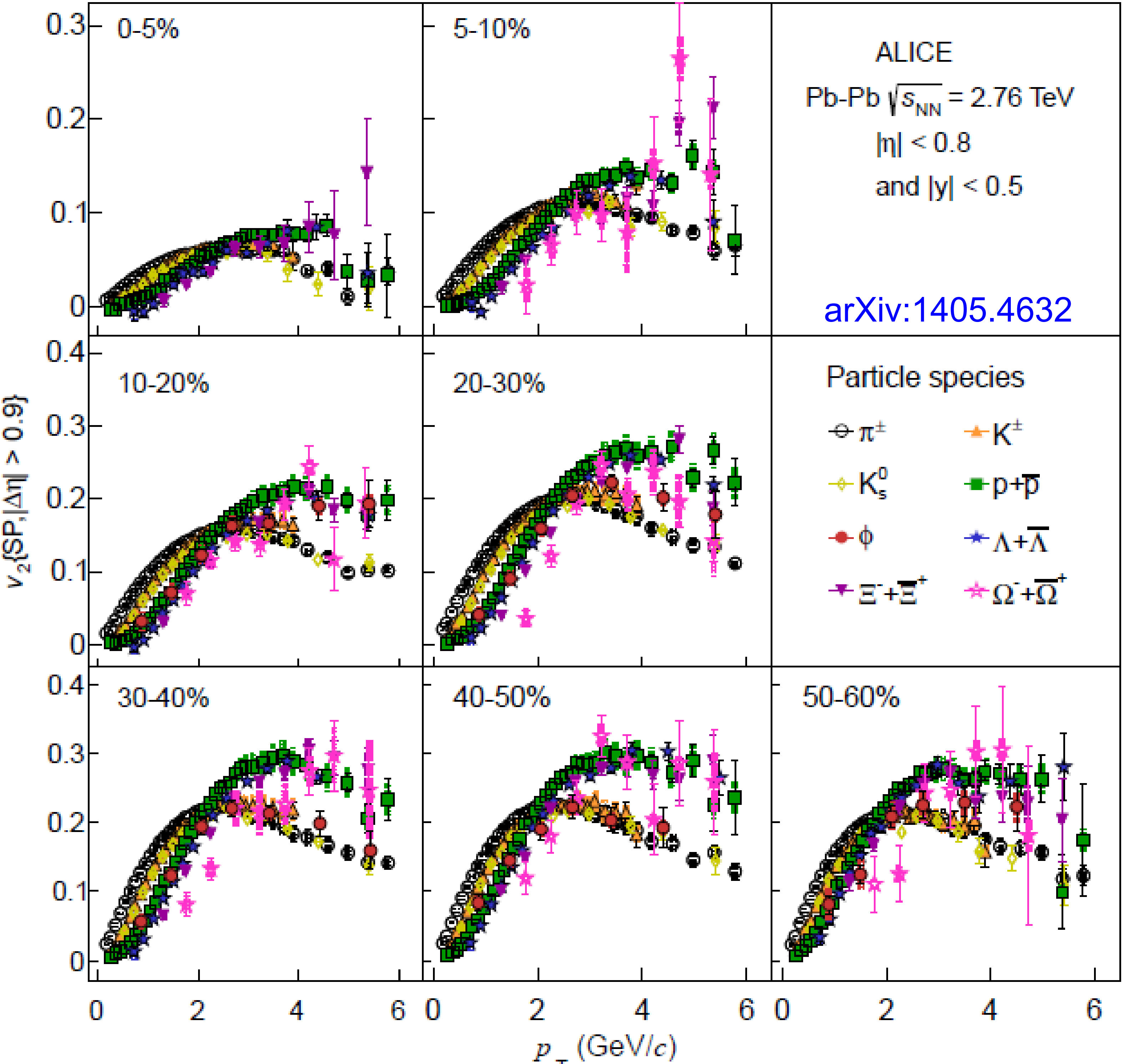
0-5%
5-10%
10-20%
20-30%
30-40%
40-50%
50-60%
ALICE
Pb-Pb $\sqrt{s_{NN}}$ = 2.76 TeV
$|\eta| < 0.8$
and $|y| < 0.5$
arXiv:1405.4632
Particle species
$\pi^{\pm}$
$K^{\pm}$
K^0_s
$p+\bar{p}$
ϕ
$\Lambda+\bar{\Lambda}$
$\Xi^-+\bar{\Xi}^+$
$\Omega^-+\bar{\Omega}^+$
$v_2\{SP, |\Delta\eta| > 0.9\}$
p_T (GeV/c)

The Φ meson

- At low p_T follows mass ordering
- At high p_T close to p in central and close to π in mid-central
- In central collisions p and Φ have similar shape up to ~4 GeV/c.
  - As expected from radial flow
- Mass (and not number of constituent quarks) scaling drives the v_2 and spectra in central collisions

arXiv:1404.0495

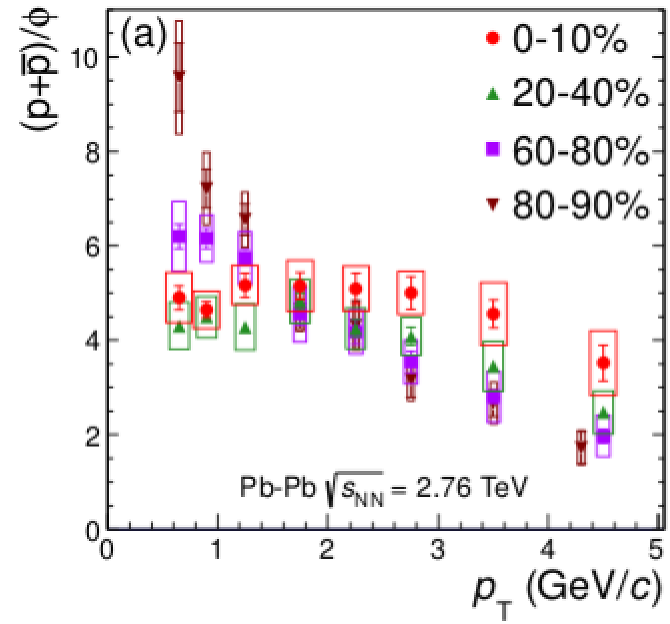

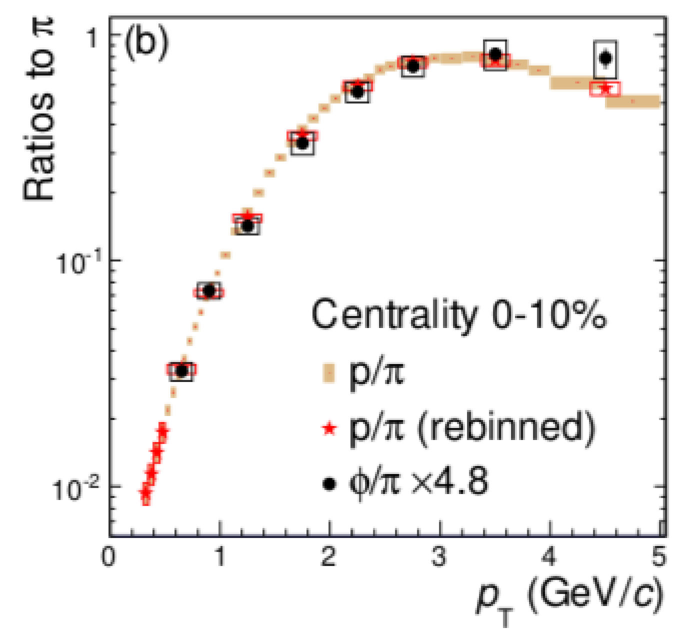

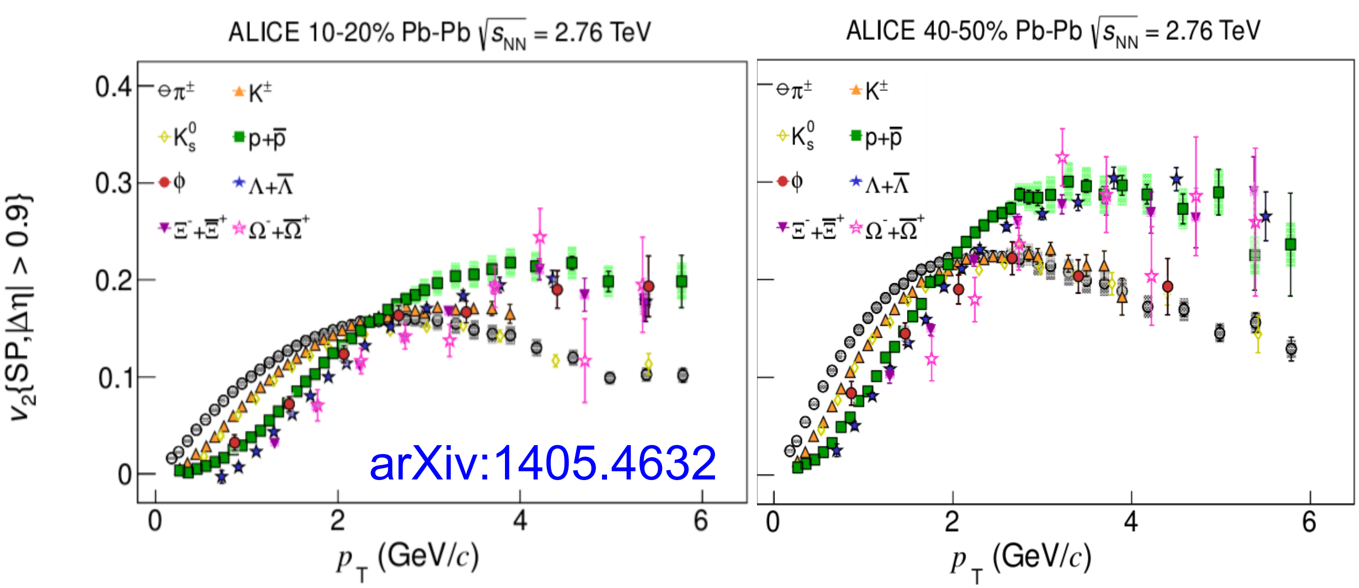

Higher harmonics and viscosity

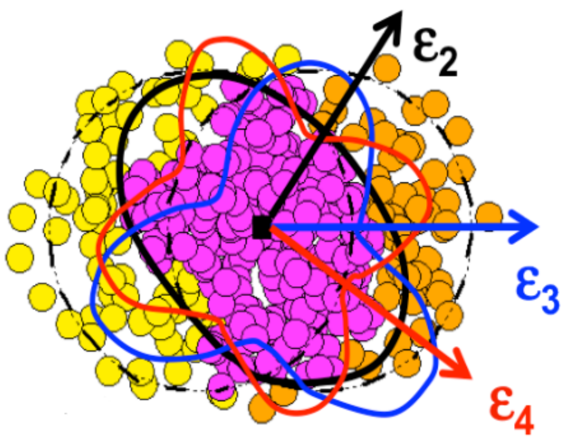

Alver, Roland

Initial spatial anisotropy not smooth, leads to higher harmonics / symmetry planes.

$$\frac{dN}{d\varphi} \sim 1 + 2v_2 \cos[2(\varphi-\psi_2)] + 2v_3 \cos[3(\varphi-\psi_3)] + 2v_4 \cos[4(\varphi-\psi_4)] + 2v_5 \cos[5(\varphi-\psi_5)] + \ldots$$

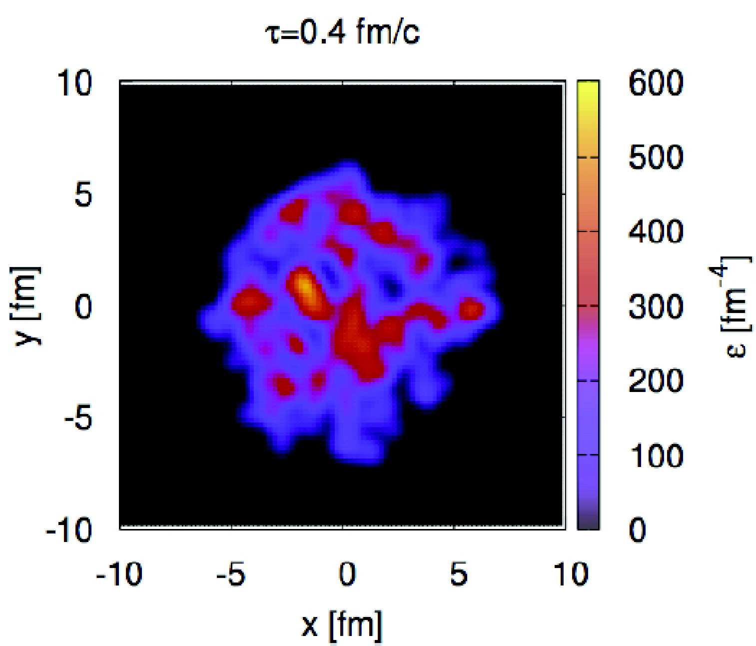

e-by-e hydro

B. Schenke et al.

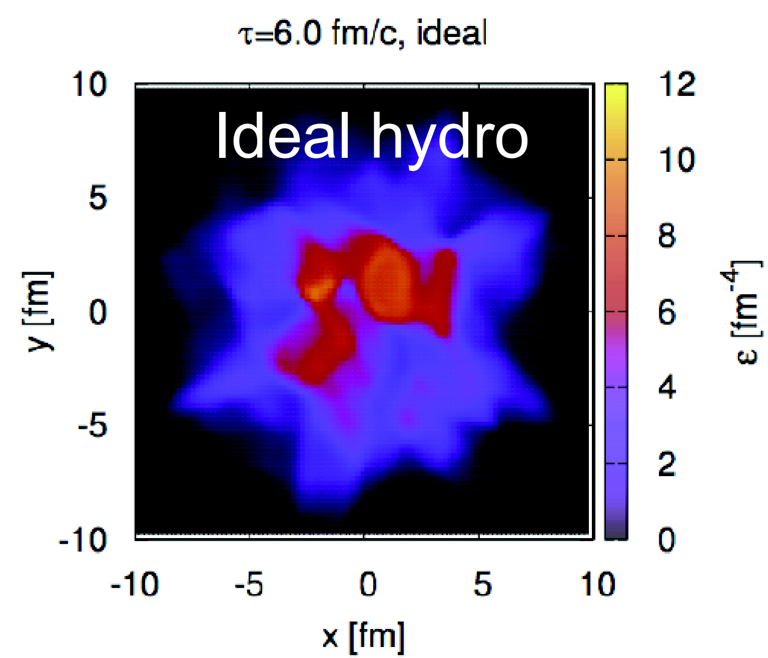

Ideal hydrodynamical models preserves these “clumpy” initial conditions

Higher harmonics and viscosity

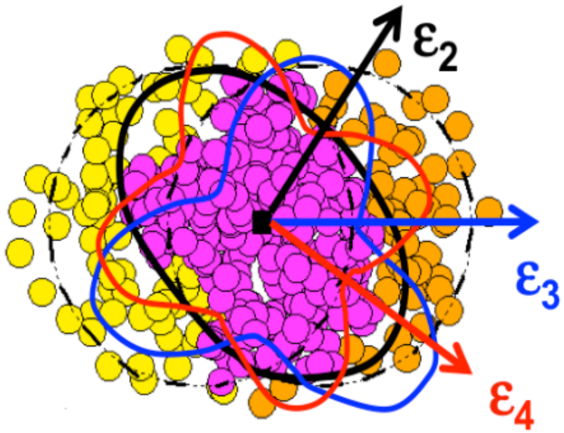

Alver, Roland

Initial spatial anisotropy not smooth, leads to higher harmonics / symmetry planes.

$$\frac{dN}{d\varphi} \sim 1 + 2v_2 \cos[2(\varphi - \psi_2)] + 2v_3 \cos[3(\varphi - \psi_3)] + 2v_4 \cos[4(\varphi - \psi_4)] + 2v_5 \cos[5(\varphi - \psi_5)] + \ldots$$

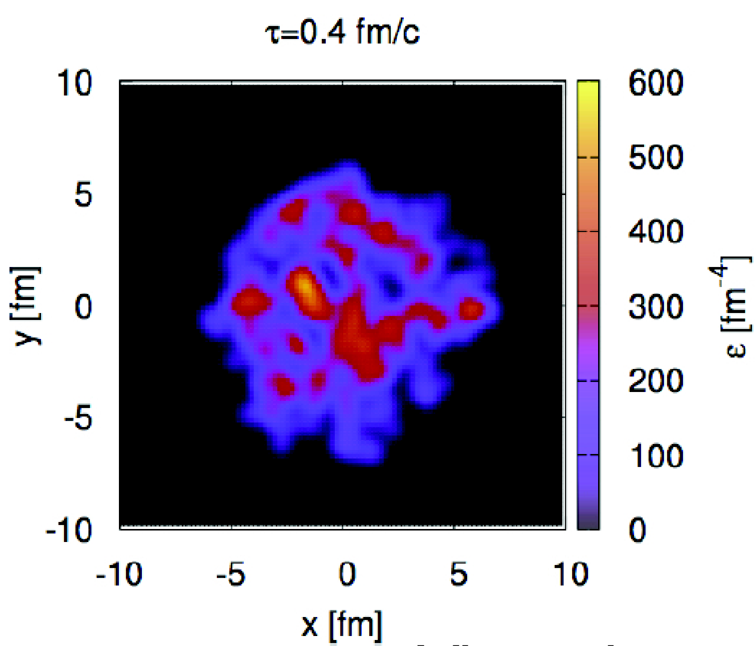

e-by-e hydro →

B. Schenke et al.

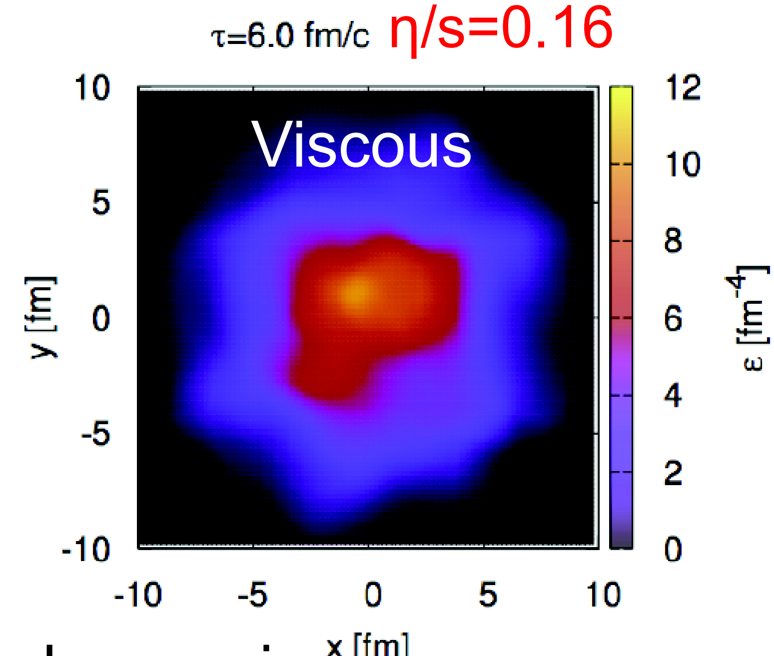

Viscosity suppresses higher harmonics,
→ v_n provide additional sensitivity to η/s

Initial state fluctuations and flow ridges

Alver+Roland, 2010

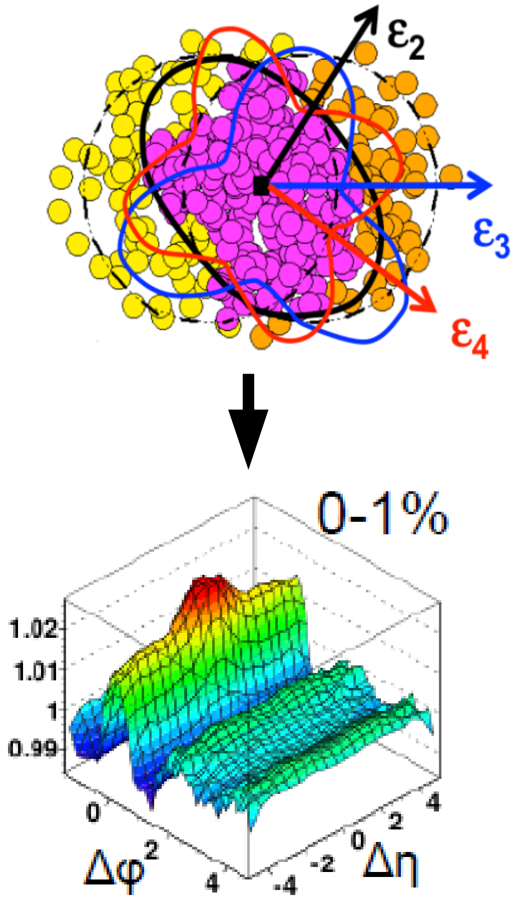

ALICE, PRL 107 (2011) 032301

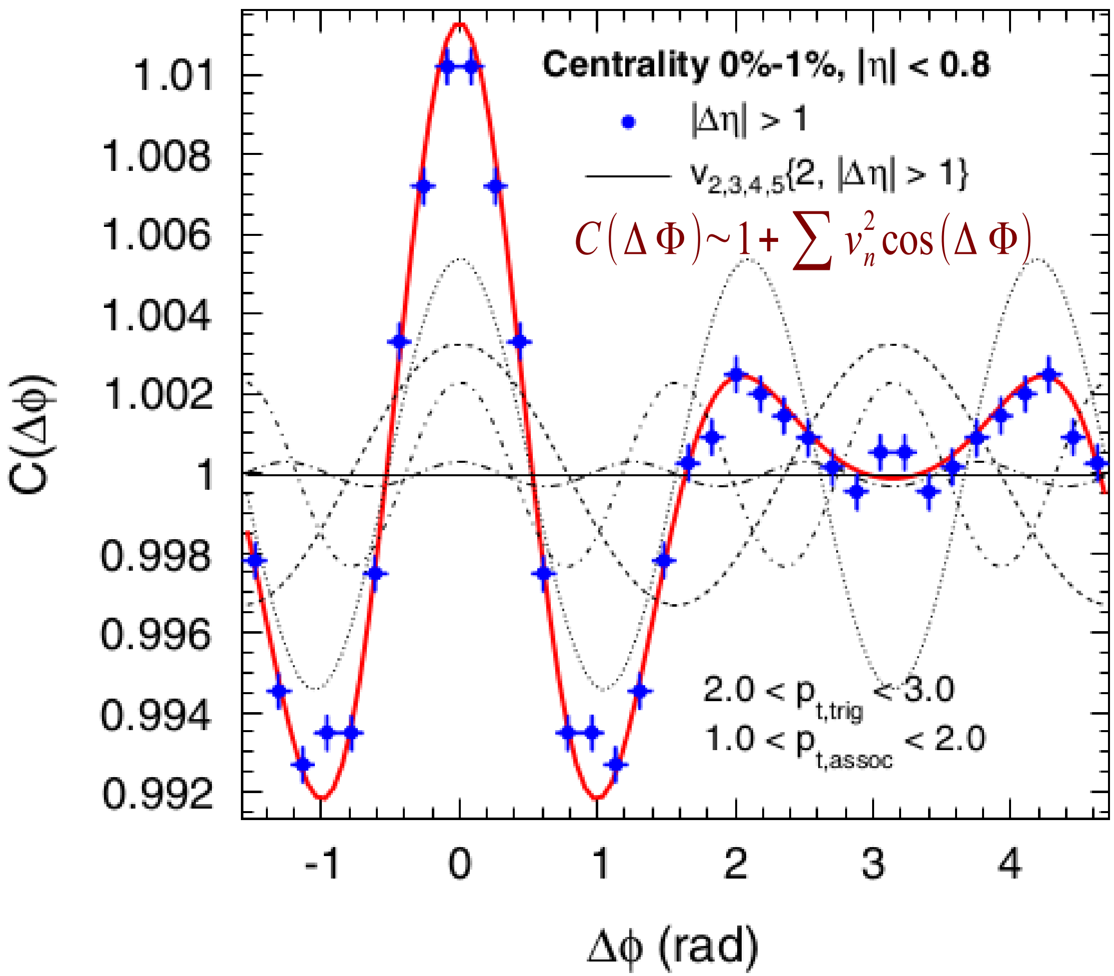

Structures seen in two particle correlations are naturally explained by measured flow harmonics assuming fluctuating initial conditions.

Mass-dependent splitting of v_2 and v_3

Elliptic flow

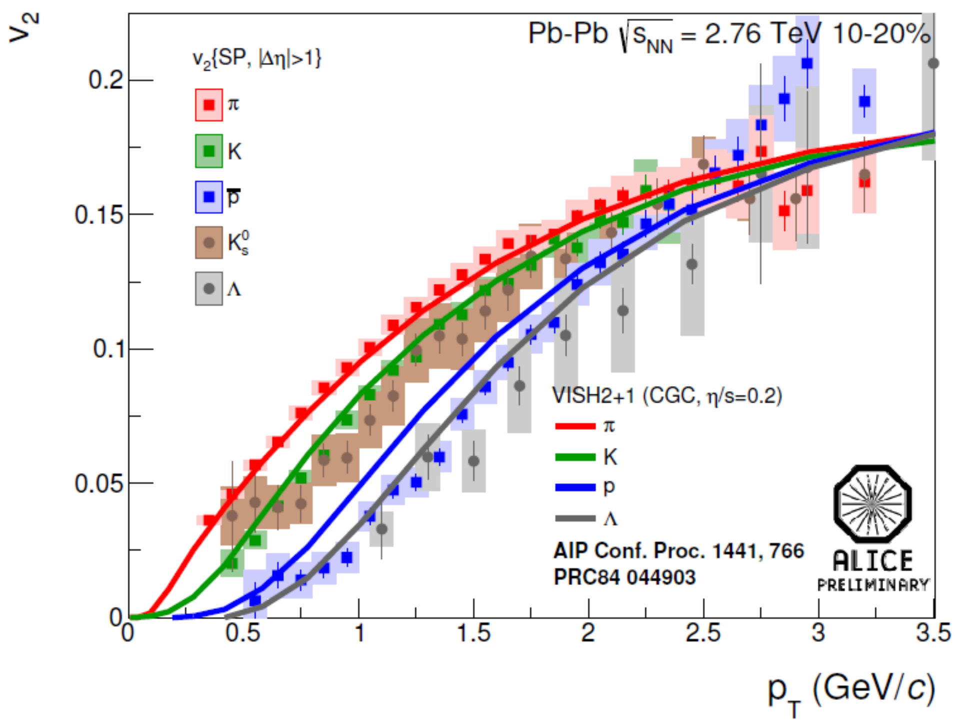

Triangular flow

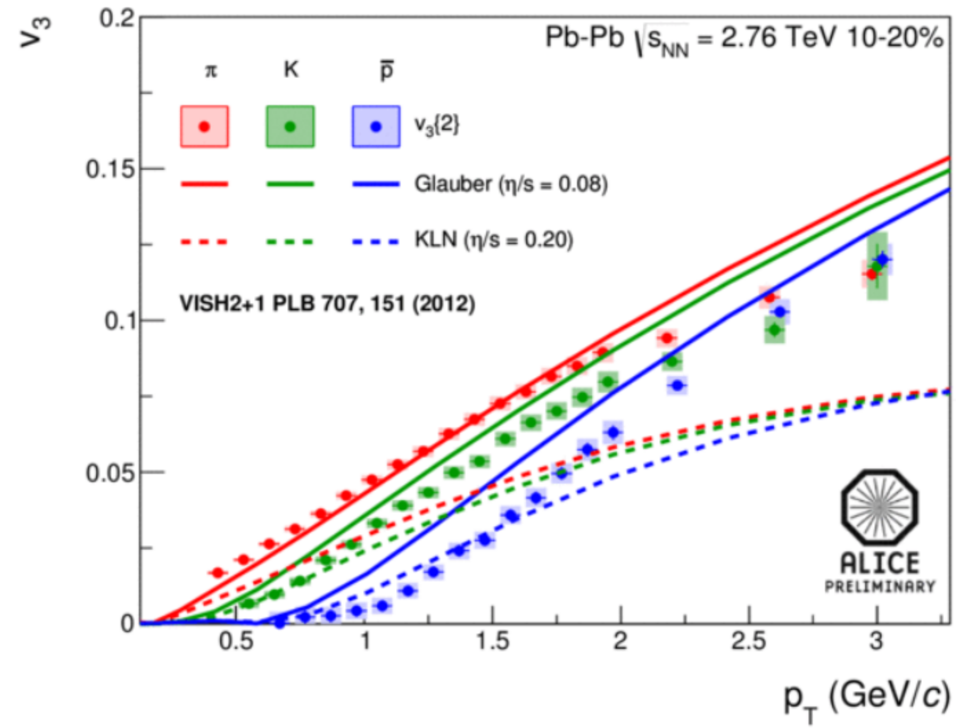

- Particle mass dependent splitting from radial flow characteristic for v_2
- Can be described by hydrodynamical models (+ hadronic afterburners)

- Similar mass splitting for v_3
- Qualitatively described by hydrodynamical models (+ hadronic afterburners)
- Provides additional constraints on η/s

D-meson elliptic flow

arXiv:1405.2001

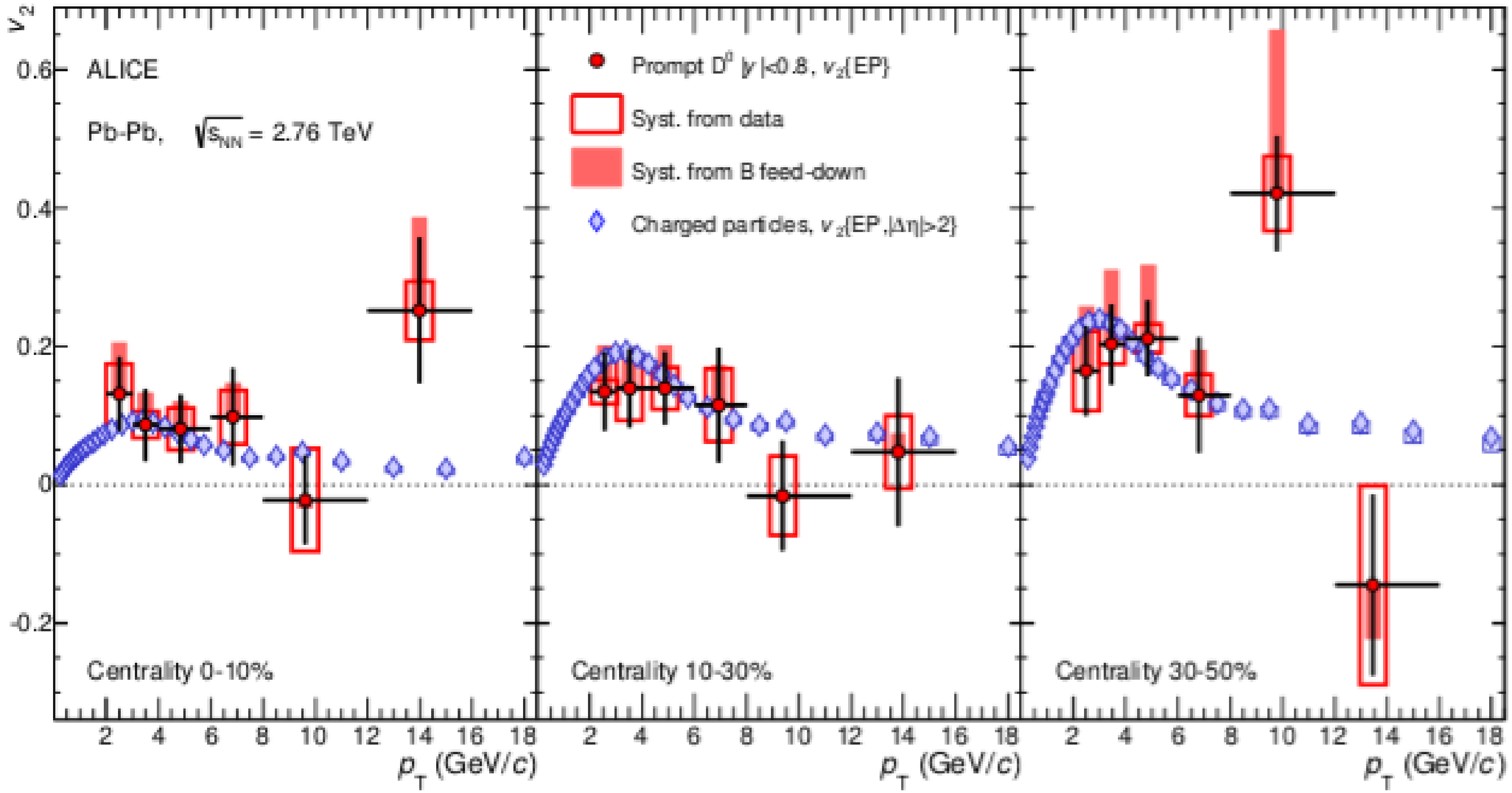

Even charm mesons exhibit elliptic flow

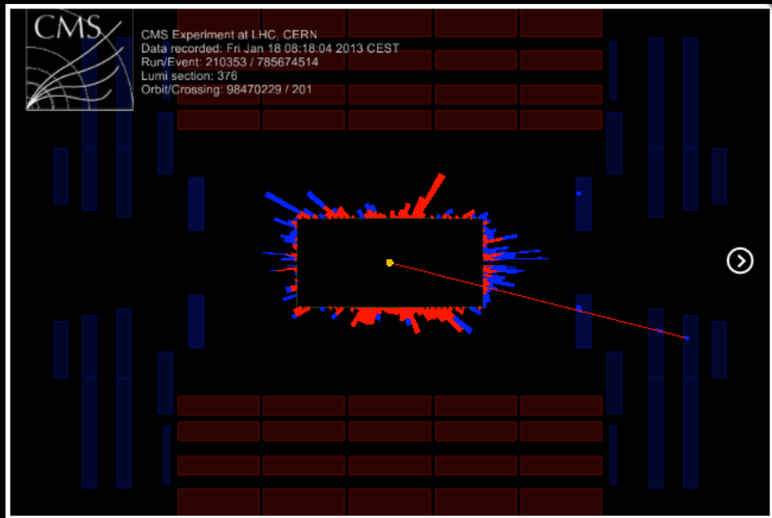

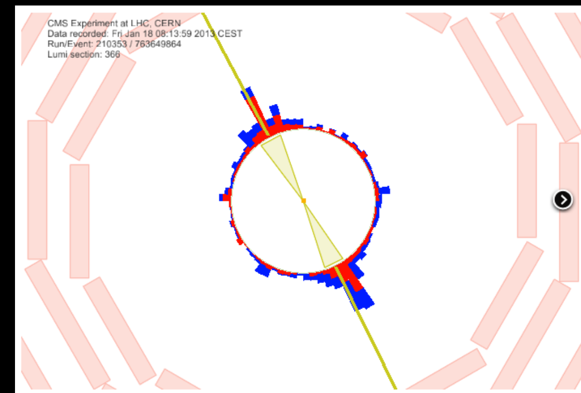

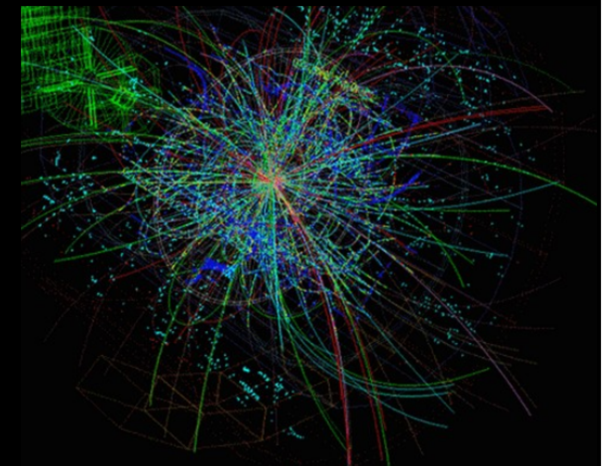

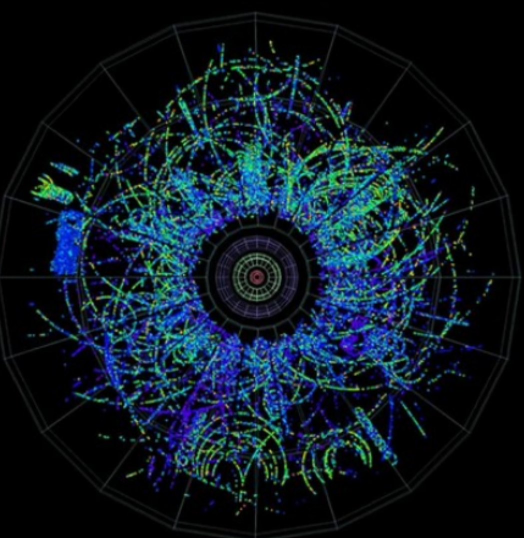

Control experiment: p+Pb collisions at the LHC

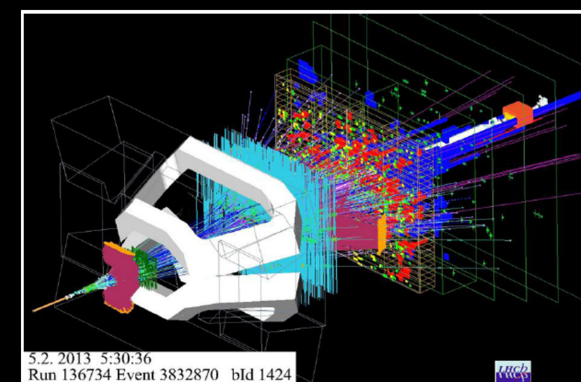

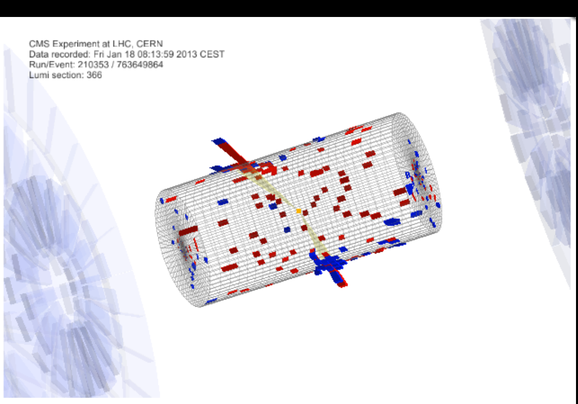

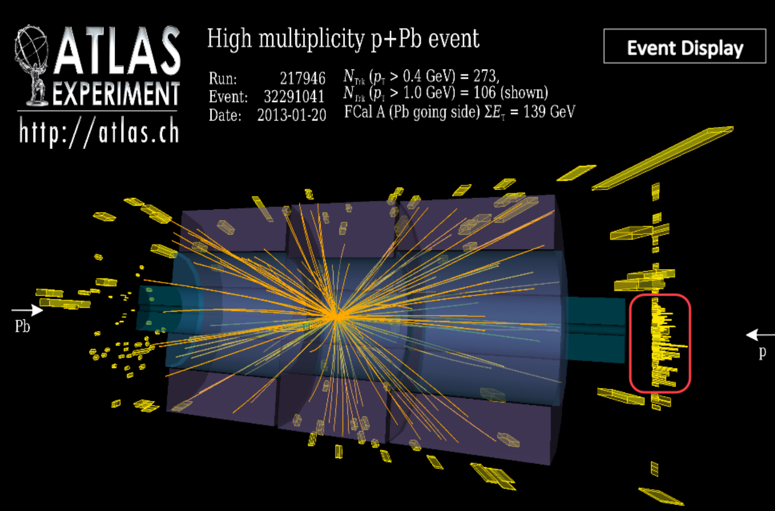

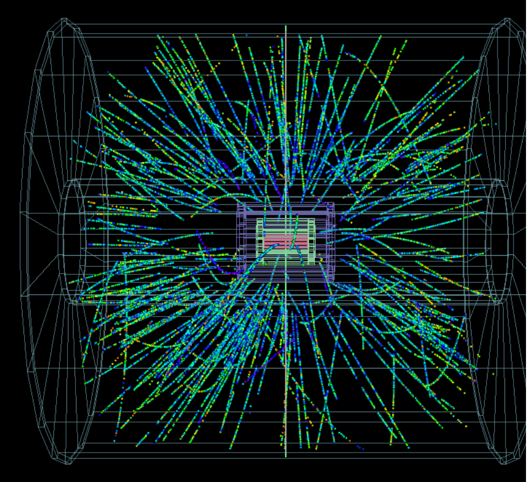

pPb and Pbp rapidity sign convention

- p-Pb
  - ⇨proton going towards muon arm (low-x in Pb)

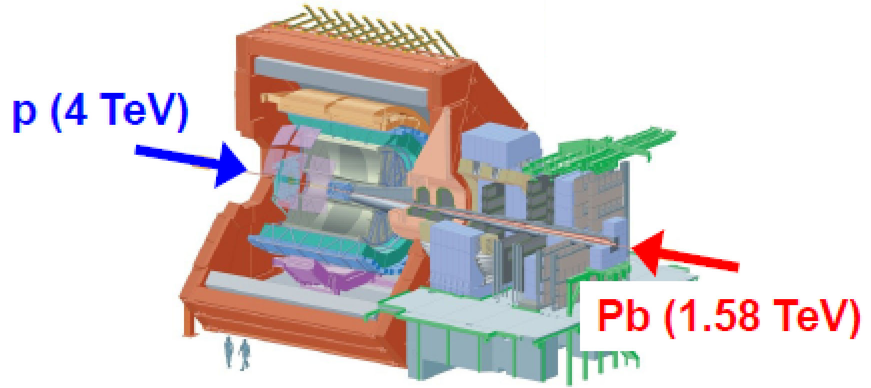

Δy_{cms}=0.465 in the p-beam direction

- Pb-p
  - ⇨Pb nucleus going towards muon arm (low-x in p)

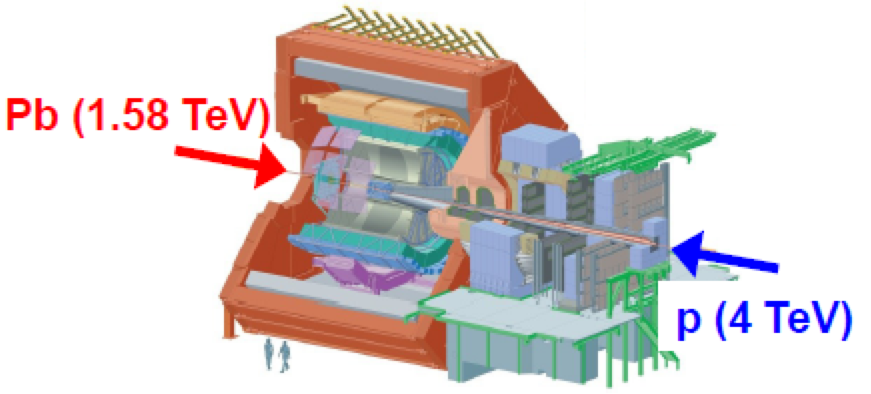

- Center-of-mass energy 5.02 with Δy=0.465 wrt lab system in direction of proton beam
- Usually results reported such that positive rapidity corresponds to proton direction and negative rapidity to Pb direction
  - Be aware that some results (in particular correlation results) are done in the laboratory frame

Nuclear modification factor

$$R_{\mathrm{pA}}^{\mathrm{X}}(p_{\mathrm{T}}) = \frac{\mathrm{d}N_{\mathrm{X}}^{\mathrm{pA}}/\mathrm{d}p_{\mathrm{T}}}{\langle N_{\mathrm{coll}}\rangle \mathrm{d}N_{\mathrm{X}}^{\mathrm{pp}}/\mathrm{d}p_T}$$

Average number of collisions from Glauber (or cross sections):
$\langle N_{coll}\rangle = A\,\sigma_{pp}/\sigma_{pA} \approx 6.9$

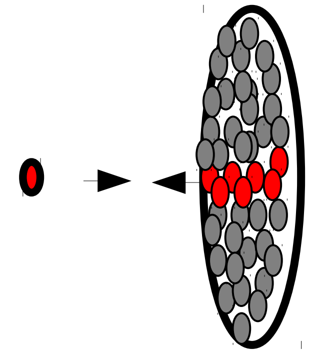

$$\frac{\mathrm{d}\sigma^{pA\to X}}{\mathrm{d}p_{\mathrm{T}}} \propto f_i^p(x_1,Q^2)\circ f_j^A(x_2,Q^2)\circ\sigma^{ij\to k}(x_1,x_2,p_{\mathrm{T}}/z,Q^2)\circ D_{k\to X}(z,Q^2)\circ FS\ effects$$

- In absence of final state effects provides information on nuclear PDF

$$f_i^A(x,Q^2) \equiv R_i^A(x,Q^2)\,f_i^{\mathrm{CTEQ6.1M}}(x,Q^2)$$

- Two regimes important at LHC:
  - Shadowing and Anti-shadowing

JHEP 0904 (2009) 065

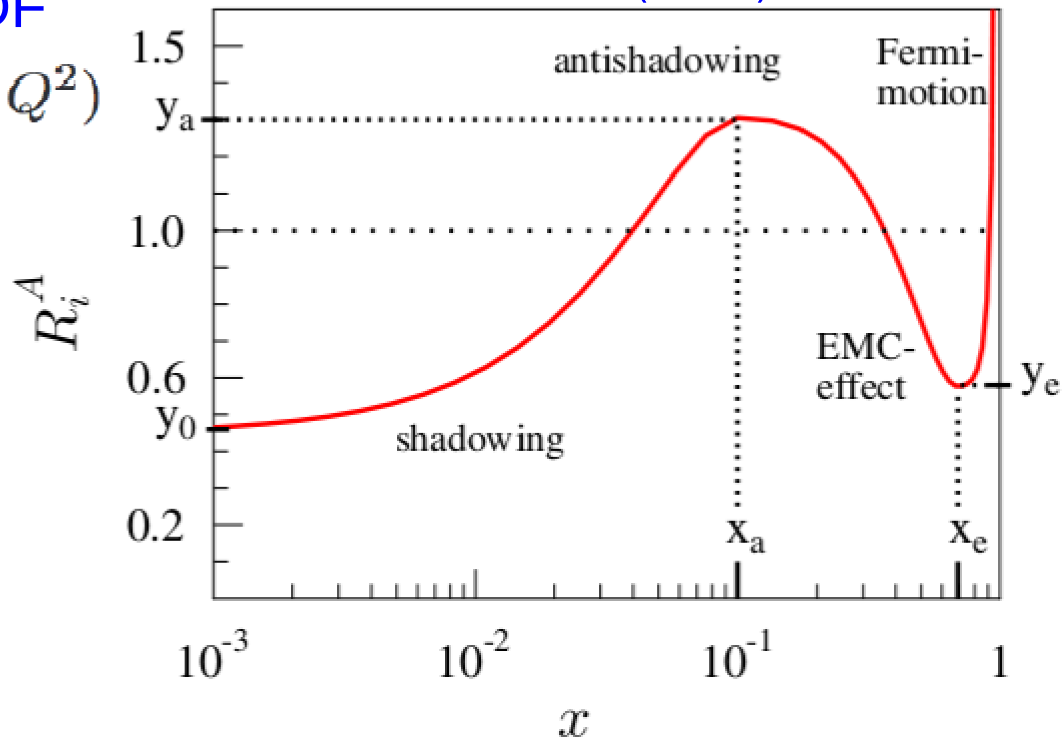

Charged particle R_{pPb}

$$R_{AB} = \frac{dN_{AB}/dp_T}{\langle N_{coll}\rangle dN_{pp}/dp_T}$$

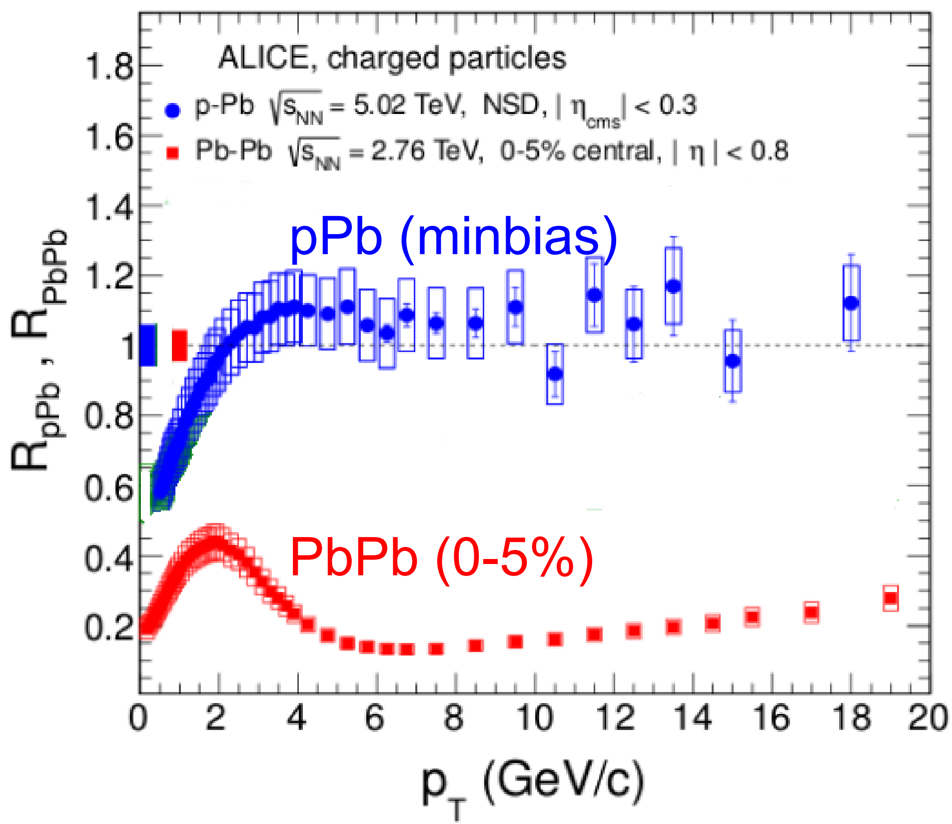

ALICE, PRL 110 (2013) 082302

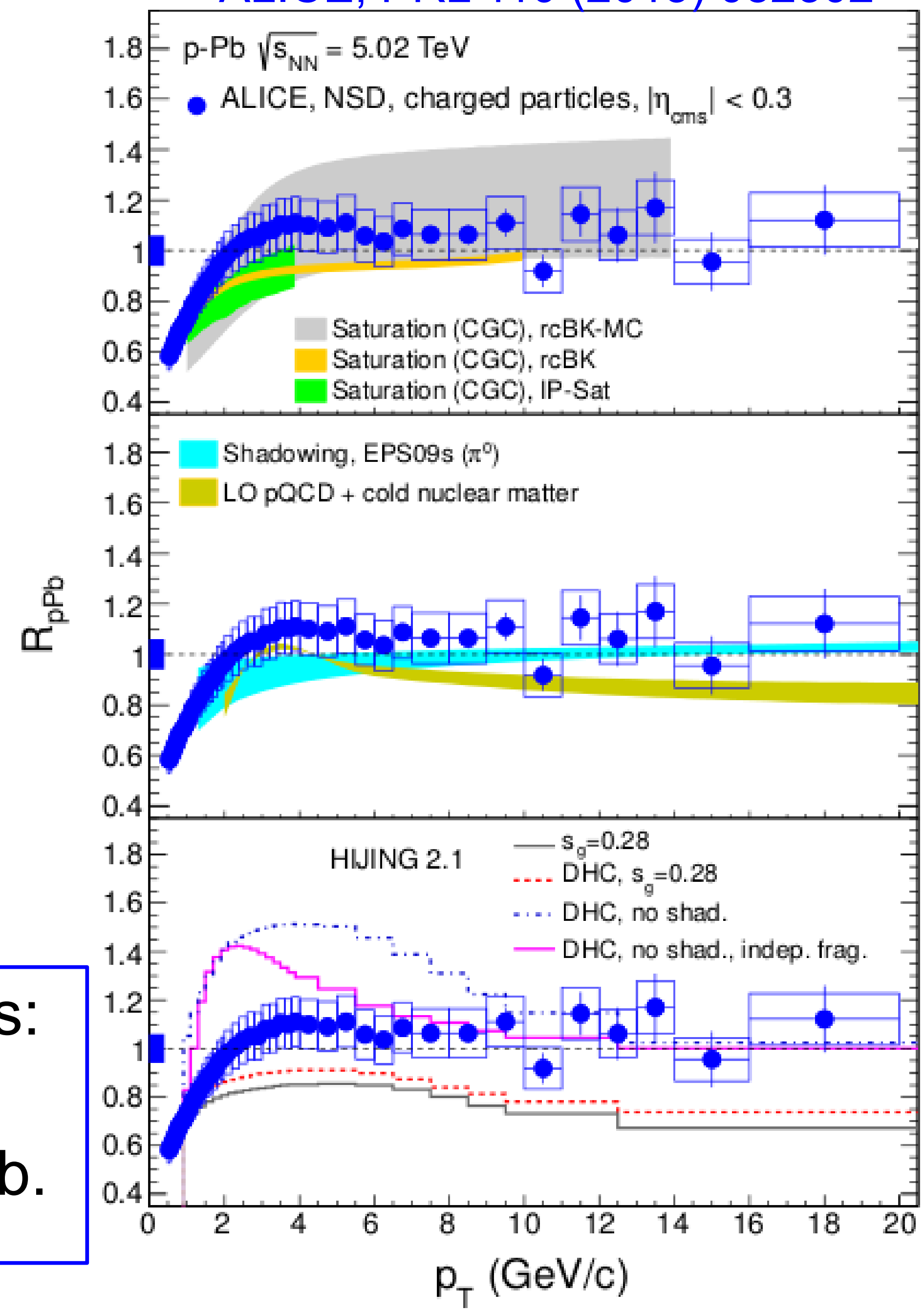

No surprises at high p_T in first results:

Supports existence of strong final state effects (at mid-rapidity) in PbPb.

Charged particle R_{pPb}

arXiv:1405.2737

$$R_{AB} = \frac{\mathrm{d}N_{AB}/\mathrm{d}p_{\mathrm{T}}}{\langle N_{\mathrm{coll}} \rangle \mathrm{d}N_{\mathrm{pp}}/\mathrm{d}p_{\mathrm{T}}}$$

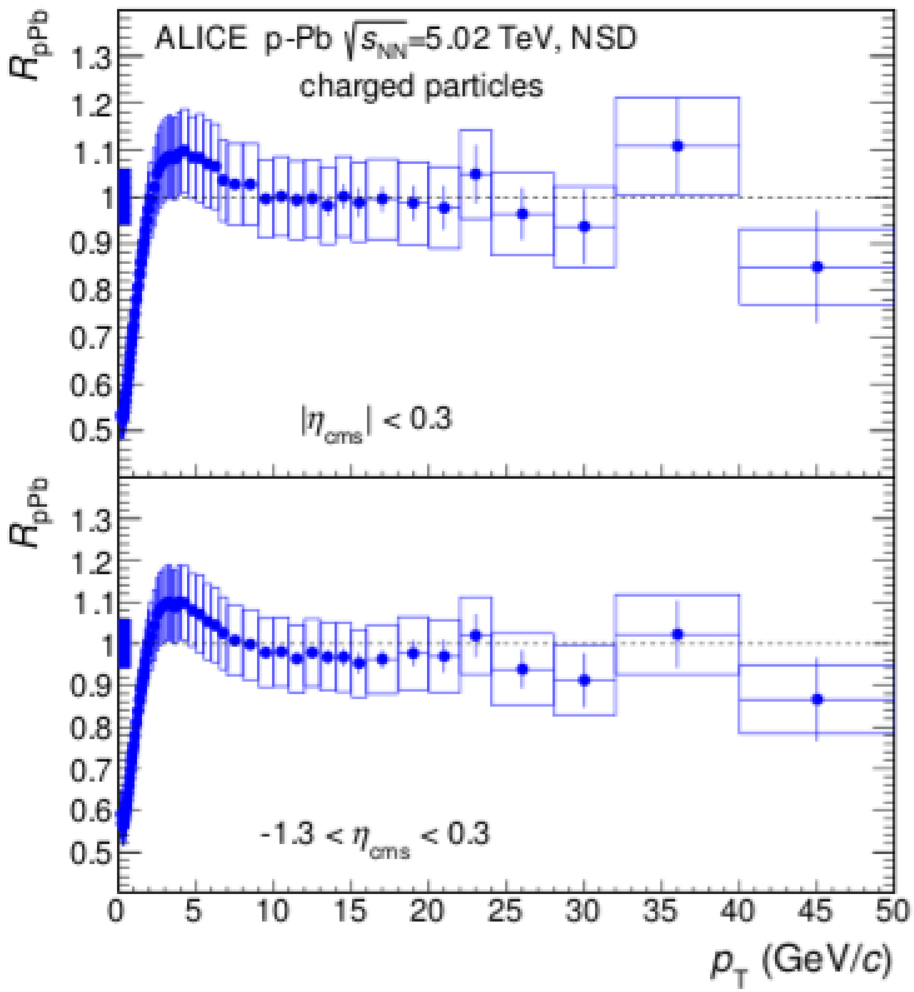

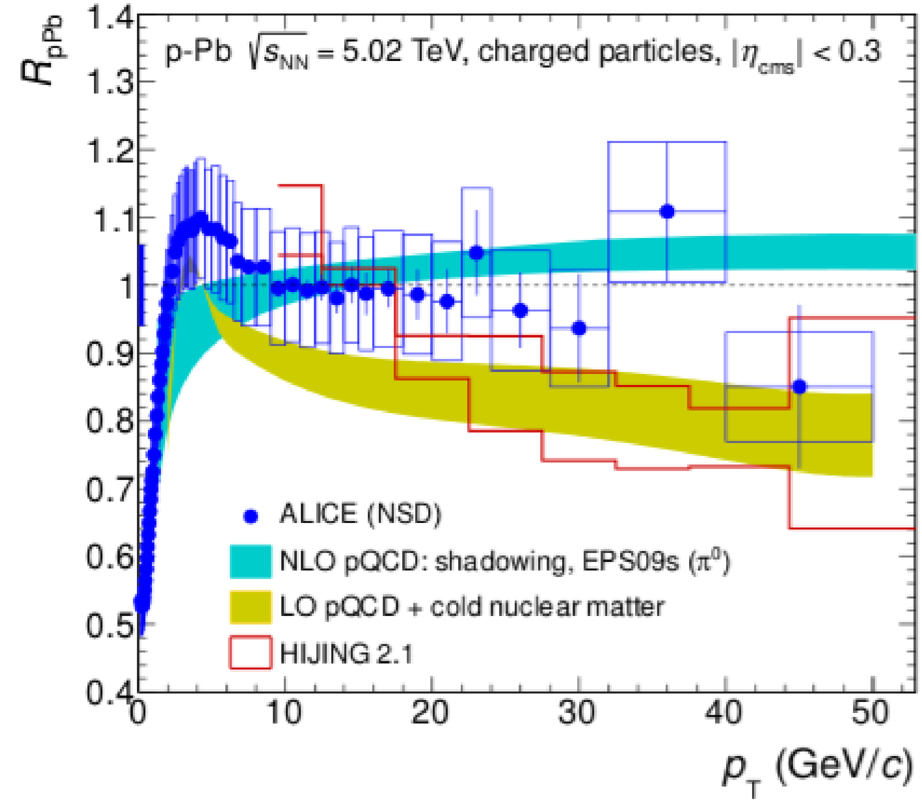

Extended measurements up to 50 GeV/c: No change of message

No significant effects at high-p_T

arXiv:1405.3452v1

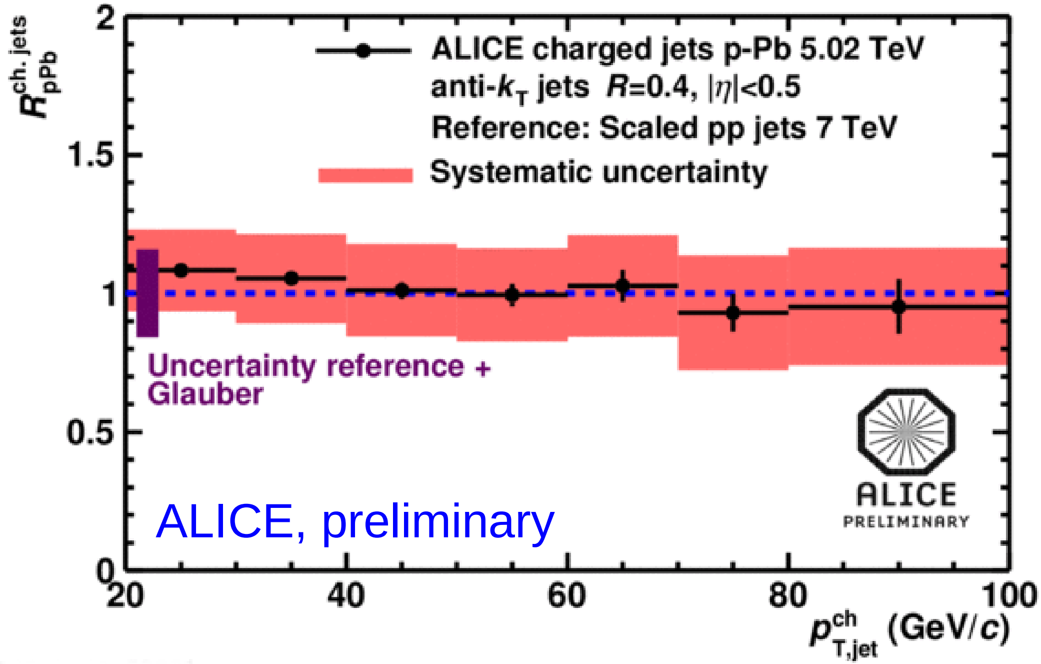

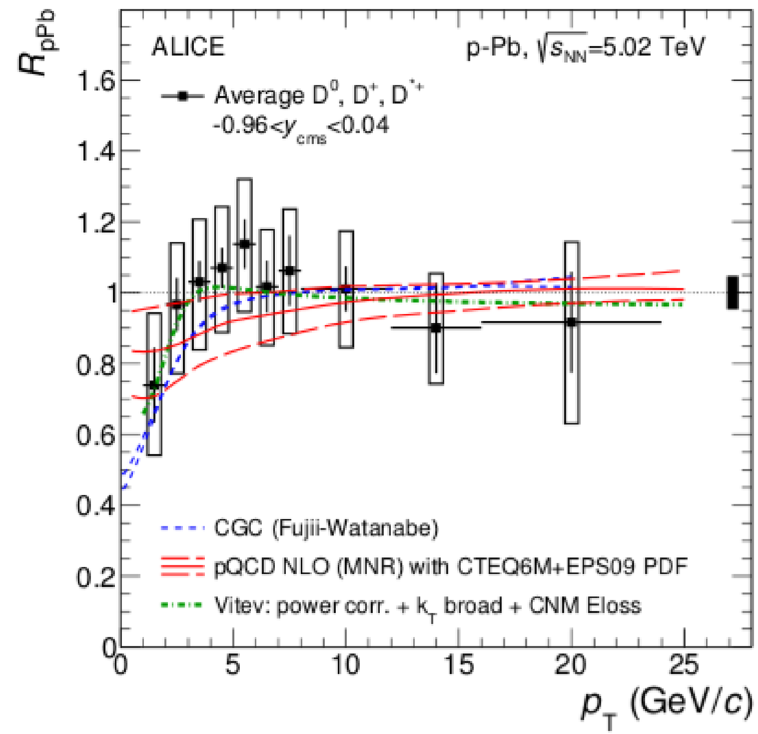

ALICE, preliminary

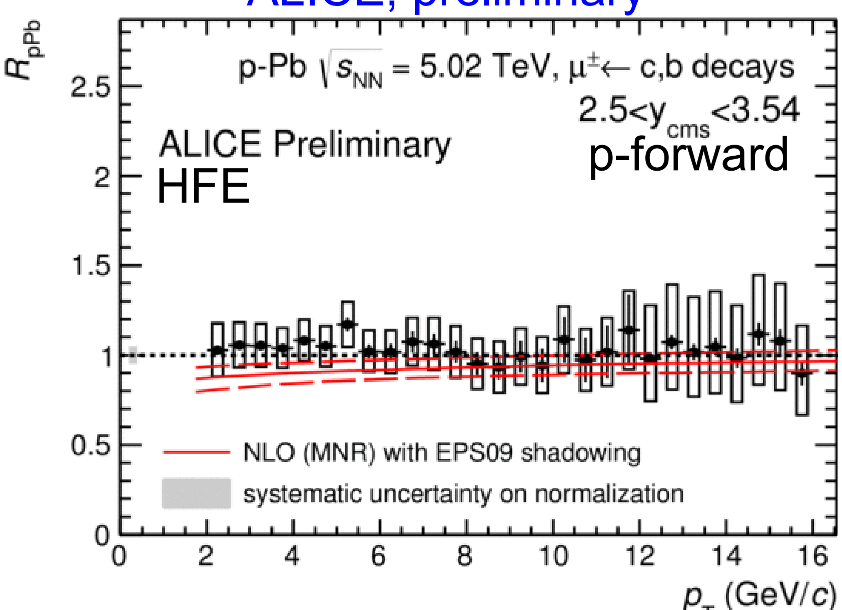

ALICE, preliminary

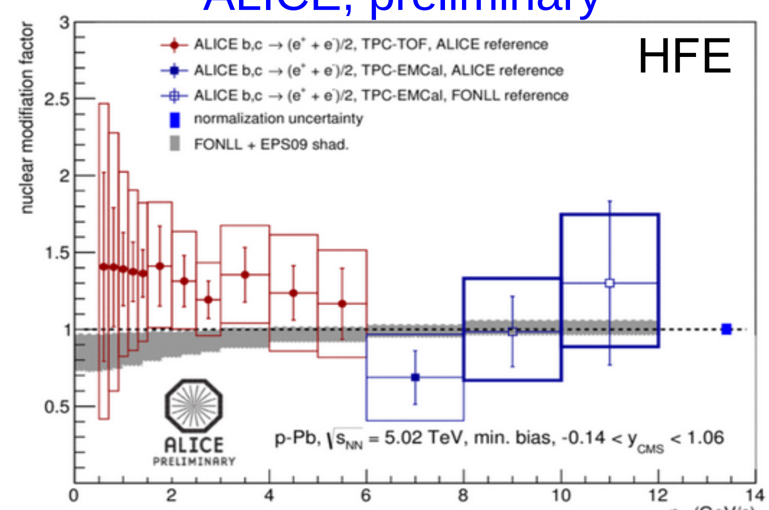

Event multiplicity/activity classes in pPb

- Define event classes by slicing various multiplicity related distributions
  - Every experiment uses its own selection and usually provides (corrected) multiplicity at mid-rapidity
  - Event class definition (aka event activity) may matter for particular measurements
  - Systematics from different selections

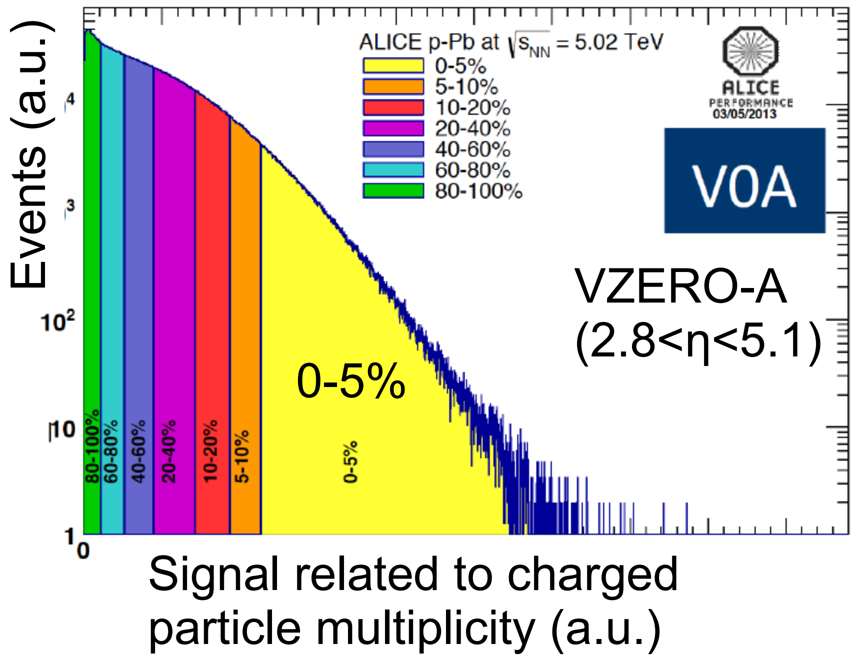

- Relation of multiplicity to centrality via Glauber model not straight-forward
  - Correlation between collision geometry and multiplicity not as strong as in AA
  - Use minimum-bias collisions instead ($N_{coll} = A\ \sigma_{pp}/\sigma_{pA}$)
  - Centrality discussion (later)

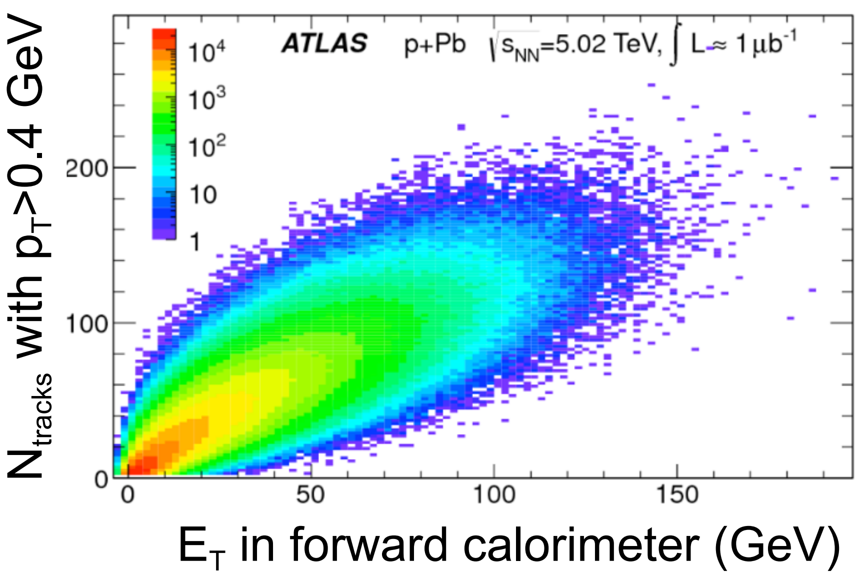

Di-Hadron Correlations (DHC)

- CMS: pp, pPb at LHC
  - Long-range near-side correlations (ridge) appear at high-multiplicity
    - Collective effects in pp and pPb?
    - CGC initial state effects?

CMS, JHEP 1009 (2010) 91 CMS, PLB 718 (2012) 795

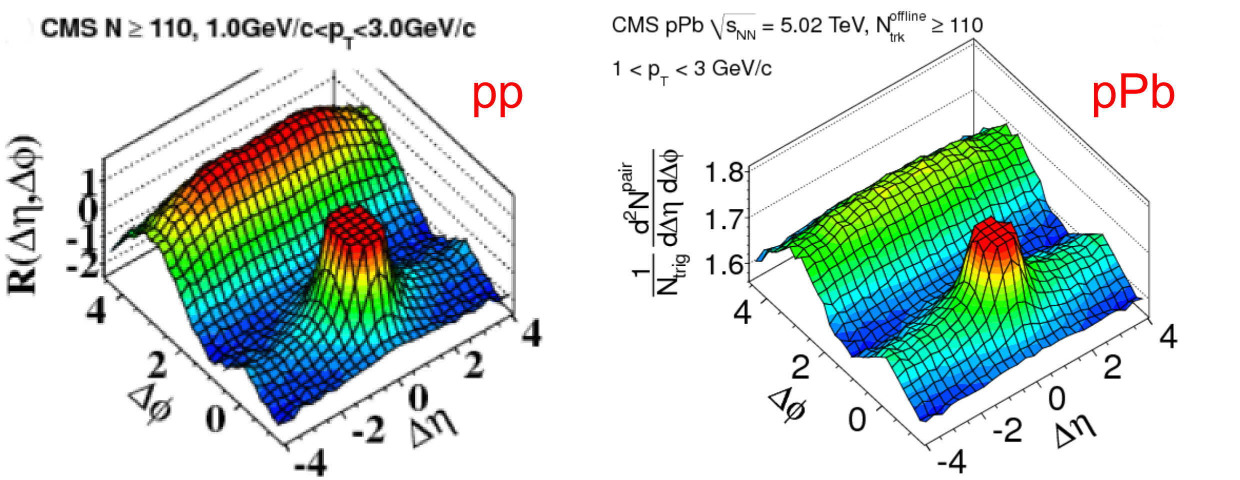

- STAR: dAu at RHIC
  - Back-to-back (jet-like) correlations in forward π^0 correlations disappear in high-multiplicity events
    - Compatible with CGC predictions
- LHC mid- and RHIC forward-η probe a similar x regime

STAR, arXiv:1005.2378

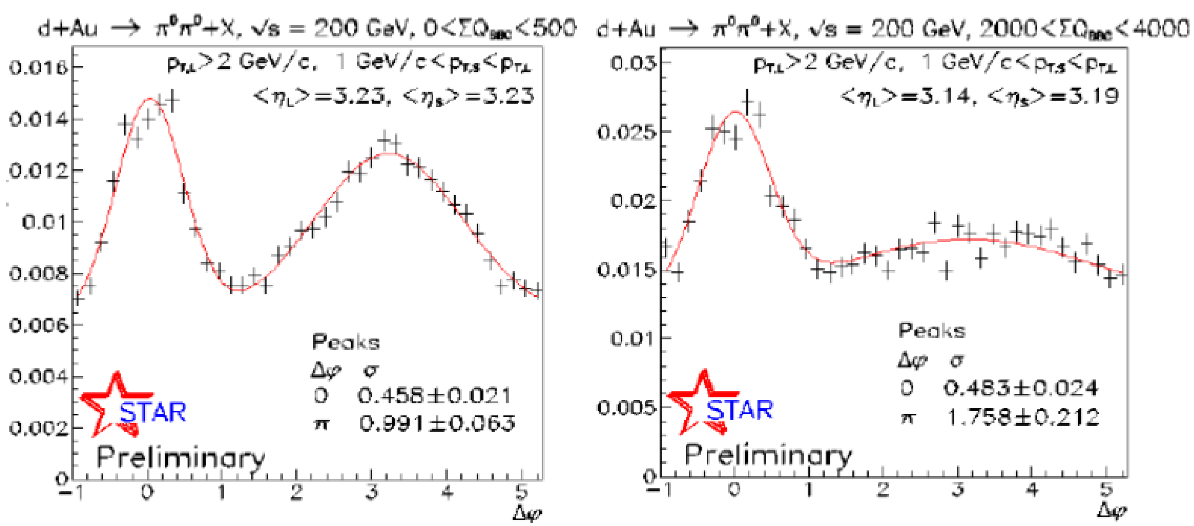

Peripheral Central

DHC: Correlation measure

ALICE, PLB 719 (2013) 29

- Associated yield per trigger particle (with $p_T^{trig} > p_T^{assoc}$)

$$\frac{1}{N_{\mathrm{trig}}} \frac{\mathrm{d}^2 N_{\mathrm{assoc}}}{\mathrm{d}\Delta\eta\,\mathrm{d}\Delta\varphi} = \frac{S(\Delta\eta, \Delta\varphi)}{B(\Delta\eta, \Delta\varphi)}$$

- Signal (same event) pair yield

$$S(\Delta\eta, \Delta\varphi) = \frac{1}{N_{\mathrm{trig}}} \frac{\mathrm{d}^2 N_{\mathrm{same}}}{\mathrm{d}\Delta\eta\,\mathrm{d}\Delta\varphi}$$

  - Definition as ratio of sums is multiplicity independent

$$\frac{N_{pair}}{N_{trig}} = \frac{\sum_{i=1}^{N_{evt}} \sum_{j=1}^{N^i_{source}} \frac{1}{2} n_{ij}(n_{ij}-1)}{\sum_{i=1}^{N_{evt}} \sum_{j=1}^{N^i_{source}} n_{ij}} = \frac{N_{evt}\langle N_{source}\rangle \frac{1}{2}\langle n(n-1)\rangle}{N_{evt}\langle N_{source}\rangle \langle n\rangle} = \frac{1}{2}\frac{\langle n(n-1)\rangle}{\langle n\rangle}$$

- Background (mixed event) pair yield

$$B(\Delta\eta, \Delta\varphi) = \frac{1}{B(0,0)} \frac{\mathrm{d}^2 N_{\mathrm{mixed}}}{\mathrm{d}\Delta\eta\,\mathrm{d}\Delta\varphi}$$

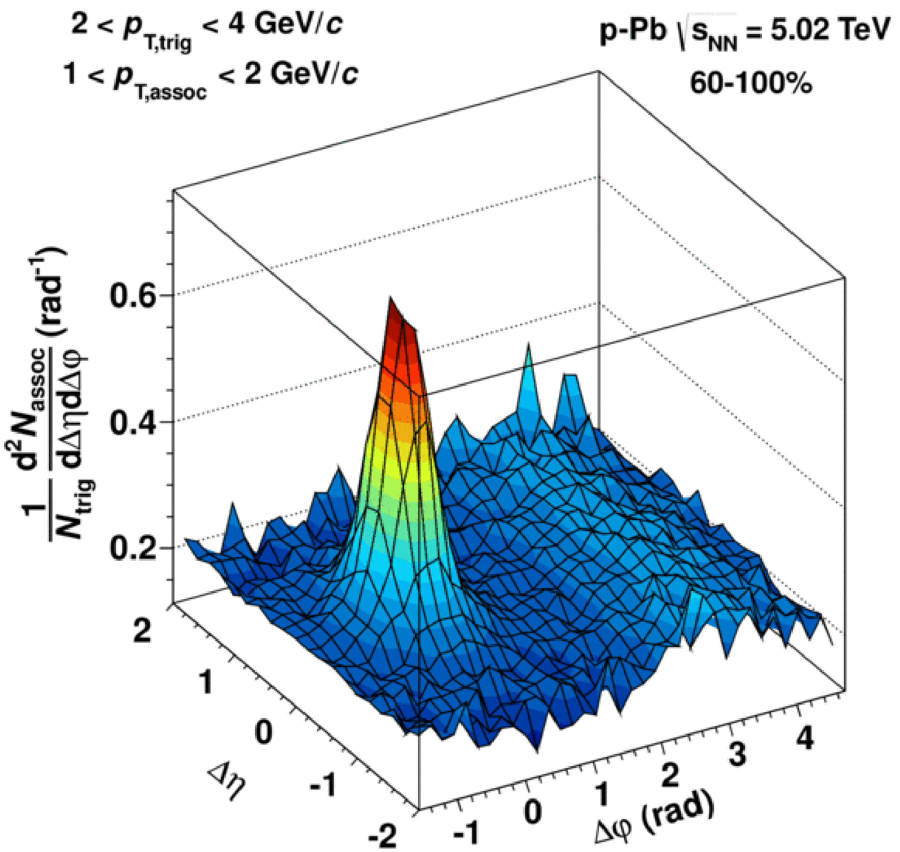

DHC: Multiplicity dependence

ALICE, PLB 719 (2013) 29

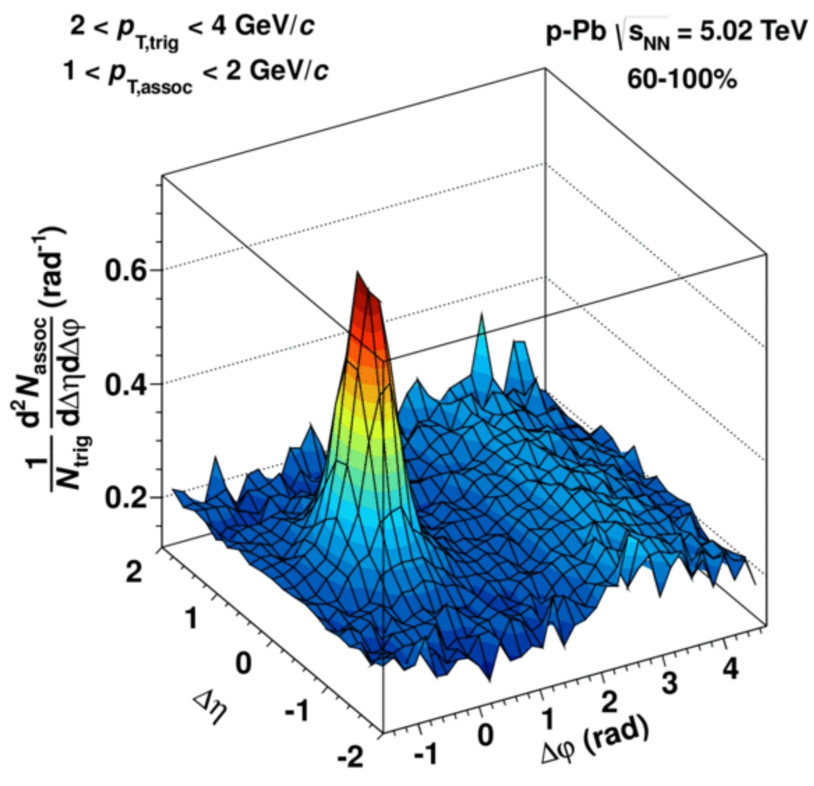

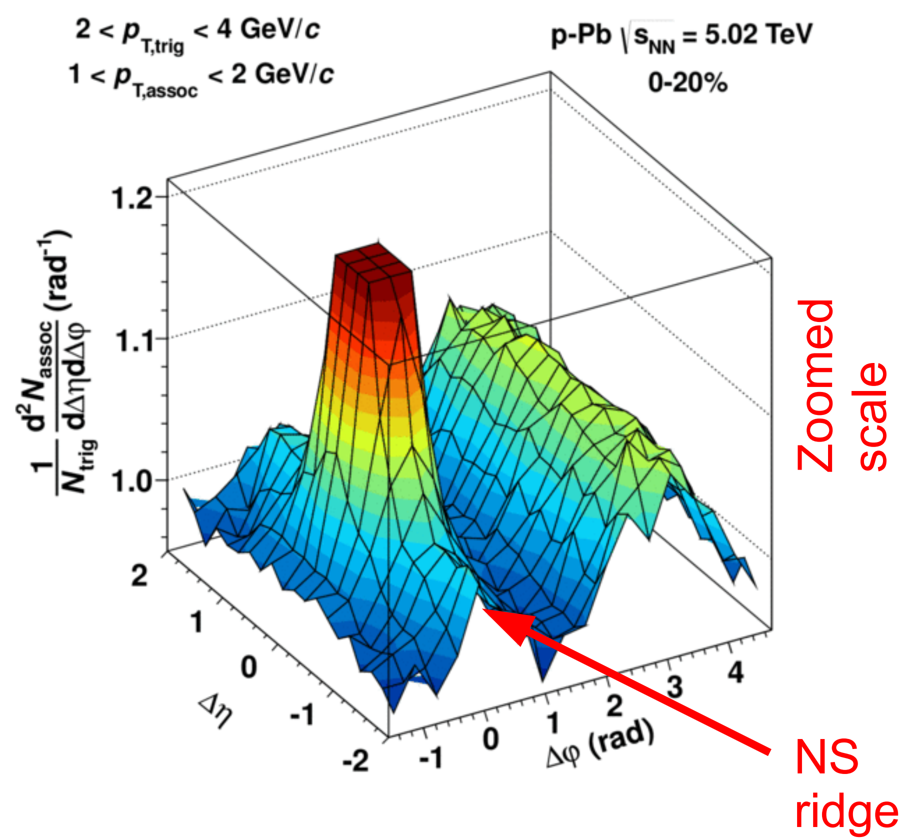

- Low-multiplicity p-Pb (60-100%)
  - pp-like (jet-like) correlation structures
- High-multiplicity p-Pb (0-20%)
  - Near-side ridge appears (first seen in CMS)
  - Higher yields on near- and away-side

DHC: Multiplicity dependence

ALICE, PLB 719 (2013) 29

- Compare associated yield in pPb multiplicity classes and pp
  - Project to Δφ over |Δη|<1.8
  - Subtract baseline at Δφ~1.3

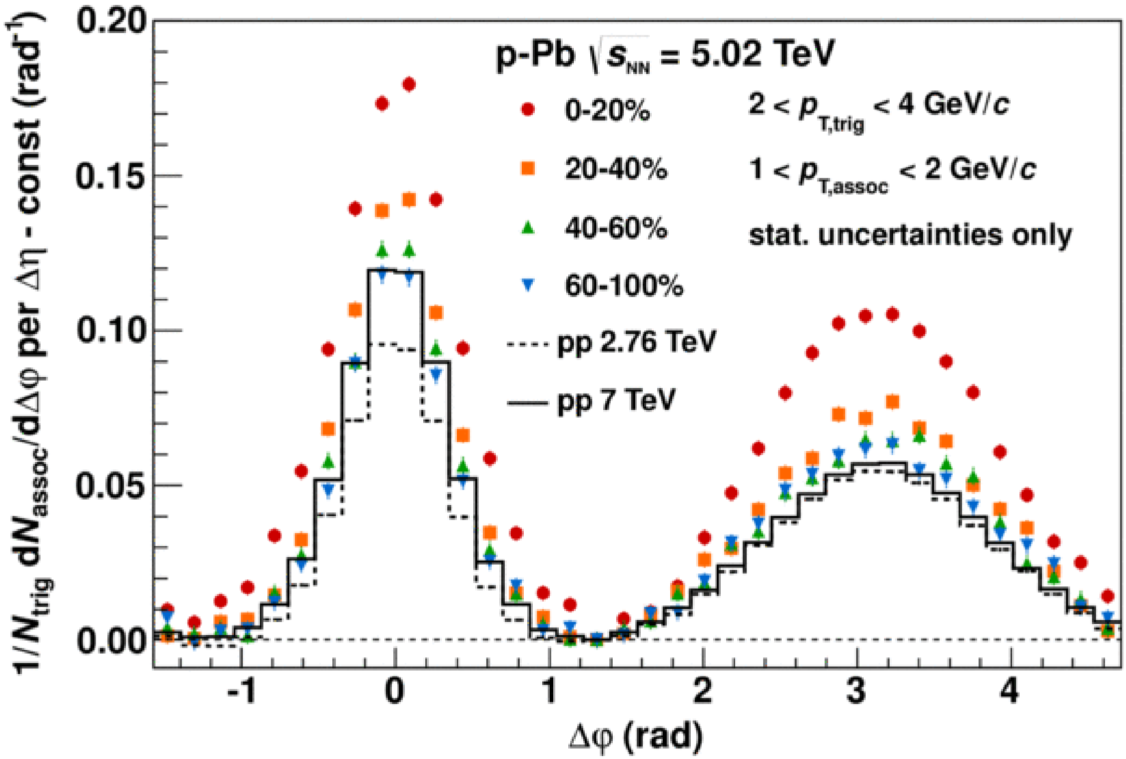

- Low multiplicity pPb is similar to pp (at 7 TeV)
- Yield rises on near and away side with increasing multiplicity
- In contrast with away-side suppression observed in dAu at RHIC at forward η (similar x)

Extraction of double ridge structure

ALICE, PLB 719 (2013) 29

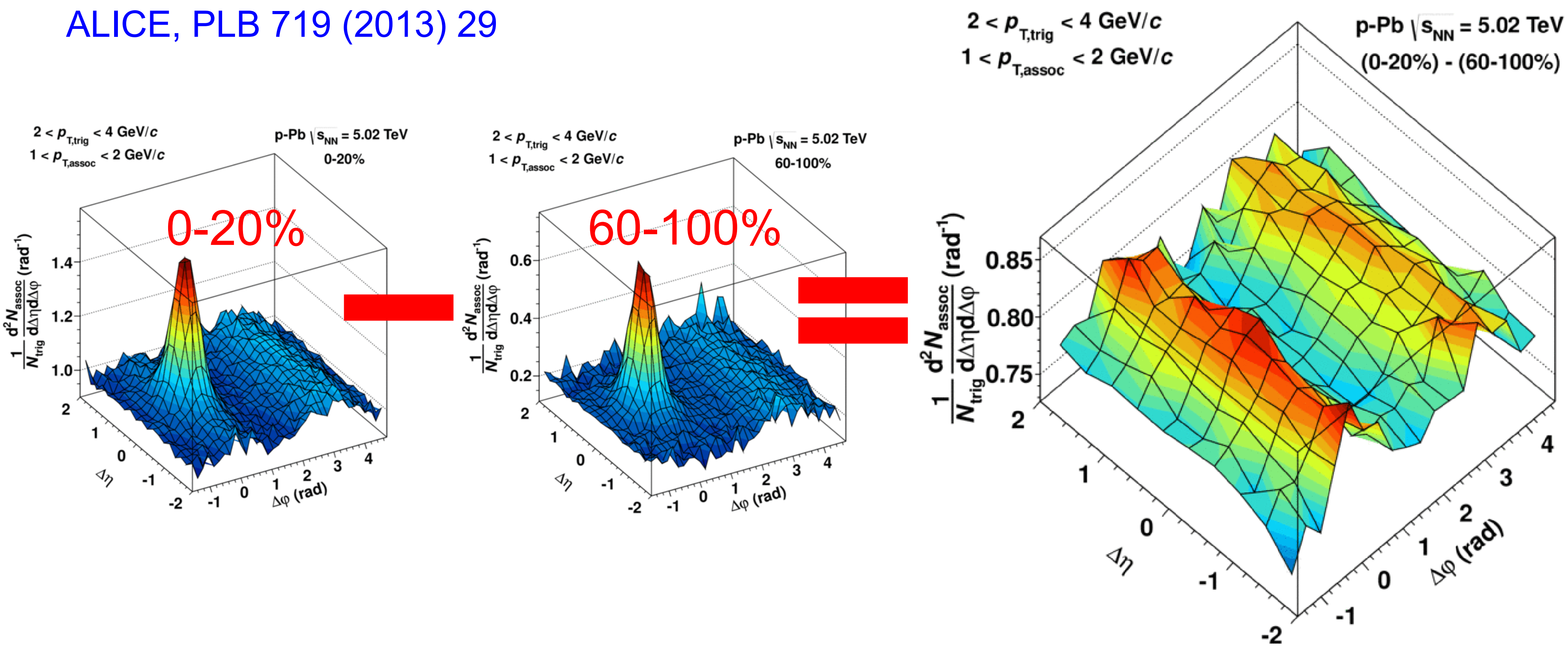

- Extract double ridge structure using a standard technique in AA collisions, namely by subtracting the jet-like correlations
    - Assumed that 60-100% class is free from non-jet like correlations

Extraction of double ridge structure

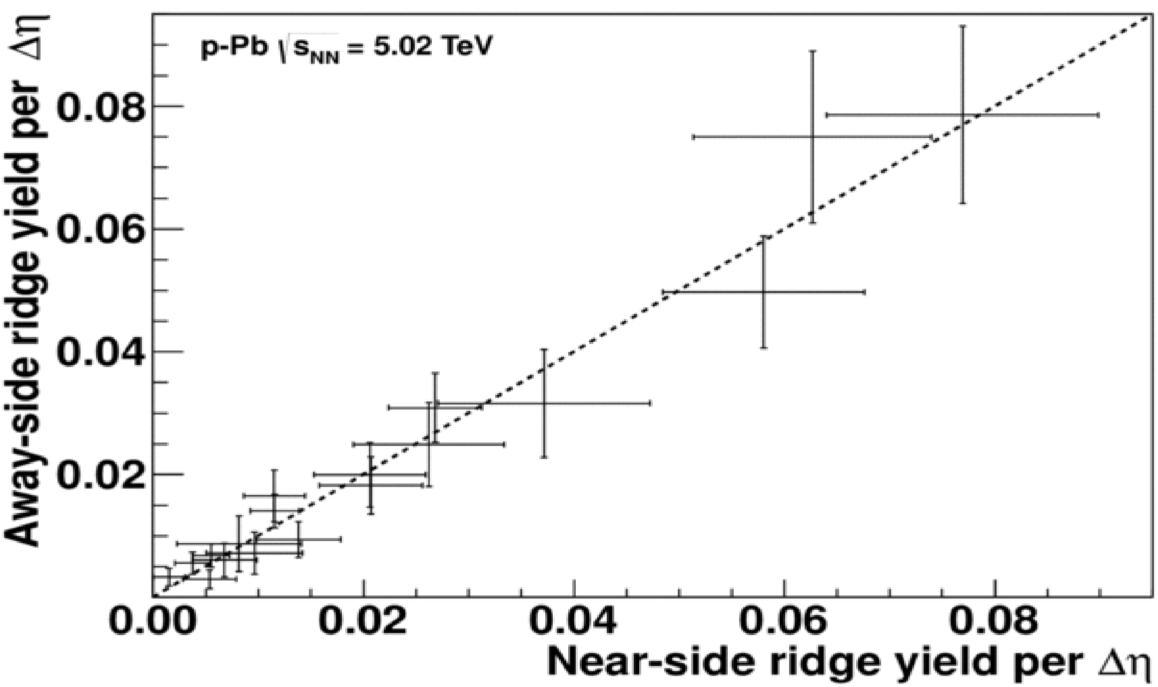

ALICE,
PLB 719 (2013) 29

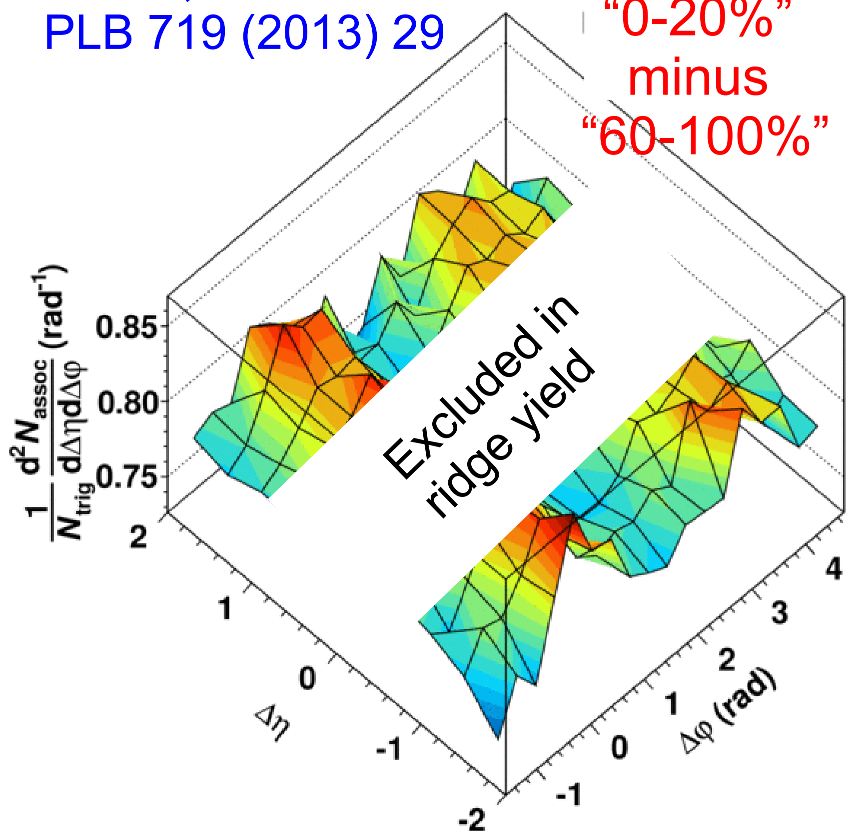

- Extract double ridge structure using a standard technique in AA collisions, namely by subtracting the jet-like correlations
  - Assumed that 60-100% class is free from non-jet like correlations
- The near-side ridge is accompanied by an almost identical ridge structure on the away-side

Dependence on event selection

ALICE, PLB 719 (2013) 29

- A residual jet peak at (0,0) remains even after subtraction of 60-100% from the 0-20% multiplicity class
- Effect at large |Δη| stable using different event class definition

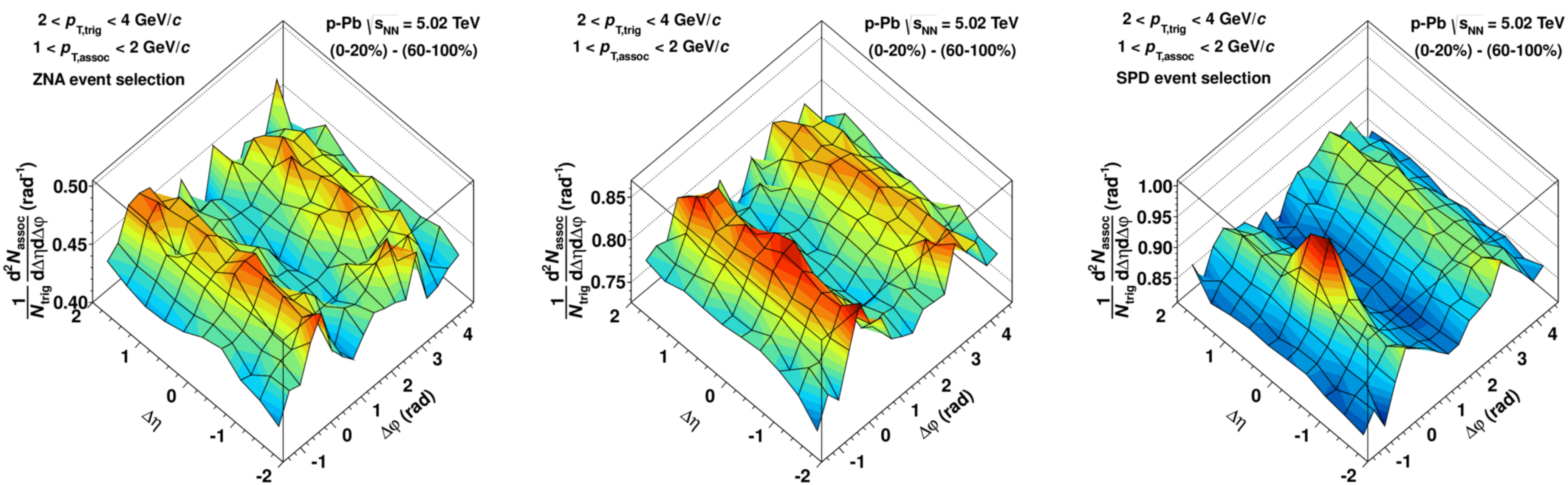

ZNA VZERO SPD

η separation

Ridge v_2 and v_3 and hydrodynamics

ALICE, PLB 719 (2013) 29

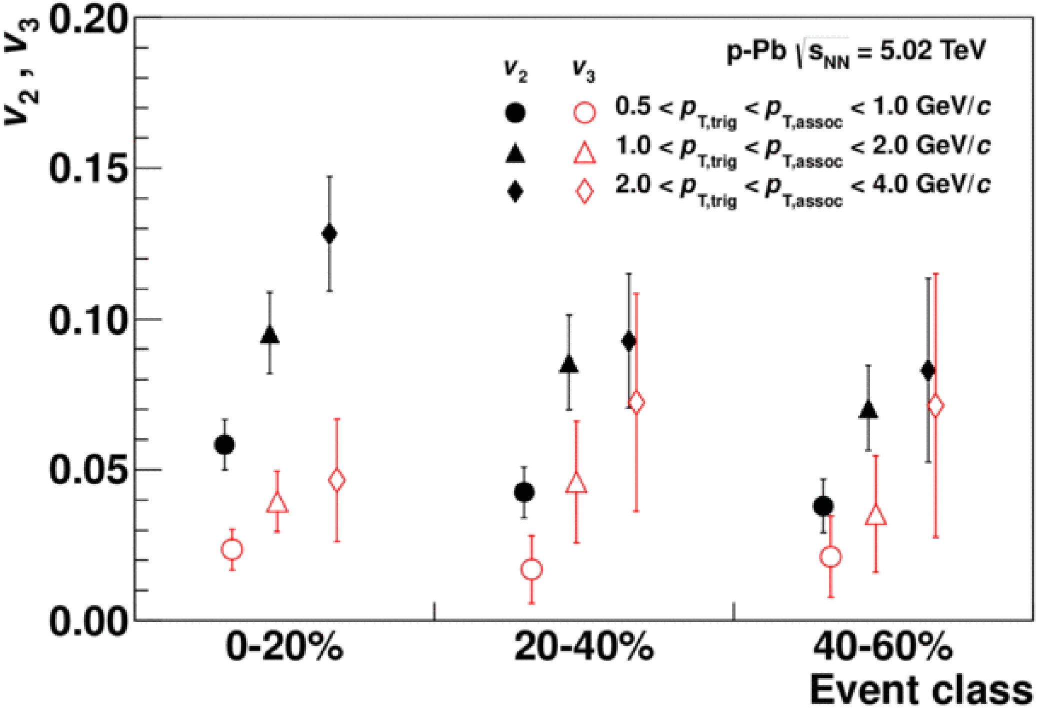

- Sizable values for v_2 and even v_3 reached for high-multiplicity events

Ridge v_2 and v_3 and hydrodynamics

ALICE, PLB 719 (2013) 29

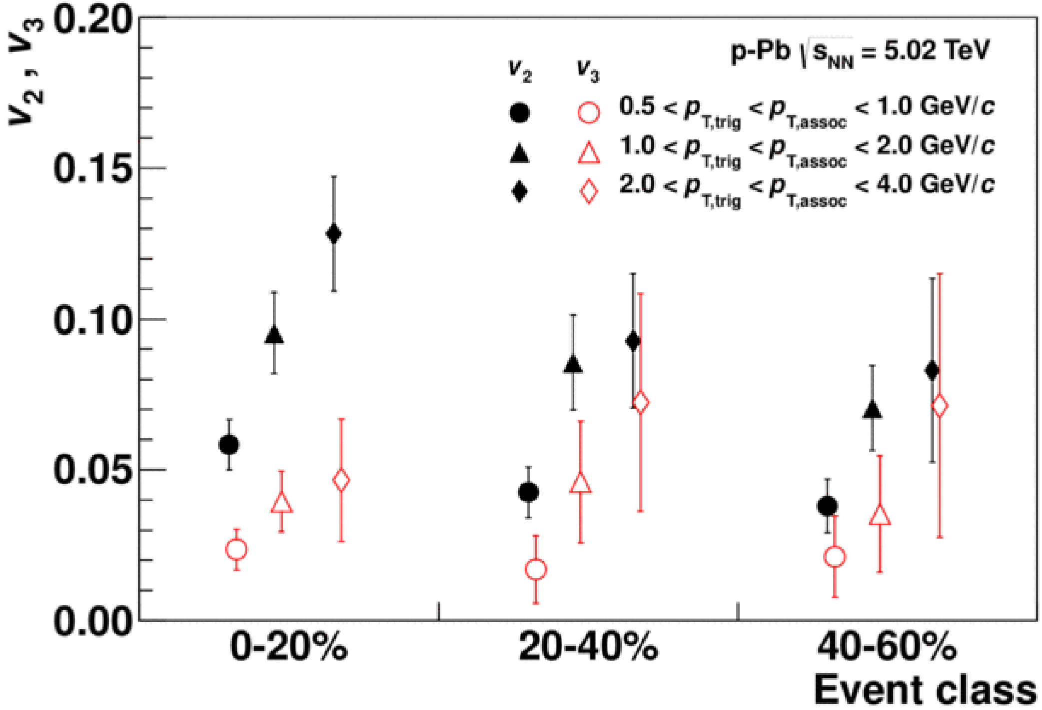

Bozek and Broniowski, PRC 88 (2013) 014903

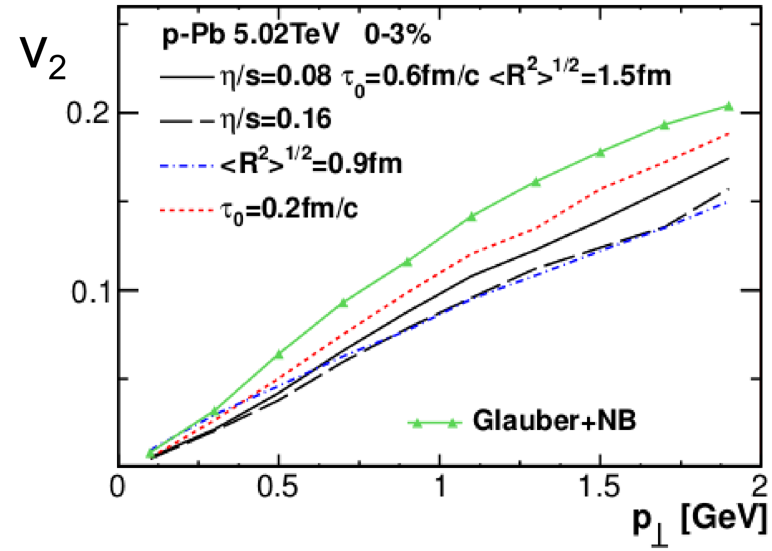

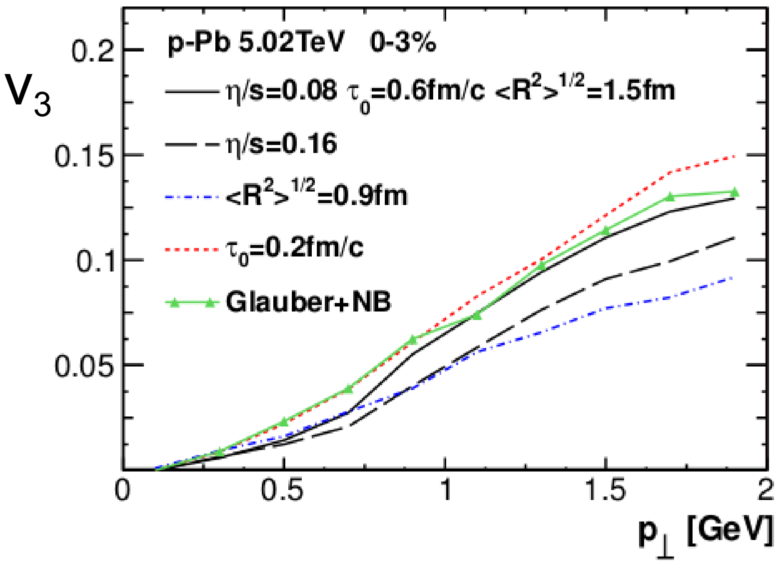

- Sizable values for v_2 and even v_3 reached for high-multiplicity events
- Results qualitatively consistent with viscous hydrodynamic calculations with initial state fluctuations from Glauber
  - Caveat: Calculations in pPb less robust wrt changes of assumptions than in AA

Multi-particle correlations: $v_2\{4\}$

Submitted
to arXiv today

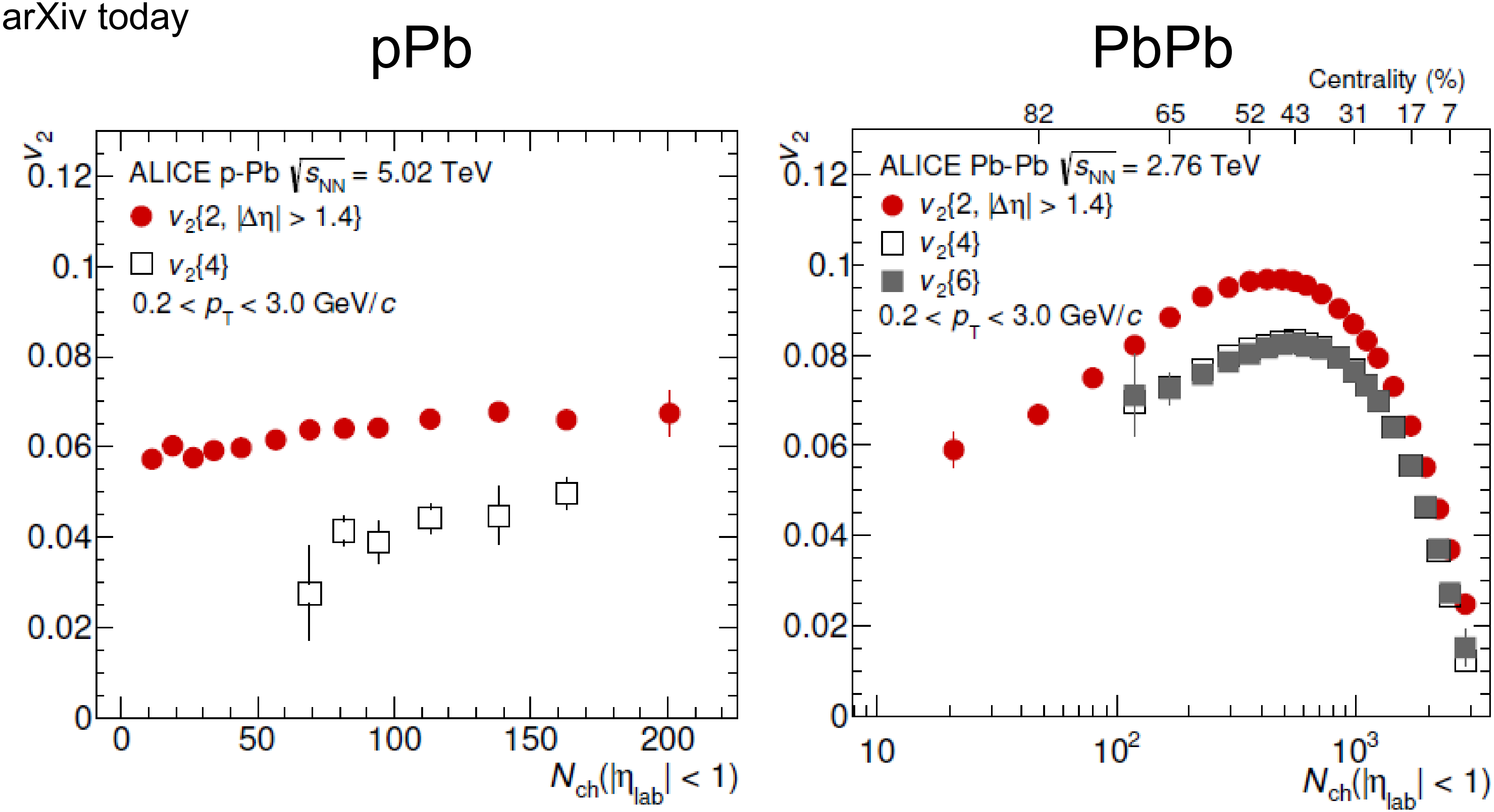

Genuine four particle correlations present in pPb, but magnitude smaller than in PbPb (which is driven also by the event plane)

Multi-particle correlations: $v_2\{6\}$

Submitted to arXiv today

$$v_2\{6\} = \sqrt[6]{\frac{1}{4}c_2\{6\}}$$

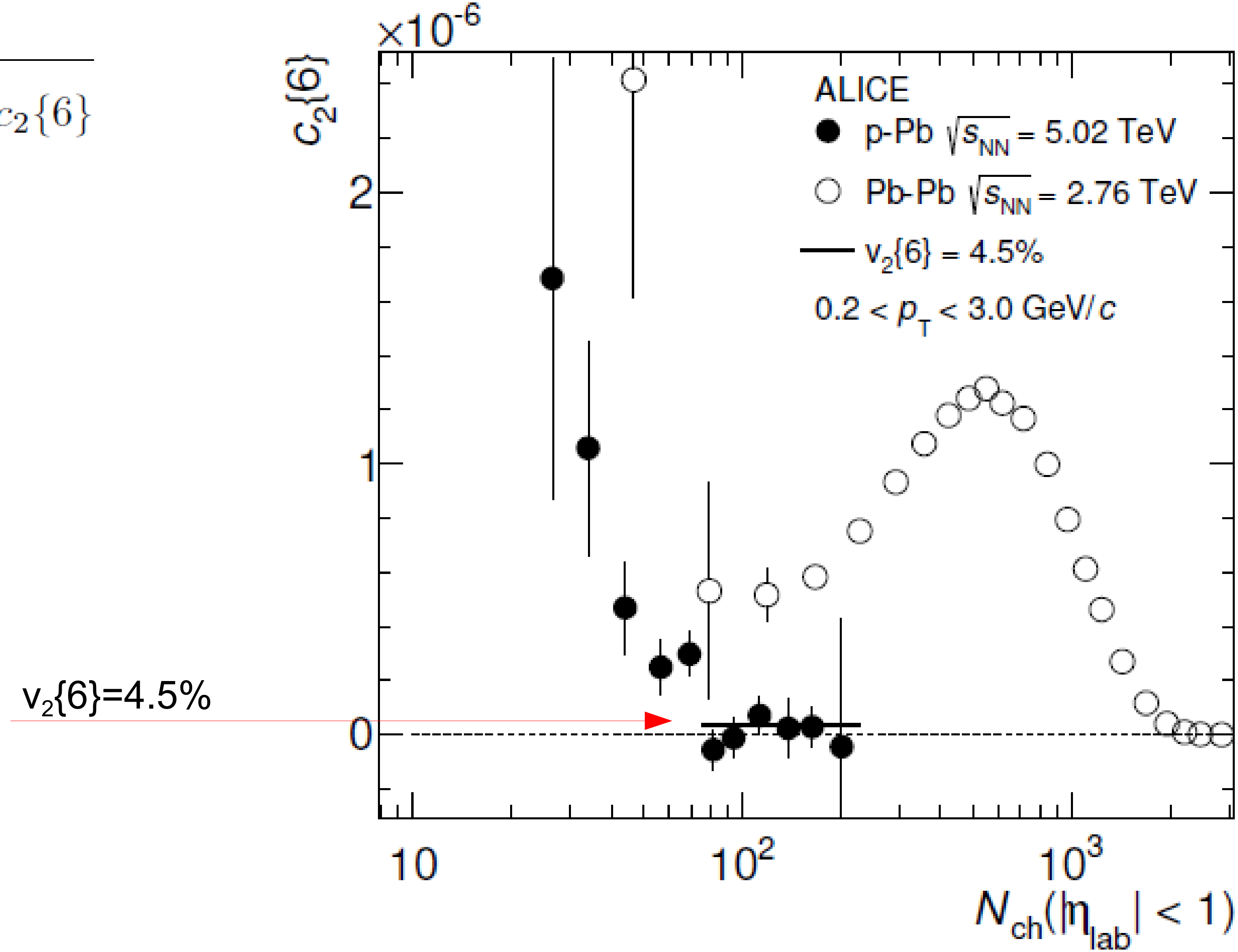

Results consistent with $v_2\{6] \approx v_2\{4\}$ in pPb, but not enough events to determine whether $v_2\{6\}$ is finite or not.

Multi-particle correlations: CMS

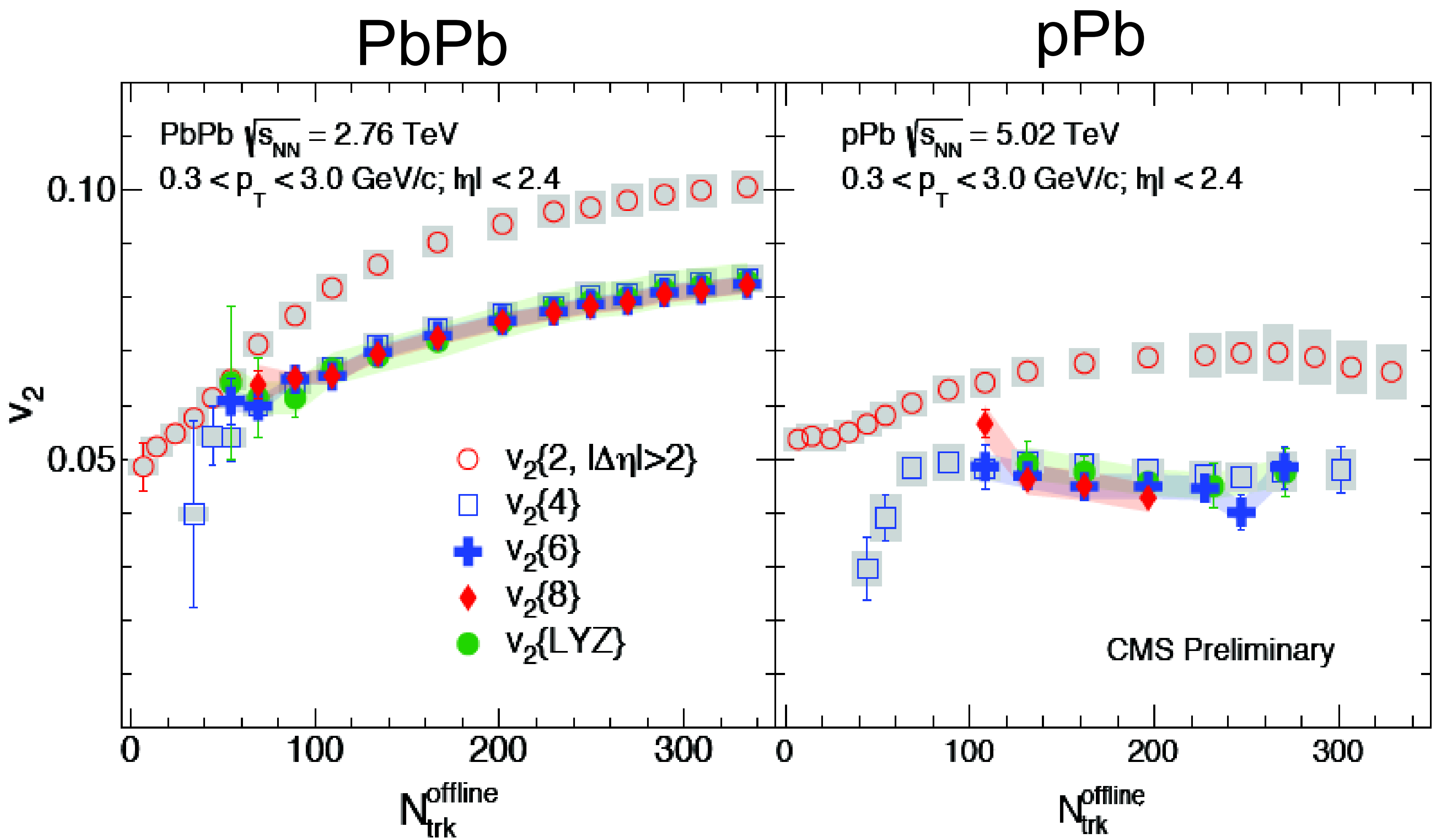

Multi-particle correlation results are the same within 10% in pPb

Submitted
to arXiv today

Multi-particle correlations: $v_3\{2\}$

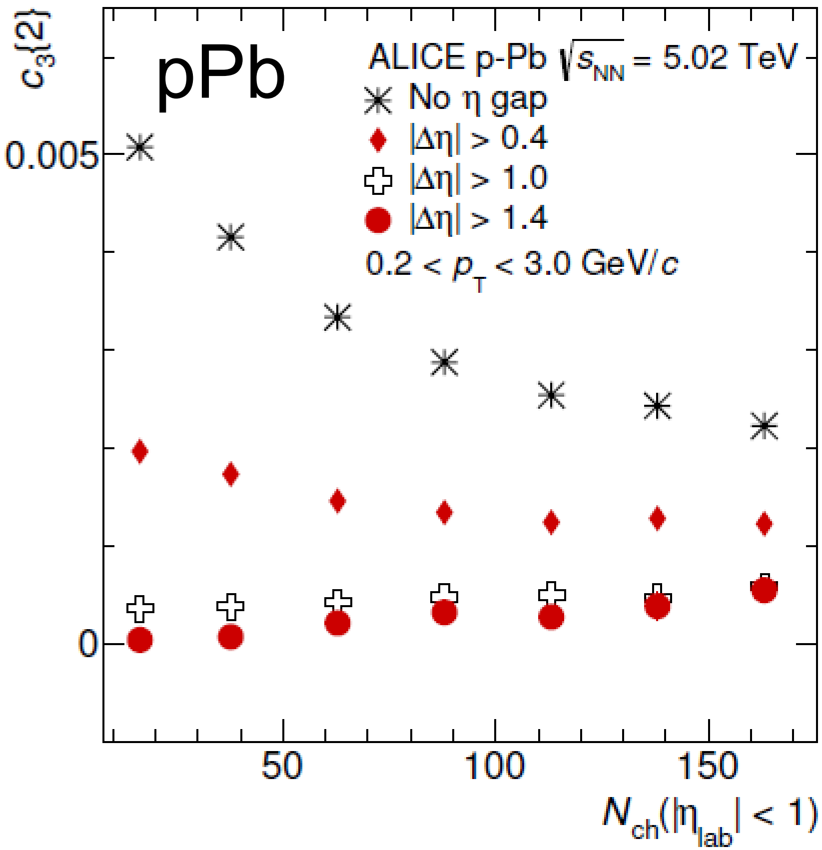

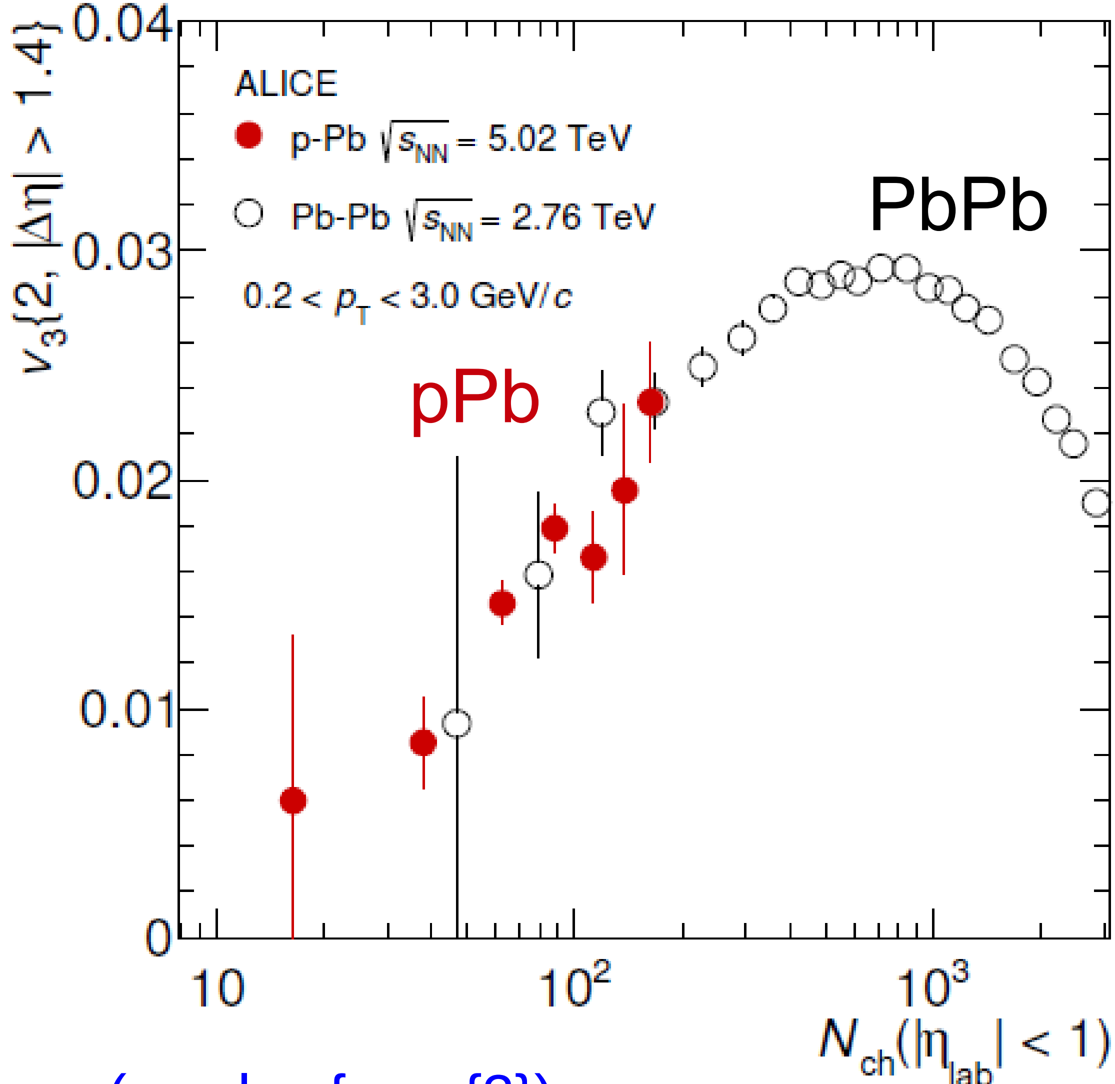

- Large dependence on Δη gap (as also for $v_2\{2\}$)
- Same dependence on Nch as in PbPb
  - Implications for understanding of initial state?

Identified particle v_2

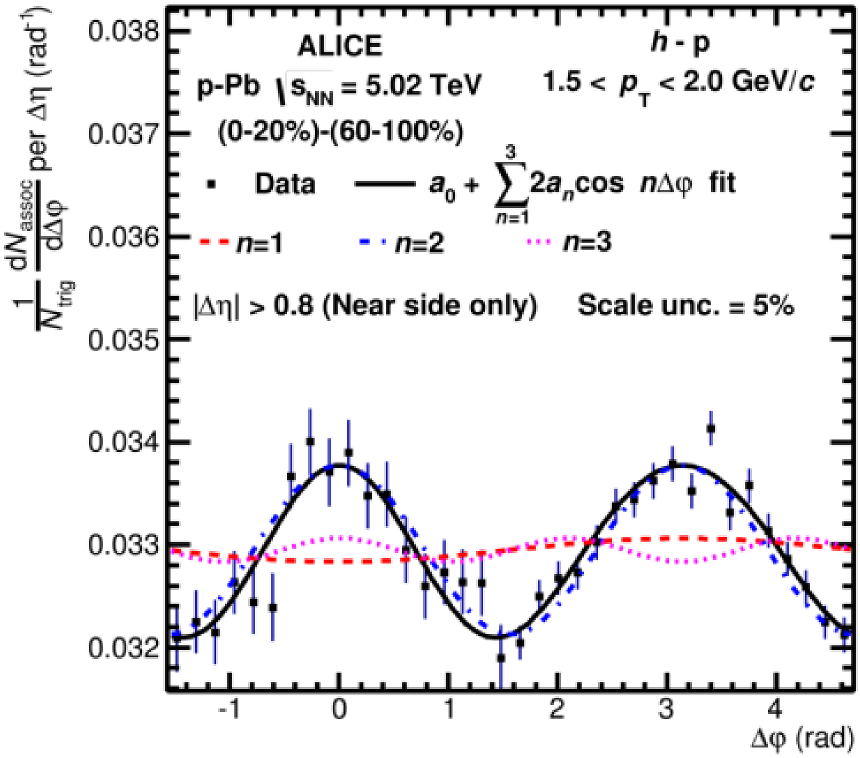

ALICE, PLB 726 (2013) 164

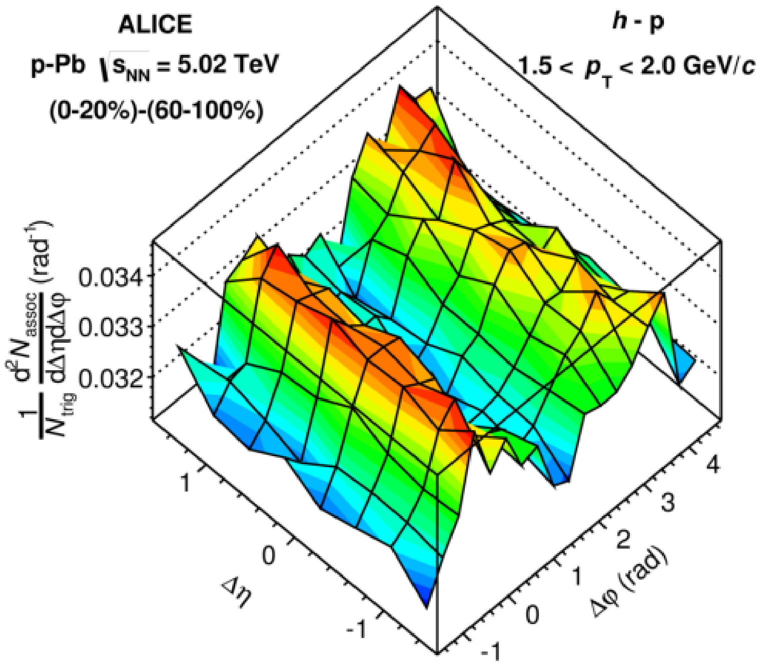

- Per-trigger yield with identified particles (π, K, or p) as associated particles of trigger particles (h)
  - Identified particle v_2: $v_n^i\{2PC\} = V_{n\Delta}^{h-i} / \sqrt{V_{n\Delta}^{h-h}}$
- Same strategy as before:
  Subtract low- (60-100%) from high-multiplicity (0-20%), then Fourier decompose long |Δη| range

Identified particle v_2

pPb

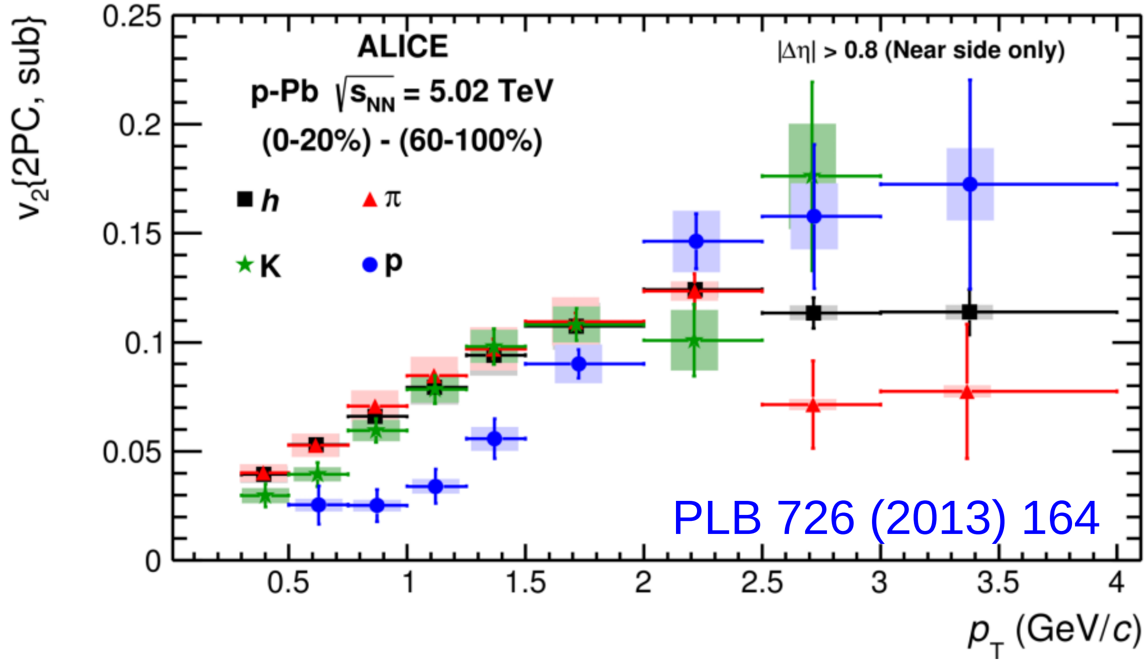

PbPb

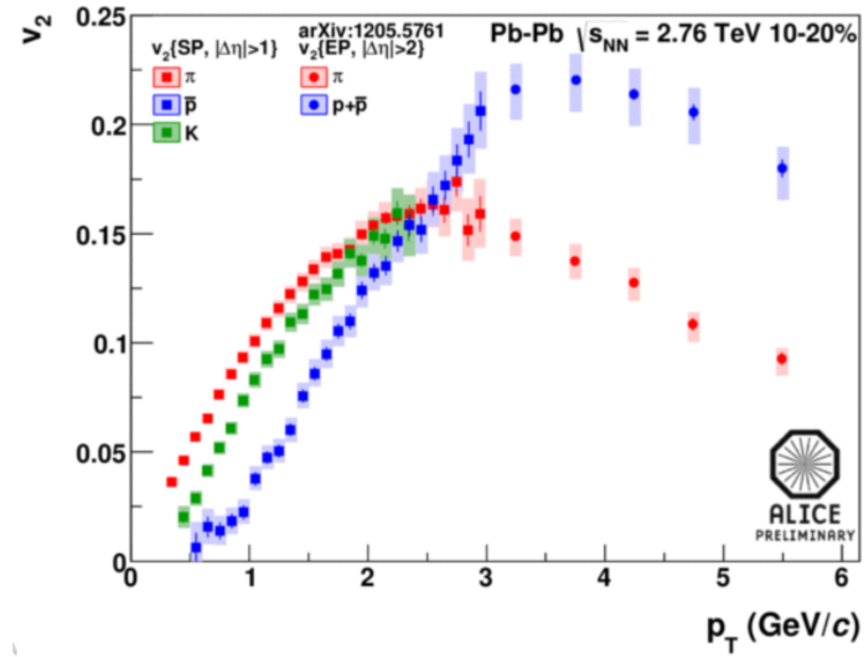

- Characteristic mass splitting observed as known from PbPb
- Crossing of proton and pion at similar p_T (2-3 GeV/c) with protons pushed further out in the pPb case
  - If interpreted in hydro picture, suggestive of strong radial flow

Identified particle v_2 versus hydro models

Werner et al., arXiv:1307.4379

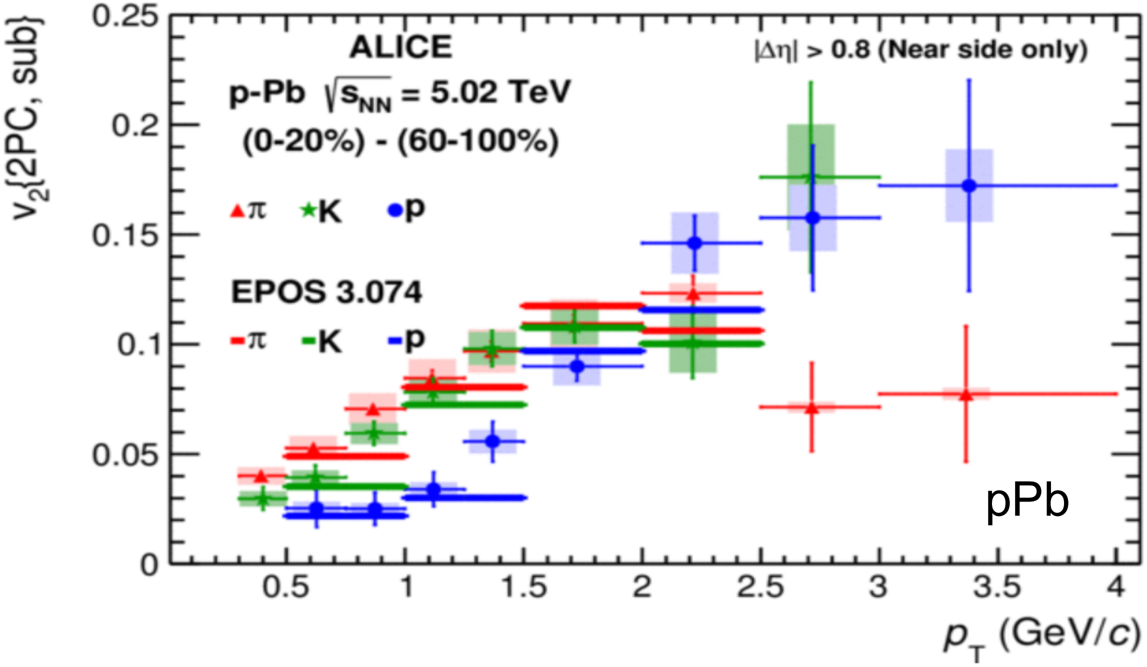

Bozek et al., arXiv:1307.5060

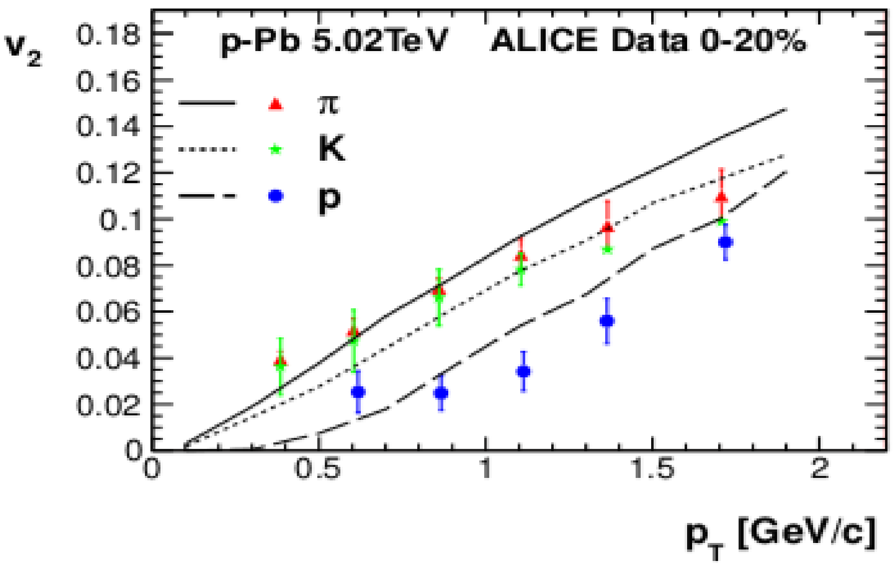

- Characteristic mass splitting observed as known from PbPb
- Crossing of proton and pion at similar p_T (2-3 GeV/c) with protons pushed further out in the pPb case
    - If interpreted in hydro picture, suggestive of strong radial flow
- Models that include a hydro phase can describe these features

Identified particle v_3 (CMS)

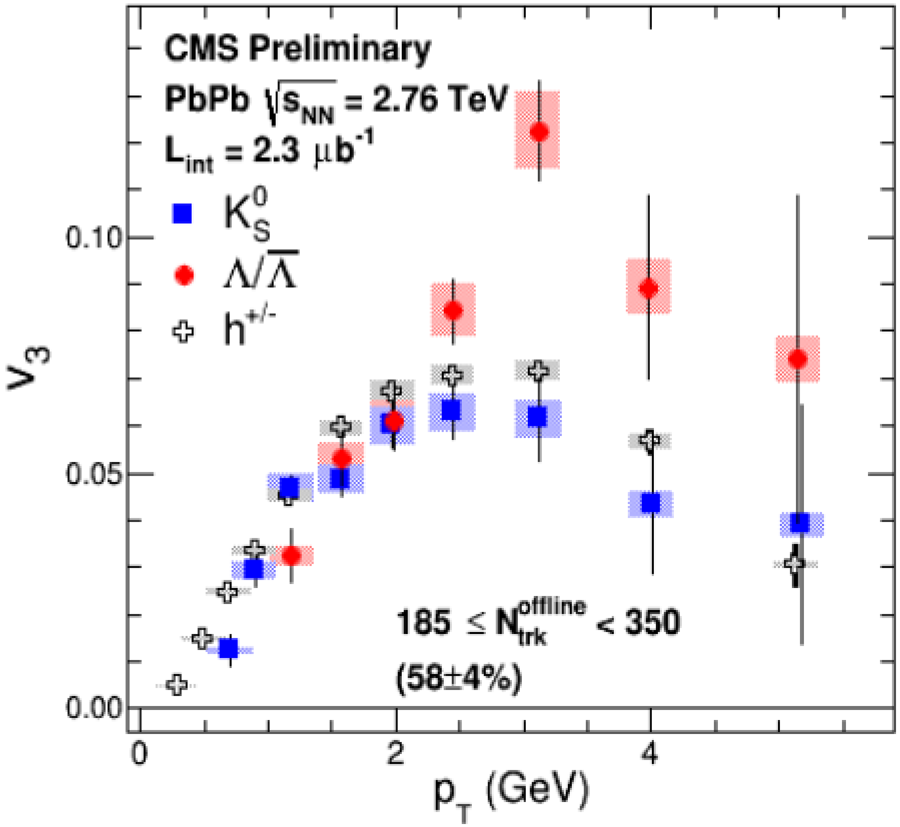

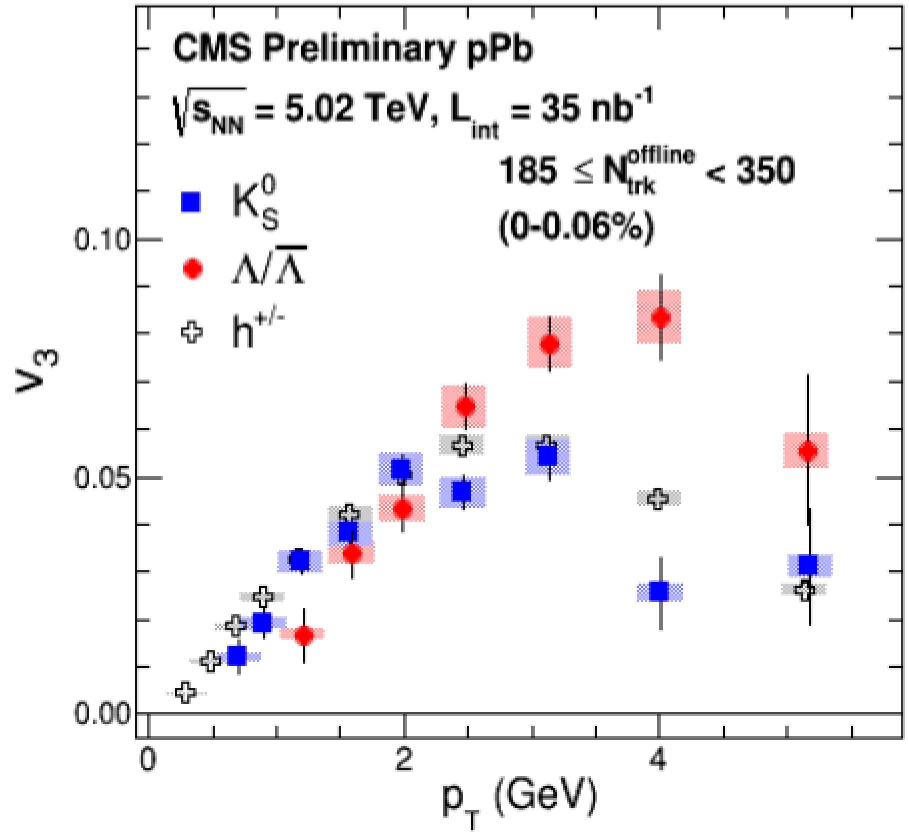

Crossing at around 2 GeV/c,
same physics origin for v_3 and v_2 in pPb as well.

Identified particle p_T spectra

$0<y_{cms}<0.5$, V0A selected

ALICE, arXiv:1307.6796

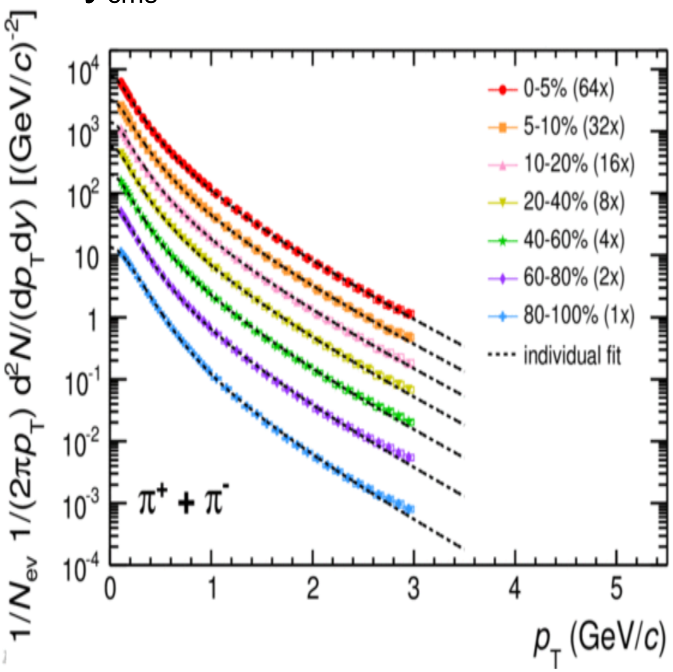

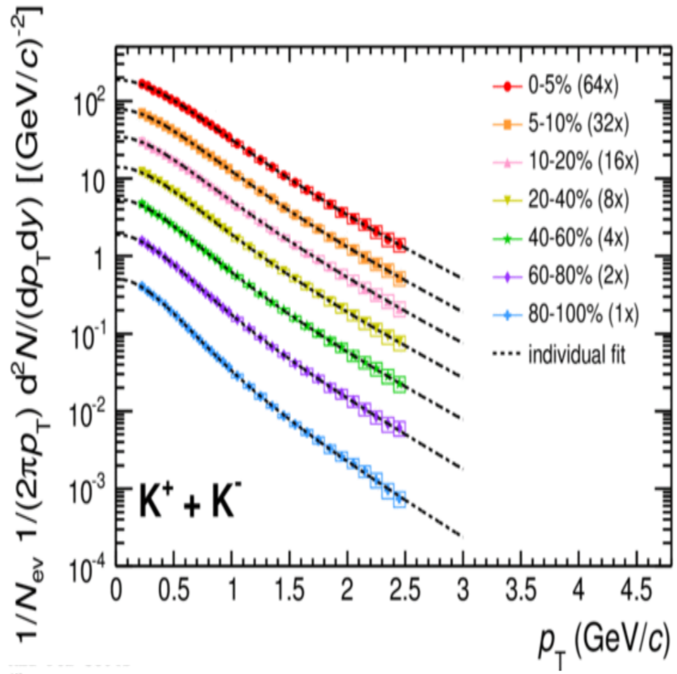

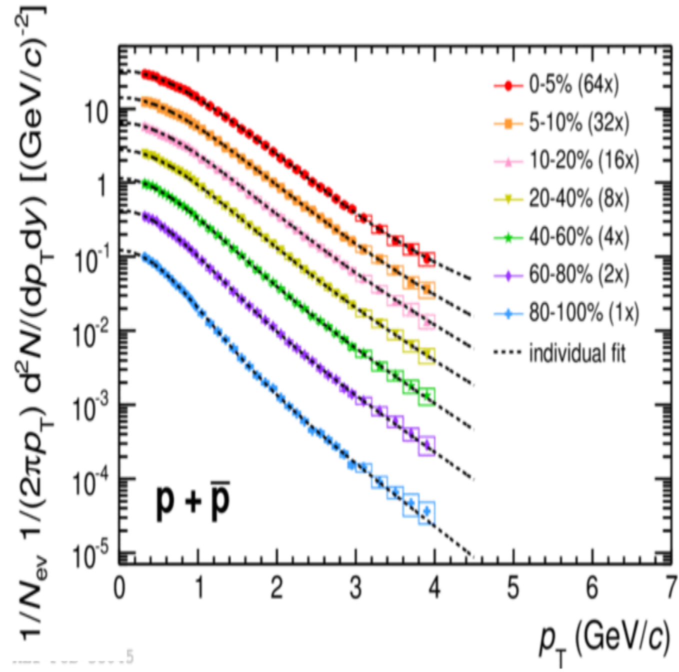

$\pi^{\pm}$	0.2 – 3.0 GeV/*c*
$K^{\pm}$	0.25 – 2.5 GeV/*c*
$p(\bar{p})$	0.45 – 4.0 GeV/*c*
K^0_S	0 – 6.0 GeV/*c*
$\Lambda(\bar{\Lambda})$	0.6 – 6.0 GeV/*c*

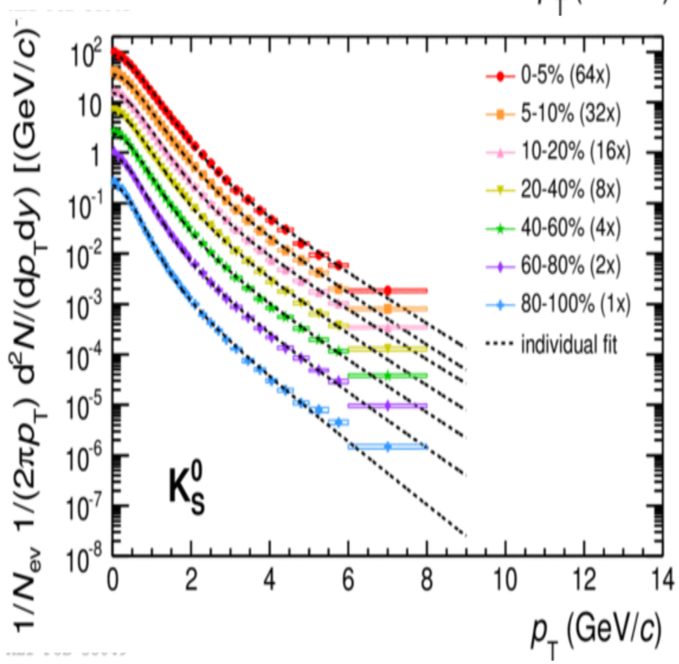

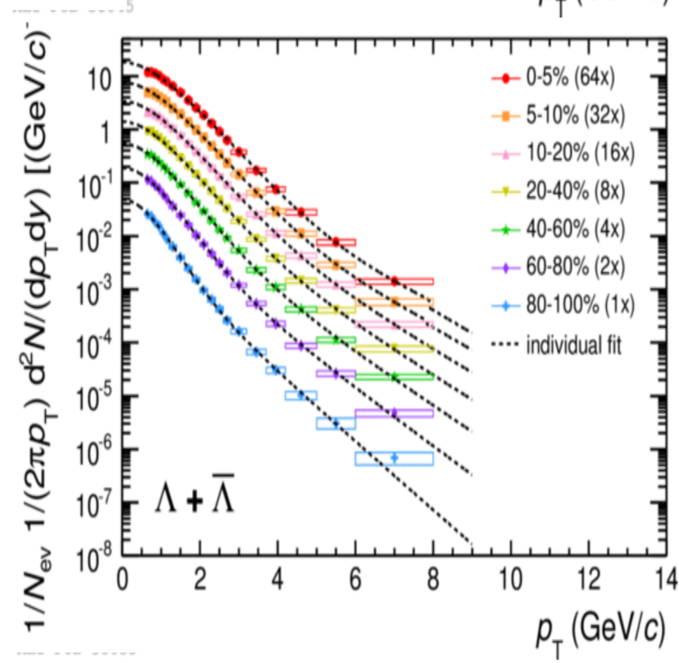

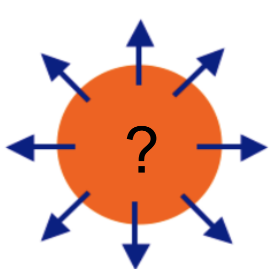

Identified particle p_T spectra

$0<y_{cms}<0.5$, V0A selected

ALICE, arXiv:1307.6796

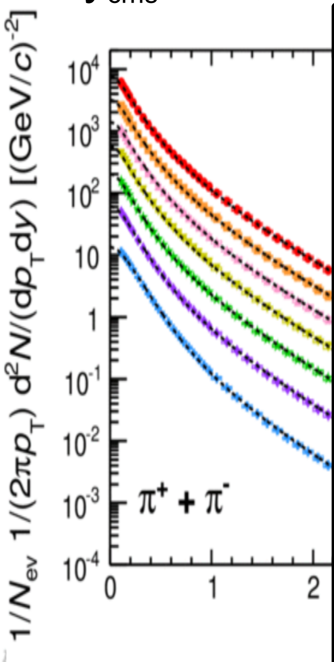

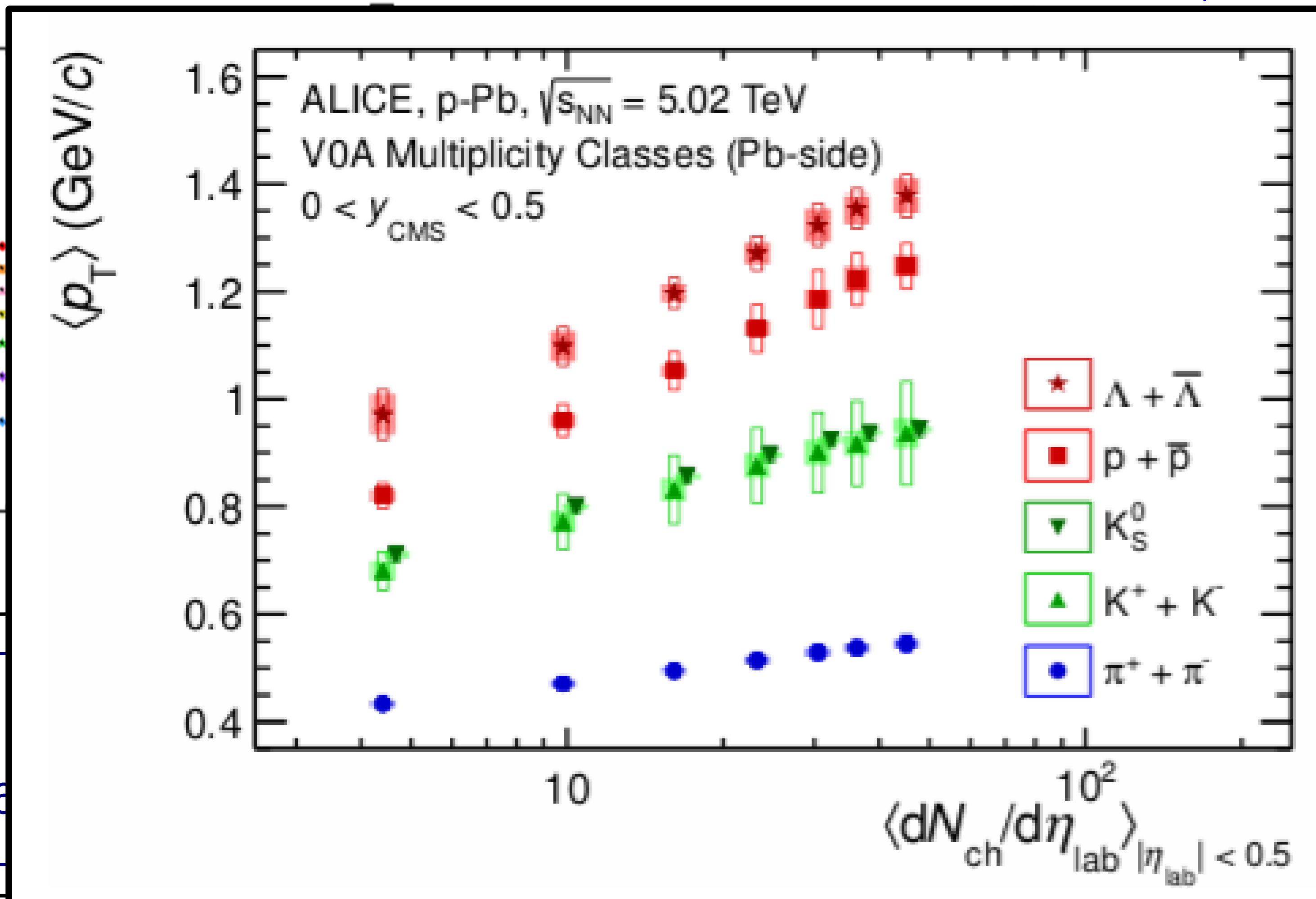

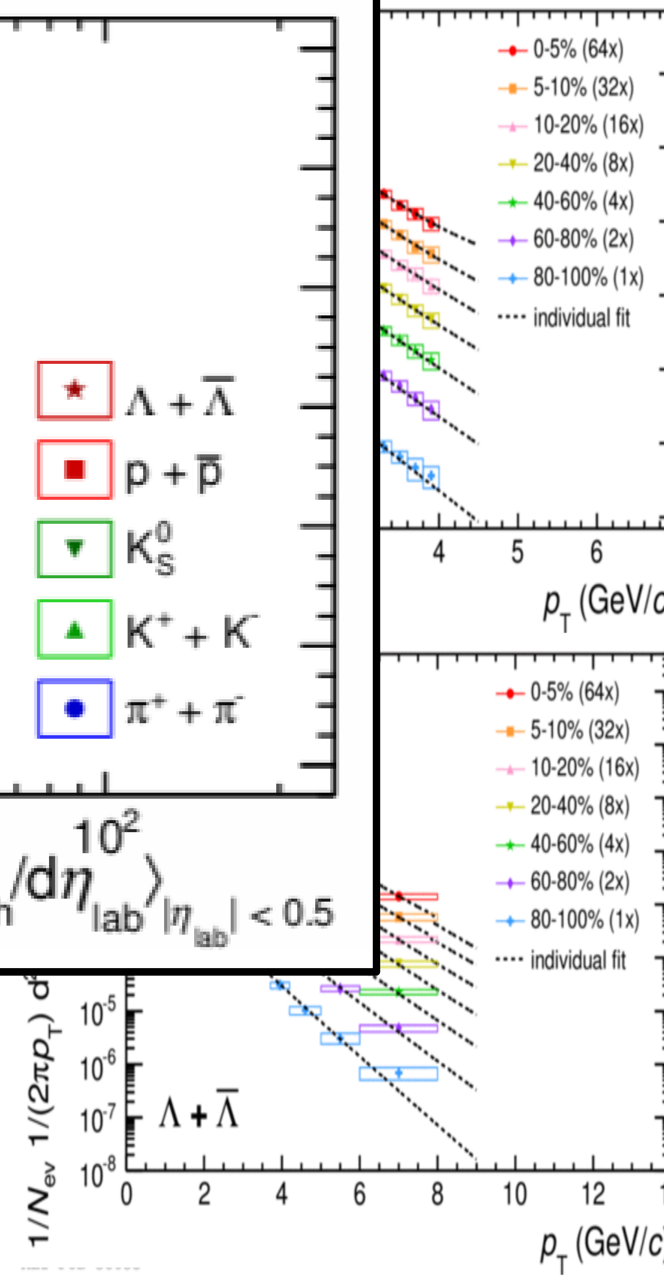

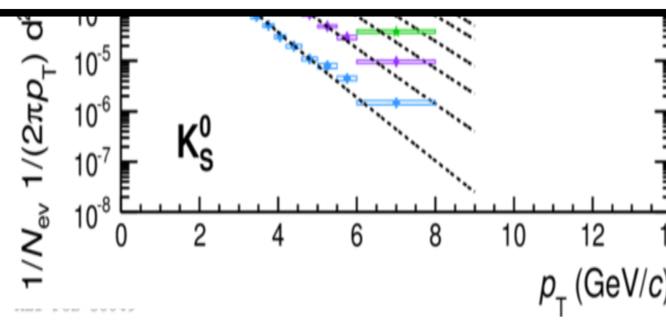

$\pi^{\pm}$	0.2 –
$K^{\pm}$	0.25
$p(\bar{p})$	0.45
K^0_S	0 – 6
$\Lambda(\bar{\Lambda})$	0.6 –

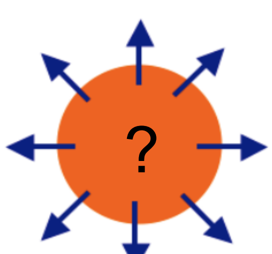

Identified particle spectra

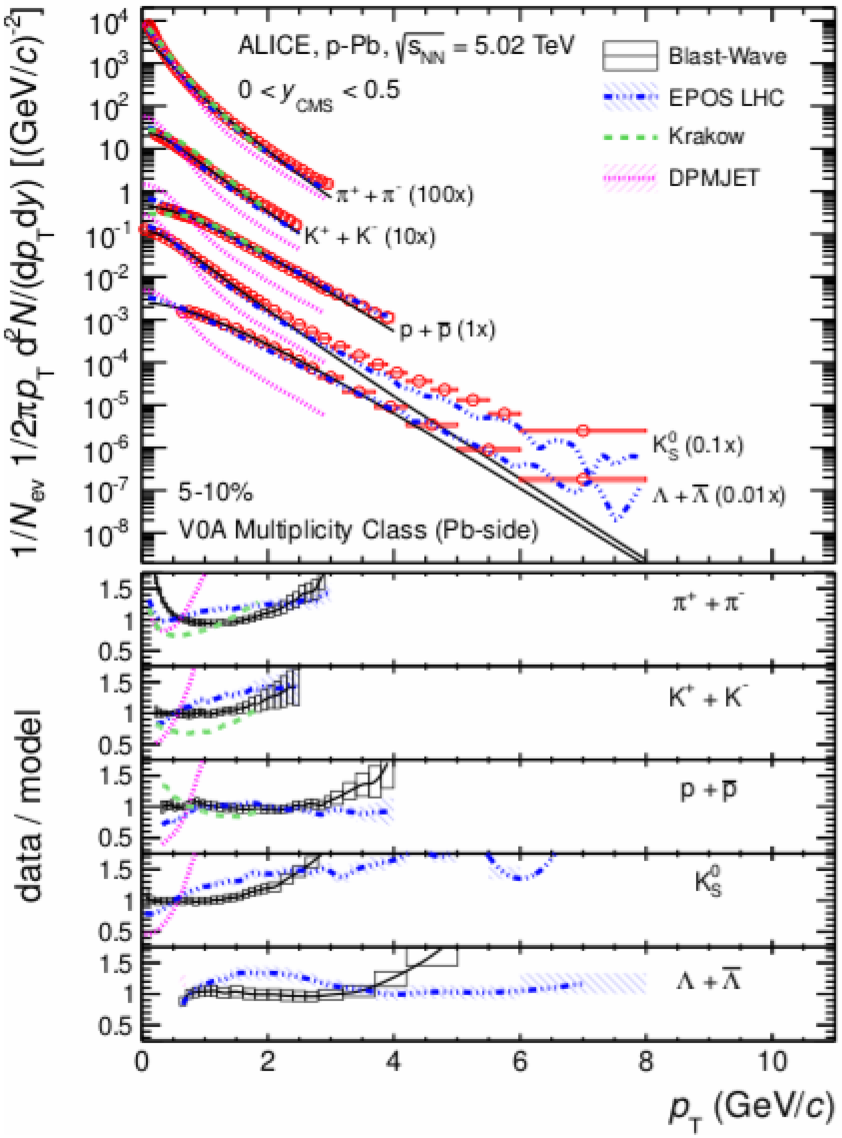

ALICE, PLB 278 (2014) 25

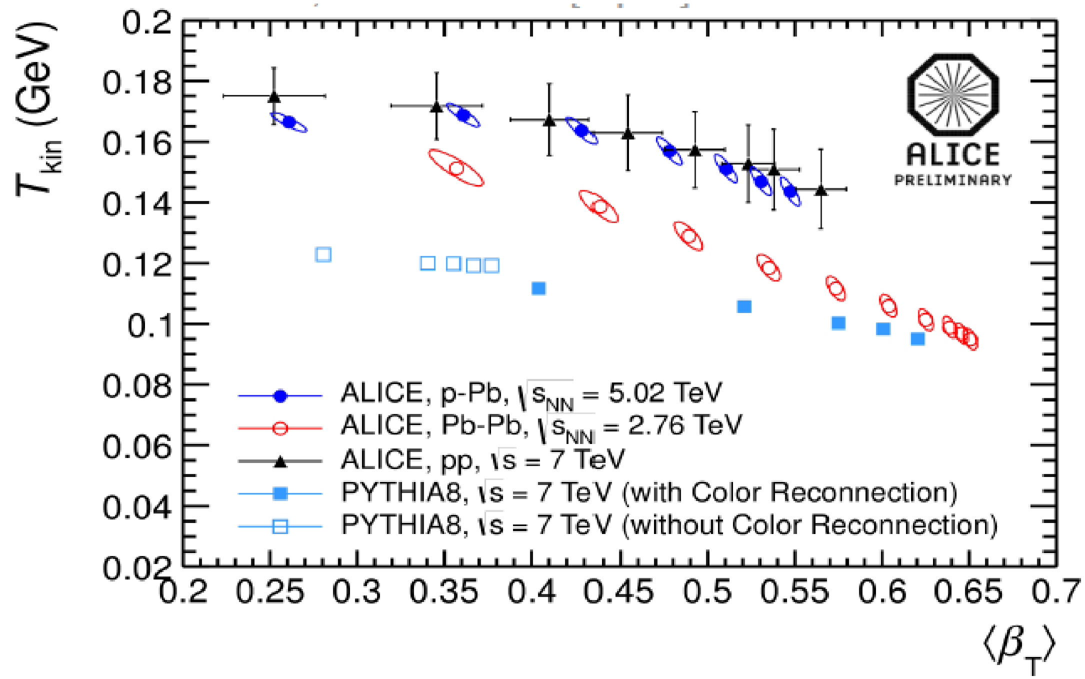

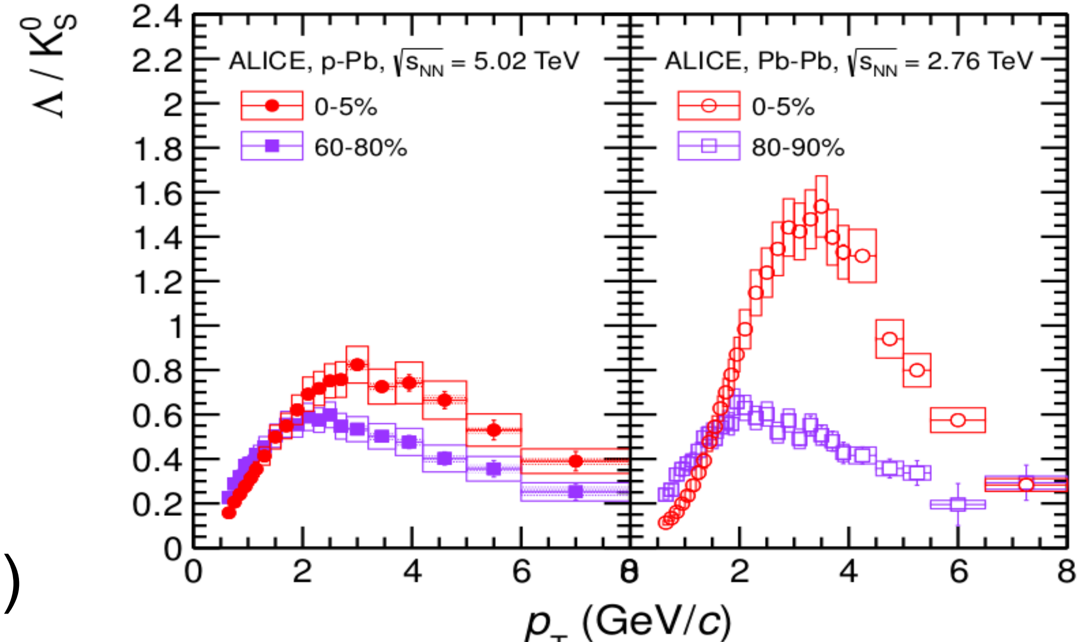

Spectra consistent with radial flow picture (also in pp)

The Cronin peak region

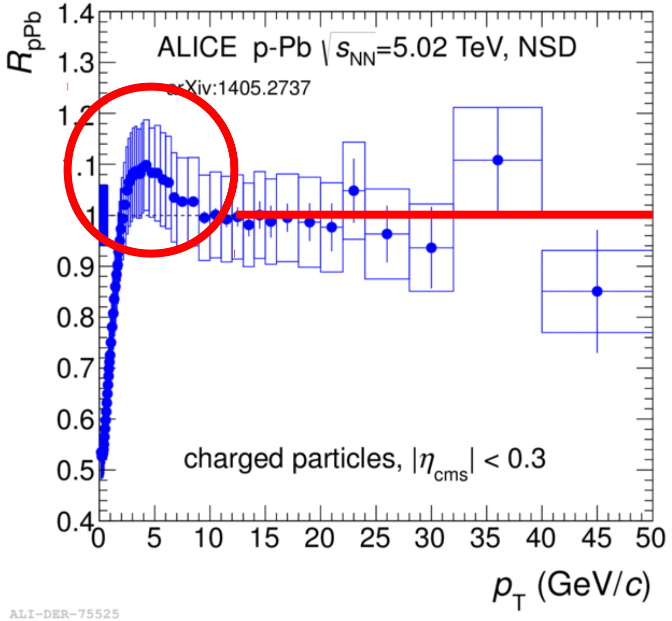

- "Cronin peak" from 2-6 GeV/c
  - Dependence on particle type
  - Enhancement dominated by protons
- Nowadays would attribute effect to be due to radial flow?
  - However, weak for the Φ

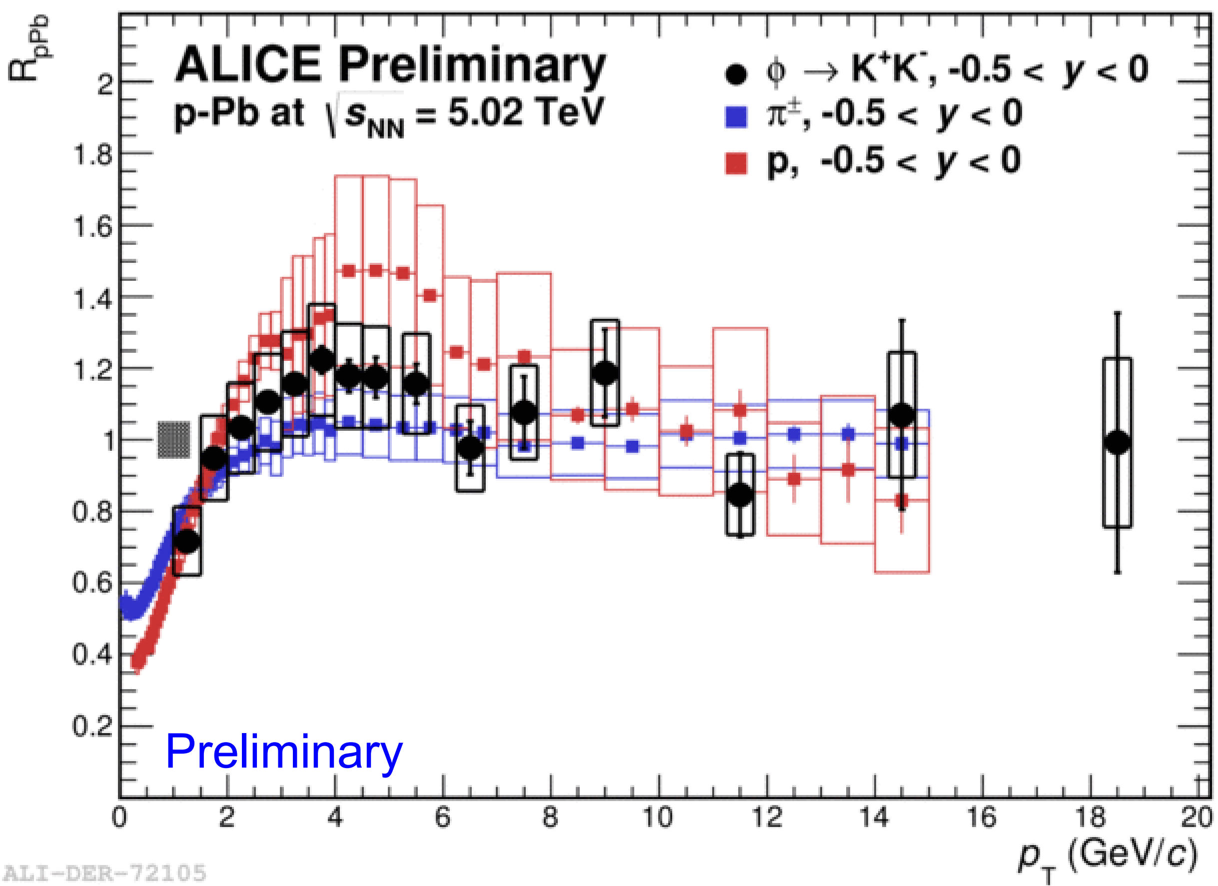

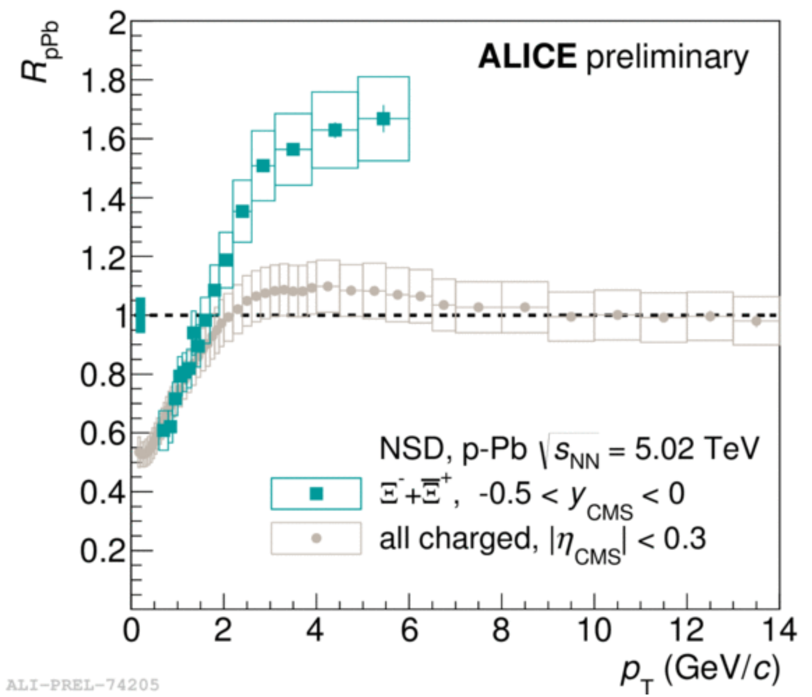

Intensity interferometry (HBT)

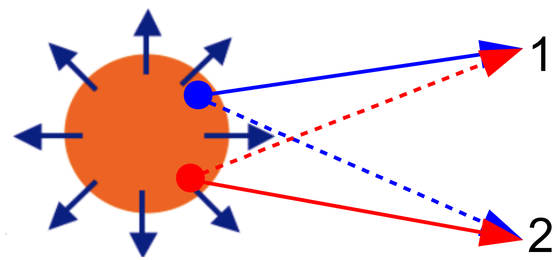

$$C_f(\mathbf{q}) = \int S(r,\mathbf{q})|\Psi(\mathbf{q},r)|^2 d^4 r$$

$q = p_1 - p_2 \quad r = r_1 - r_2$

- Two particles whose origin or propagation are correlated exhibit wave properties in the relative measures (e.g. momentum difference)
- Correlation sources range from actual interactions (Coulomb, Strong) to quantum statistics (QS) correlations
- Measurements of two same-particle correlations at low momentum allows to access the space-time characteristics of the source

- At freeze-out the characteristic distance of particles is O(fm)
- Need $\Delta p < 0.5$ GeV/c so that $\Delta x \Delta p \sim 1$ to be sensitive to BE correlations
- Expect a moving source to look smaller than at rest
  - Study source as function of pair transverse momentum
  - $k_T = |p_{T,1} + p_{T,2}|/2$

Intensity interferometry: Rinv

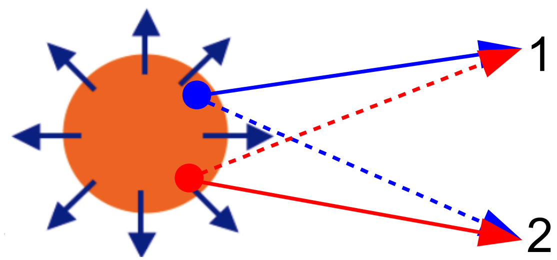

$$C_f(\mathbf{q}) = \int S(r,\mathbf{q})|\Psi(\mathbf{q},r)|^2 d^4r$$

$$q = p_1 - p_2$$

- Experimentally measure (in bins of k_T)

$$C_2(q) = \frac{N_2(p_1, p_2)}{N_1(p_1)/N_1(p_2)}$$

- Parameterize the source (and address background)

Non-femtoscopic background

$$C_2(q) = \mathcal{N}[(1 - f_c^2) + f_c^2 K_2(q) C_2^{QS}(q)]\, B(q)$$

Correlated fraction + interaction term

$$C_2^{\mathrm{QS}}(q) \;=\; 1 + \lambda\, E_{\mathrm{w}}^2(R_{\mathrm{inv}}\, q)\, e^{-R_{\mathrm{inv}}^2\, q^2}$$

in PRF ($p_1+p_2=0$)

Intensity interferometry: 3d radii

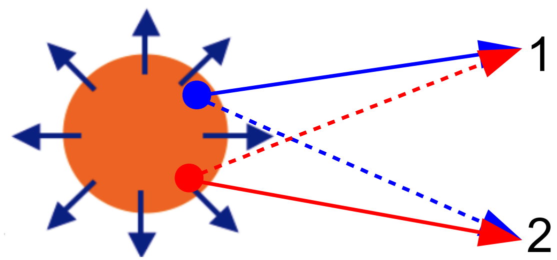

$$C_f(\mathbf{q}) = \int S(r,\mathbf{q})|\Psi(\mathbf{q},r)|^2 d^4r$$

$q = p_1 - p_2$

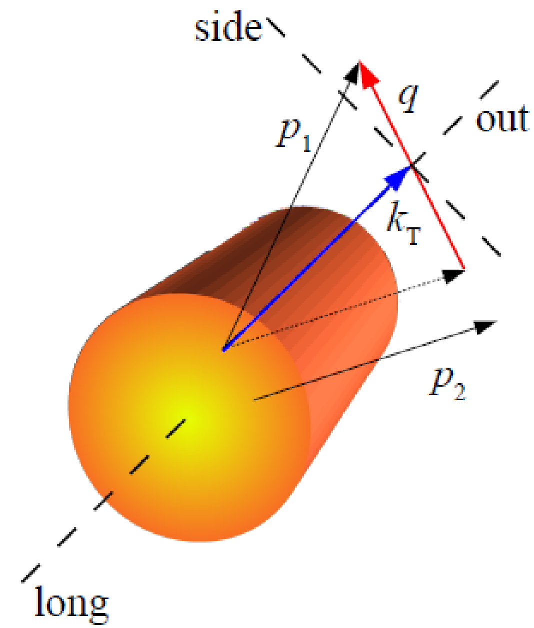

- Experimentally measure (in bins of k_T)

$$C_2(q) = \frac{N_2(p_{1,}p_2)}{N_1(p_1)/N_1(p_2)}$$

- Parameterize the source
(and address background)

$$C_2(q) = \mathcal{N}[(1 - f_c^2) + f_c^2 K_2(q) C_2^{QS}(q)]\, B(q)$$

Correlated fraction +
interaction term

$$C_2^{\mathrm{QS}}(q) \quad = \quad 1 + \lambda \exp(-R_{out}^2 q_{out}^2 - R_{side}^2 q_{side}^2 - R_{long}^2 q_{long}^2)$$

in LCMS ($p_{L,1}+p_{L,2}=0$)

k_T dependence of radii in PbPb

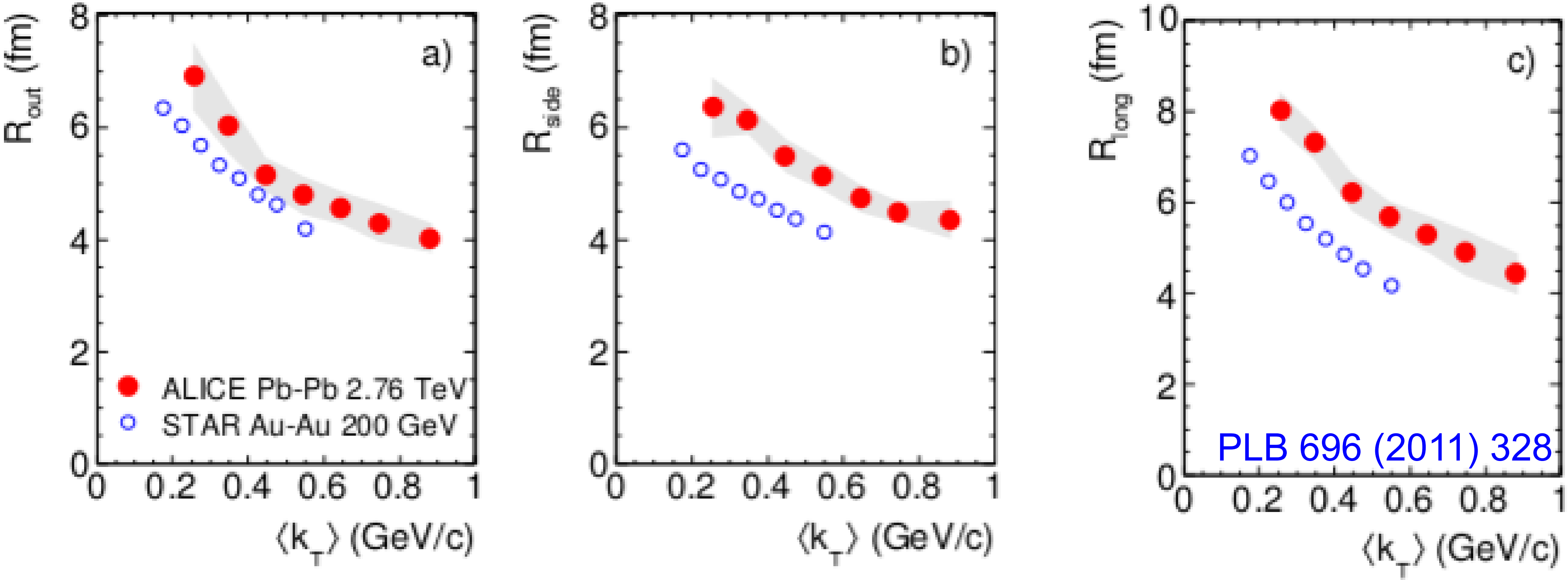

The expected trends with k_T are clearly observed in central PbPb

k_T dependence of radii in pPb

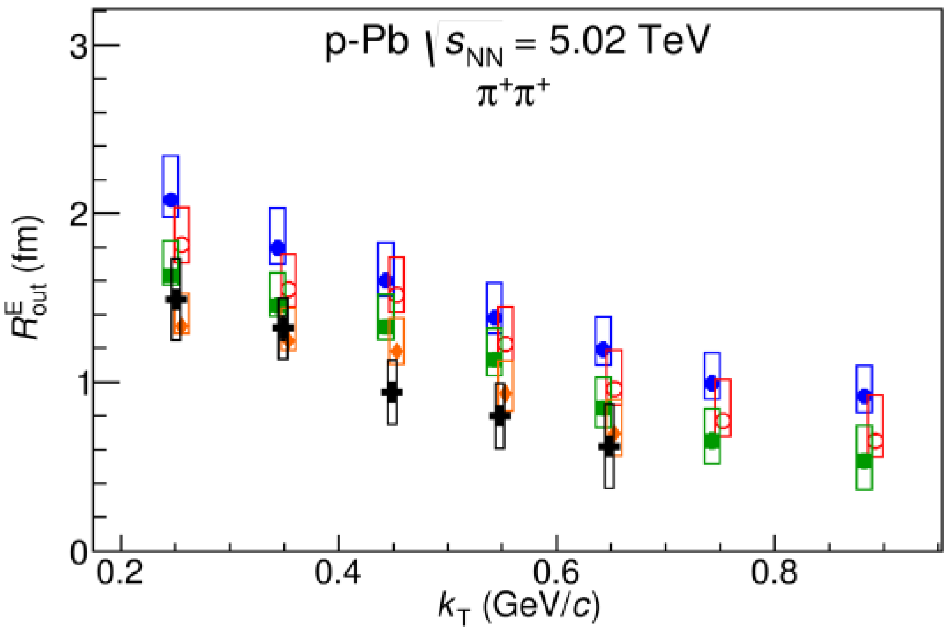

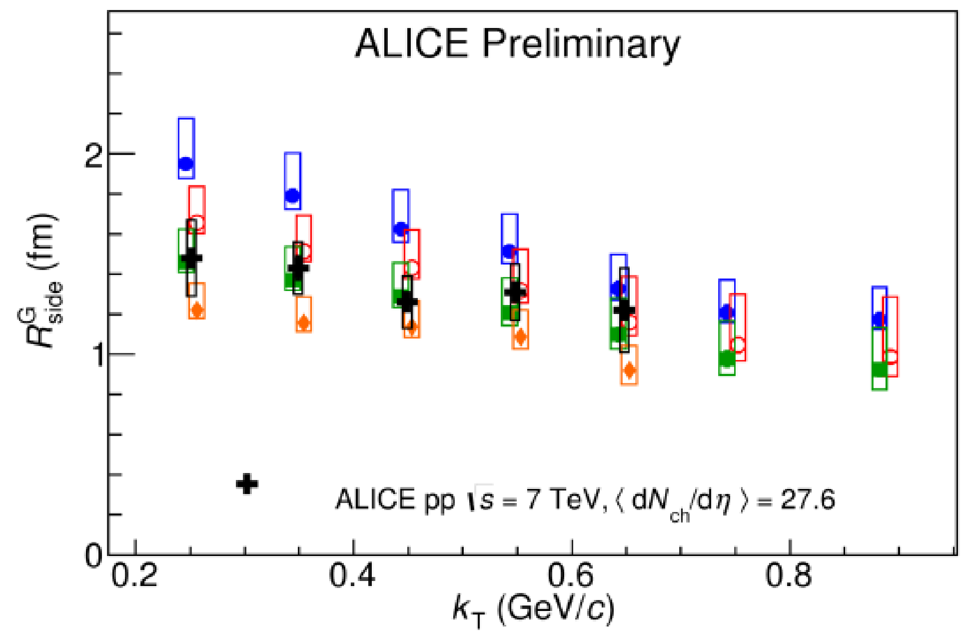

- Similar trends seen for pPb
- Also for high multiplicity pp
  - pp similar to pPb,
    but devil in details

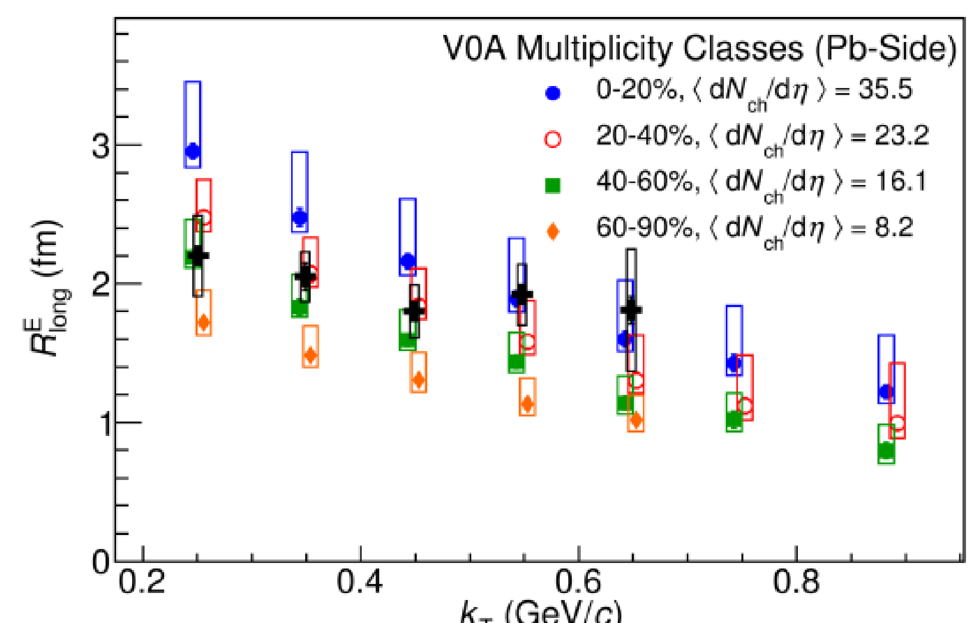

System comparison: R_{inv} vs N_{ch}

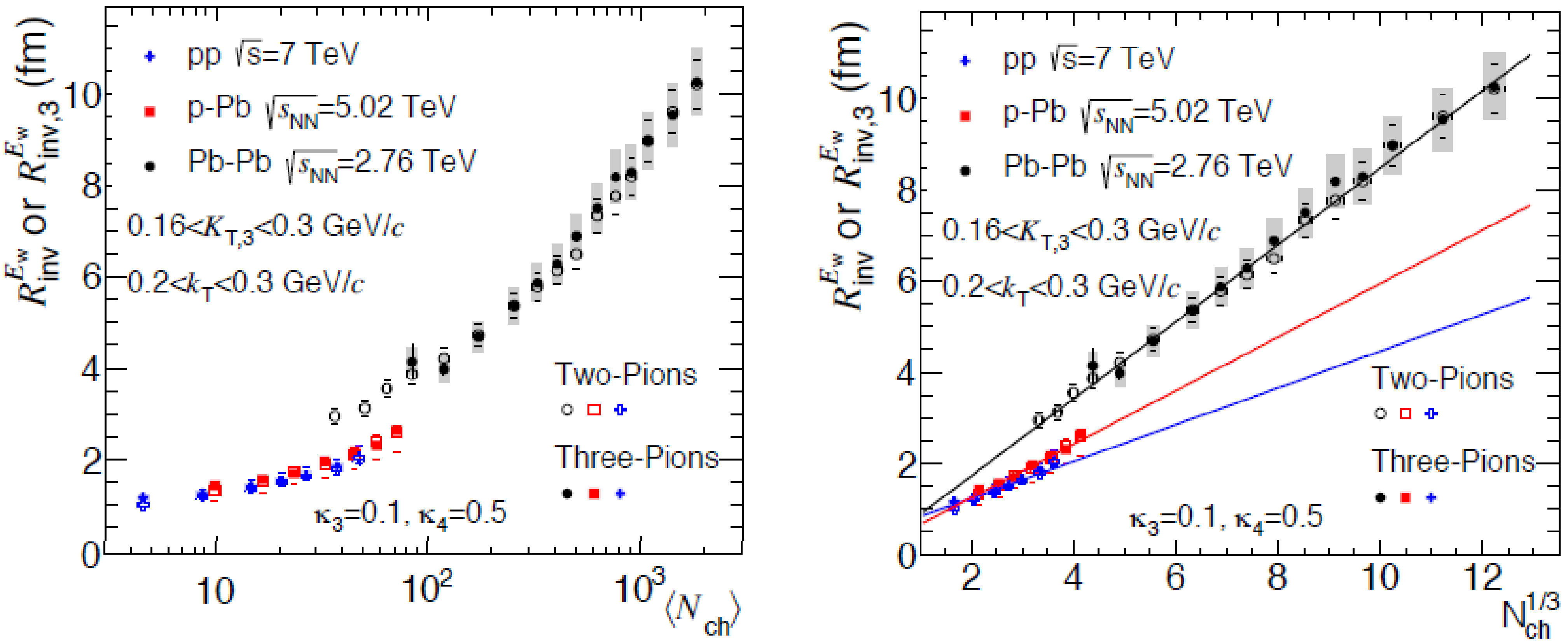

- Exhibit different trend (with linear fit over measured region)
- Radii in pp and pPb at similar measured Nch are with 5-15% while larger difference (up to 30-50%) between pPb and PbPb
- Not much room for a hydro-dynamical expansion in pPb beyond what might already be there in pp

Comparison with IP-Glasma

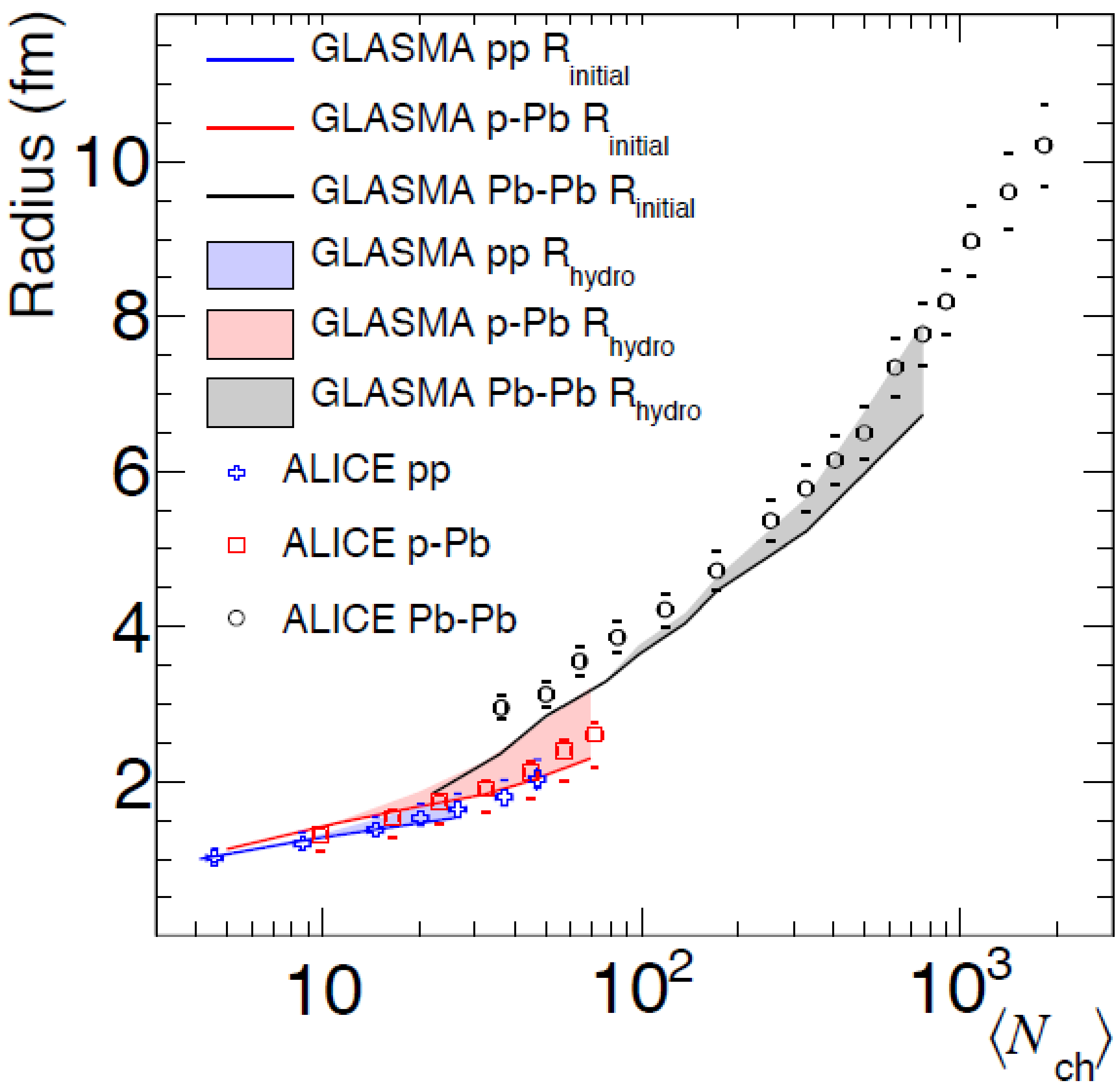

- Similarity between radii in pPb and pp can be described by Yang-Mills evolution alone
- They also can be reproduced by adding a hydrodynamic phase

GLASMA points are first scaled such that the calculations in pp match the ALICE pp data. Scale = 1.15. GLASMA calculations have uncertainty due to infrared cutoff (m=0.1 GeV).

Schenke, Venugopalan, arXiv:1405.3605

Initial system size scaling across systems

arXiv:1404.5291

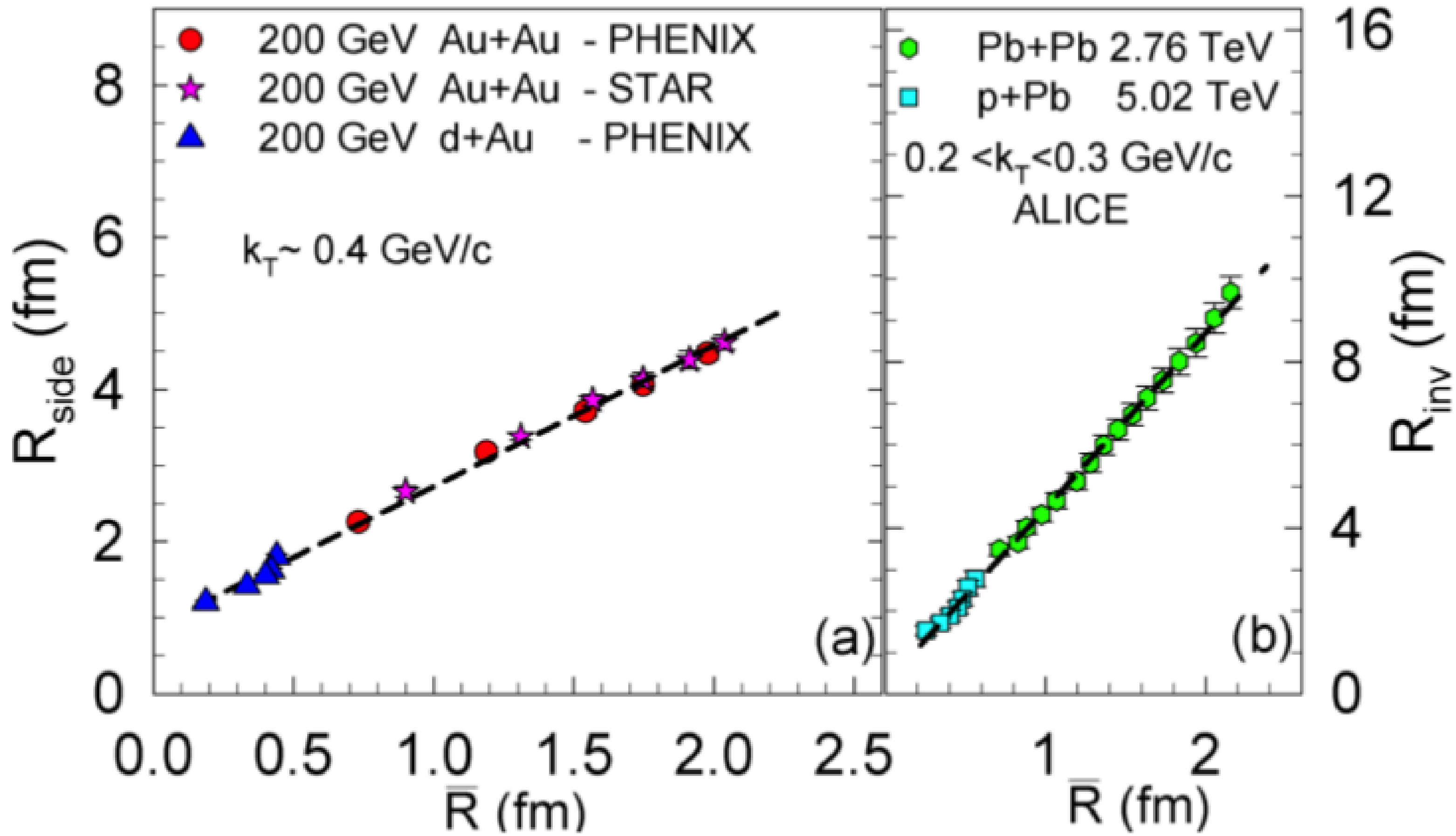

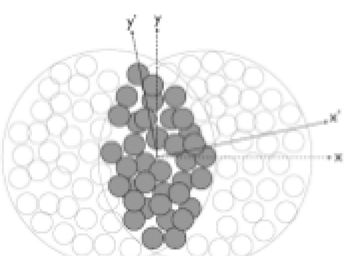

$$\frac{1}{\bar{R}} = \sqrt{\left(\frac{1}{\sigma_x^2} + \frac{1}{\sigma_y^2}\right)}$$

(proxy for gradients in initial size)

Scaling with $\bar{R}$ across systems:
Implies evidence for radial expansion

And the jet at low p_T?

- Ridge and jet seem additive in 2PC
- Subtract ridge to obtain jet yields
- Resulting jet yields are constant over ~60% of the pPb cross section
  - No modification even at low p_T
- Consistent with picture of minijets in pPb from independent superpositions of NN collisions with incoherent fragmentation

What happens to jet at low p_T?

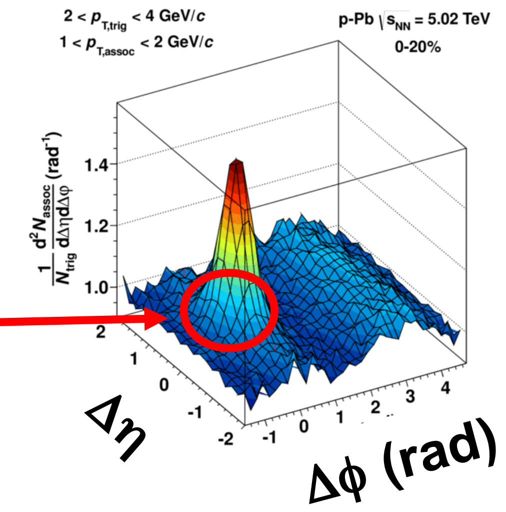

ALICE preliminary

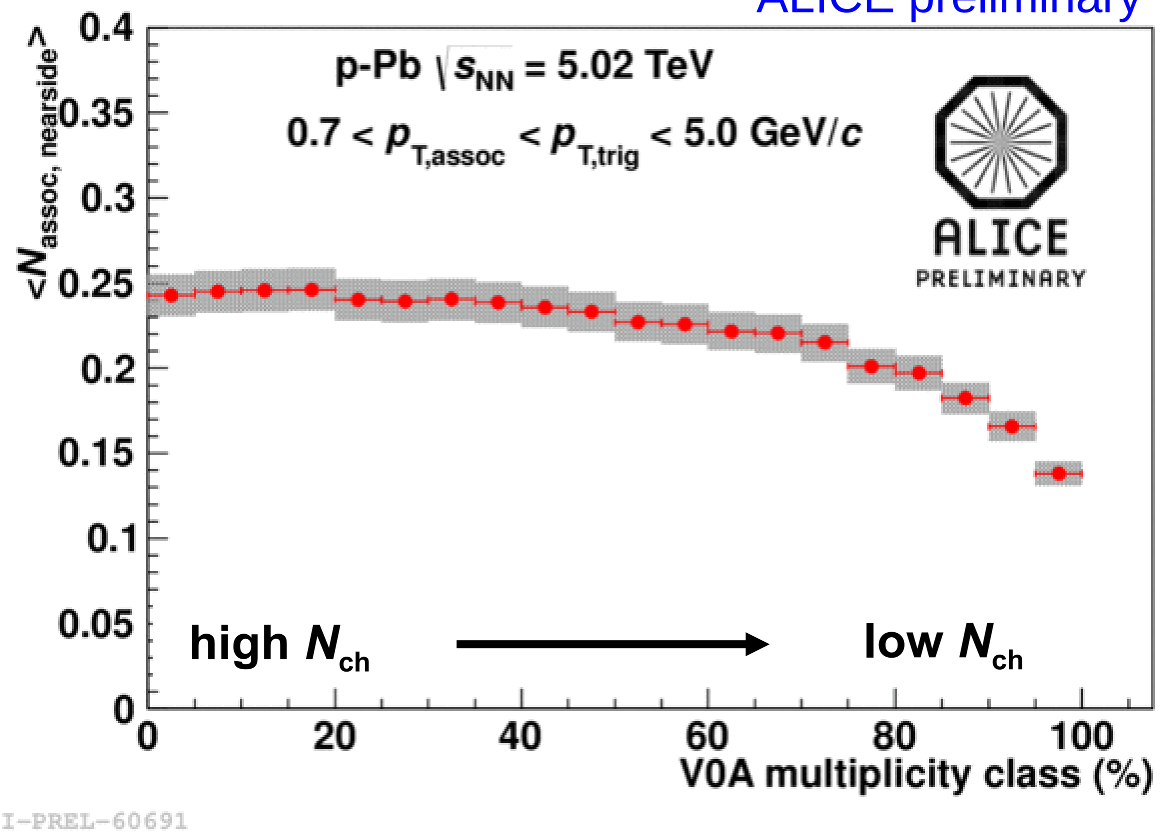

ψ(2S) production in p-Pb

arXiv:1405.3796

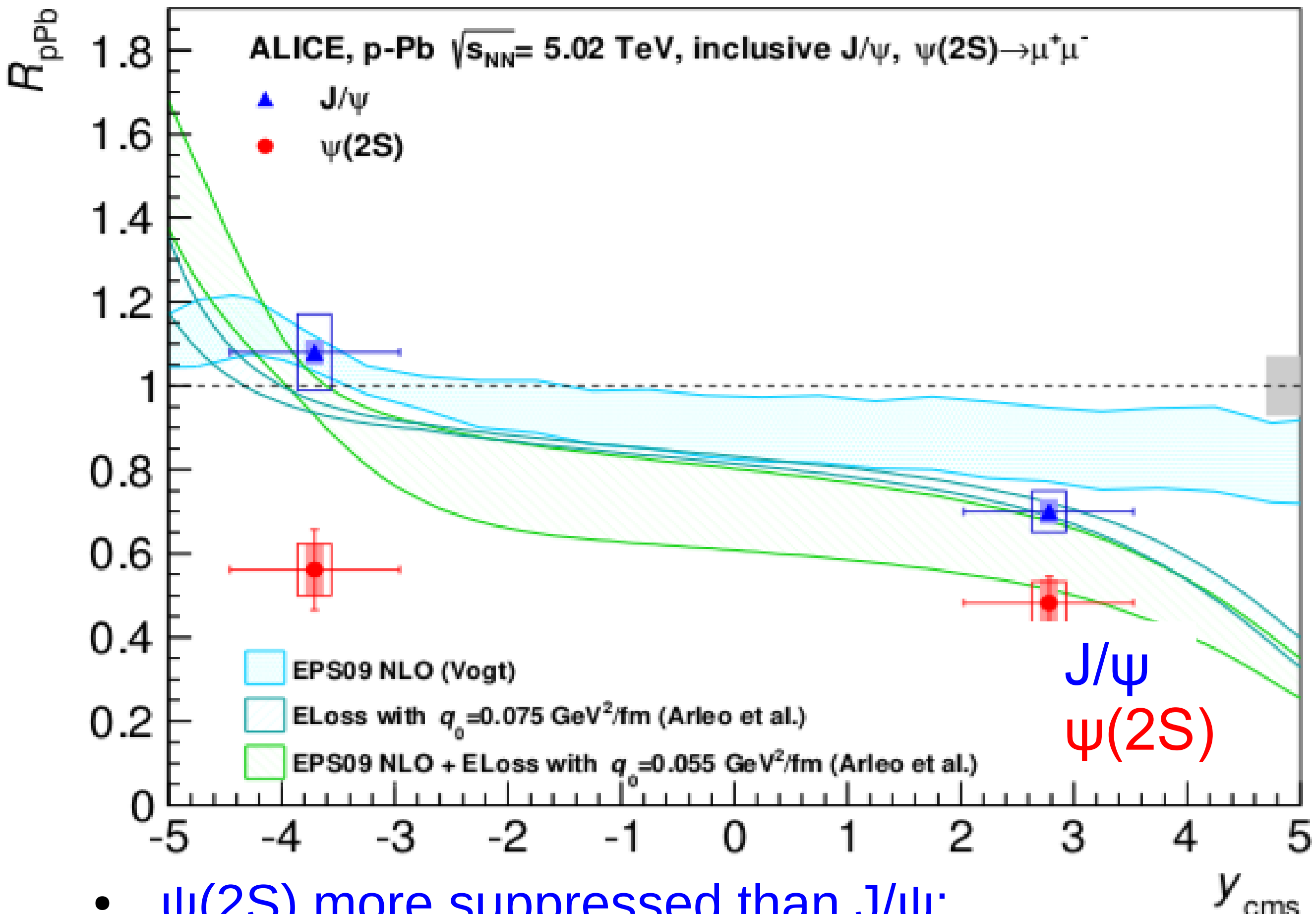

New preliminary

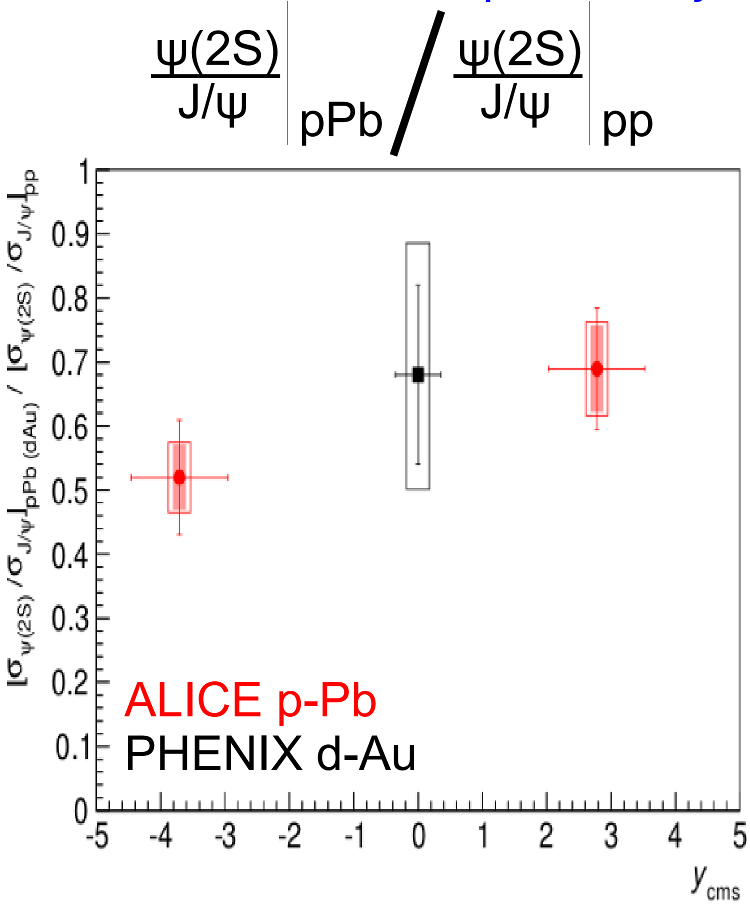

- ψ(2S) more suppressed than J/ψ:
  Not expected by initial state + CNM effects and coherent energy loss
- Stronger relative suppression in backward direction:
  Qualitatively expected from break-up due to comoving system
- But also strong suppression in forward direction
  - Final state effects?

Centrality dependent nuclear modification

$$R_{AB} = \frac{\mathrm{d}N_{AB}/\mathrm{d}p_{\mathrm{T}}}{\langle N_{\mathrm{coll}} \rangle \mathrm{d}N_{\mathrm{pp}}/\mathrm{d}p_{\mathrm{T}}}$$

ALICE, PRL 110 (2013) 082302

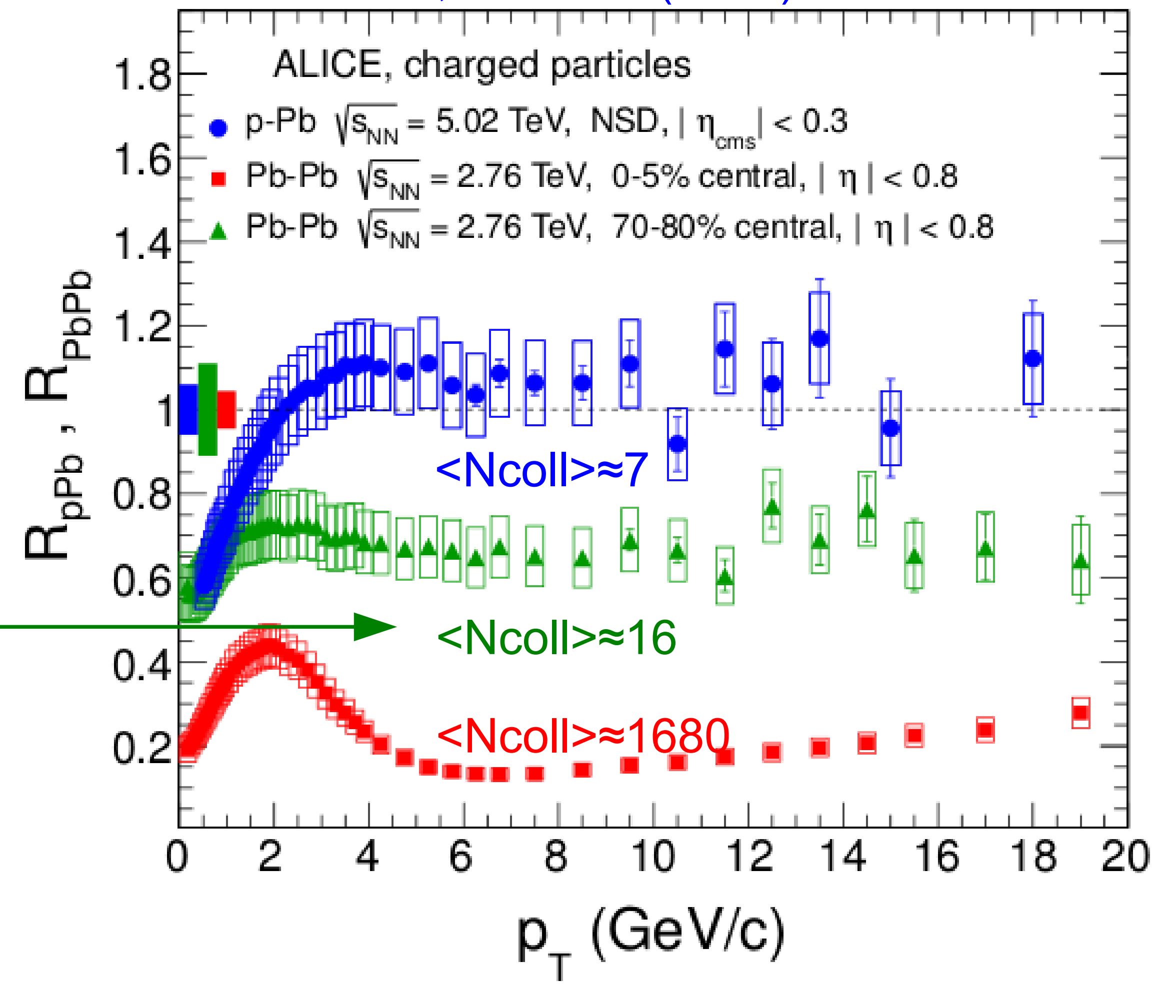

In reach for
central pPb collisions

How to perform a centrality dependent measurement?

$$R_{\mathrm{pA}}^{\mathrm{cent}}(p_{\mathrm{T}}) = \frac{\mathrm{d}N^{\mathrm{pA}}/\mathrm{d}p_{\mathrm{T}}}{\langle T_{\mathrm{pA}}^{\mathrm{cent}} \rangle \mathrm{d}\sigma^{\mathrm{pp}}/\mathrm{d}p_{\mathrm{T}}} = \frac{\mathrm{d}N^{\mathrm{pA}}/\mathrm{d}p_{\mathrm{T}}}{\langle N_{\mathrm{coll}}^{\mathrm{cent}} \rangle \mathrm{d}N^{\mathrm{pp}}/\mathrm{d}p_{\mathrm{T}}}$$

Nuclear geometry and collision centrality

Nuclei are "macroscopic": Characterize collisions by impact parameter

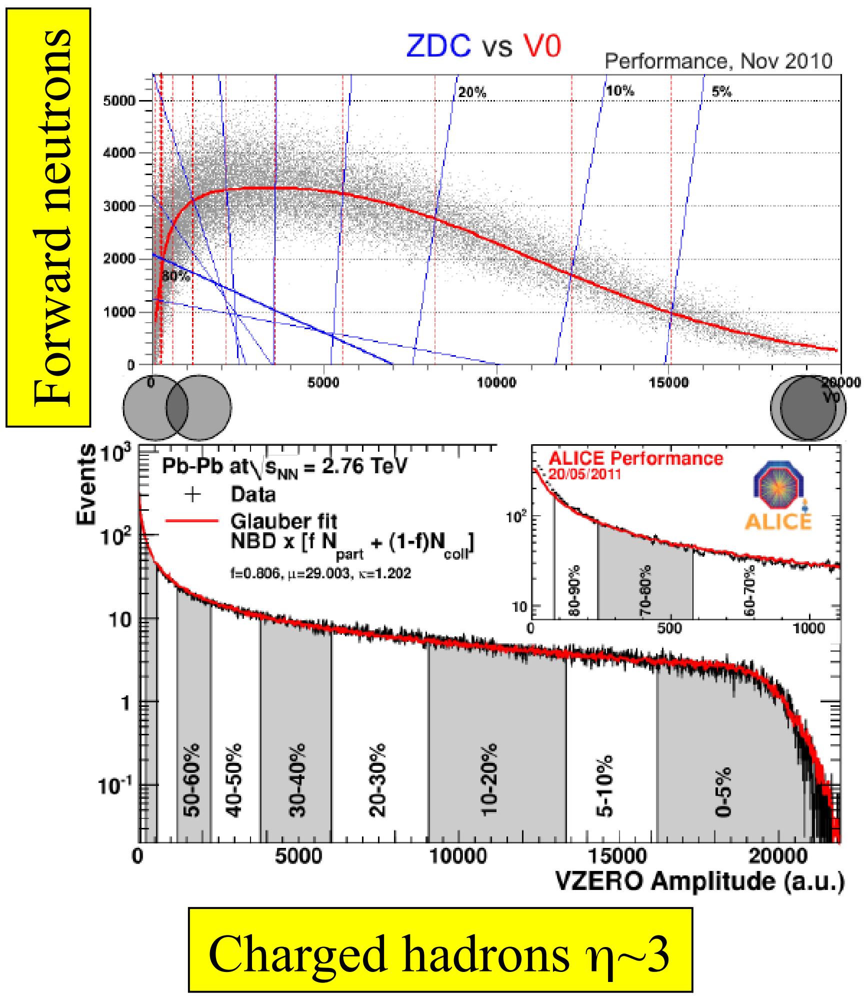

- Correlate yields from disconnected parts of phase space
  - Correlation arises from common dependence on collision impact parameter
- Order events by centrality metric
  - Typically, classify them as "ordered" fraction of total cross section
    - eg. 0-5% most central
  - Number of participants (volume)

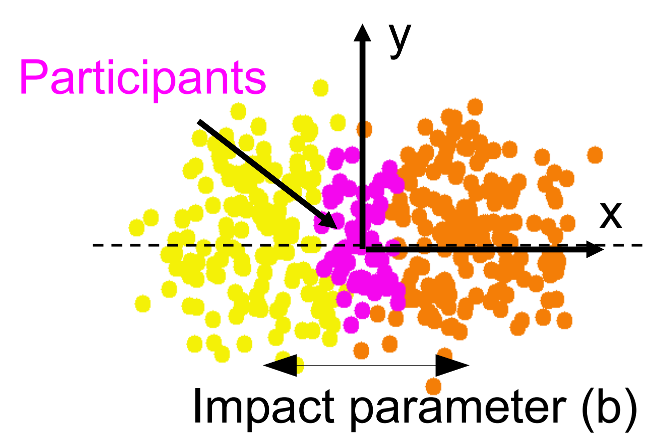

Centrality from multiplicity

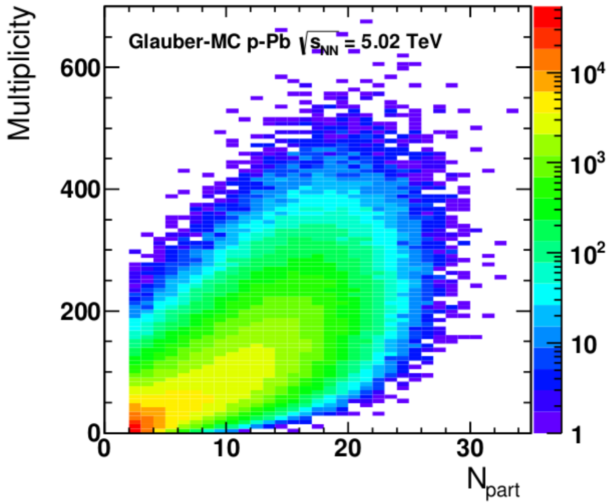

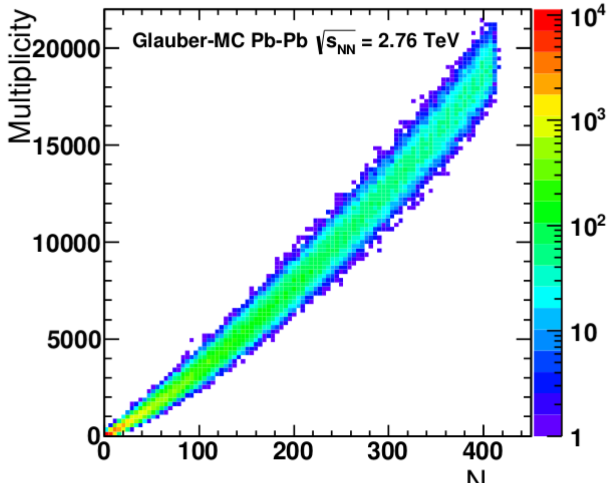

- Due to small dynamic range several biases are present
  - Multiplicity bias
  - Jet veto bias
  - Geometrical bias
- Include (and indicate) bias in the definition

$$Q_{pPb,\,cent} = \langle N_{cent}^{Glauber} \rangle \frac{\langle dN^{pPb}/dp_T \rangle_{cent}}{dN^{pp}/dp_T}$$

- Not R_{pPb} as not 1 in absence of nuclear effects

Toy Model: Glauber+Pythia

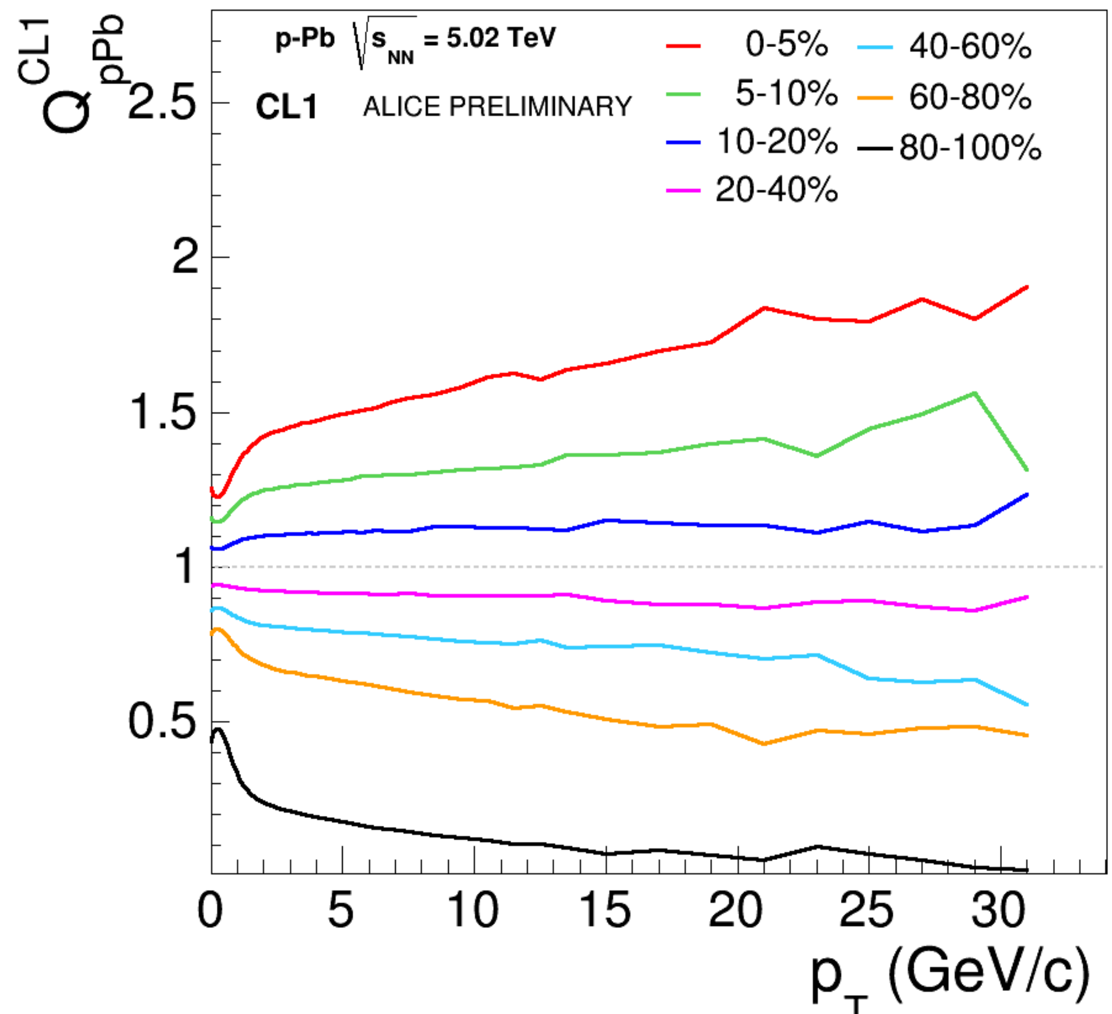

Centrality from multiplicity

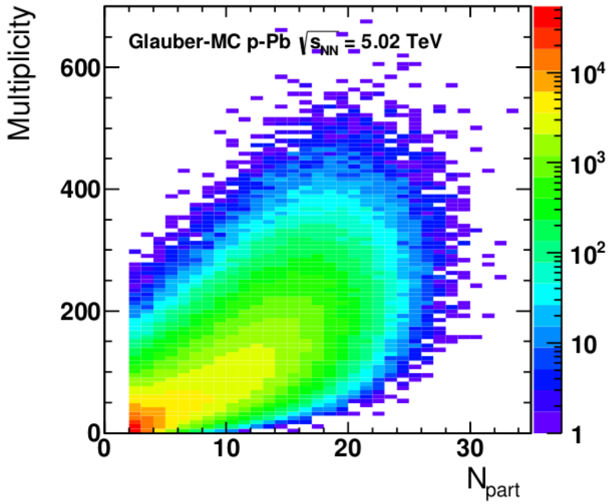

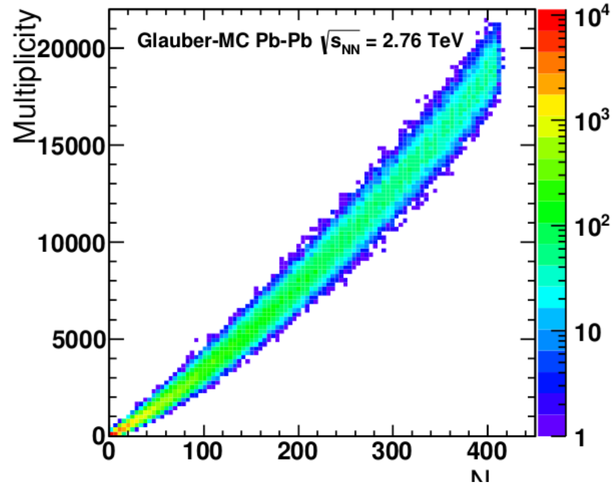

Using hits
at mid-rapidty (CL1)

- Due to small dynamic range several biases are present
  - Multiplicity bias
  - Jet veto bias
  - Geometrical bias
- Include (and indicate) bias in the definition

$$Q_{pPb,\,cent} = \langle N_{cent}^{Glauber} \rangle \frac{\langle dN^{pPb} / dp_T \rangle_{cent}}{dN^{pp} / dp_T}$$

- Not R_{pPb} as not 1 in absence of nuclear effects

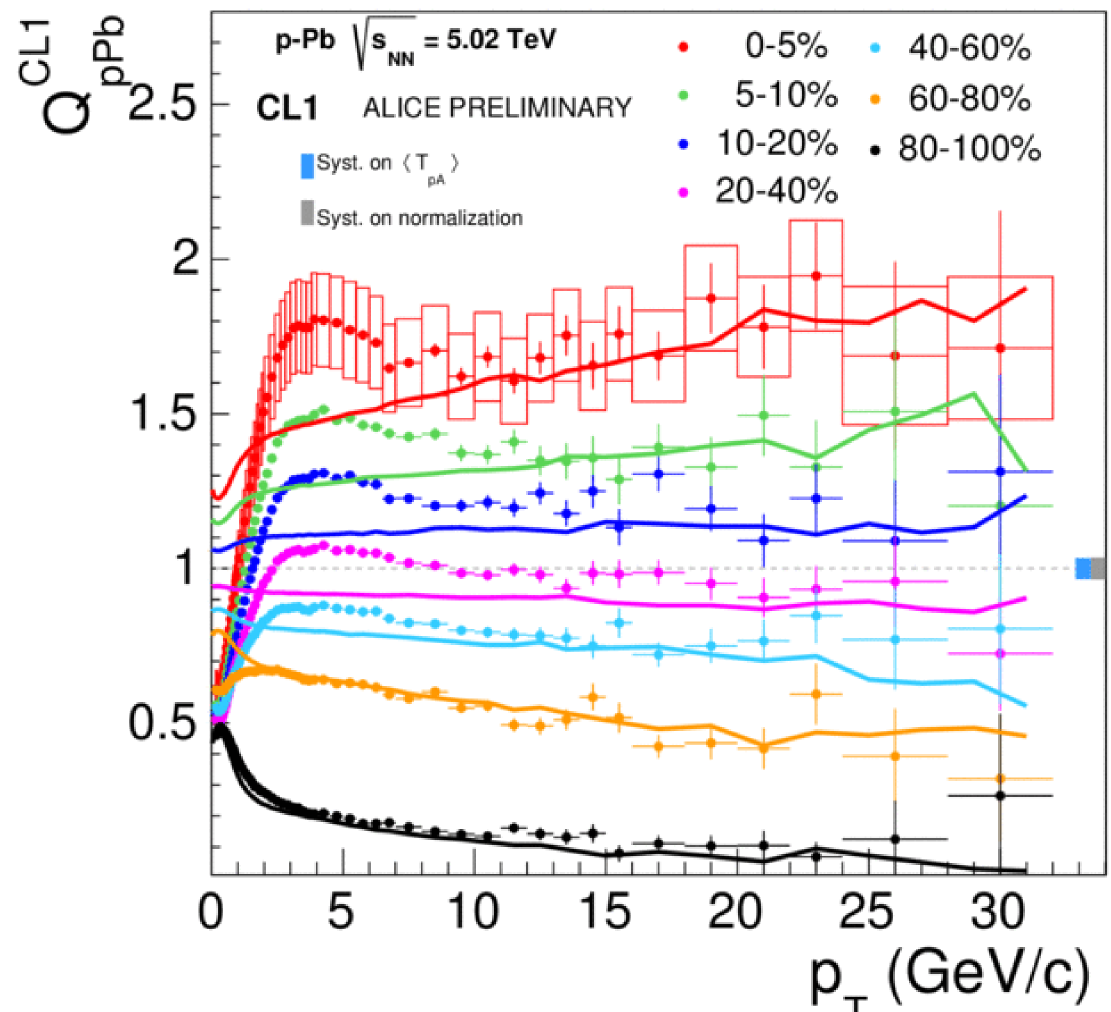

Centrality from multiplicity

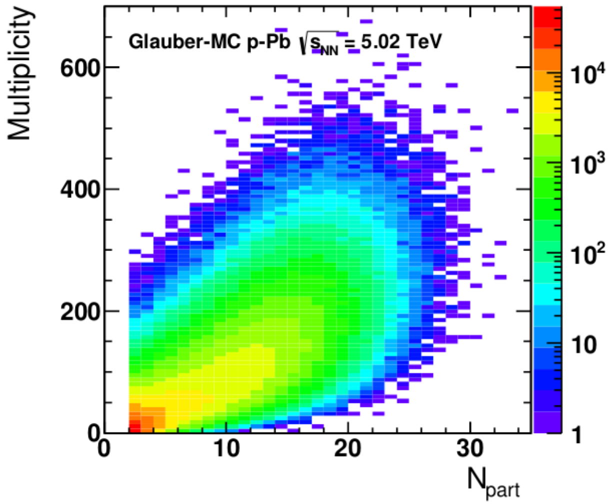

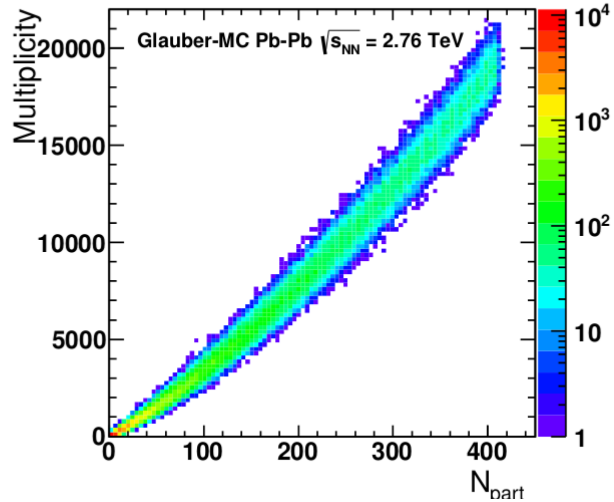

Using amplitudes
at forward rapidity (V0A)

- Due to small dynamic range several biases are present
  - Multiplicity bias
  - Jet veto bias
  - Geometrical bias
- Include (and indicate) bias in the definition

$$Q_{pPb,\,cent} = \langle N_{cent}^{Glauber} \rangle \frac{\langle dN^{pPb}/dp_T \rangle_{cent}}{dN^{pp}/dp_T}$$

- Not R_{pPb} as not 1 in absence of nuclear effects

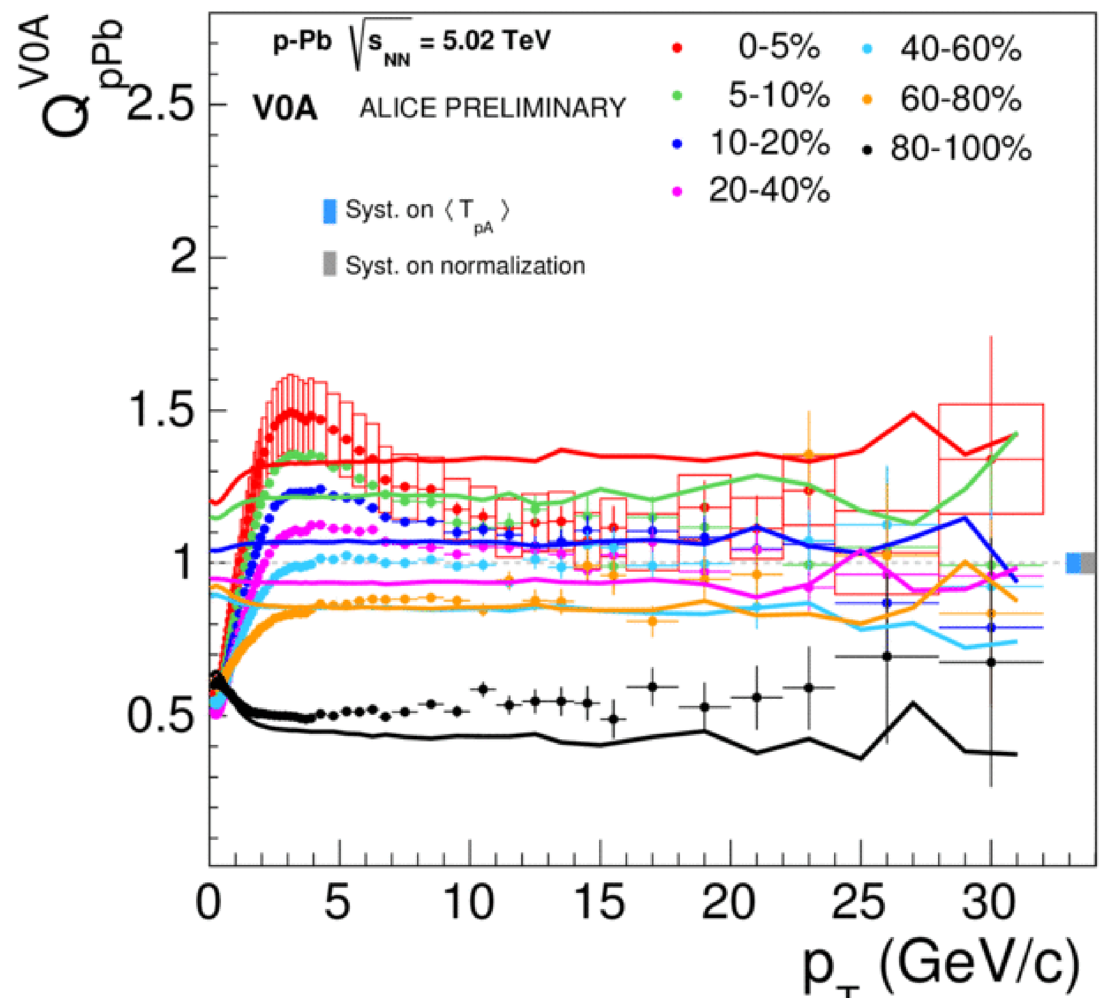

Alternative approach using neutrons

Preliminary

- Use forward neutrons to bin event classes
  - Not expected to lead to selection bias
  - But smaller dynamic range
- Obtain scale factor from data using only minbias values for Glauber $\langle N_i \rangle = \langle N_i \rangle \langle S_i \rangle / \langle S \rangle$
- Assume
  - <Npart>: mid-rapidity signal
  - <Npart>-1: forward signal
  - <Ncoll>: high-p_T yield
- Methods lead to consistent results
  - Q_{pPb} flat at high p_T (>10 GeV/c)
  - <Ncoll> within 10%

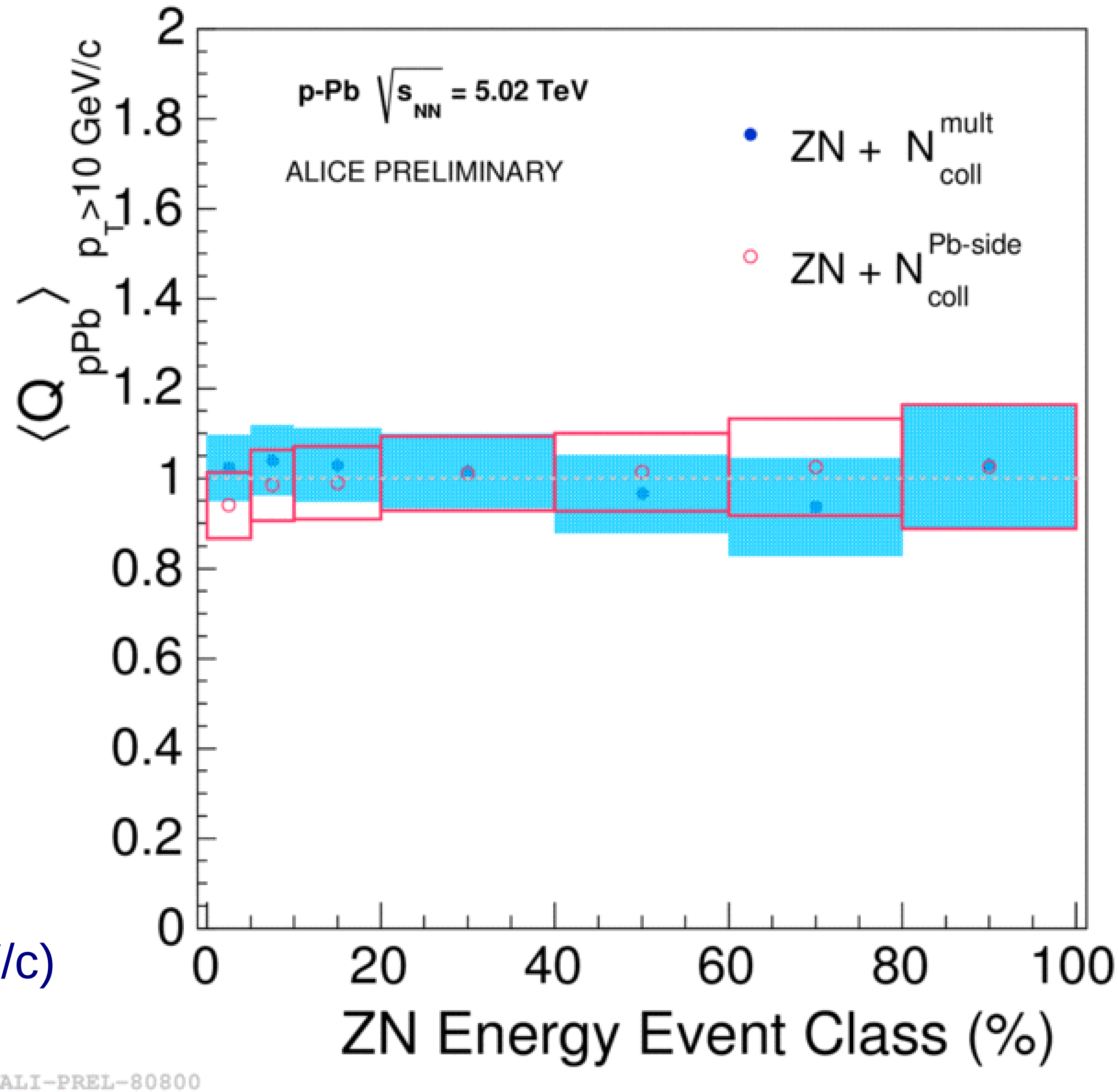

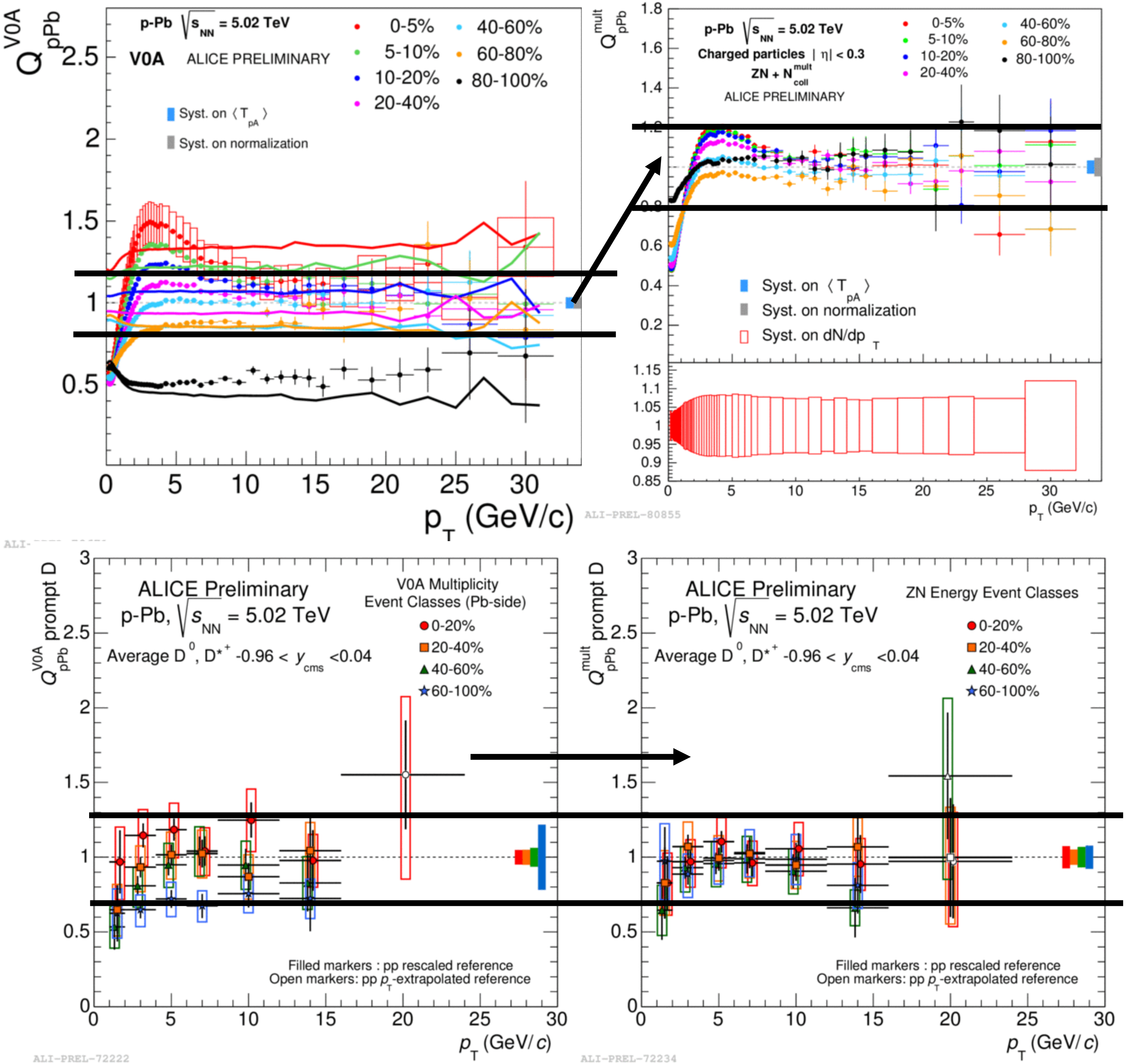

- Charged particle Q_{pA} consistent with unity at high p_T
  - Cronin peak develops with multiplicity
- D meson Q_{pA} independent of p_T above 2 GeV/c
  - Consistent with unity

NB. Estimators have different dynamic range

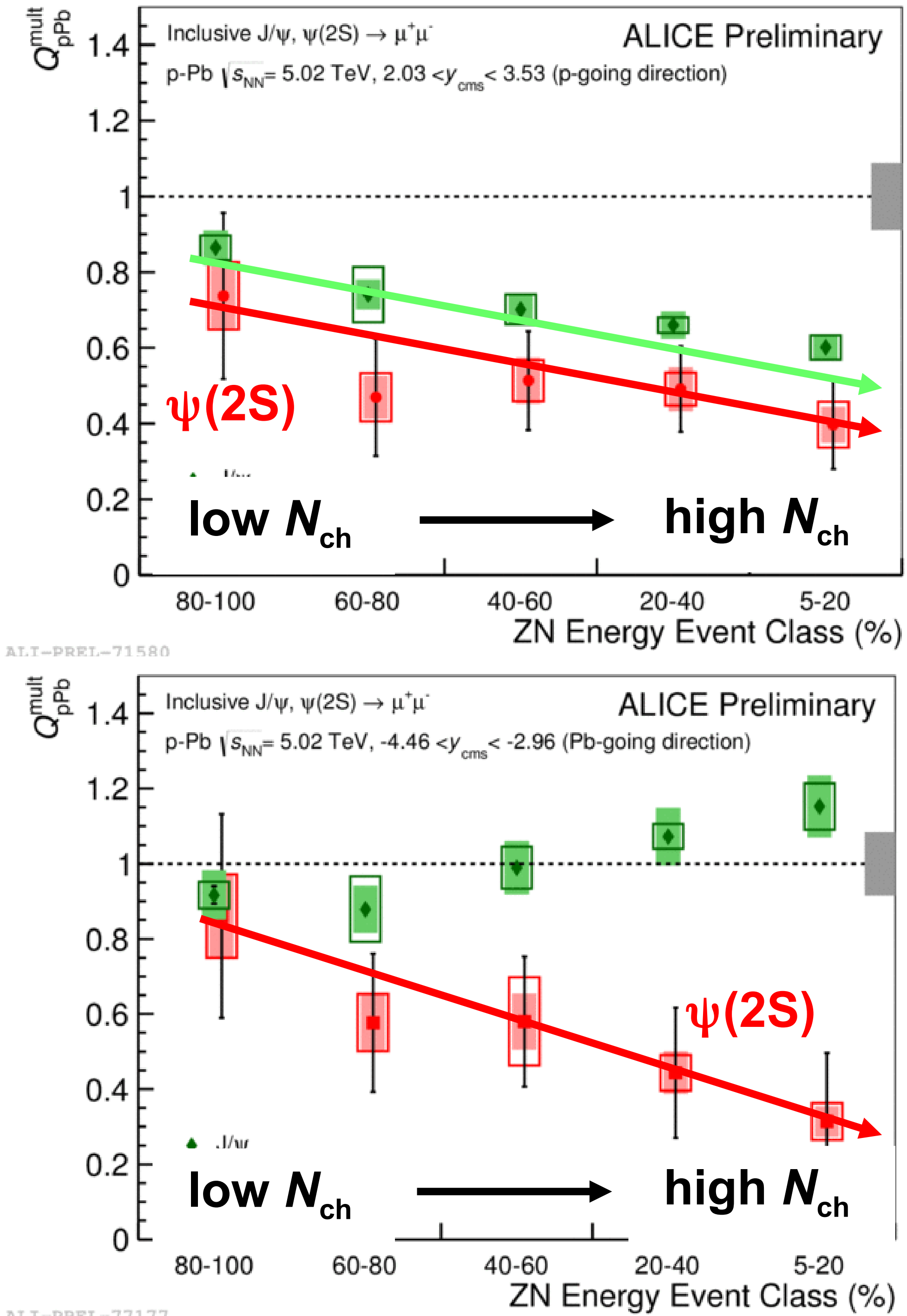

- J/ψ → μμ: Multiplicity dependent suppression in p-going direction:
  - Shadowing region; <*x*> ~ 10^{-4}
- No suppression in Pb-going direction
  - Anti-shadowing region; <*x*> ~ 10^{-2}

- ψ(2S) → μμ: Multiplicity dependent suppression in both directions
- Similar as at RHIC
- J/ψ consistent with shadowing
- ψ(2S) needs additional effects → Final state?

Summary

- The pPb control experiment did not give the expected “null” results
- Observables known to exhibit collective effects in PbPb show the same in pA
  - In particular at high multiplicity where the effects are almost as strong
  - Some effects are also present in high multiplicity pp collisions
- Not surprisingly, most can be described by hydrodynamical model calculations, but some also with microscopical models
- Jet quenching not observed but ψ(2S) suppressed relative to J/ψ may be first indication

Some questions

- What is the smallest (in terms of size and energy content) droplet of QGP to which a fluid dynamical description can be applied?
- Is observed collectivity in momentum space driven by the spatial structure (i.e. the pressure gradients) of the initial matter distribution?
- Are there mechanisms other than hydrodynamics that can generate and quantitatively reproduce the observed collective features in these collisions?
- How does collectivity emerge as a function of system size and energy density? What are the relevant scales (time, energy, size) controlling the degree of collectivity observed in the final state?
- Can one (does it make sense to) disentangle initial from final effects?
- To which extent can a collective effect observed in a larger system be reduced to a superposition of more elementary collisions?
- How can we use our ability to probe different collision energies, centralities and other event characteristics for further measurements?
- How is collectivity in small systems correlated with hard probes of the medium, such as jet quenching and quarkonium spectroscopy?

Some interesting topics I left out

Collective flow without fluid dynamics

arXiv:1401.1364v1

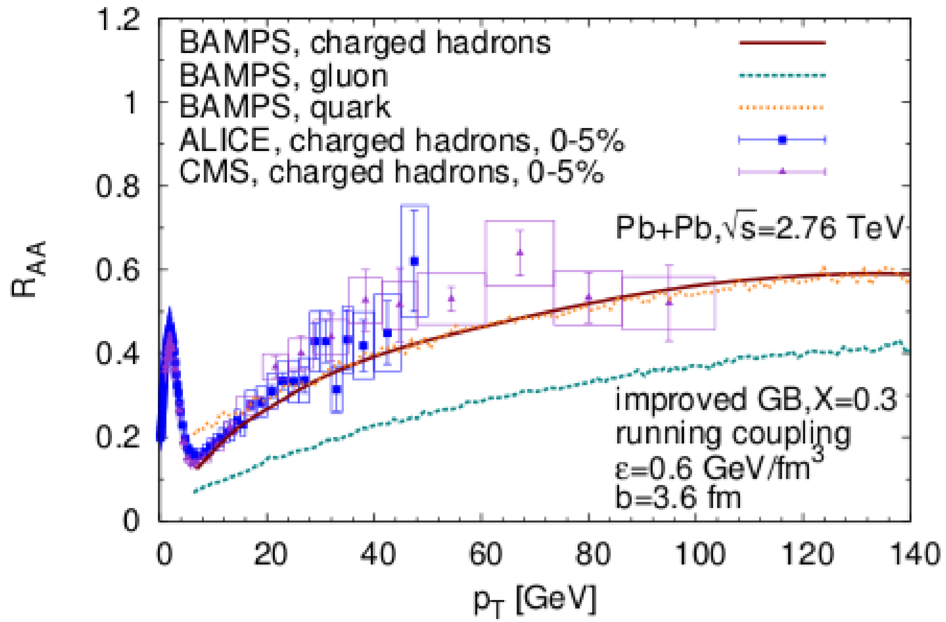

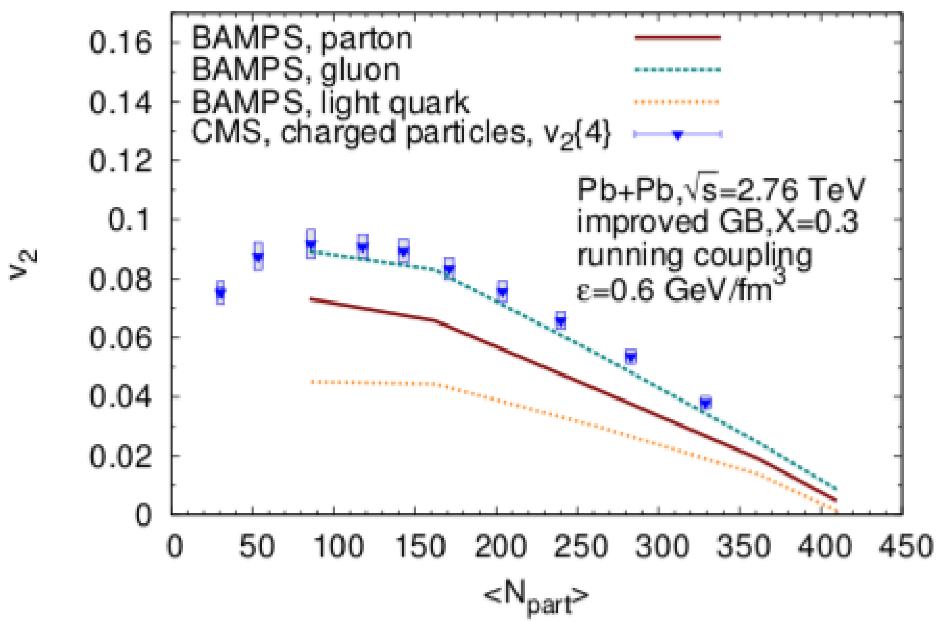

- BAMPS: Boltzman equation with 2->2 and 2->3 processes
- Can get R_{AA} and v_2 qualitatively
  (by adjusting one parameter at RHIC energy)

Ridge modulation v_2 and v_3 and CGC

- Two symmetric ridges predicted by CGC glasma graphs found to describe the ridge yields and shape
- However, a large v_3 component and multi-particle correlations would be a challenge for the model

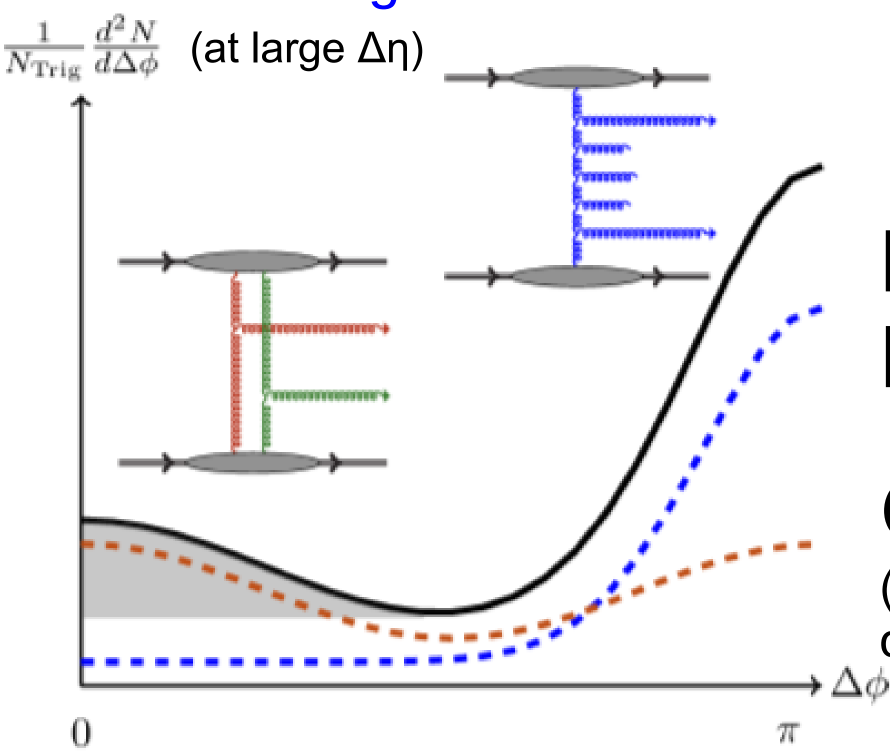

BFKL-Minijets

Glasma (enhanced by α_s^{-8} for $k_T < Q_s$)

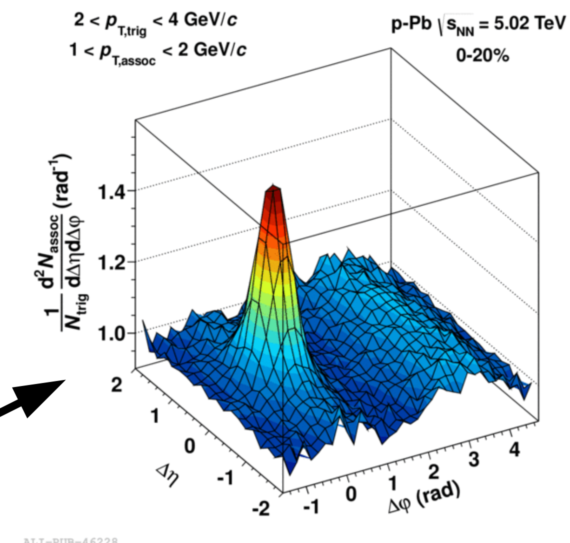

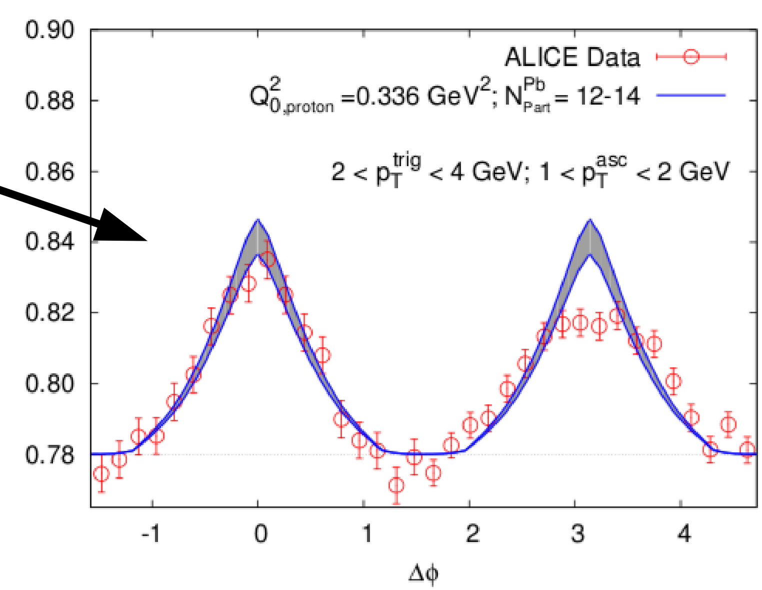

Dusling and Venugopalan, PRD 87 (2013) 094034

IP-Glasma model

Dusling QM 2014

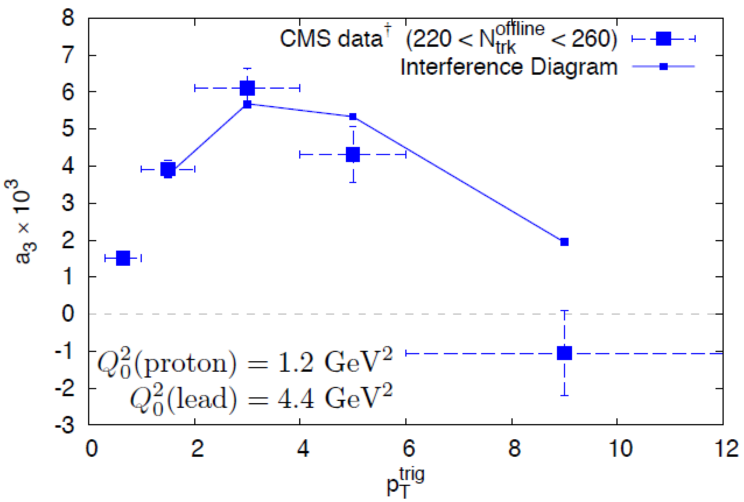

Jet-Glasma interference

Schenke QM 2014

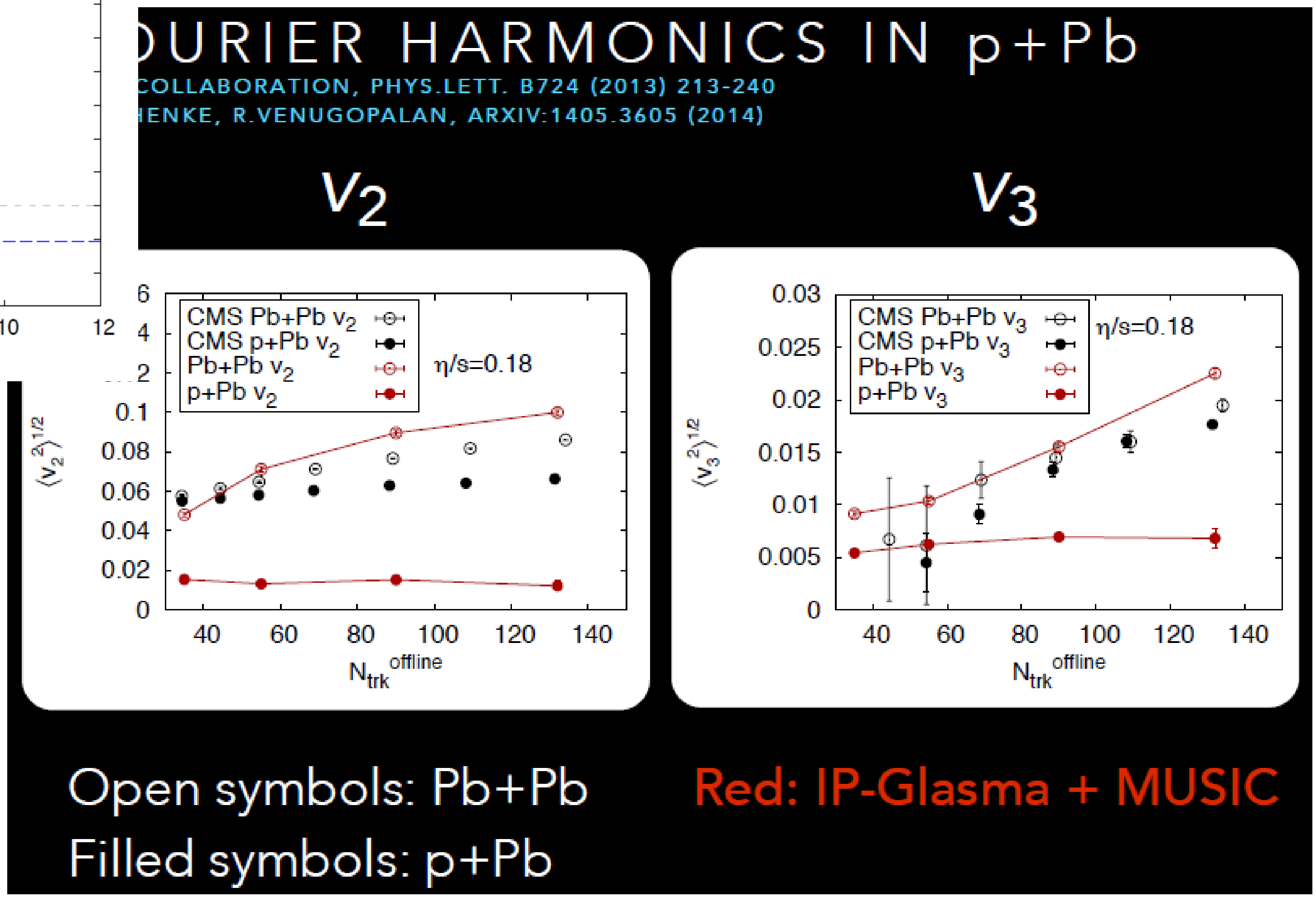

IP-Glasma (which otherwise is very successful) fails to describe pPb:
Maybe because:
a) It does not keep the IS Glasma induced correlations
b) Initial configuration of proton simply taken symmetric

Identified-particle mean p_T vs multiplicity

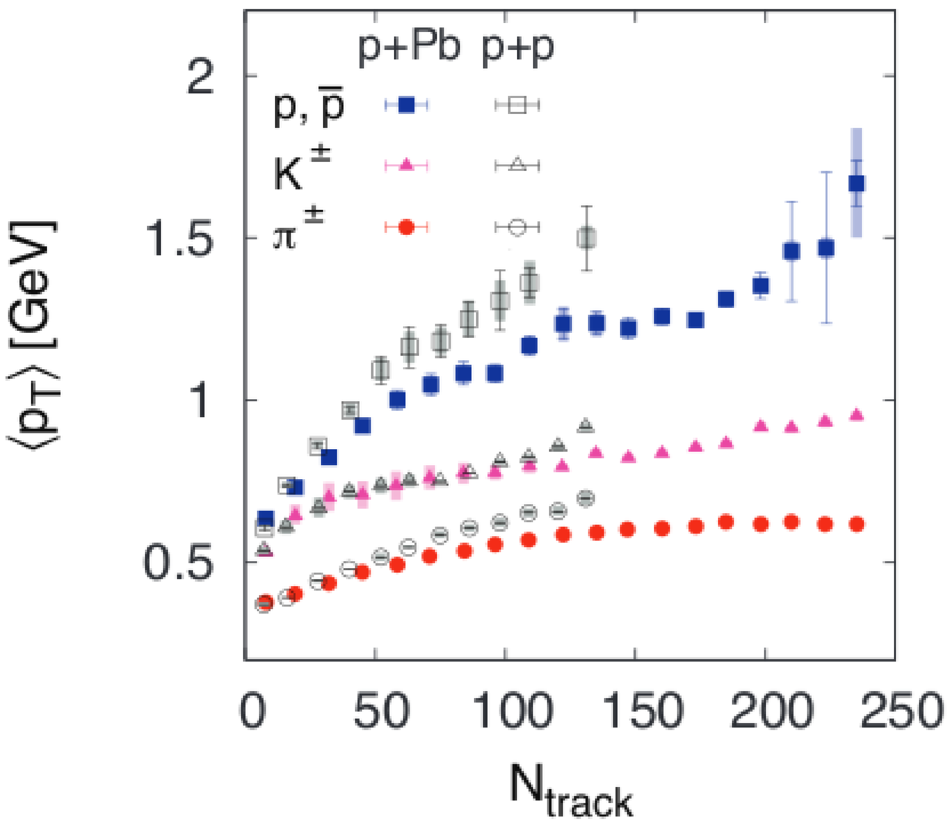

McLerran et al., arXiv:1306.2350

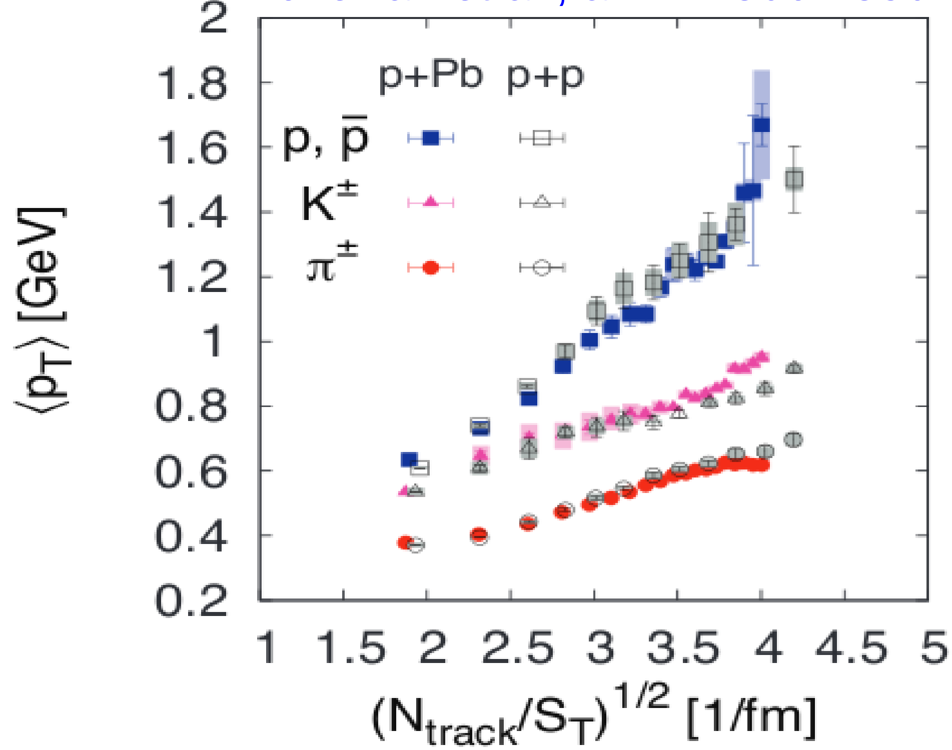

The data in pp and pPb can also be related via geometrical scaling assuming at high multiplicity

$$\frac{1}{S_\mathrm{T}}\frac{dN_i}{dyd^2p_\mathrm{T}} = F_i\left(\frac{p_\mathrm{T}}{Q_\mathrm{s}}, \frac{m_i}{Q_\mathrm{s}}\right)$$

(S_T is calculated in the CGC framework)

Implications of RpPb rising?

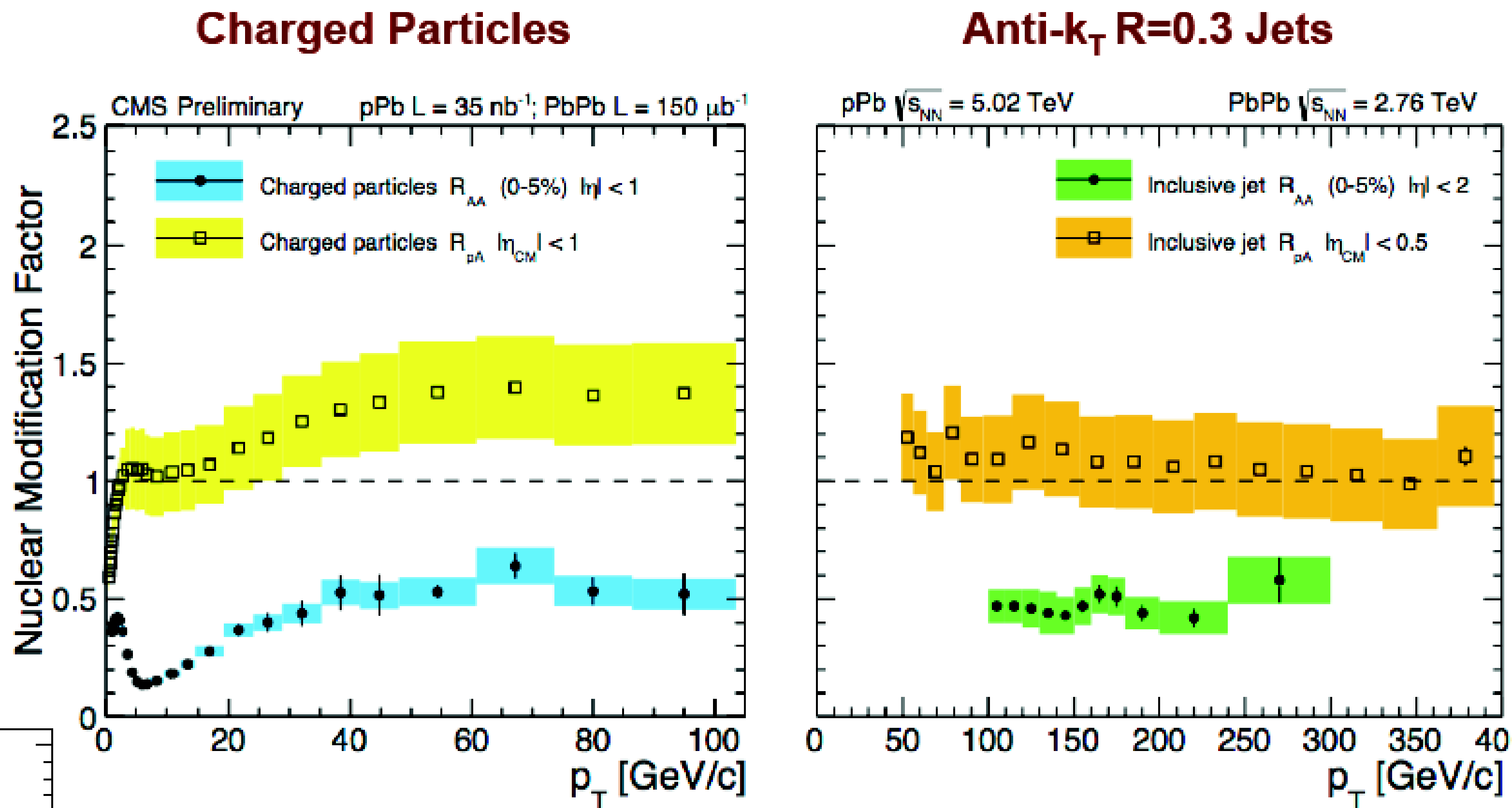

Also ATLAS:

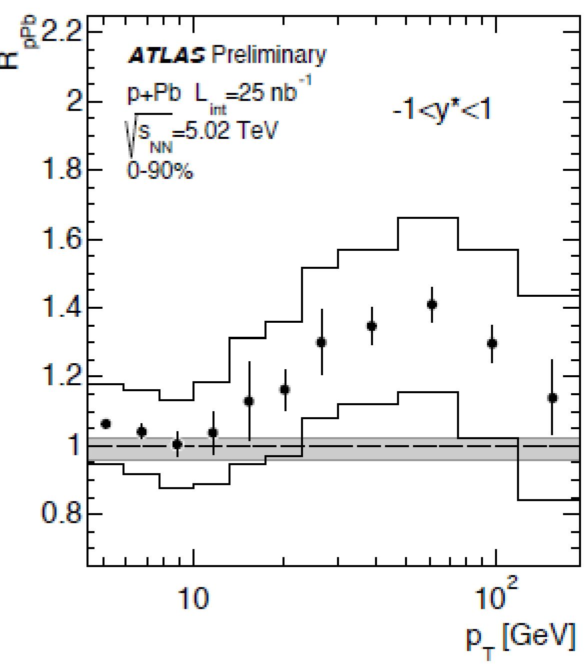

MS: EPJC 72 (2012) 1945 , HIN-12-004, HIN-12-017, HIN-14-001

If taken literally leading hadron suppression must be must stronger.

Average p_T versus N_{ch}

PLB 727 (2013) 371

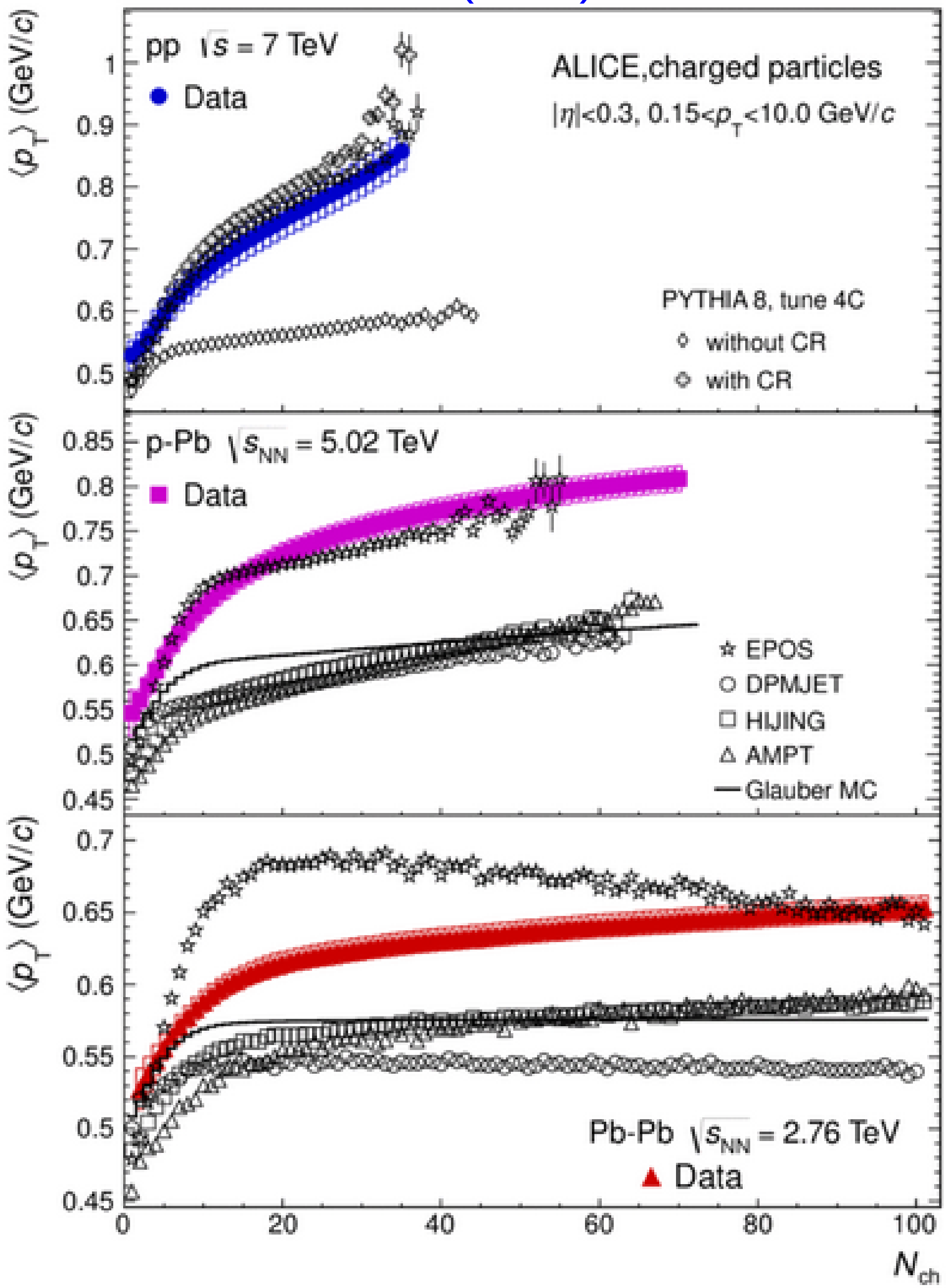

- pp
  - Within PYTHIA model increase in mean p_T can be modeled with Color Reconnections between strings
  - Can be interpreted as collective effect (e.g. Velasquez et al., arXiv:1303.6326v1)
- pPb
  - Increase follows pp up to N_{ch}~14 (90% of pp cross section, pp already biased)
  - Glauber MC (as other models based on incoherent superposition) fails
  - Like in pp: Do we need a (microscopic) concept of interacting strings?
  - EPOS LHC which includes a hydro evolution describes the data (also pp)
- PbPb
  - As expected, incoherent superposition can not describe data

Coherent MPI effects

ALICE, PLB 727 (2013) 371

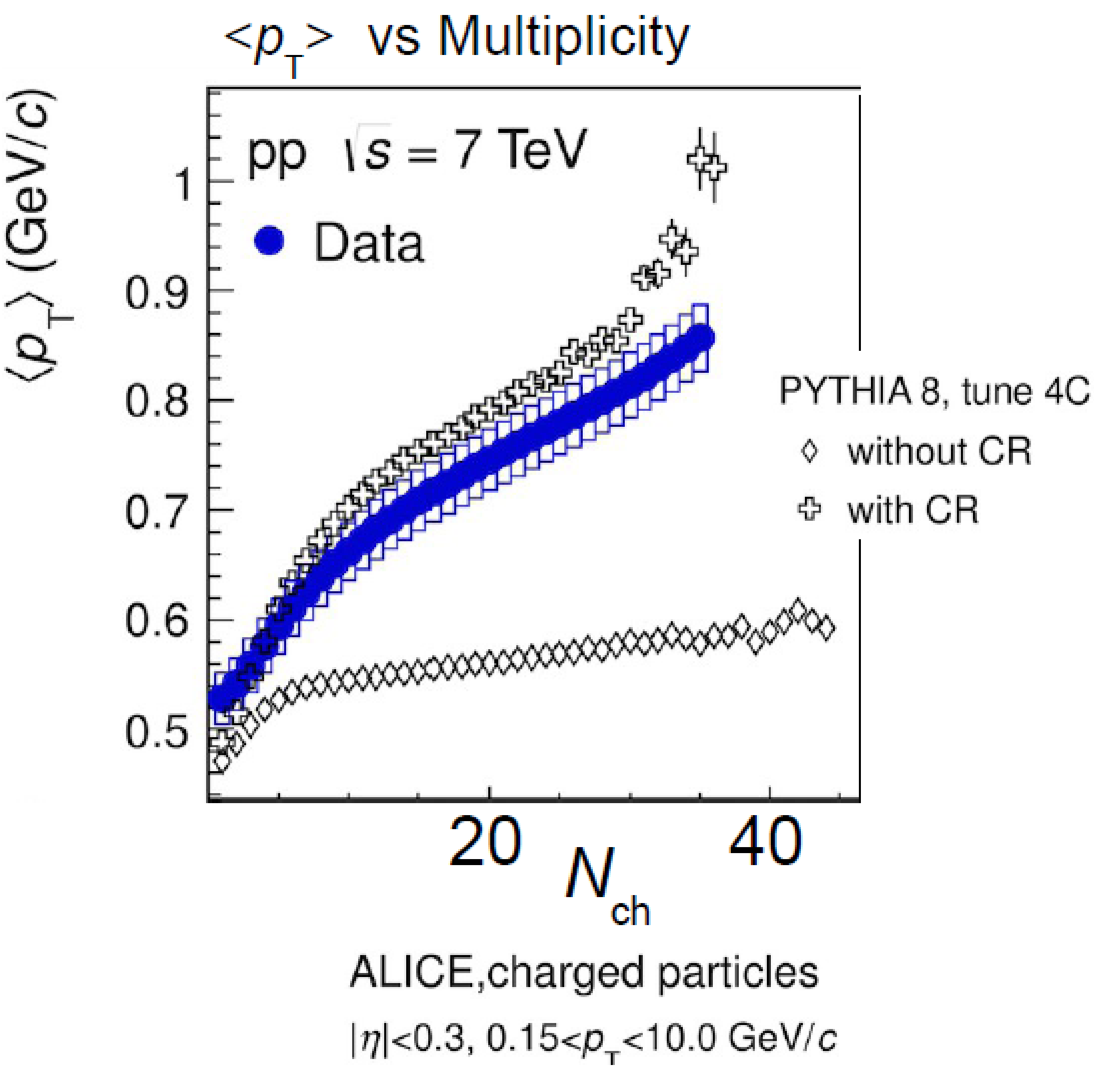

Rise of $<p_T>$ can not be reproduced by incoherent superposition of MPI

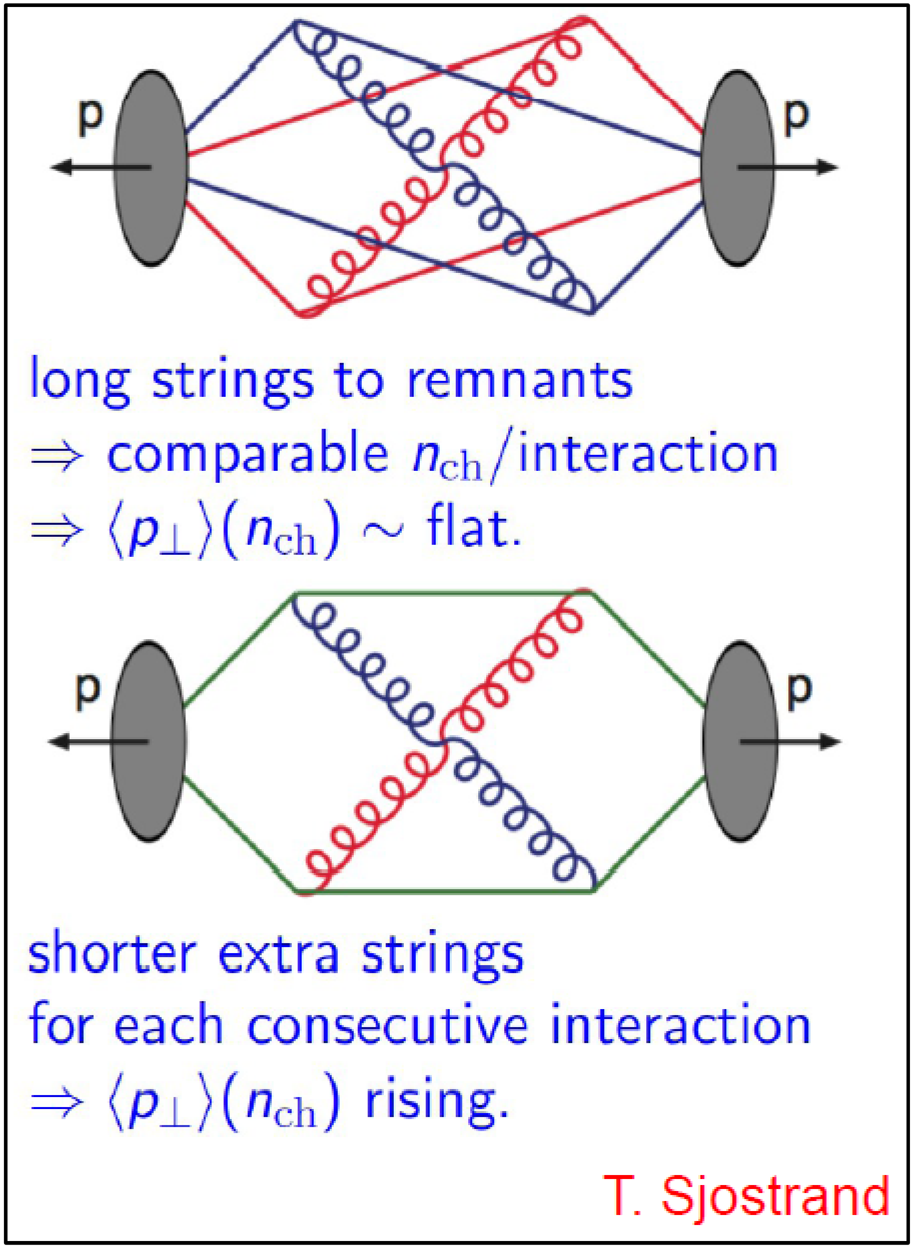

Centrality (and energy) dep. of dN/dη

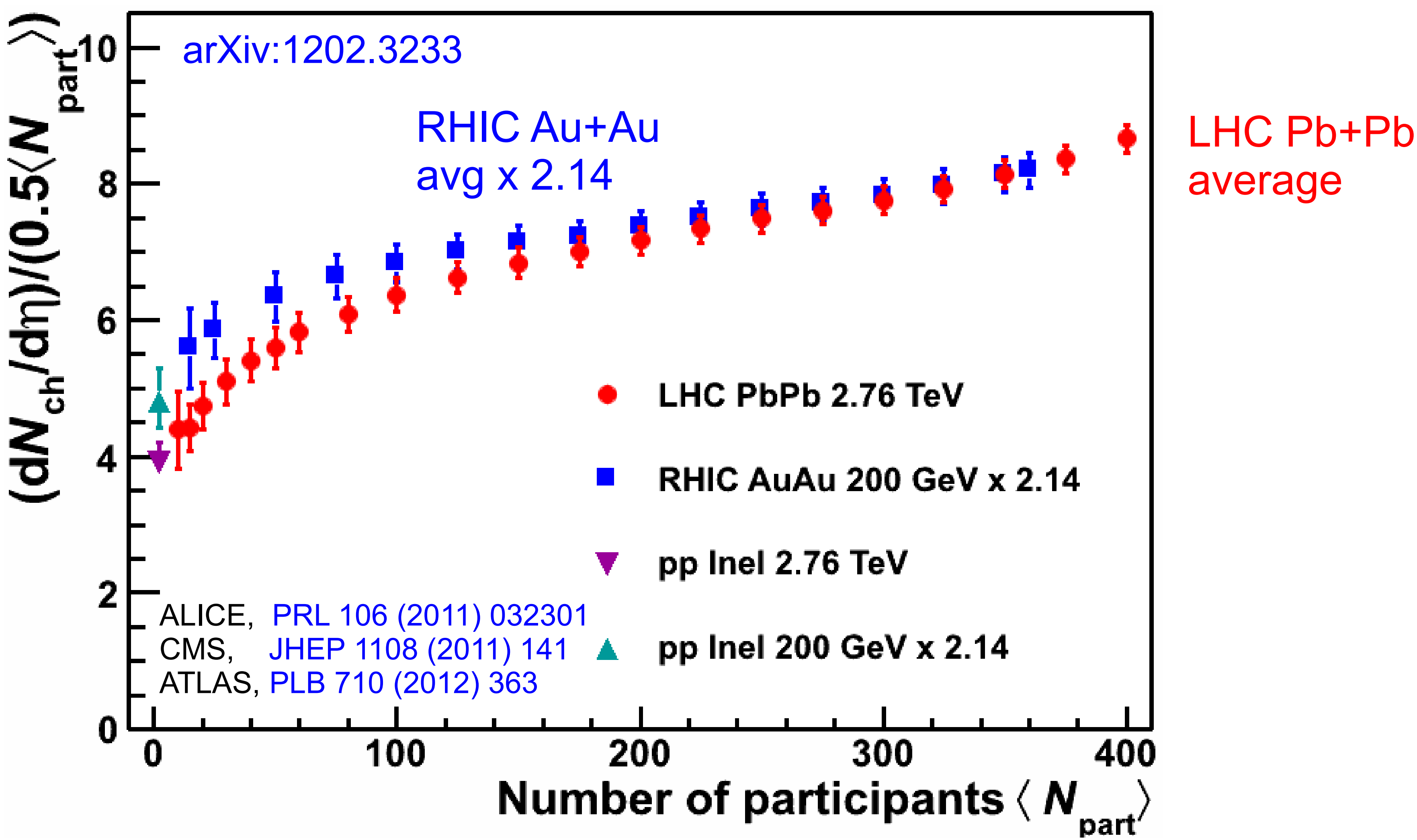

Centrality dependence is strikingly similar to RHIC.

This actually holds all the way down to 19.6 GeV (not shown)

Charged particle elliptic flow versus p_T

PRL 105 (2010) 252302

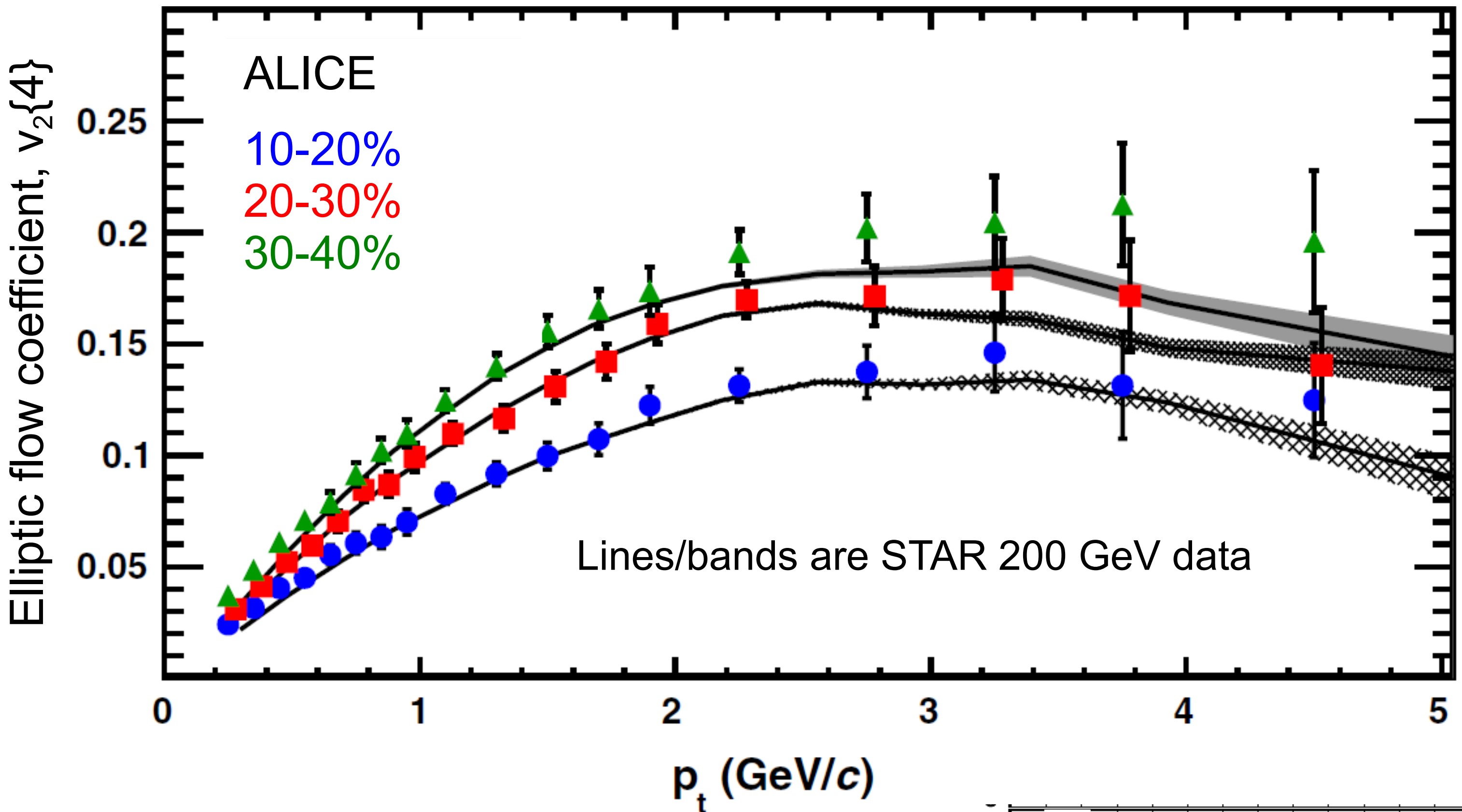

Observe $v_2(p_T)_{LHC} \approx v_2(p_T)_{RHIC}$ above 1 GeV to about 5% despite factor 14 increase in energy, but consistent with hydro predictions! (Int.v_2 30% larger due to radial flow)

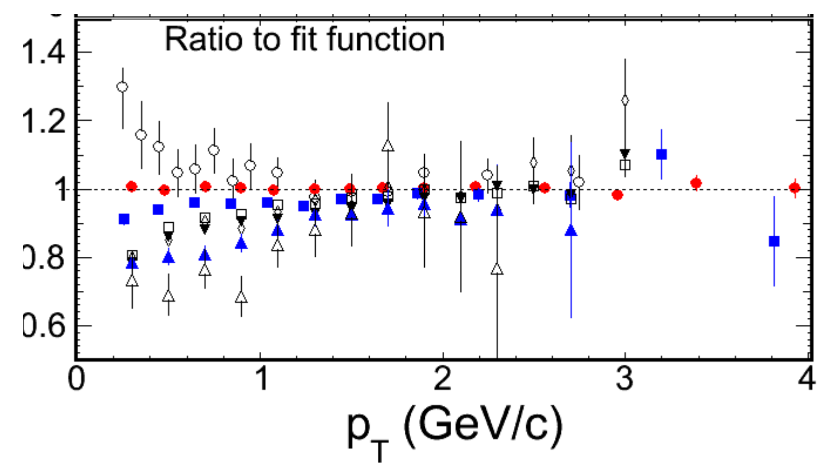

Extra

QGP cross-over phase transition

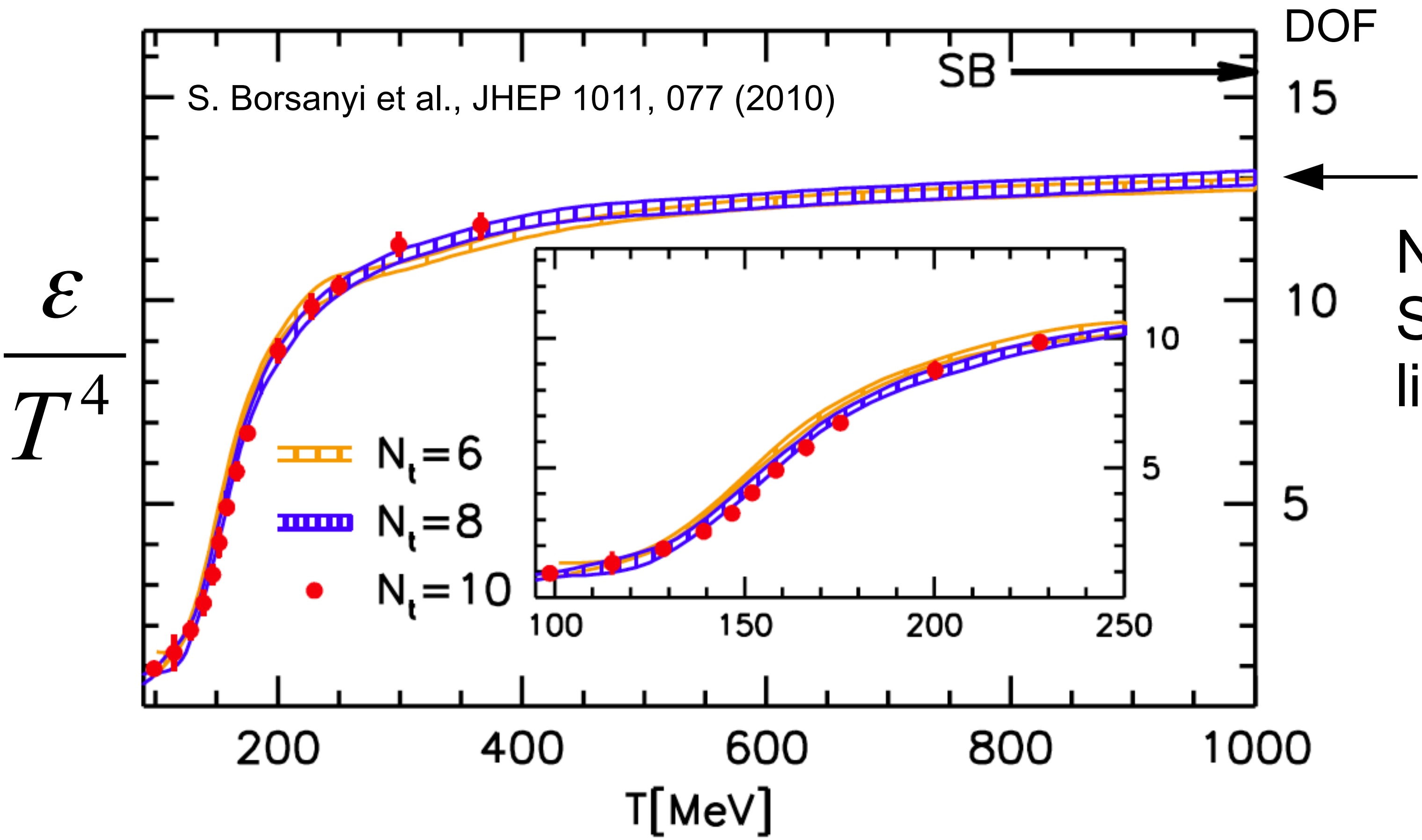

Lattice predicts a cross-over phase transition from hadronic to partonic degrees of freedom

$T_c \approx$ 145-175 MeV
$\varepsilon_c \sim$ 1 GeV/fm3

Shear viscosity in fluids

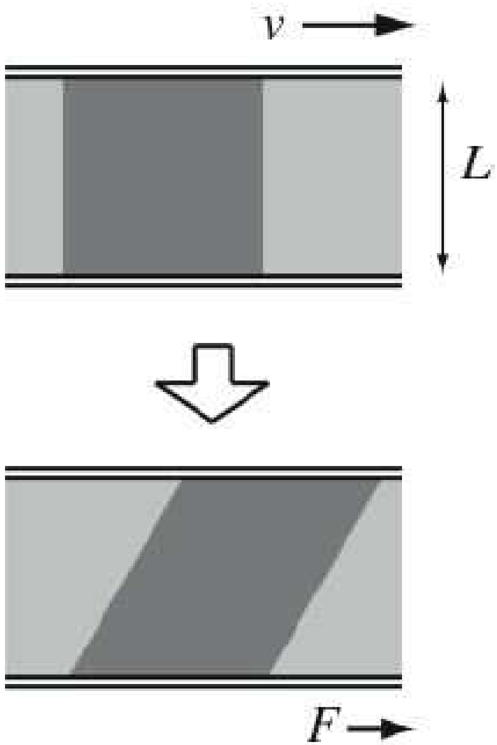

Shear viscosity characterizes the efficiency of momentum transport

quasi-particle interaction cross section

$$\frac{F}{A} = \eta \frac{v}{L}$$

$$\eta = \rho \langle v \rangle \lambda_{mfp} \sim \frac{1}{\sigma}$$

Comparing relativistic fluids: η/s

- s = entropy density
- scaling param. η/s emerges from relativistic hydro eqns.
- generalization for non-rel. fluids: η/w (w=enthalpy) (Liao and Koch, Phys.Rev. C81 (2010) 014902)

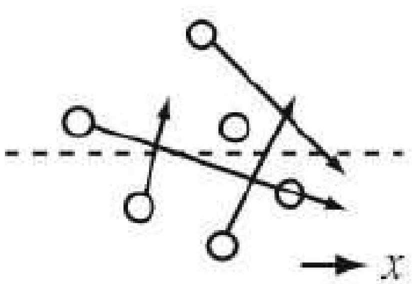

Large σ ➔small η/s
➔Strongly-coupled matter
➔"perfect liquid"

Tomography of QCD matter

- Hard (large Q^2) probes of QCD matter: jets, heavy-quark, $Q\overline{Q}$, γ, W, Z
  - "Self-generated" in the collision at τ<1/Q (or τ<1/m) < 0.1 fm/c
  - "Tomographic" probes of hottest and densest phase of medium

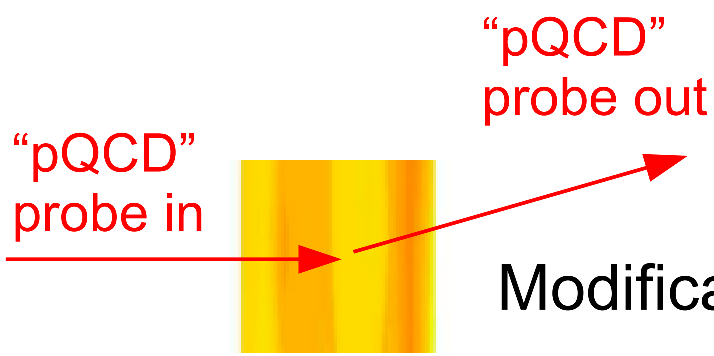

QCD medium

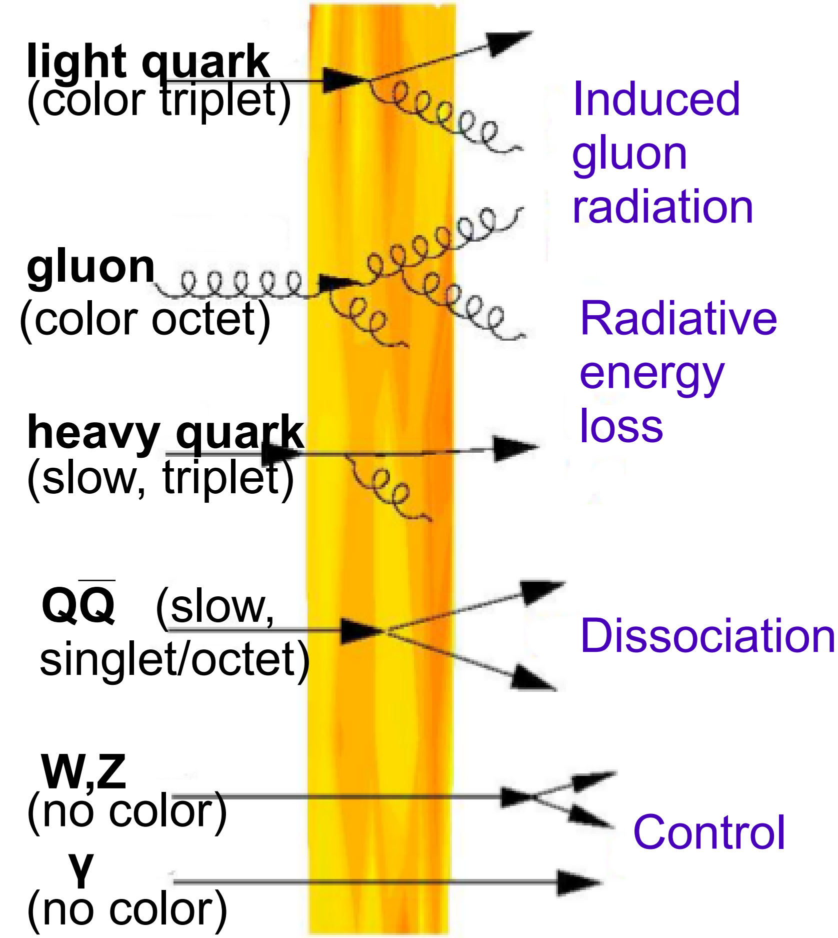

QCD medium

- Nuclear modification factor
  - $R_{AA} = \frac{\text{Yield(AA)}}{\text{Yield(pp)}} \sim \frac{\text{Yield("Medium")}}{\text{Yield("Vacuum")}}$

$$R_{AA}(,p_T) = \frac{1}{N_{coll}} \times \frac{dN_{AA}/dp_T}{dN_{pp}/dp_T} = \frac{dN_{AA}/dp_T}{T_{AA}\, d\sigma_{pp}}$$

  - Quantify change of production rates from expected binary scaling

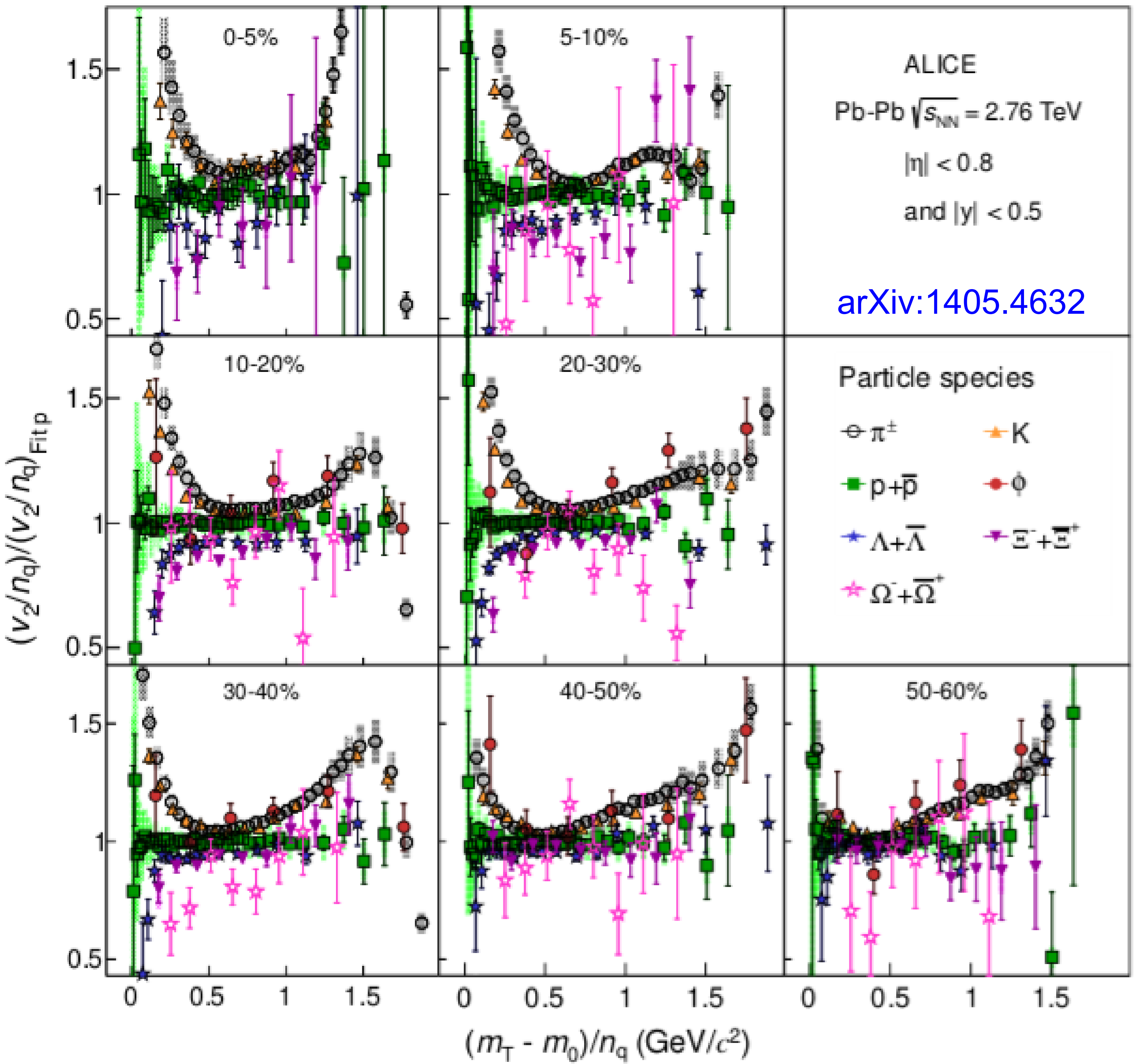
0-5%
5-10%
ALICE
Pb-Pb $\sqrt{s_{NN}}$ = 2.76 TeV
$|\eta| < 0.8$
and $|y| < 0.5$
arXiv:1405.4632
10-20%
20-30%
Particle species
$\pi^{\pm}$
K
$p+\bar{p}$
ϕ
$\Lambda+\bar{\Lambda}$
$\Xi^{-}+\bar{\Xi}^{+}$
$\Omega^{-}+\bar{\Omega}^{+}$
30-40%
40-50%
50-60%
$(v_2/n_q)/(v_2/n_q)_{\mathrm{Fit\,p}}$
$(m_T - m_0)/n_q$ (GeV/c^2)
0
0.5
1
1.5

Azimuthally sensitive pion femtoscopy

New preliminary

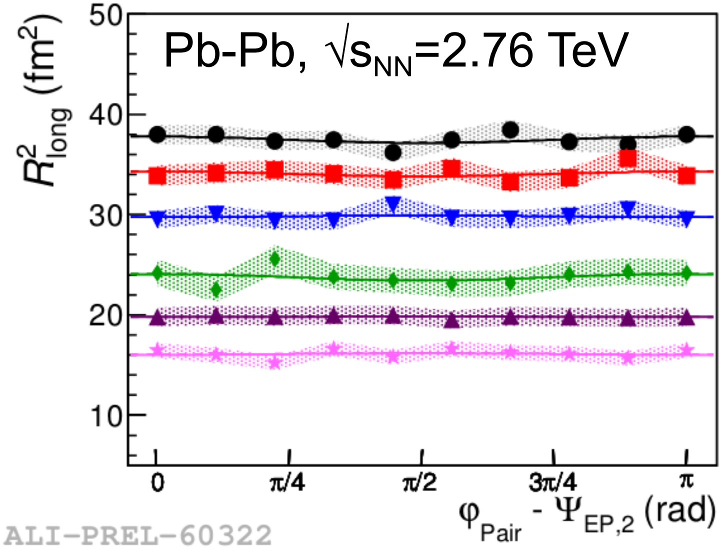

Local co-moving system (LCMS)

Δφ=0
Rside large
Rout small

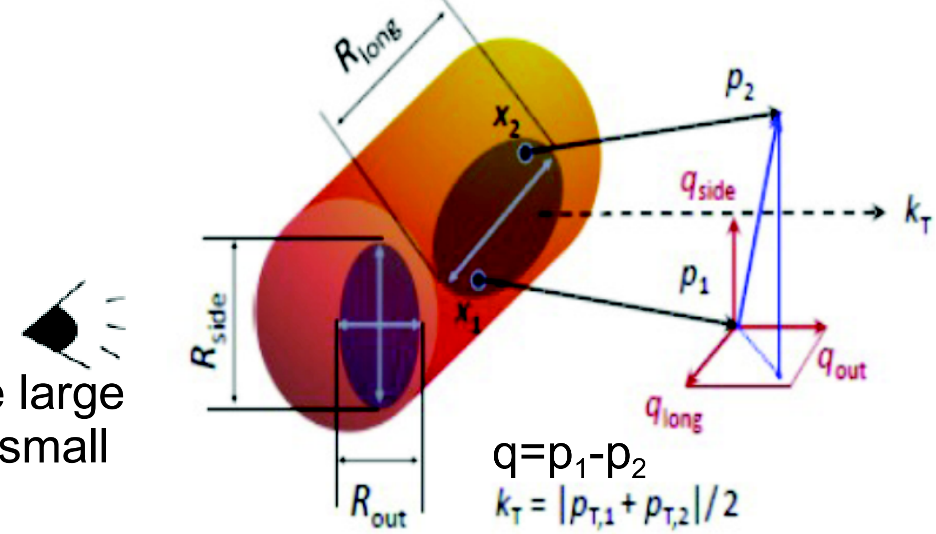

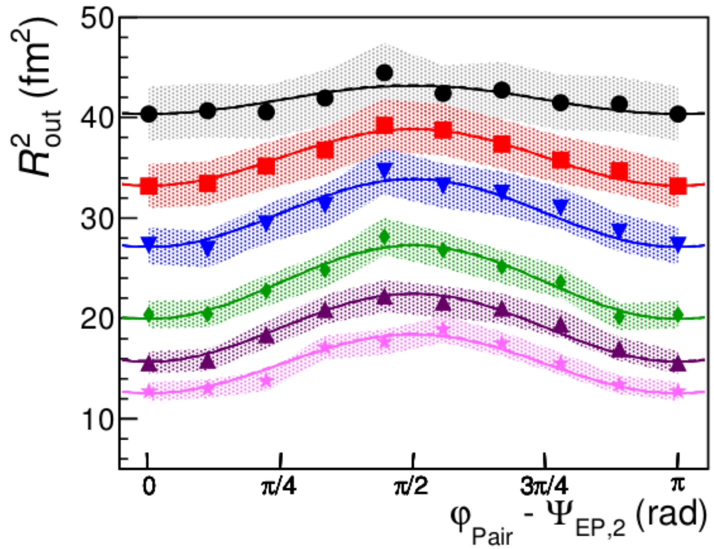

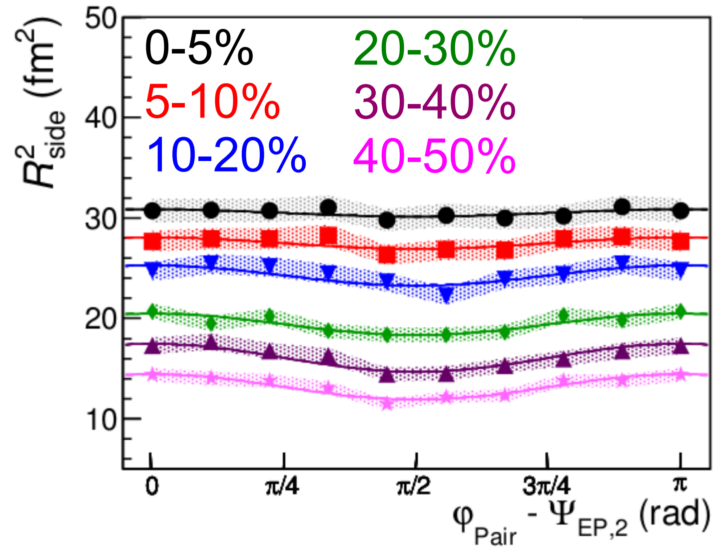

Expected dependence of 3D radii in LCMS relative to event plane angle

Particle ratios and chemical freeze-out

- Statistical (thermal) model

$$N_i \propto V \int \frac{d^3 p}{2\pi^3} \frac{1}{e^{(E_i - \mu_B B_i)/Tch} \pm 1}$$

  - Chemical potential depends on baryon number, strangeness and isospin
  - Two parameters: T_{ch}, μ_B
- Obtain: $T_{ch} \approx 164$ MeV $\approx T_c$
  - Holds for $\sqrt{s_{NN}} > 10–20$ GeV
- Ratios except p/π well described
- Disagreement for p/π may point to the relevance of other effects like
  - Rescattering in hadronic phase
  - Non-equilibrium effects
  - Flavor-dependent freeze-out

PRL 109 (2012) 252301

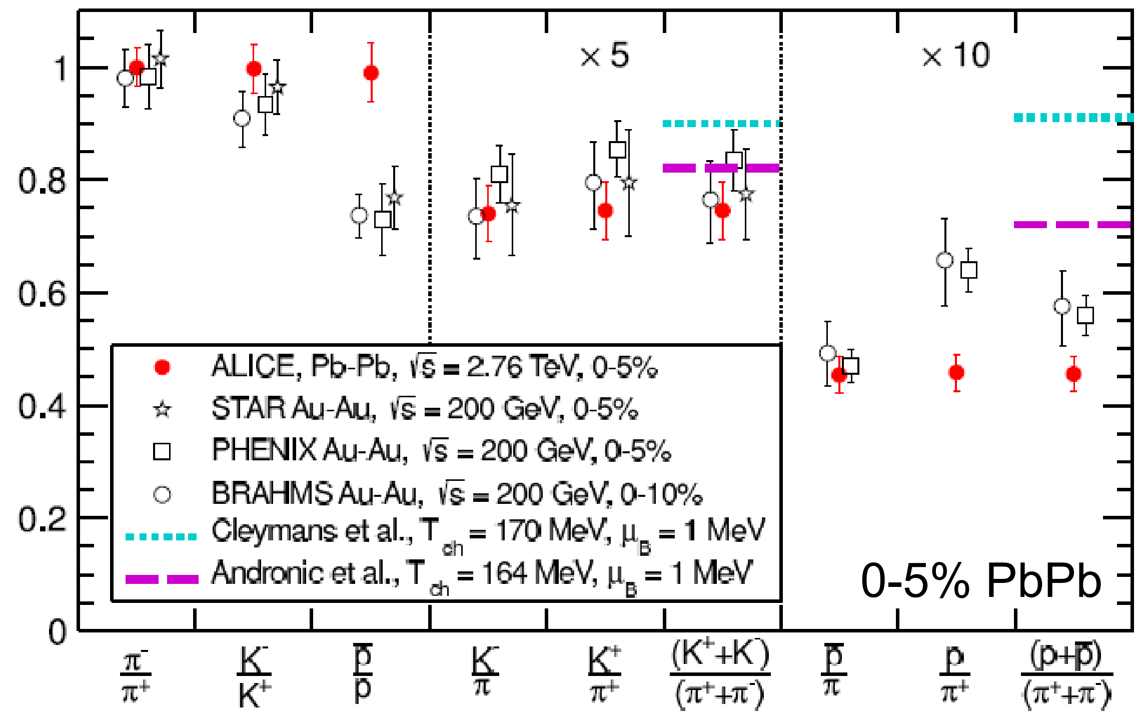

New preliminary results using a much larger set of particles including mult-strange particles points to slightly lower Tch

Jet suppression

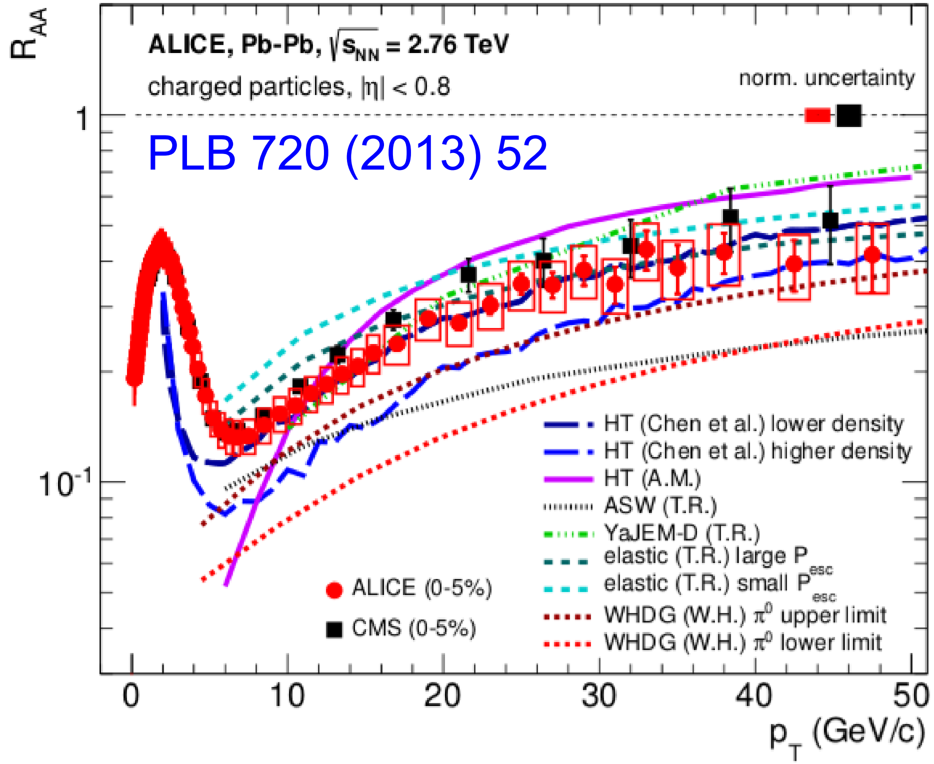

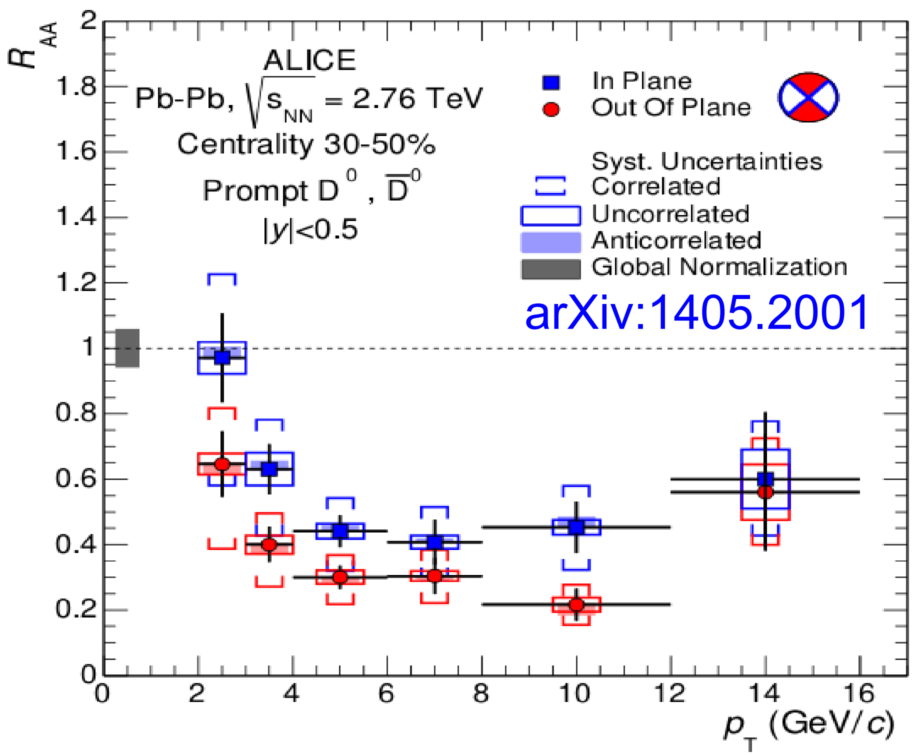

JHEP 1403 (2014) 013

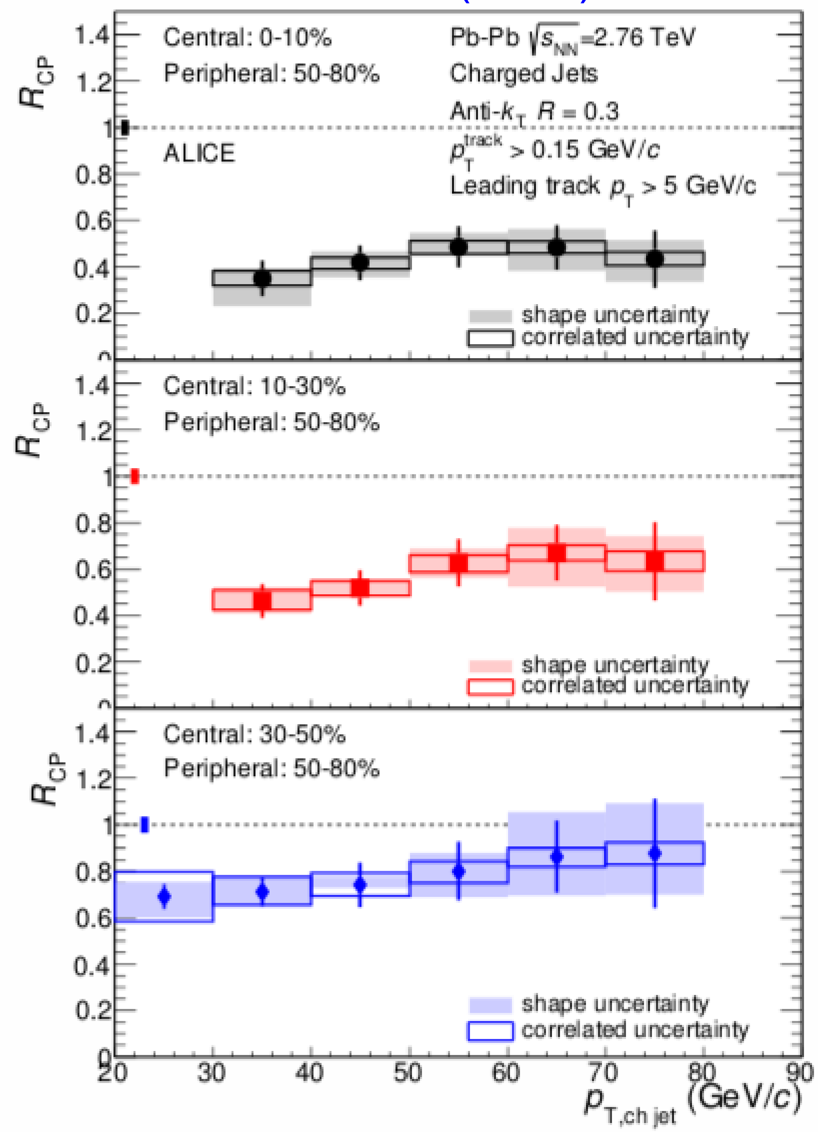

J/ψ production in Pb-Pb

arXiv:1311.0214

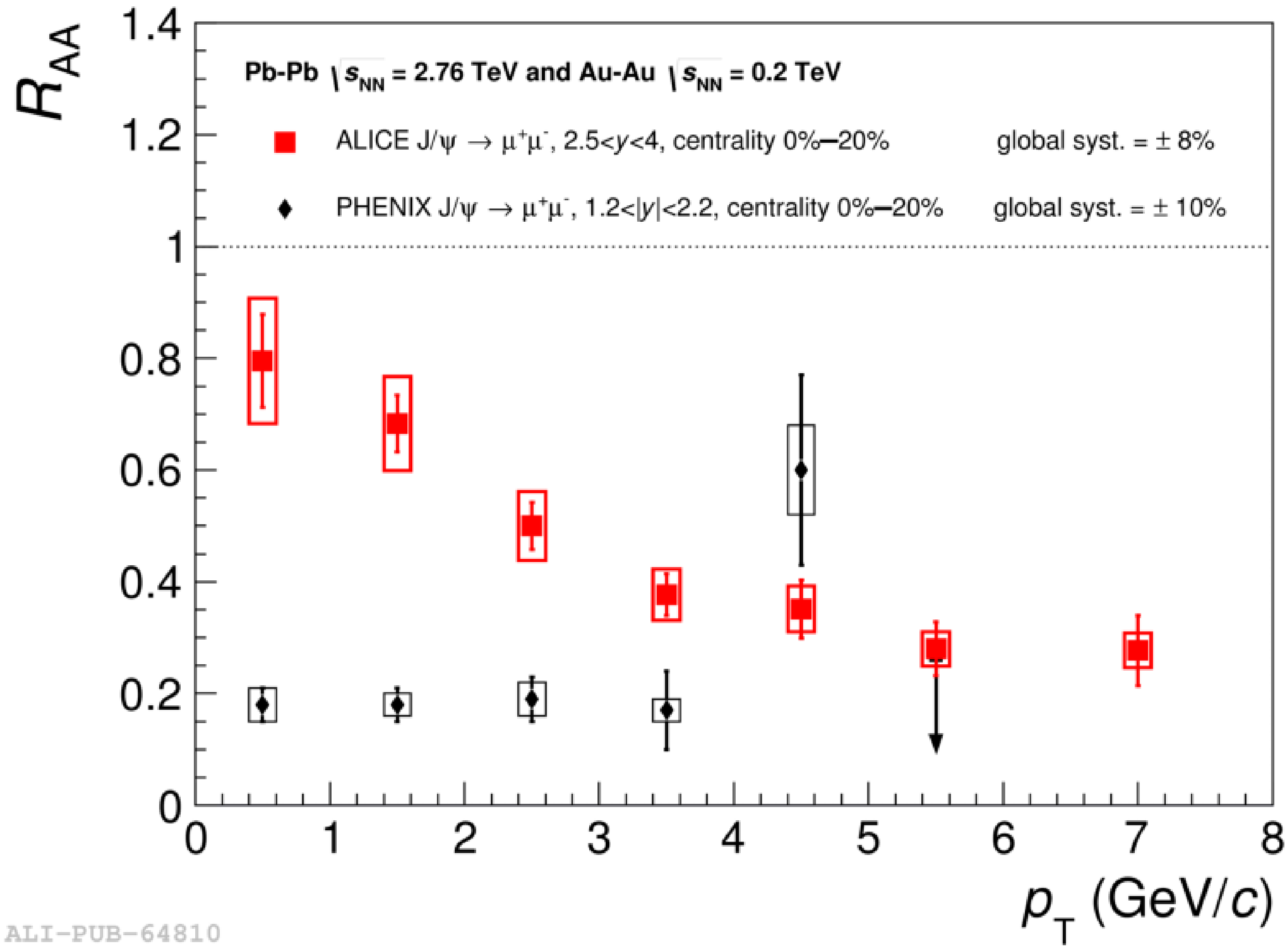

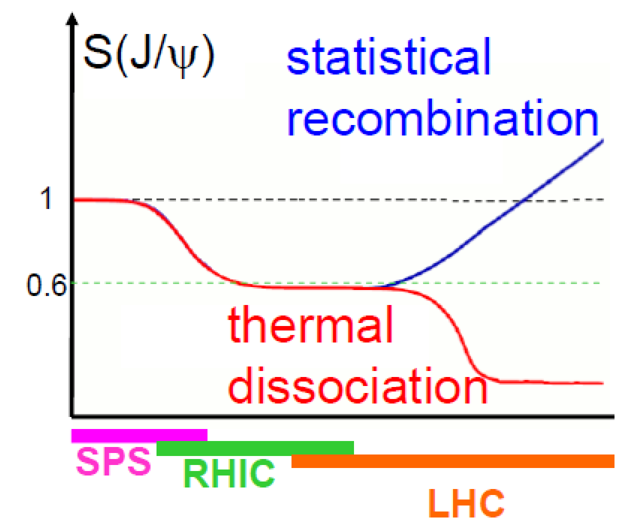

Different p_T (and centrality) dependence of J/ψ R_{AA} at LHC and RHIC

J/ψ production in Pb-Pb

arXiv:1311.0214

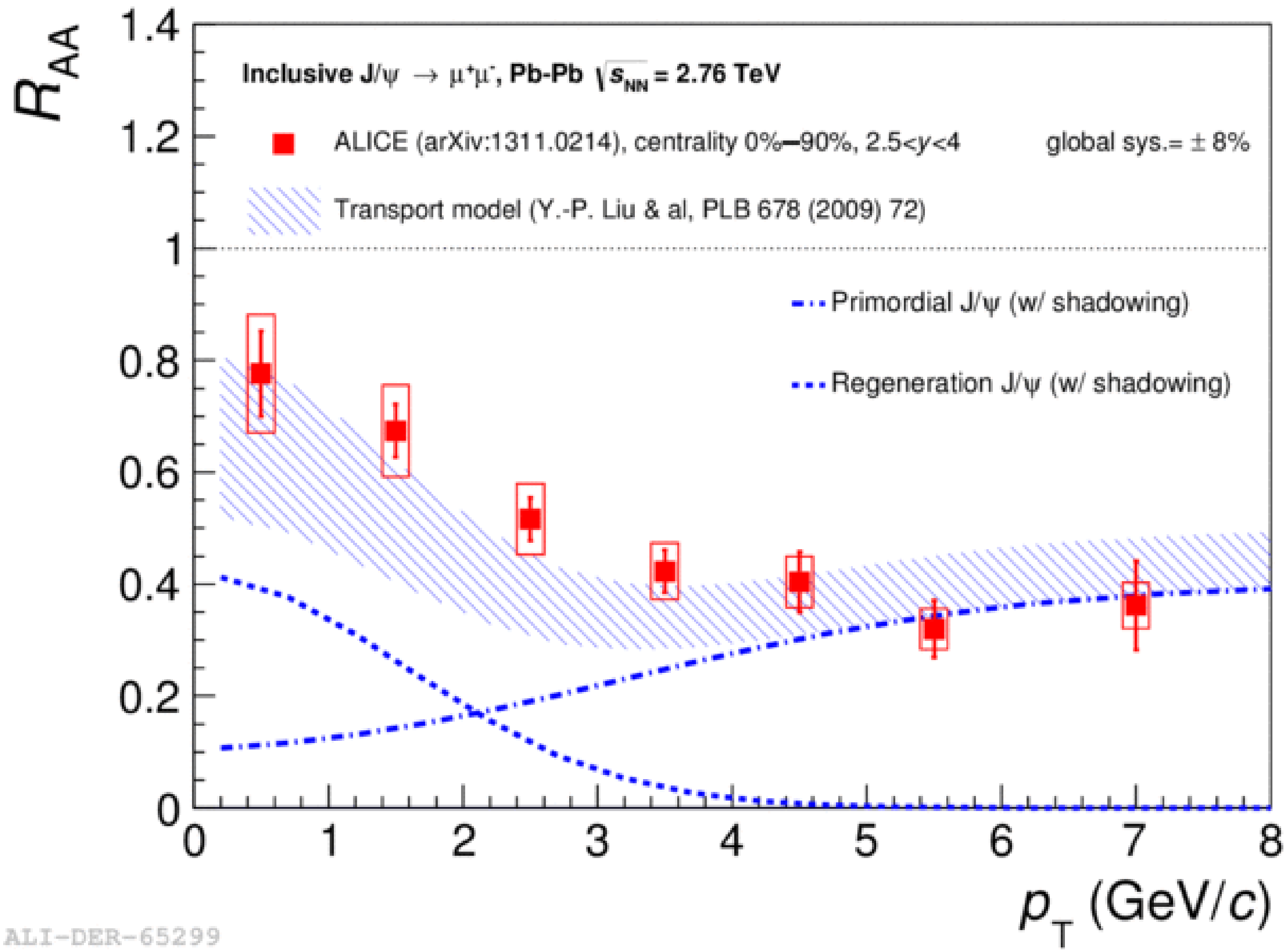

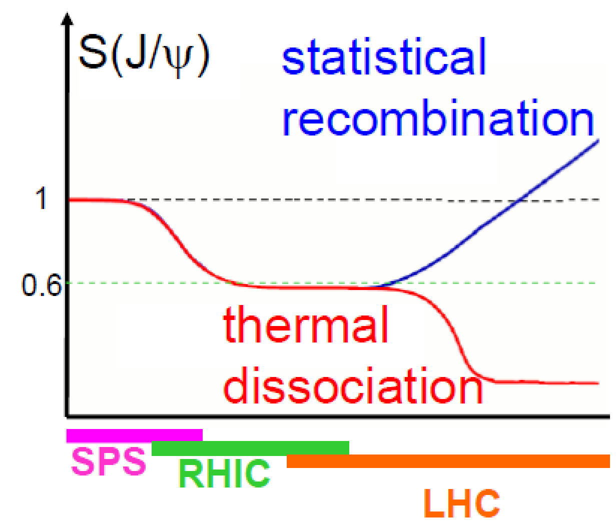

As expected in a scenario with $c\bar{c}$ recombination, especially at low p_T

pPb and Pbp collisions at the LHC

- 2-in-1 design for magnets
  - Identical bending field in two beams
  - Locks the relation between the two beams:
    - p(Pb) = Z p(proton)
    - Different speeds for the two beams!
  - Adjust length of closed orbits to compensate different speeds
  - Different RF freq for two beams at injection and ramps
- Short low lumi (~2/μb) pilot run on 12/9/2012
- First run in Jan-Feb 2013: ~ 30/nb
  - p(proton) = 4 TeV
  - Center-of-mass energy 5.02 TeV
  - Center-of-mass with Δy=0.465 wrt lab system in direction of proton beam
  - Two beam configurations were provided

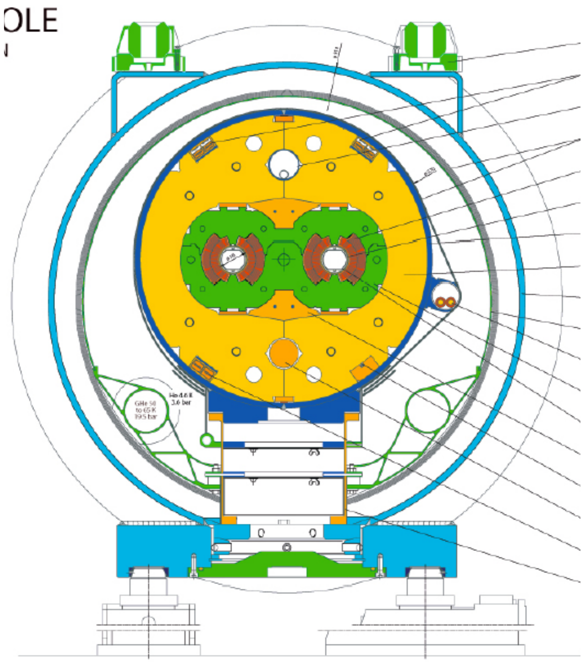

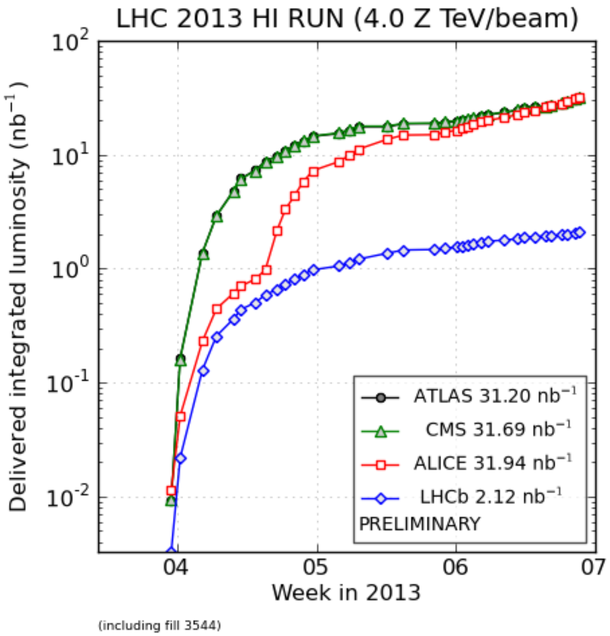

Charged particle pseudorapidity density

- Tracklet based analysis
  - Dominant systematic uncertainty from NSD normalization of 3.1%
- Reach of SPD extended to |η|<2 by extending the z-vertex range
- Results in ALICE laboratory system
  - Δy_{cms} = - 0.465 (direction of proton)
- Comparison with models
  - Most models within 20%
  - Saturation models have too steep rise between p and Pb region
  - See for further comparisons Albacete et al., arXiv:1301.3395

ALICE, PRL 110 (2013) 032301

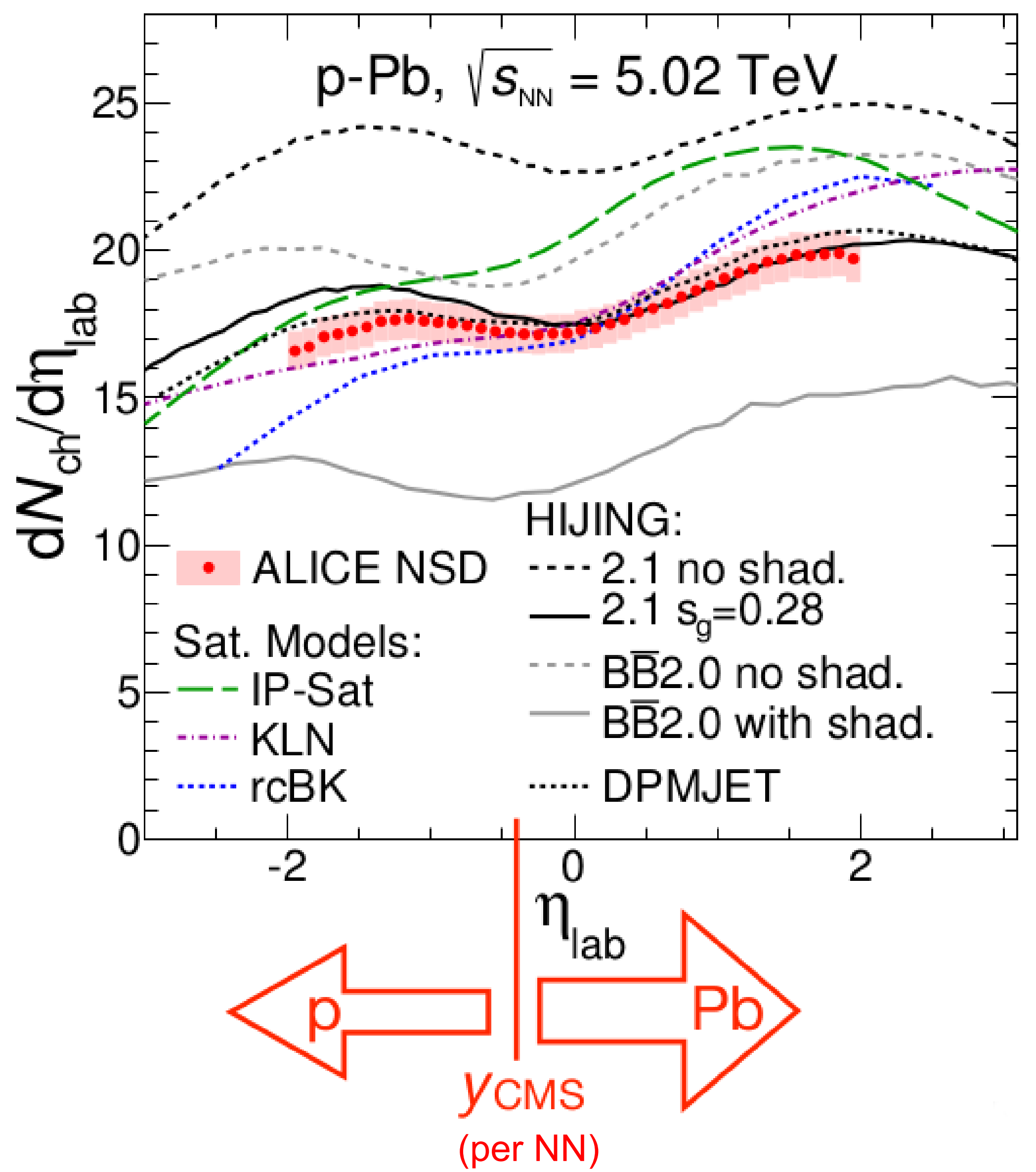

NB: HIJING calculations are expected to increase by ~4% from INEL to NSD

DHC: Two ridges

ALICE, PLB 719 (2013) 29

- A closer look at the two ridges: the near- and away-side ridges
  - Are essentially flat in Δη
    - Slight excess on near side due to small residual jet peak
  - Have the same magnitude

- Projection to Δφ
  - Exclude residual peak (|Δη<0.8| on near-side) exhibits a modulation
  - In HIJING, the correlation shows no qualitative changes with multiplicity
  - Quantify the ridges
    - Ridge yields
    - Fourier coefficients

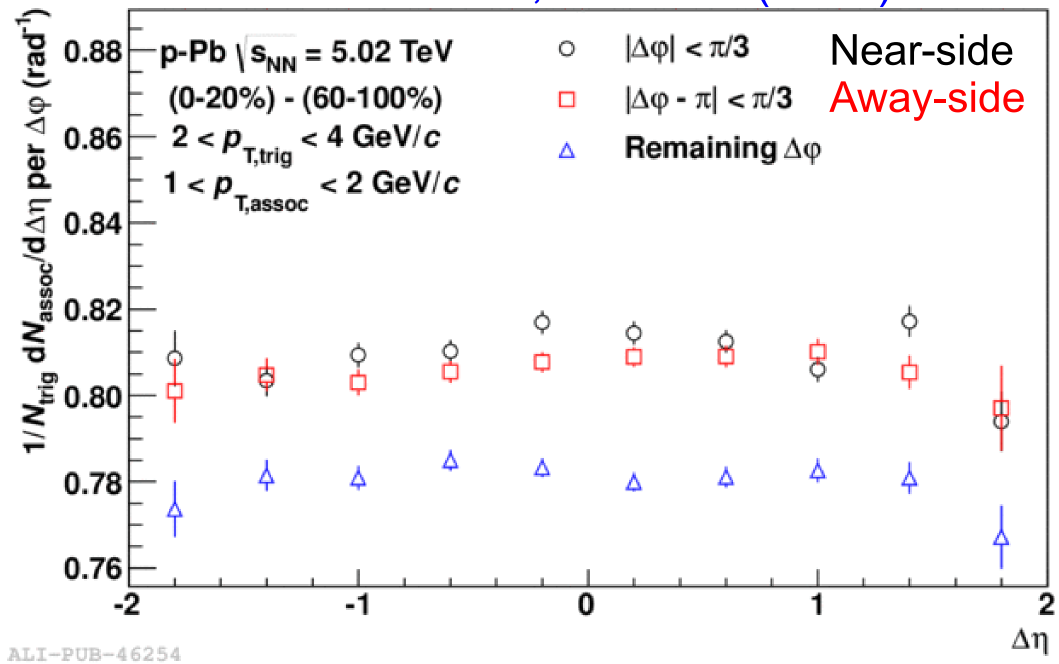

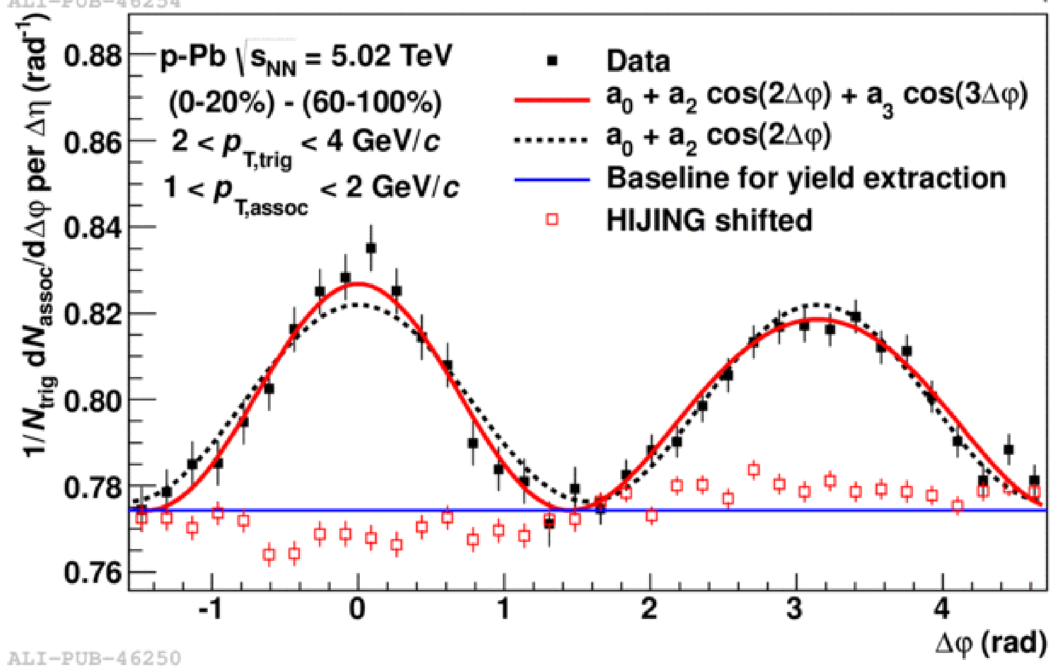

DHC: Ridge yields

- Integrate two ridges above baseline on the
  - Near side (|Δ|<π/2)
  - Away side (π/2<|Δ|<3π/2)
- Near and away-side ridge yields
  - Change significantly
  - Agree for all p_T and multiplicity ranges
  - Increase with trigger p_T and multiplicity
  - Widths are approximately the same (not shown)
- The correlation between near- and away-side yields suggests a common underlying origin

ALICE, PLB 719 (2013) 29

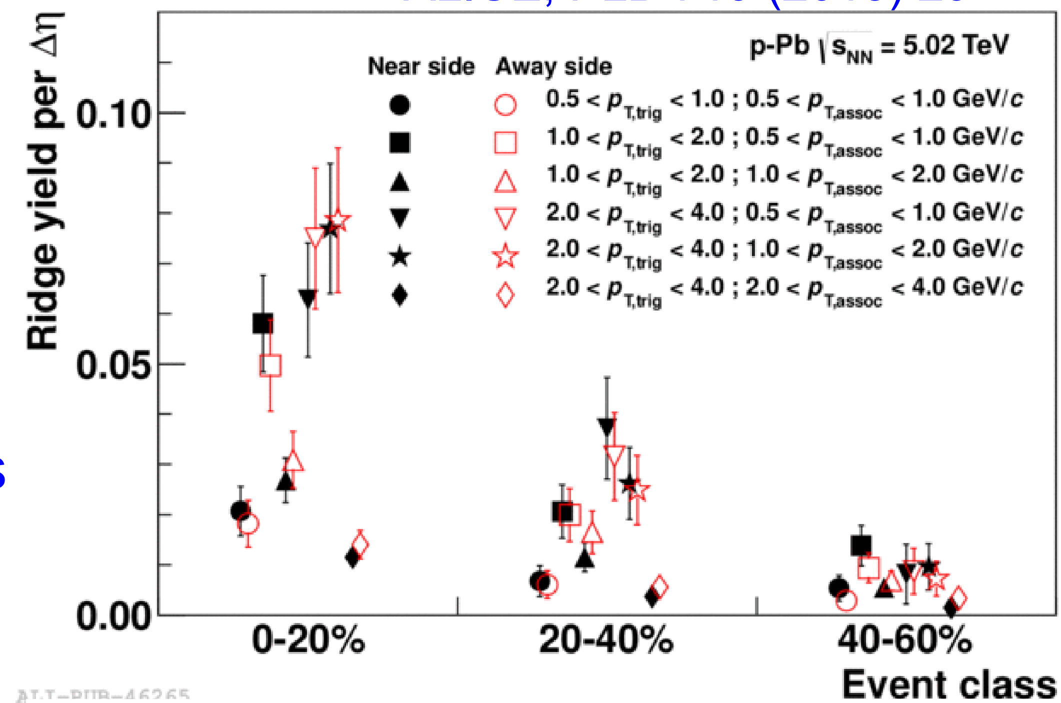

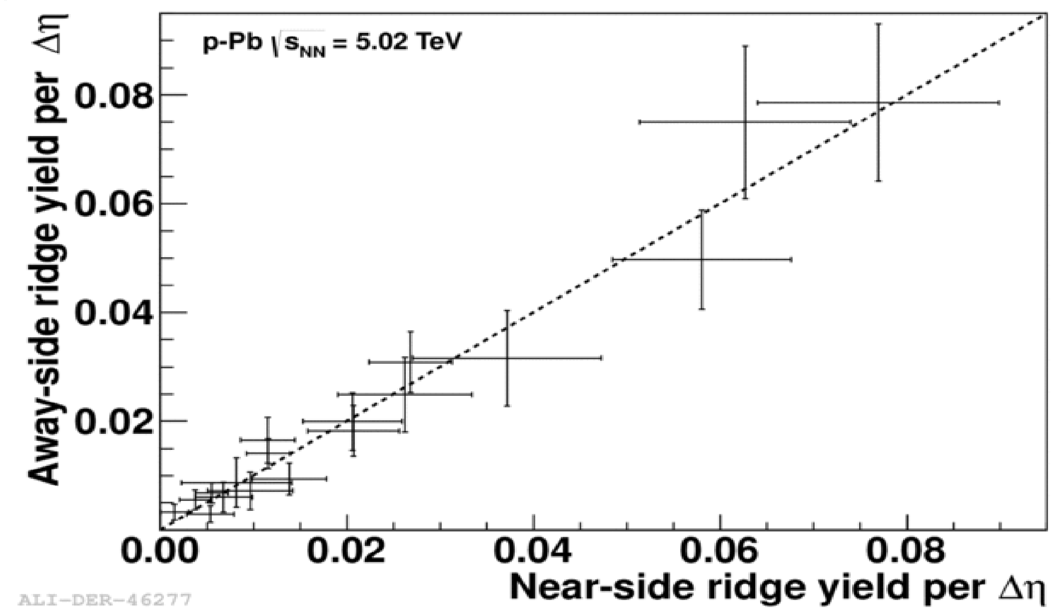

DHC: Symmetric ridge

ALICE, PLB 719 (2013) 29

- What would the assumption of a symmetric ridge give?
  - Determine the near-side ridge in $1.2 < |\Delta\eta| < 1.8$
  - Mirror to away-side and subtract

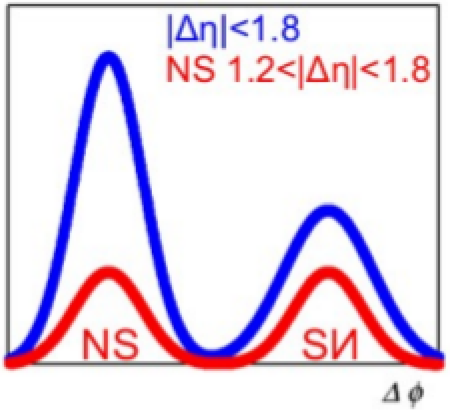

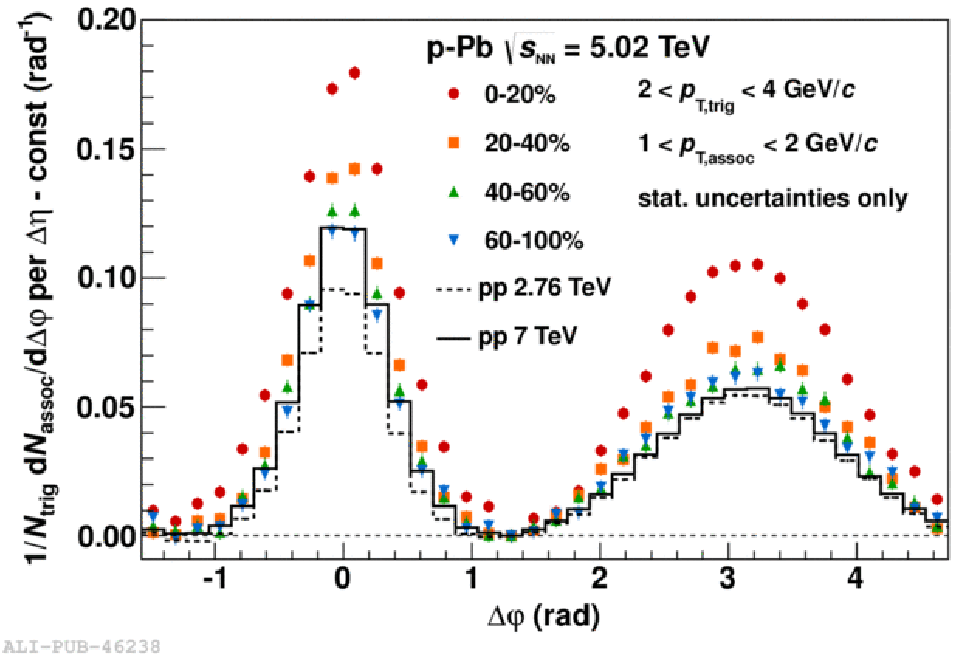

Subtract →

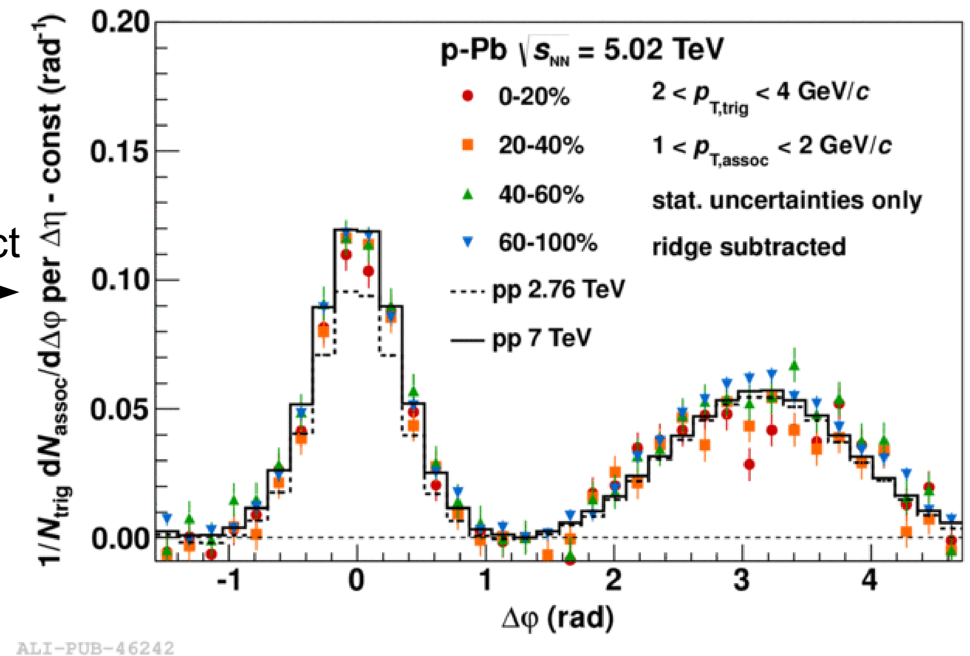

- No significant other multiplicity dependent structures left over

Particle ratios versus p_T

$0<y_{cms}<0.5$

ALICE, arXiv:1307.6796

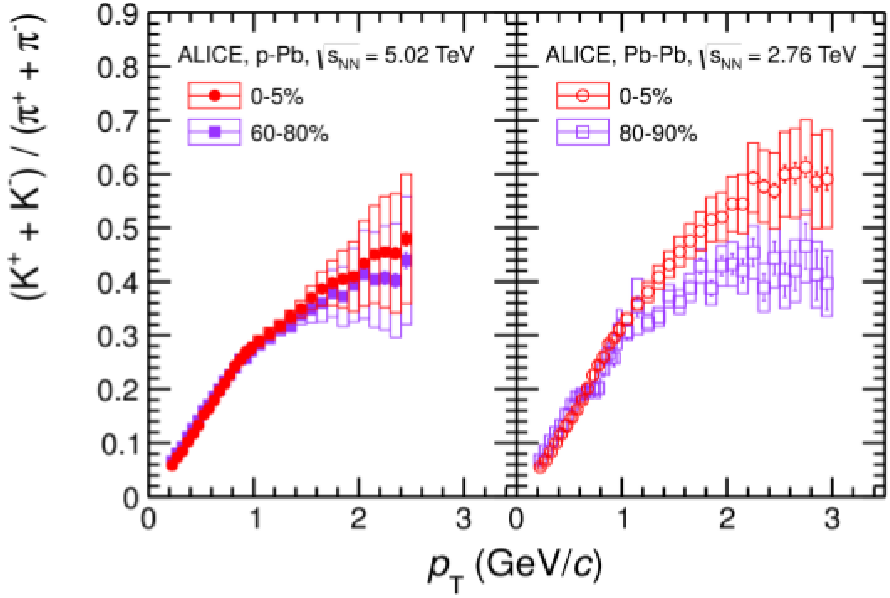

- Particle ratios in pPb show similar trends than those in PbPb
- The strength of the effects is similar to those in peripheral PbPb collisions
- Increase of p/π and Λ/K in PbPb usually explained by radial flow and/or parton recombination

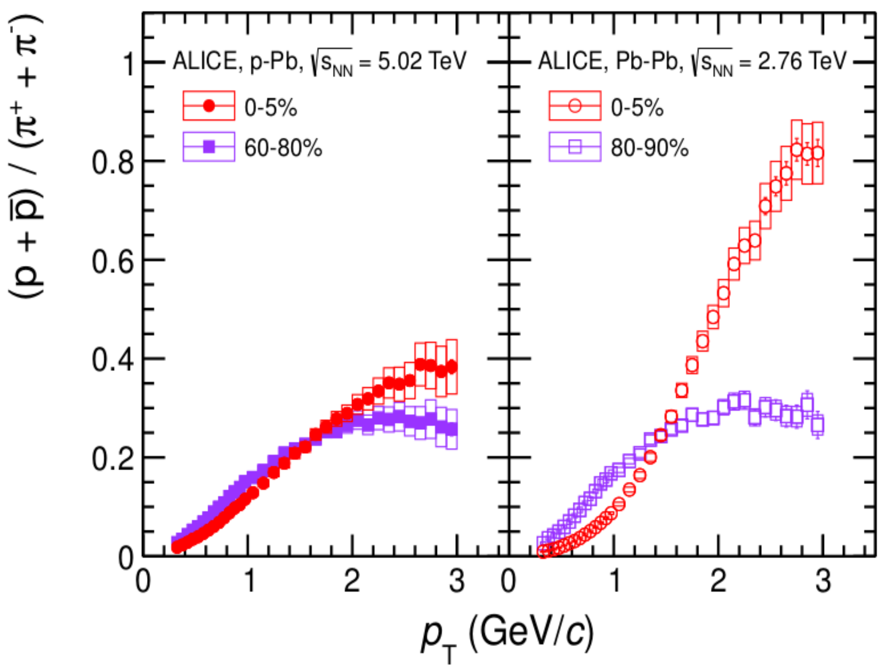

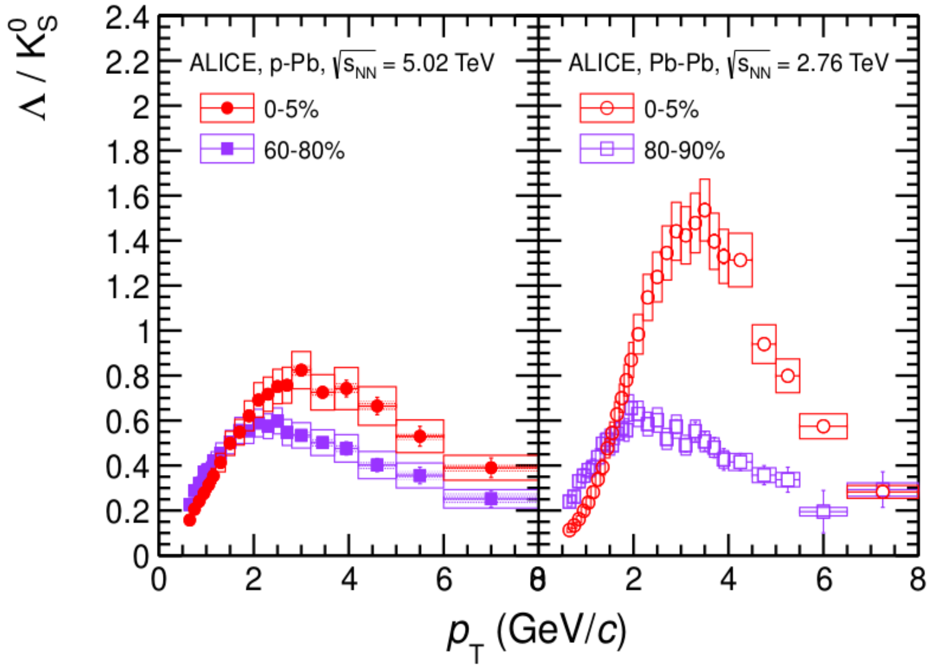

Multiplicity scaling of ratios

$0<y_{cms}<0.5$

ALICE, arXiv:1307.6796

- Fit ratio vs dN/dη in p_T bins with power-law ($A\,x^B$ with x=dN/dη)
- Same increase of ratio for similar increase of dN/dη in pPb and PbPb
- Same power-law scaling exponent (B) in pPb and PbPb
  - Underlying mechanism?
- Similar scaling found for p/π

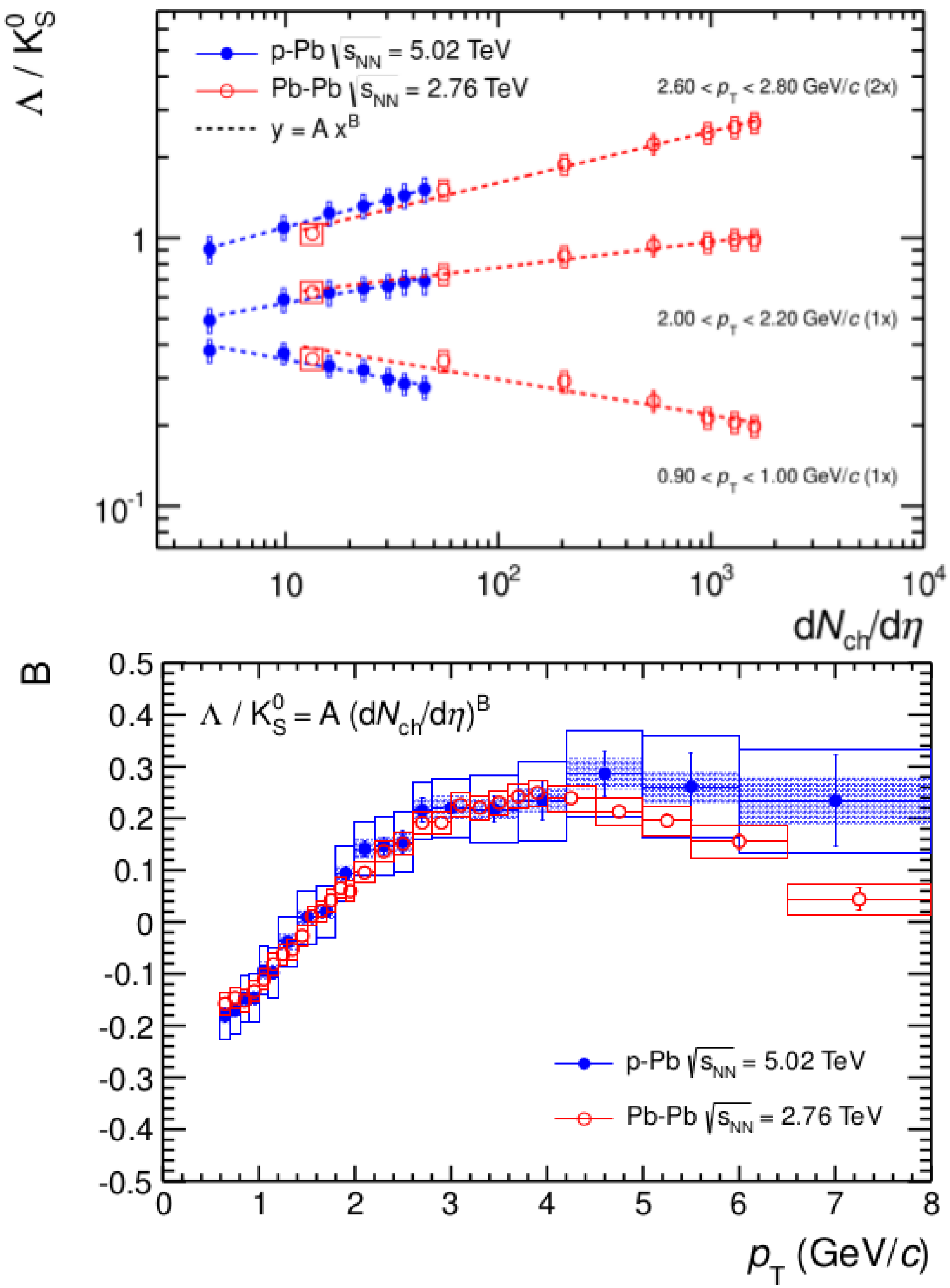

Similar scaling also holds for pp

Insights from data

- Two-particle angular correlation analysis at low p_T are ideal to statistically study mini-jet production
- $p_T > 0.7$ GeV/c ($>>\Lambda_{QCD}$ to be insensitive to string breaking)
- Analysis similar to pp (ALICE, JHEP 1309 (2013) 049) except subtraction of double ridge
- Obtain yields from fit as

$$< N_{\mathrm{trigger}} >= \frac{N_{\mathrm{trigger}}}{N_{\mathrm{events}}}$$

$$< N_{\mathrm{assoc,nearside}} >= \frac{\sqrt{2\pi}}{N_{\mathrm{trigger}}}(A_1 \cdot \sigma_1 + A_2 \cdot \sigma_2)$$

$$< N_{\mathrm{assoc,awayside}} >= \frac{\sqrt{2\pi}}{N_{\mathrm{trigger}}}(A_3 \cdot \sigma_3)$$

ALICE preliminary

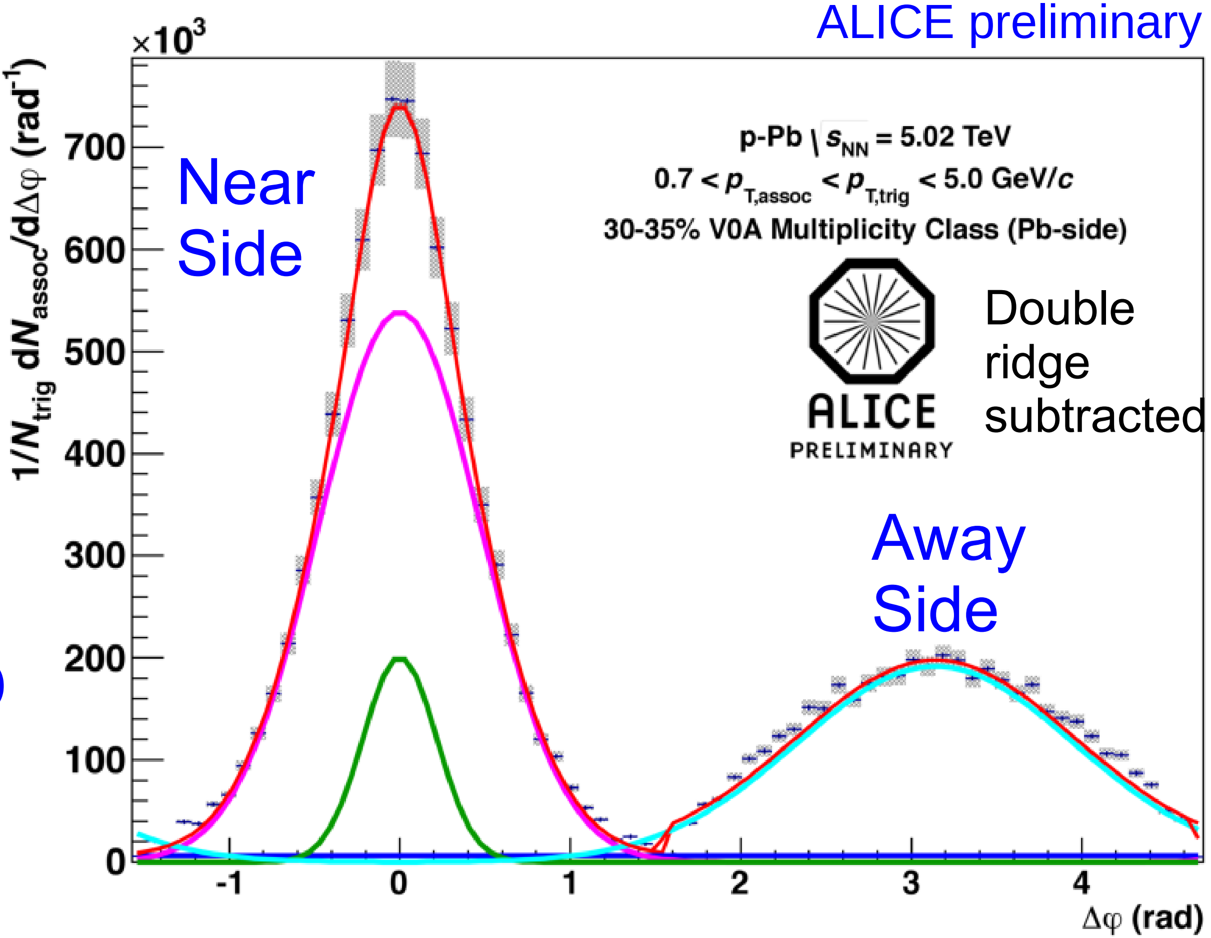

Fit with Double Gaussians:

$$f(\Delta\varphi) = C + A_1\ exp\left(-\frac{\Delta\varphi^2}{2\cdot\sigma_1^2}\right) + A_1\ exp\left(-\frac{(\Delta\varphi-2\pi)^2}{2\cdot\sigma_1^2}\right) +$$

$$+A_2\ exp\left(-\frac{\Delta\varphi^2}{2\cdot\sigma_2^2}\right) + A_2\ exp\left(-\frac{(\Delta\varphi-2\pi)^2}{2\cdot\sigma_2^2}\right) +$$

$$+A_3\ exp\left(-\frac{(\Delta\varphi-\pi)^2}{2\cdot\sigma_3^2}\right) + A_3\ exp\left(-\frac{(\Delta\varphi+\pi)^2}{2\cdot\sigma_3^2}\right).$$

Number of uncorrelated seeds

ALICE preliminary

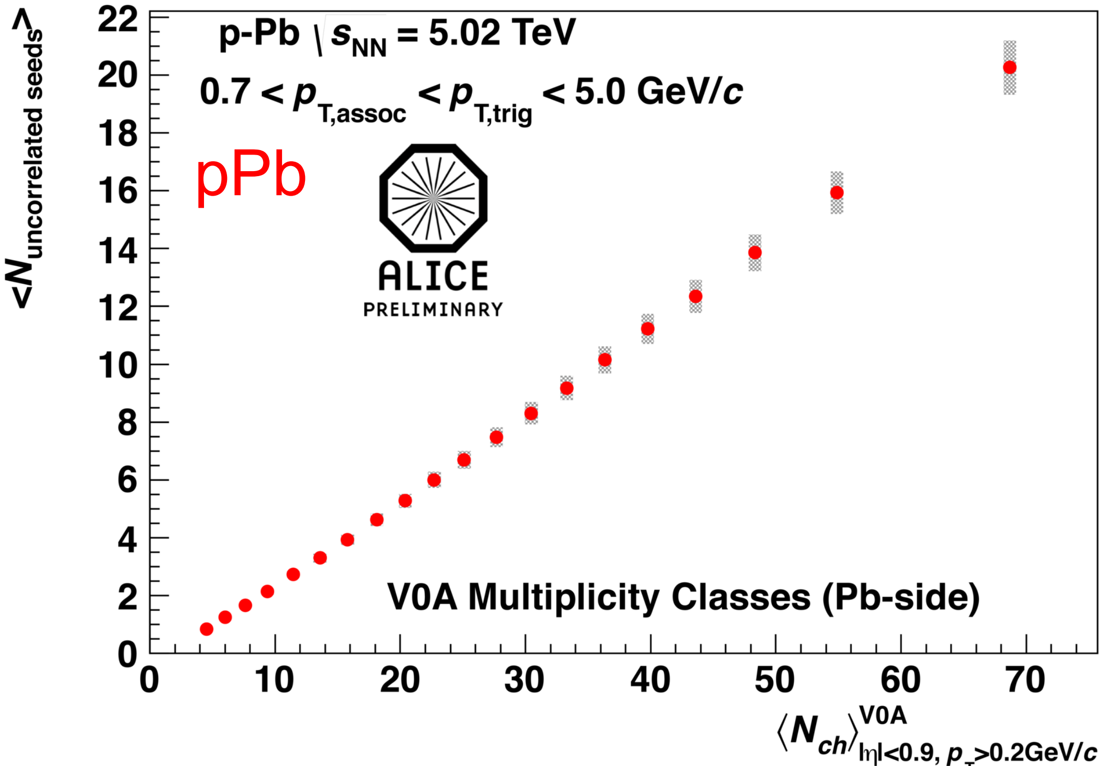

ALICE, JHEP 1309 (2013) 049

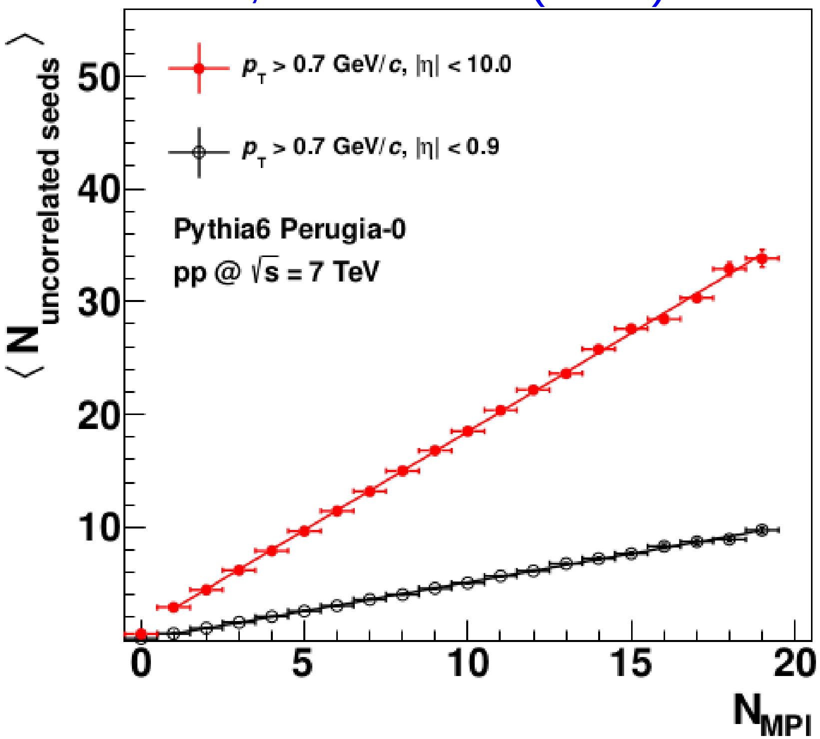

Define number of uncorrelated seeds:

$$< N_{\text{uncorrelated seeds}} >= \frac{< N_{\text{trigger}} >}{< N_{\text{trigger correlated}} >} = \frac{< N_{\text{trigger}} >}{< 1 + N_{\text{assoc,near+away}} >}$$

- In pPb, the number of uncorrelated seeds scales with V0A multiplicity
- In Pythia, the number of uncorrelated seeds scale with number of MPI

Bias in number of hard scatters

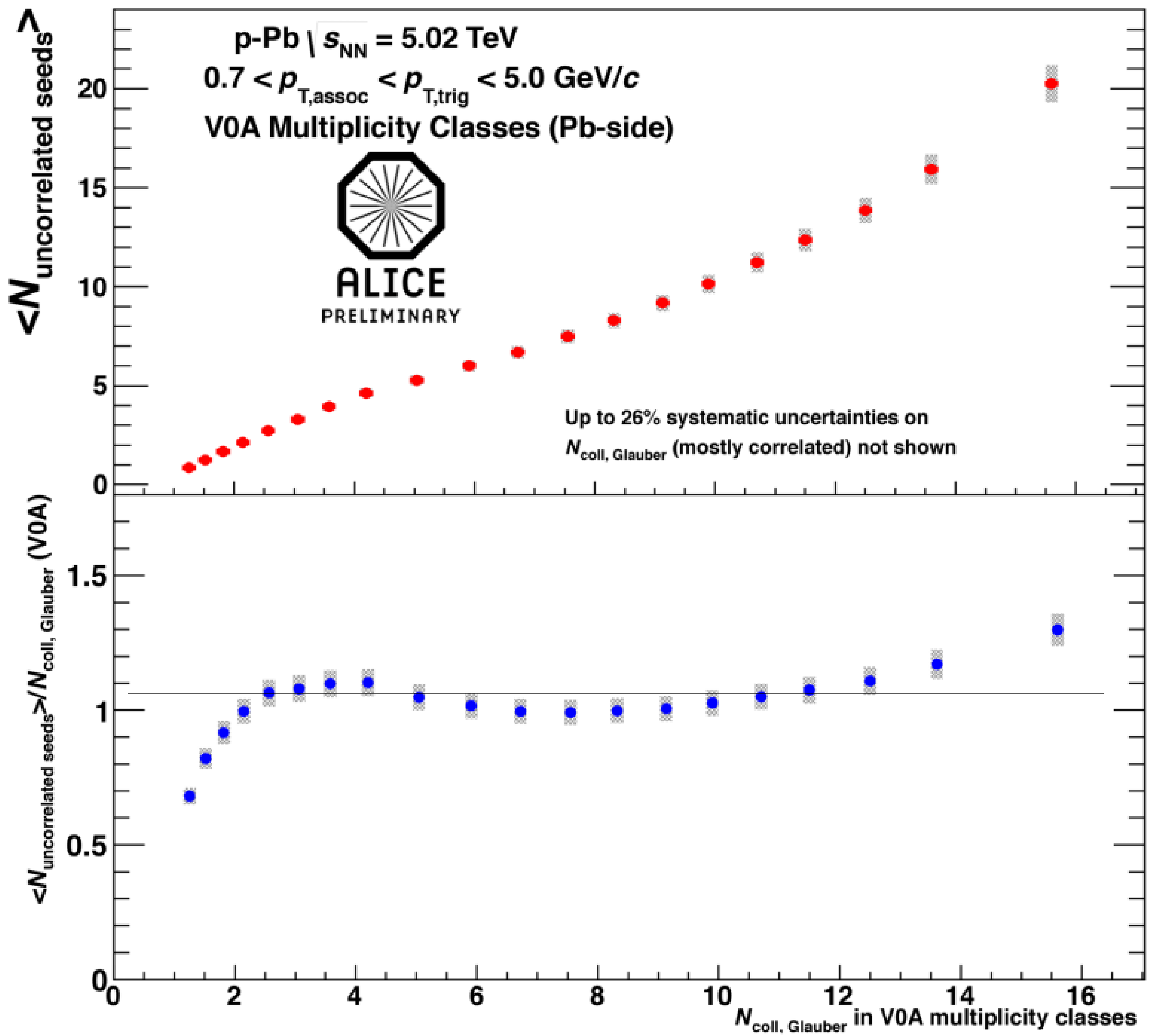

Approximate scaling (~10%) for N_{coll} between 3 and 13, and strong deviation for peripheral and central collisions

Near-side yield

ALICE preliminary

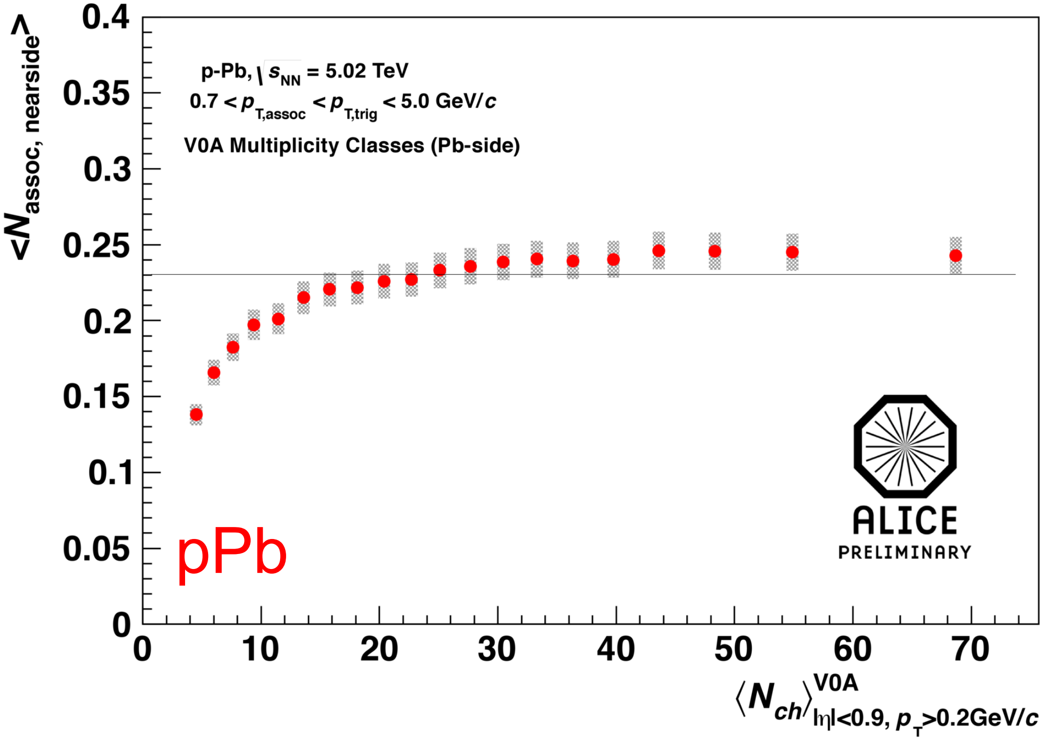

ALICE, JHEP 1309 (2013) 049

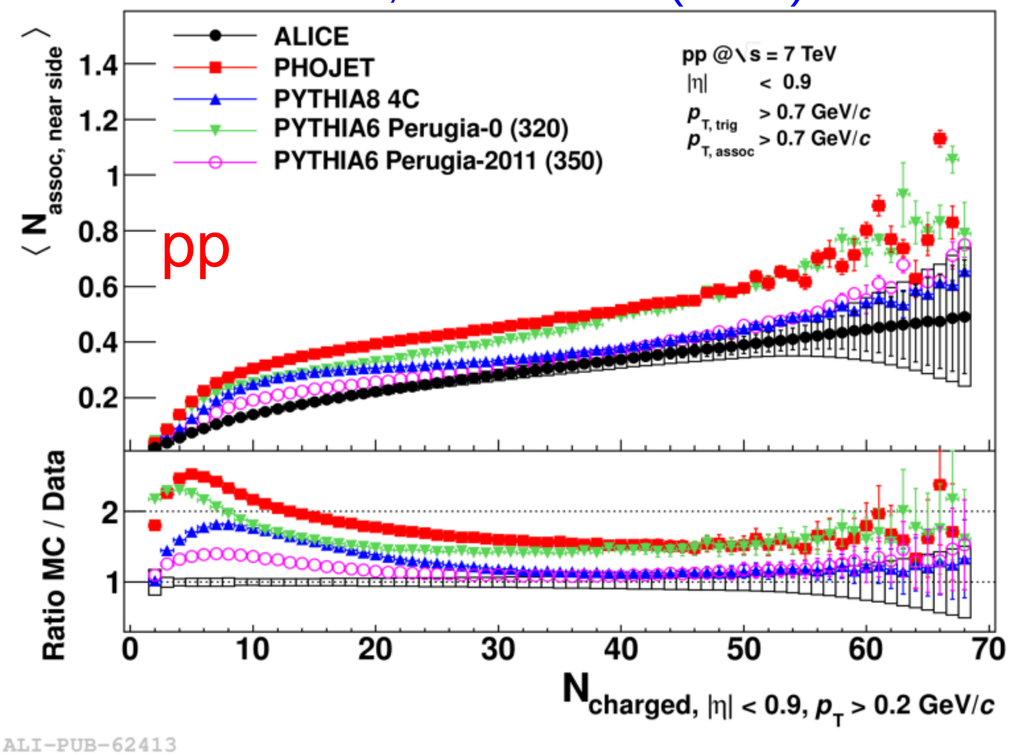

- In pPb, no bias on the near-side per trigger yield except for low multiplicities
- Bias to softer than average collisions
- Caveat: Different event selection than in pp

Away-side yield

ALICE preliminary

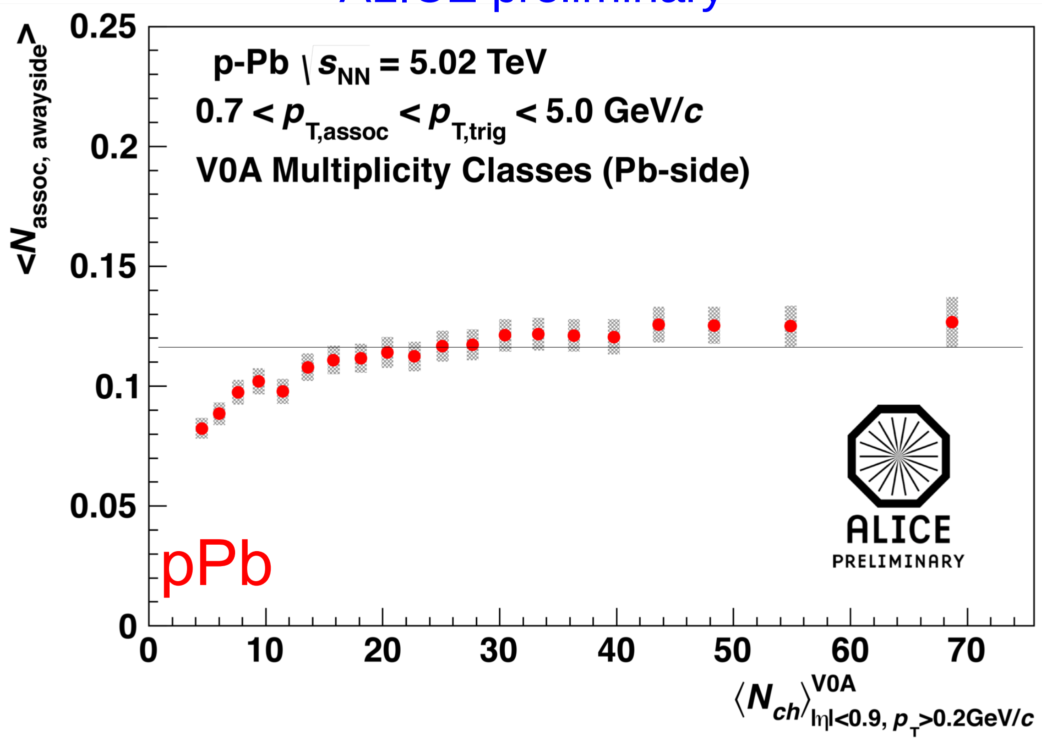

ALICE, JHEP 1309 (2013) 049

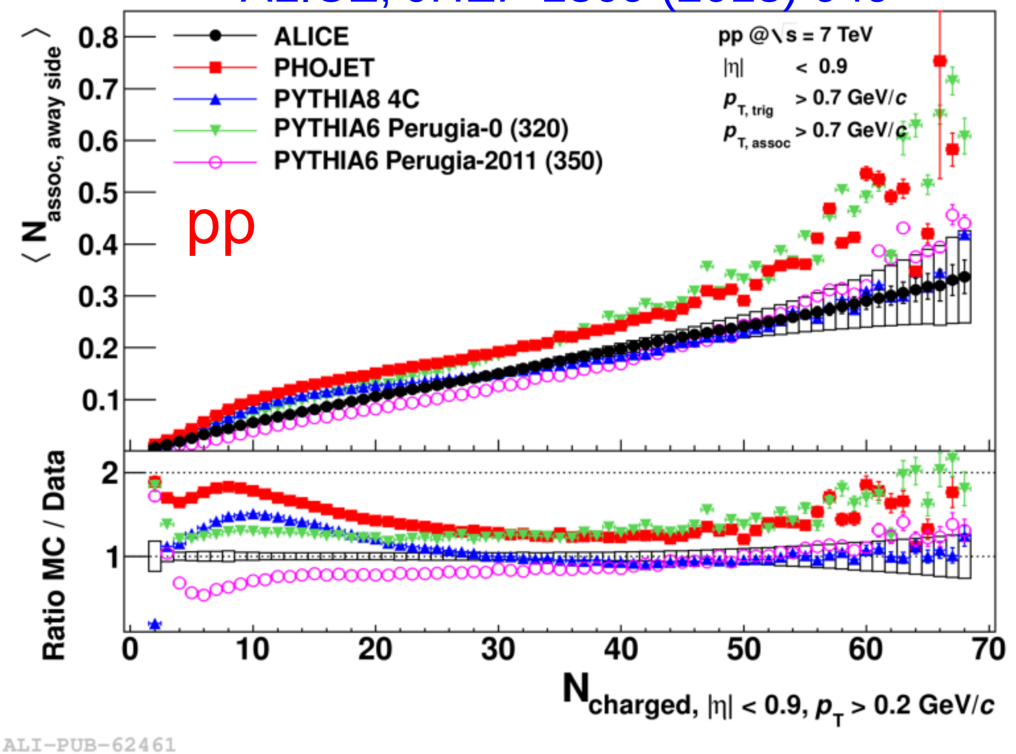

- In pPb, no bias on the away-side per trigger yield except for low multiplicities
- Bias to softer than average collisions
- Caveat: Different event selection than in pp

The Φ meson

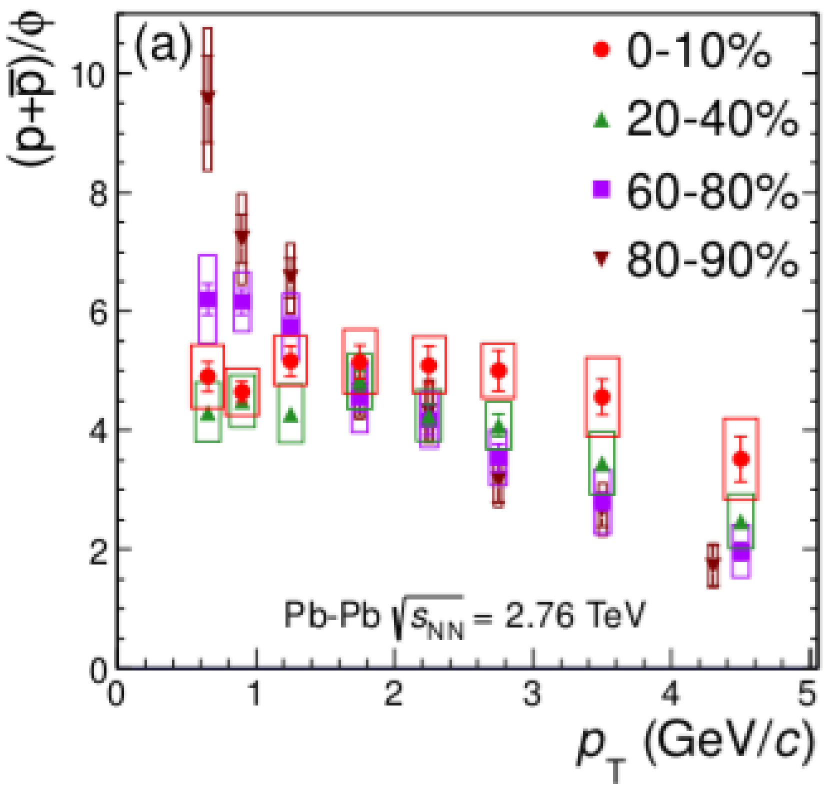

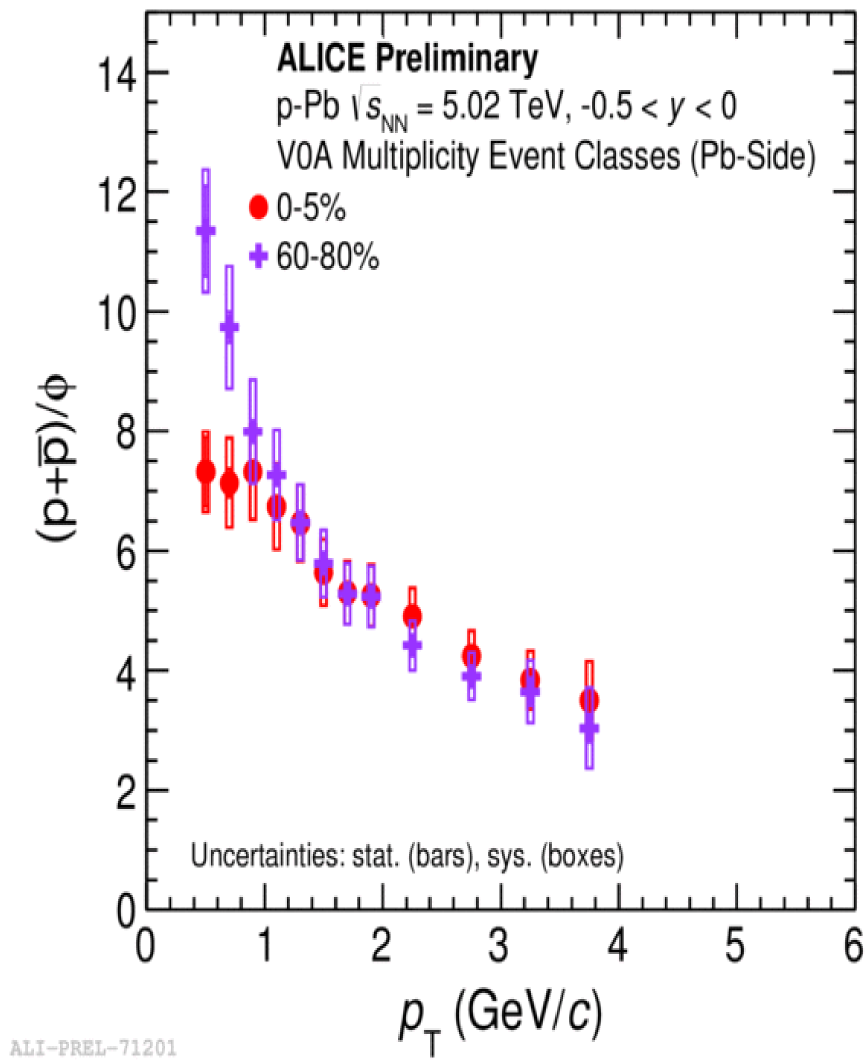

Unlike in PbPb, the Φ meson does not have the same shape as the p in 0-5% V0A class.

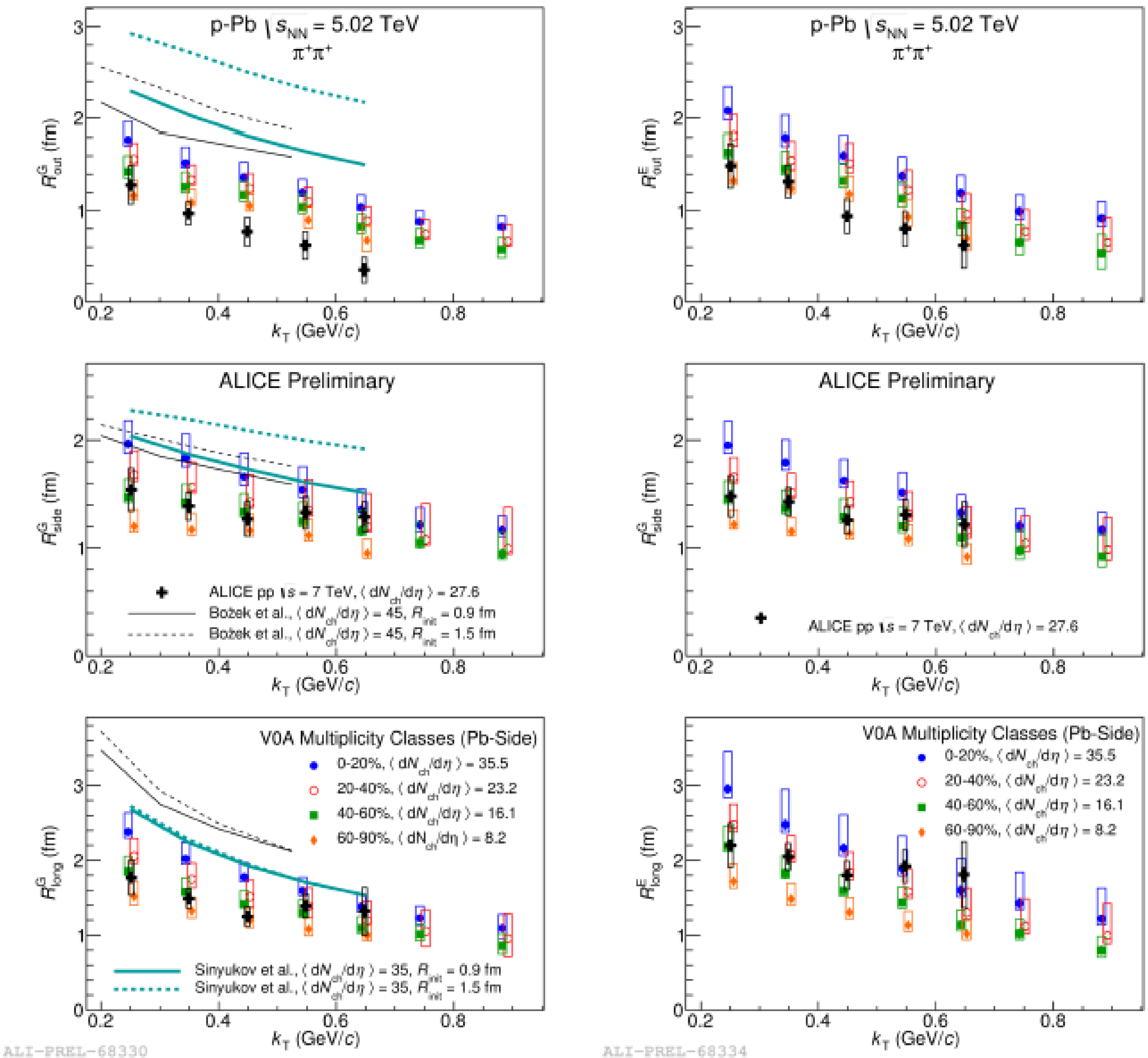
p-Pb $\sqrt{s_{NN}}$ = 5.02 TeV
$\pi^+\pi^+$
ALICE Preliminary
V0A Multiplicity Classes (Pb-Side)
0-20%, ⟨ $dN_{ch}/d\eta$ ⟩ = 35.5
20-40%, ⟨ $dN_{ch}/d\eta$ ⟩ = 23.2
40-60%, ⟨ $dN_{ch}/d\eta$ ⟩ = 16.1
60-90%, ⟨ $dN_{ch}/d\eta$ ⟩ = 8.2
ALICE pp $\sqrt{s}$ = 7 TeV, ⟨ $dN_{ch}/d\eta$ ⟩ = 27.6
Božek et al., ⟨ $dN_{ch}/d\eta$ ⟩ = 45, R_{init} = 0.9 fm
Božek et al., ⟨ $dN_{ch}/d\eta$ ⟩ = 45, R_{init} = 1.5 fm
Sinyukov et al., ⟨ $dN_{ch}/d\eta$ ⟩ = 35, R_{init} = 0.9 fm
Sinyukov et al., ⟨ $dN_{ch}/d\eta$ ⟩ = 35, R_{init} = 1.5 fm
R^G_{out} (fm)
R^G_{side} (fm)
R^G_{long} (fm)
R^E_{out} (fm)
R^G_{side} (fm)
R^E_{long} (fm)
k_T (GeV/c)
ALI-PREL-68330
ALI-PREL-68334

Comparison of 1d and 3d results

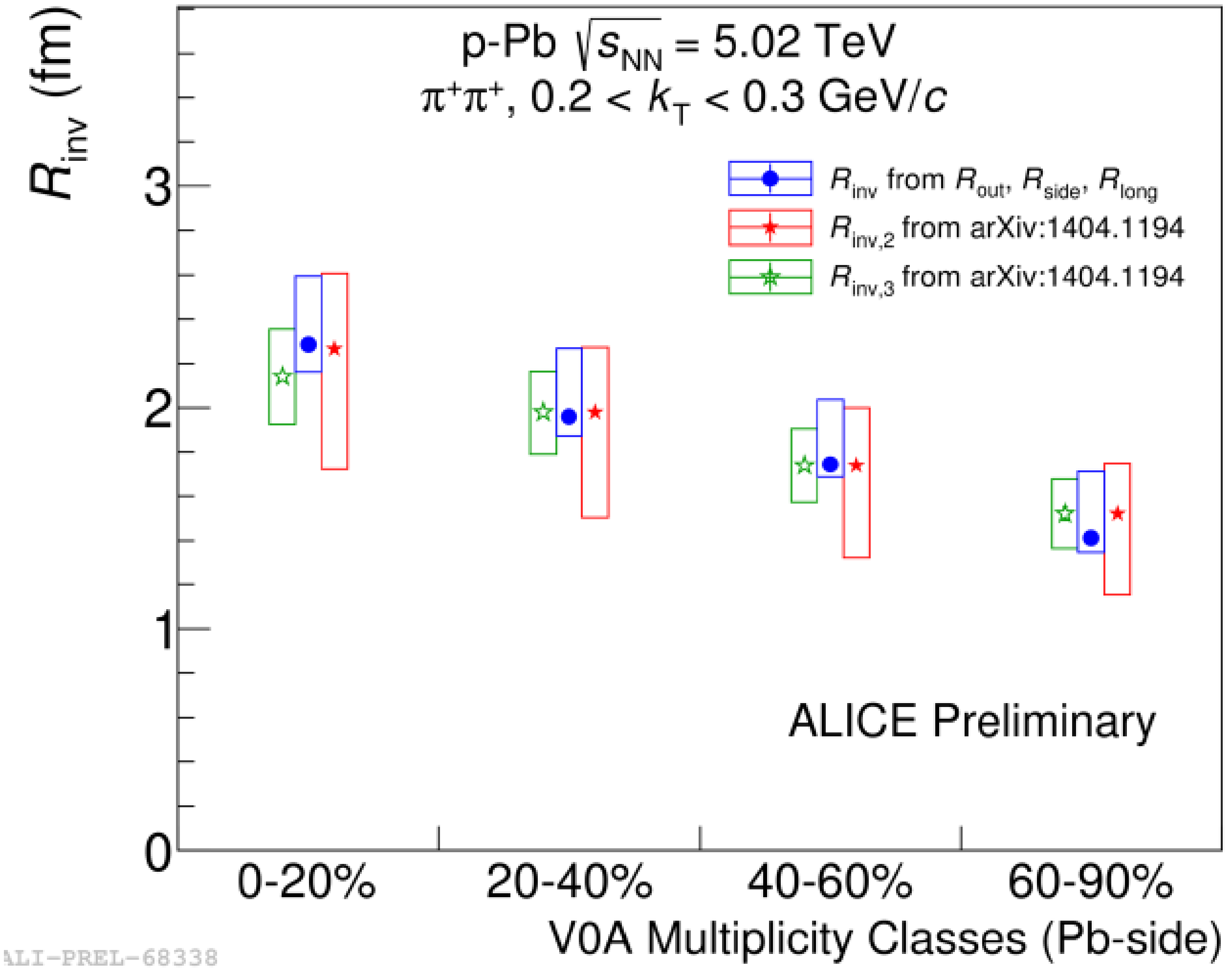

Correlation functions in extended range

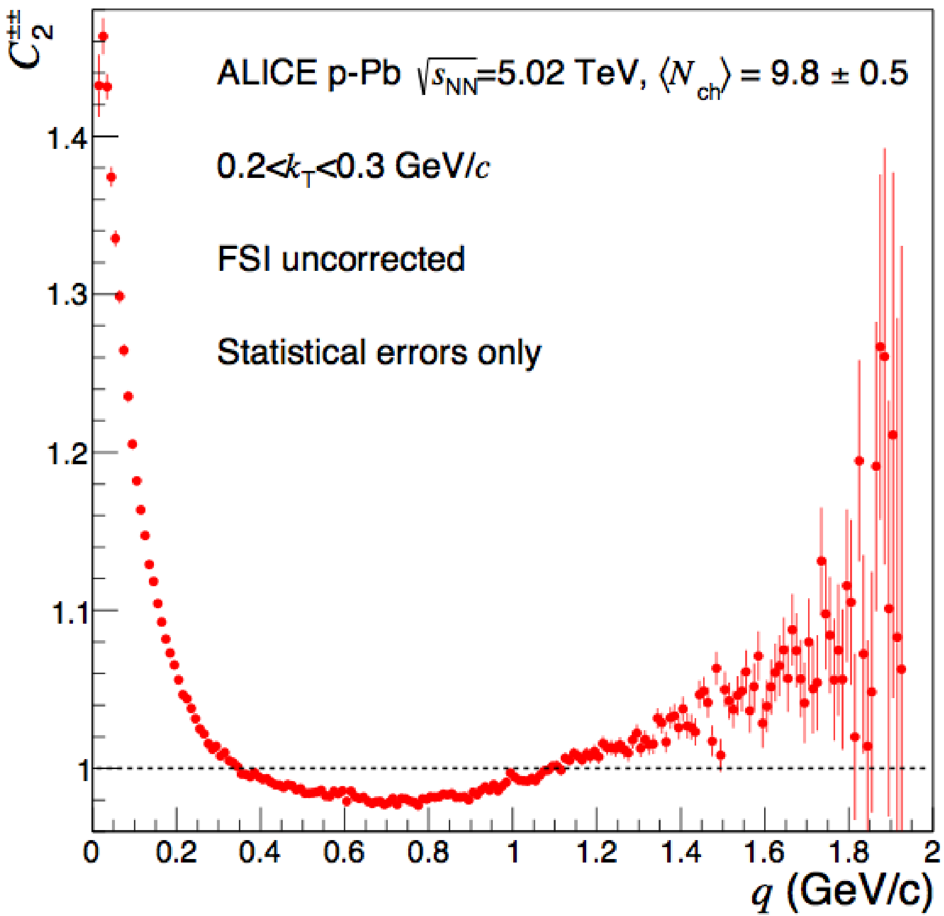

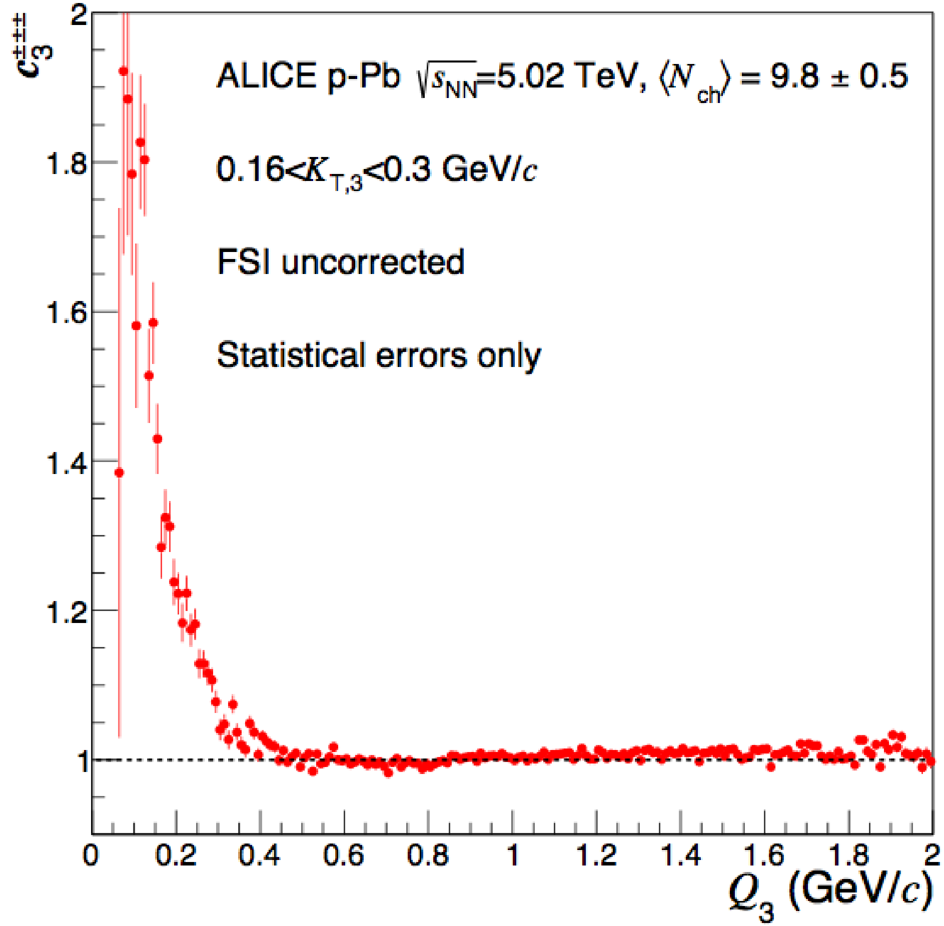

The baseline for 3-pion correlation functions is more flat than for 2-pions.
Fit more reliable since neither source nor background shape well known.
For a given parametrization main uncertainty from chosen fit range in q.

Isolation of 2-pion correlations

$$C_2(q) = \mathcal{N}[(1 - f_c^2) + f_c^2 K_2(q) C_2^{QS}(q)]\, B(q)$$

Measured correlation function

Quantum-Statistics correlation

Coulomb+strong FSI

Correlated fraction of pairs
Obtained from mixed-charge pion C_2.
(cleaner method to determine dilution).
$f_c^2 = 0.7 \pm 0.05$ in ALICE
PRC 89 024911 (2014)

Non-femtoscopic background

Sinyukov et al.,
Phys. Lett. B 432, 249 (1998)

Fitting of 2-pion correlations

$$C_2^{QS}(q) \;=\; 1 + \lambda\, E_w^2(R_{inv}\, q)\, e^{-R_{inv}^2\, q^2}$$

Quantum-Statistics correlation

Suppression parameter related to incorrect fit functions and coherence

$$E_w(R_{inv}\, q) \;=\; 1 + \sum_{n=3}^{\infty} \frac{\kappa_n}{n!(\sqrt{2})^n} H_n(R_{inv}\, q)$$

Edgeworth expansion for non-Gaussian features

Gaussian Fit when $E_w = 1.0$

Non-Gaussian features parameterized with an Edgeworth expansion.

- κ_3 and κ_4 expansion parameters retained and extracted from 3-pion cumulants.
- Free fit performed for all 3 systems and all multiplicity bins.
- $\langle\kappa_3\rangle = 0.1$
- $\langle\kappa_4\rangle = 0.5$

Csorgo & Hegyi,
Phys. Lett. B 489, 15 (2000)

Isolation of 3-pion correlations

3 pions from the same event

All 3 pions from different events

2 pions from the same event
Other pion from mixed event

$$
\begin{aligned}
N_3(p_1,p_2,p_3) &= f_1 N_1(p_1) N_1(p_2) N_1(p_3) \\
&+ f_2 \left[N_2(p_1,p_2) N_1(p_3) + N_2(p_3,p_1) N_1(p_2) + N_2(p_2,p_3) N_1(p_1)\right] \\
&+ f_3 K_3(q_{12},q_{31},q_{23}) N_3^{QS}(p_1,p_2,p_3)\,,
\end{aligned}
$$

3-pion FSI correlation

Full 3-pion
Quantum-Statistics
correlation

f_1, f_2 and f_3 are functions of f_c

$f_1 = -0.08$

$f_2 = 0.16$

$f_3 = 0.59$

Isolation and fitting of 3-pion correlations

Cumulant isolation

$$
\begin{aligned}
\mathbf{c}_3(p_1,p_2,p_3) \; = \; & \mathcal{N}_3[1+[2N_1(p_1)N_1(p_2)N_1(p_3) \\
- \; & N_2^{\mathrm{QS}}(p_1,p_2)N_1(p_3) - N_2^{\mathrm{QS}}(p_3,p_1)N_1(p_2) - N_2^{\mathrm{QS}}(p_2,p_3)N_1(p_1) \\
+ \; & N_3^{\mathrm{QS}}(p_1,p_2,p_3)]/N_1(p_1)N_1(p_2)N_1(p_3)],
\end{aligned}
$$

Cumulant fitting

$$
\mathbf{c}_3(q_{12},q_{31},q_{23}) = 1 + \lambda_3 E_{\mathrm{w}}(R_{\mathrm{inv},3}\, q_{12}) E_{\mathrm{w}}(R_{\mathrm{inv},3}\, q_{31}) E_{\mathrm{w}}(R_{\mathrm{inv},3}\, q_{23}) e^{-R^2_{\mathrm{inv},3} Q_3^2/2}
$$

New suppression parameter

Edgeworth factors to account for non-Gaussian features

3-pion correlation functions

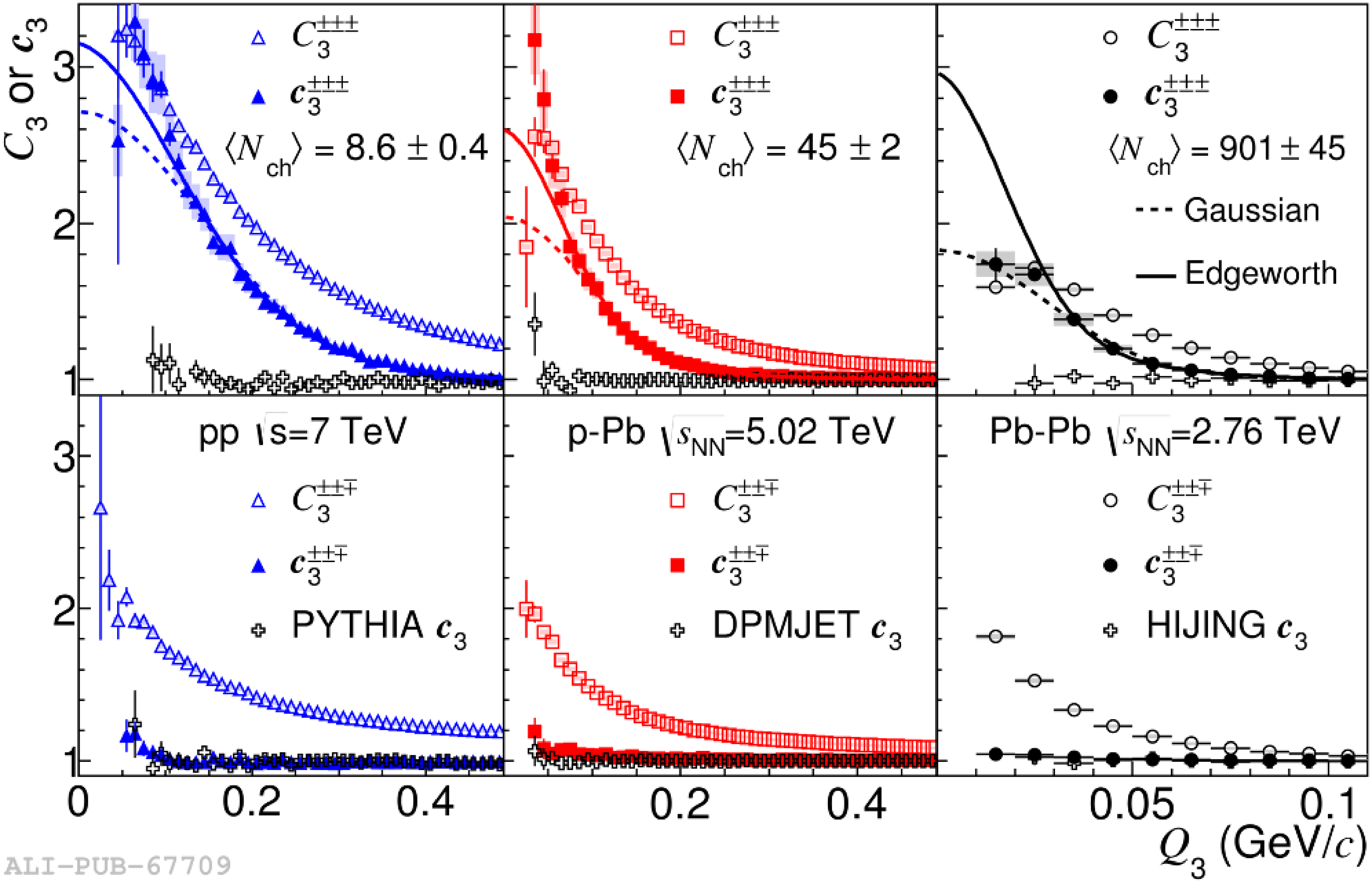

Comparison of c_3 at similar N_{ch}

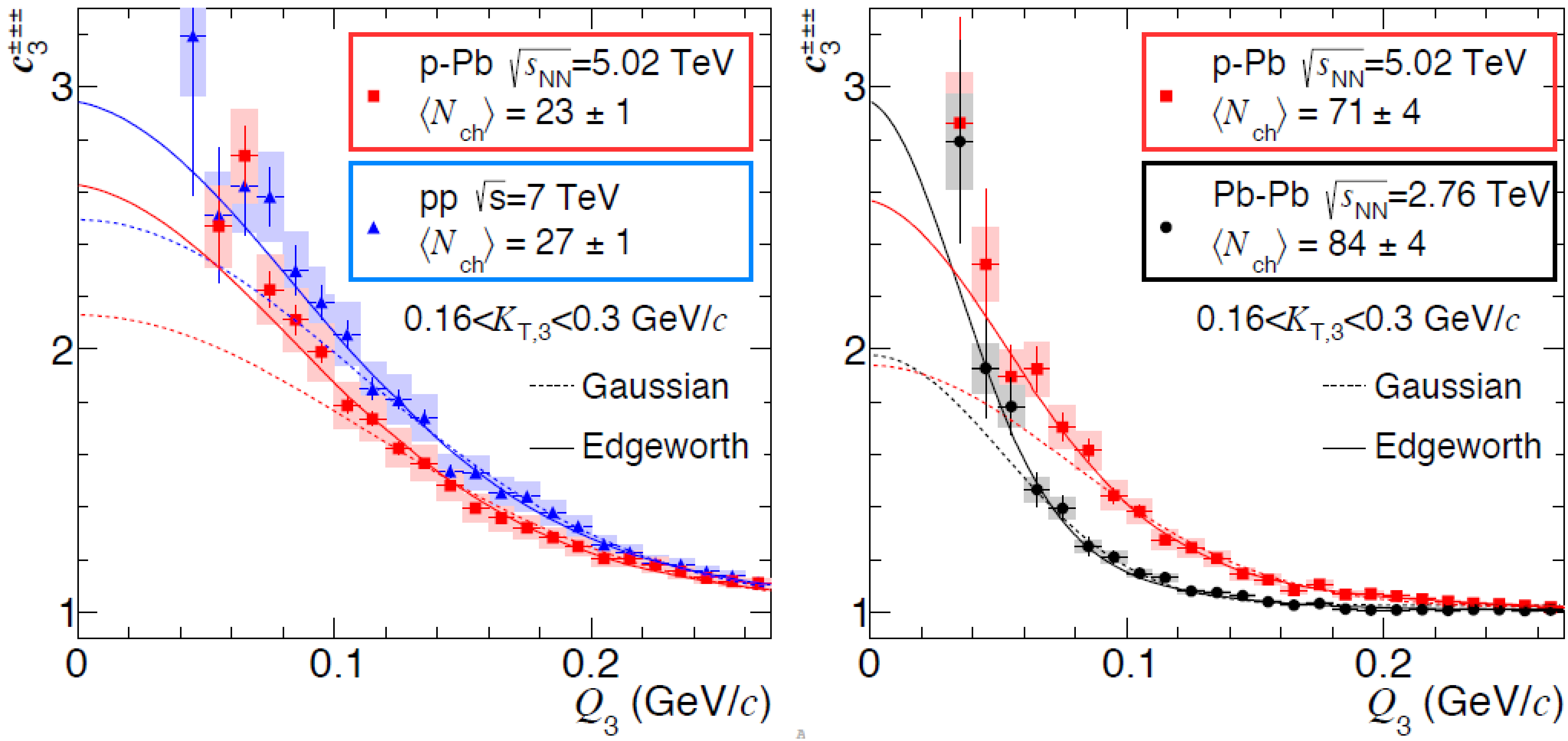

The correlation function is very similar for pp and pPb at similar Nch (unlike for pPb and PbPb)

Edgeworth radii and intercepts

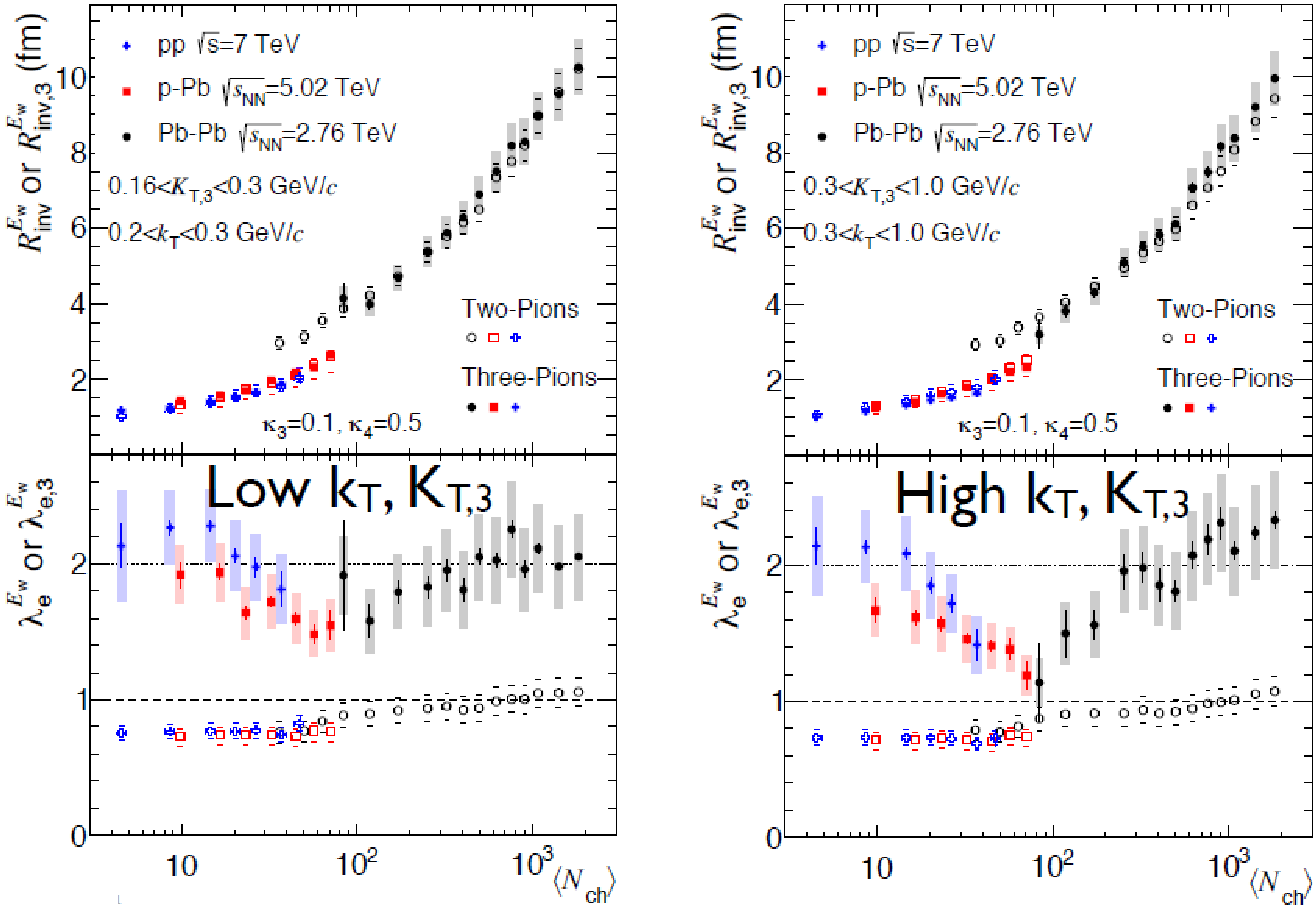

Edgeworth radius ratios

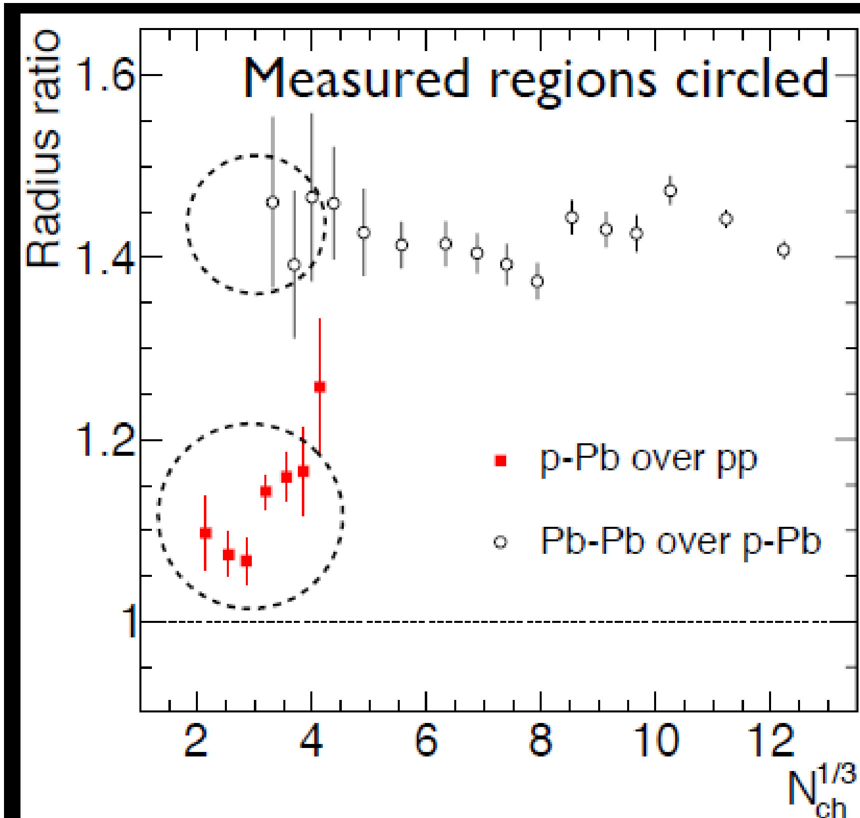

Low $K_{T,3}$

pp Fit: $R = 0.44 + 0.402*N_{ch}^{1/3}$

p-Pb Fit: $R = 0.08 + 0.586*N_{ch}^{1/3}$

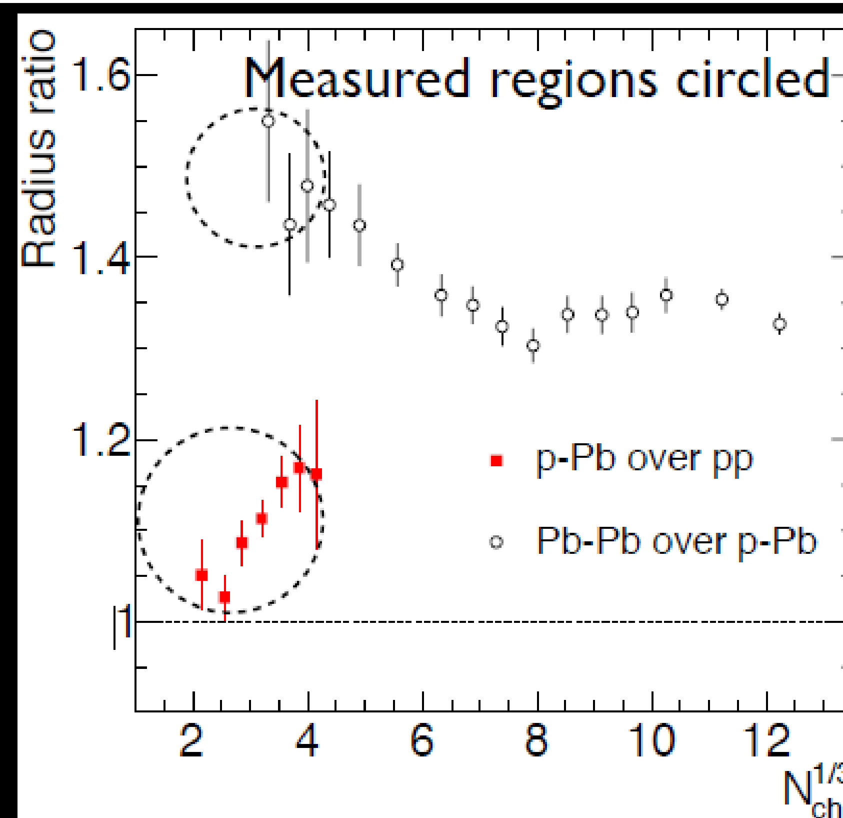

High $K_{T,3}$

pp Fit: $R = 0.33 + 0.405*N_{ch}^{1/3}$

p-Pb Fit: $R = -0.05 + 0.585*N_{ch}^{1/3}$

Red Points: p-Pb data divided by pp radii trend fit (linear with $N_{ch}^{1/3}$).
Black Points: Pb-Pb data divided by p-Pb radii trend.

J/ψ production versus rapidity in p-Pb

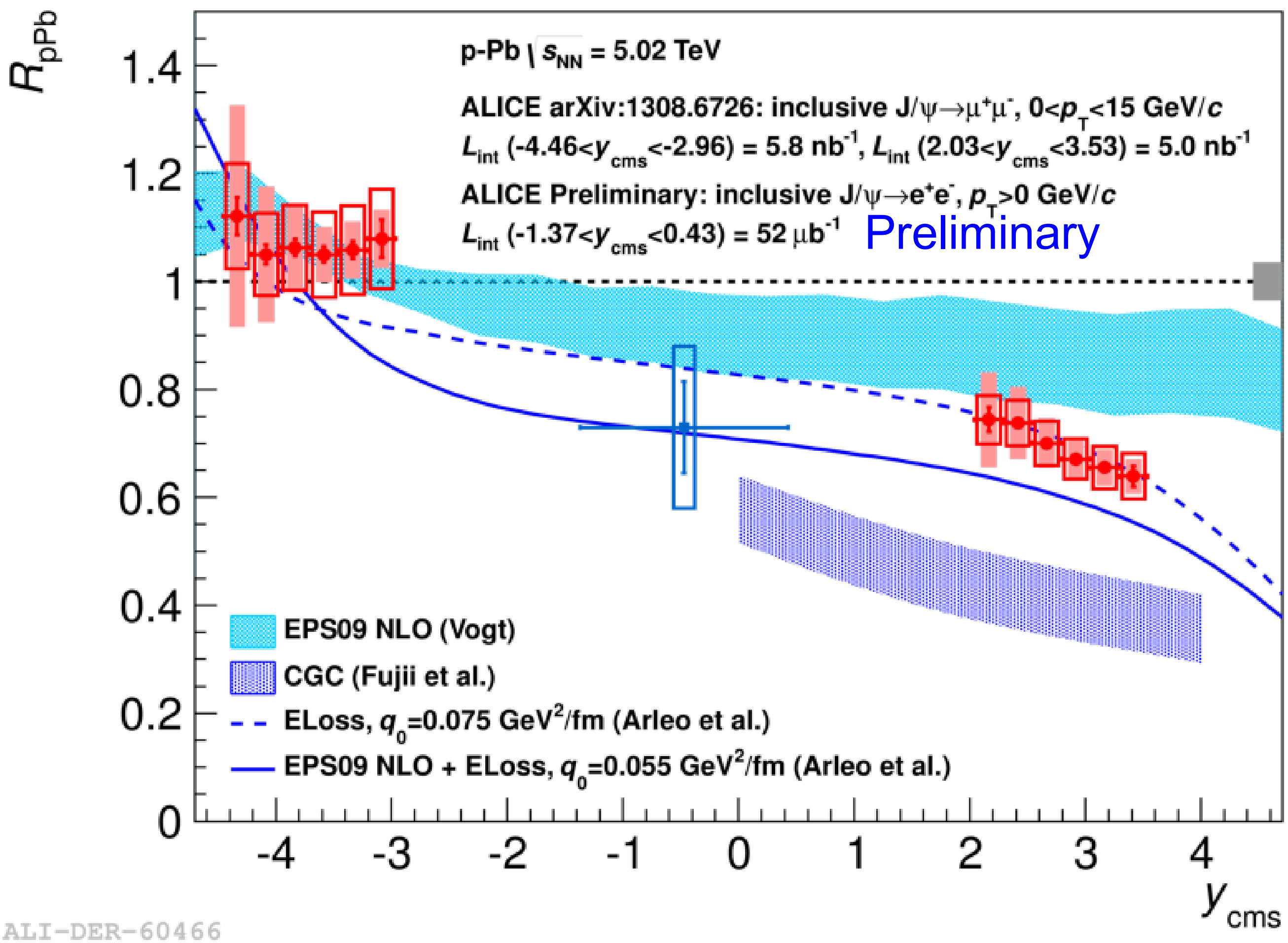

- Suppression at mid- and forward rapidity
  - Consequences for R_{AA}: Suggests even stronger recombination
- Consistent with shadowing models (EPS09 NLO) and/or coherent parton energy loss
- Specific CGC calculation disfavored

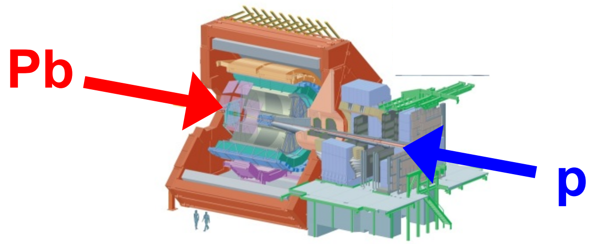

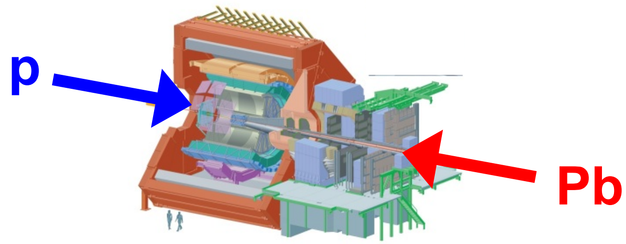

Centrality estimators

MULTIPLICITY

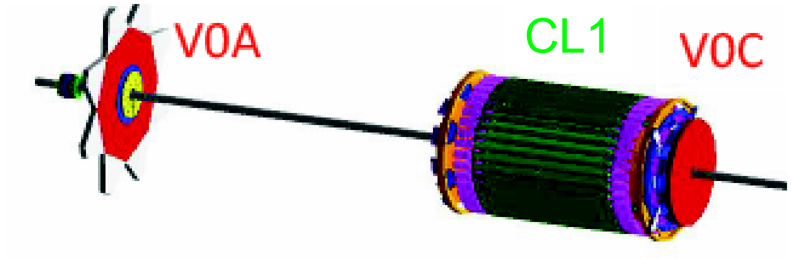

MIDRAPIDITY

2 innermost ITS layers (pixel)
$|\eta| < 2$, $|\eta| < 1.4$

FORWARD RAPIDITY

V0 scintillator hodoscopes
V0A z = 3.4 m $2.8 < \eta < 5.1$
V0C z = -0.9 m $-3.7 < \eta < -1.7$

VERY FORWARD ENERGY

ZERO DEGREE

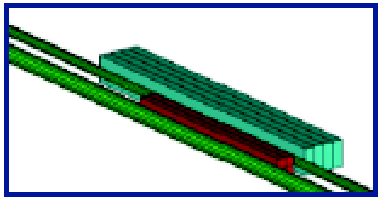

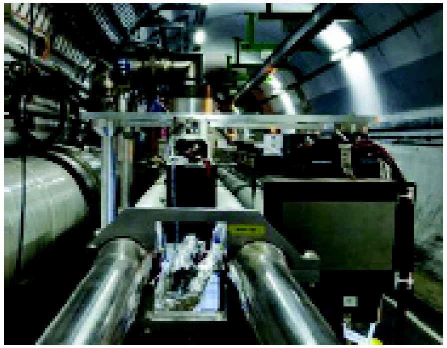

Zero Degree Calorimeters (ZDC) ±112.6 m
neutron ZDC (ZN) $|\eta| > 8.7$
proton ZDC (ZP)

Particle production is modeled by
Negative Binomial Distribution (NBD)

Centrality estimators:
- CL1 ➡ clusters in 2nd pixel layer
- V0M ➡ total (V0A+V0C) multiplicity
- V0A ➡ V0 multiplicity (Pb-remnant side)

Need a model to describe nucleus fragmentation and the following
nucleon emission
"Slow" Nucleon Model (SNM)

- ZNA ➡ ZN energy (Pb-remnant side)
- ZPA ➡ ZP energy (Pb-remnant side)

N_{coll} from fits to multiplicity distributions

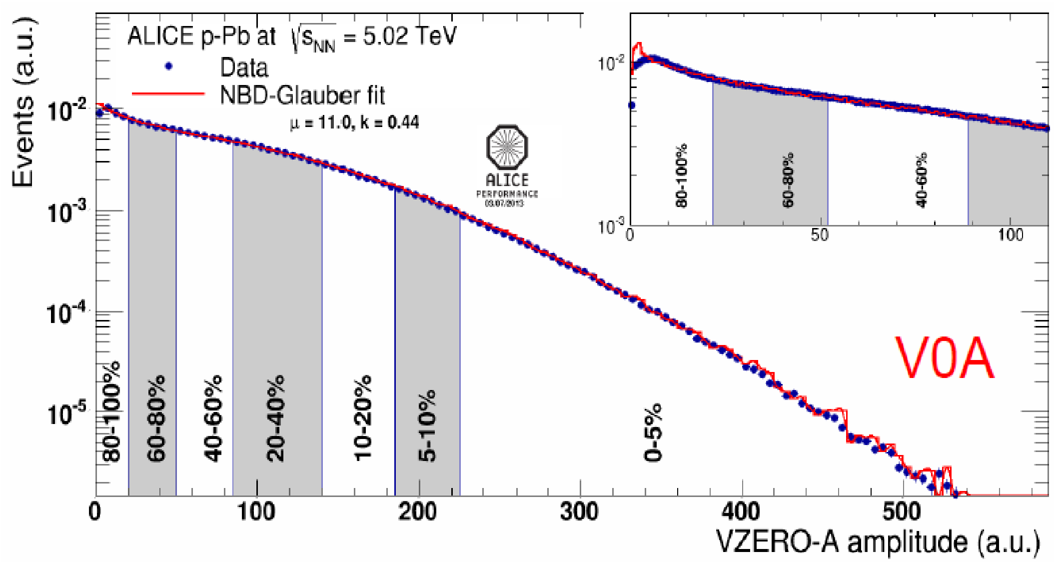

ALICE, preliminary

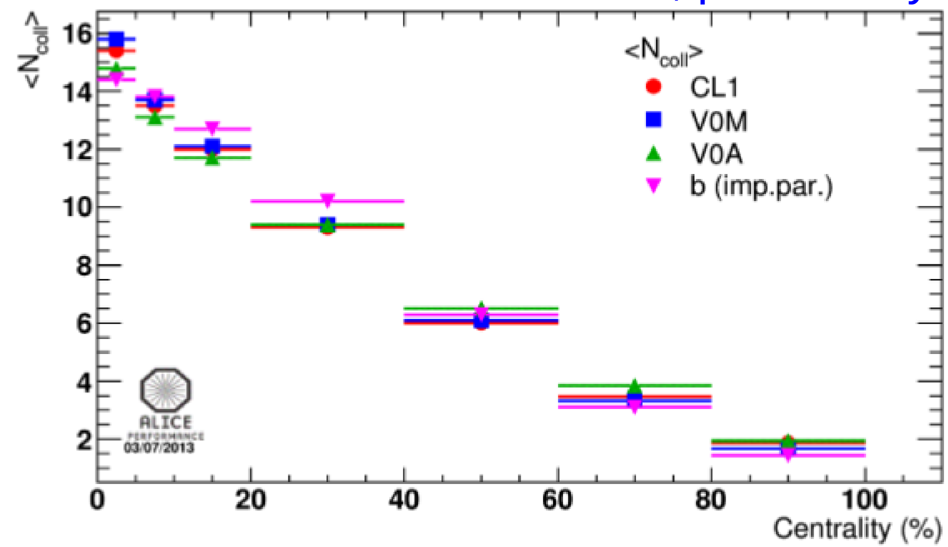

- Glauber fit to multiplicity distribution (V0A) with Negative Binomial ansatz coupled to Glauber MC
  - Obtain $P(N_{part}, \mu, k)$ in centrality slices
  - Same approach as in ALICE, PRC 88 (2013) 044909
- Obtain $\langle N_{coll} \rangle$ (= $\langle N_{part} \rangle$ -1) from Glauber
  - Similar for different estimators (CL1, V0M, V0A)
  - Similar to MC closure (done with HIJING)
  - Systematic uncertainty from variation of Glauber parameters

Glauber MC Parameters

$$\rho(r) = \rho_0 \frac{1}{1+\exp\left(\frac{r-R}{a}\right)}$$

R = 6.62 ± 0.06 fm

a = 0.546 ± 0.01fm

Minimum NN distance:
0.4±0.4 fm

pN Cross-section

σ_{pN} = 70 ± 5 mb

Proton radius

R_p = 0.6 ± 0.2 fm

N_{coll} from multiplicity

Slicing (percentiles)

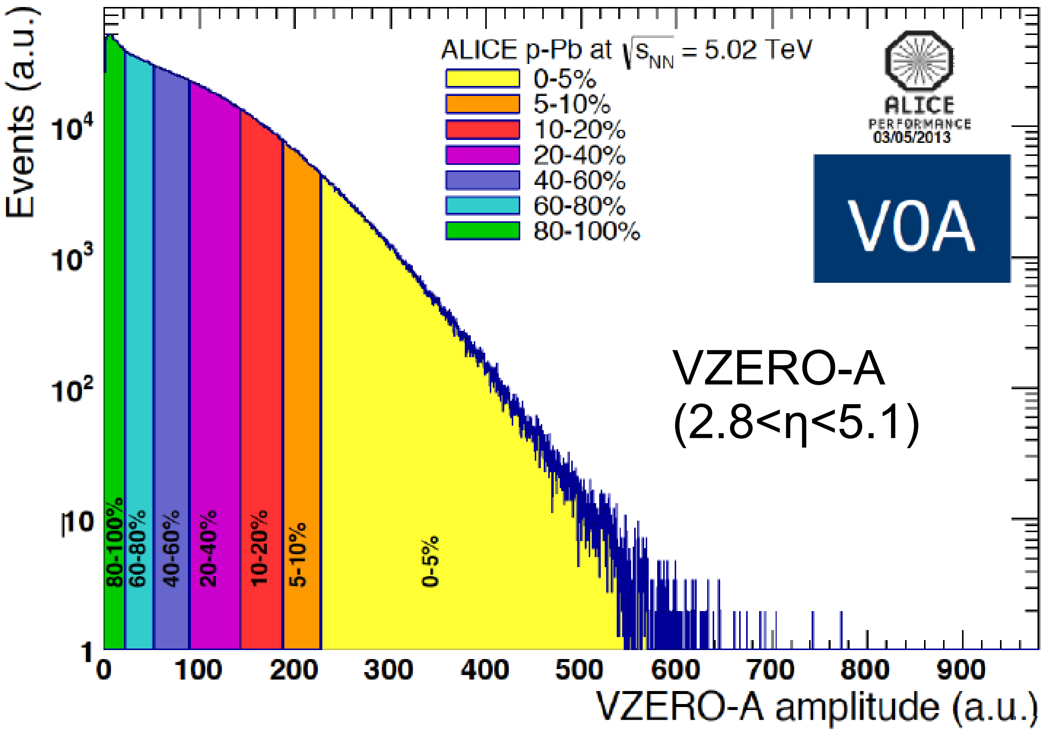

Correspondence in Glauber

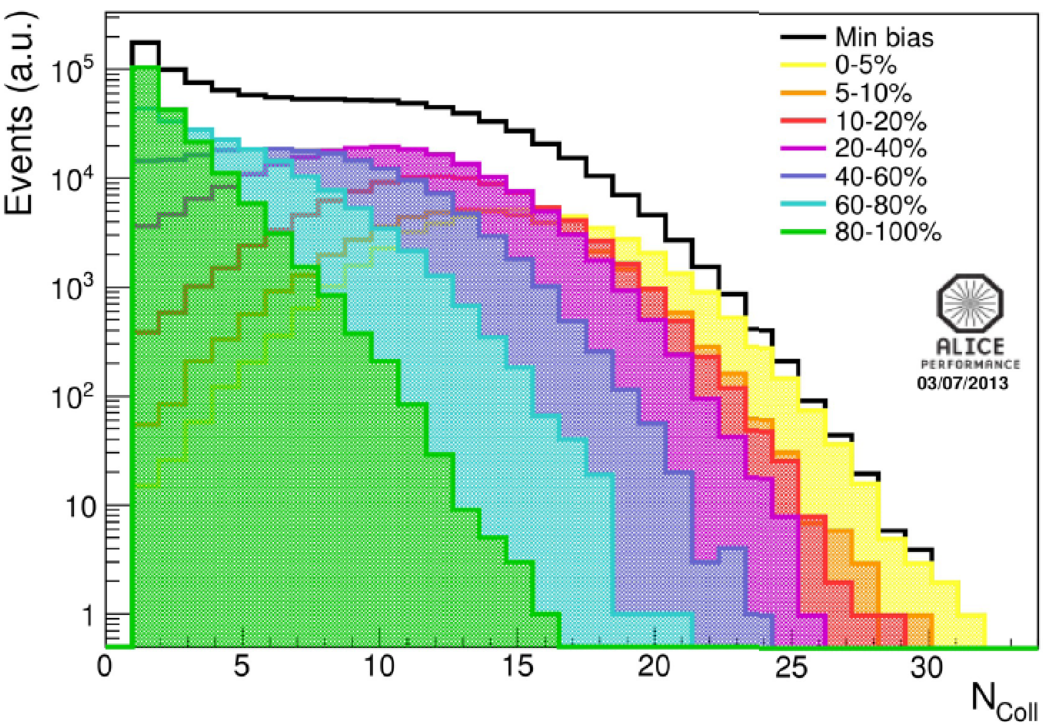

Average N_{coll} well determined, but fluctuations within the same class are large

Multiple (semi-)hard collisions

JHEP 0901 (2009) 065

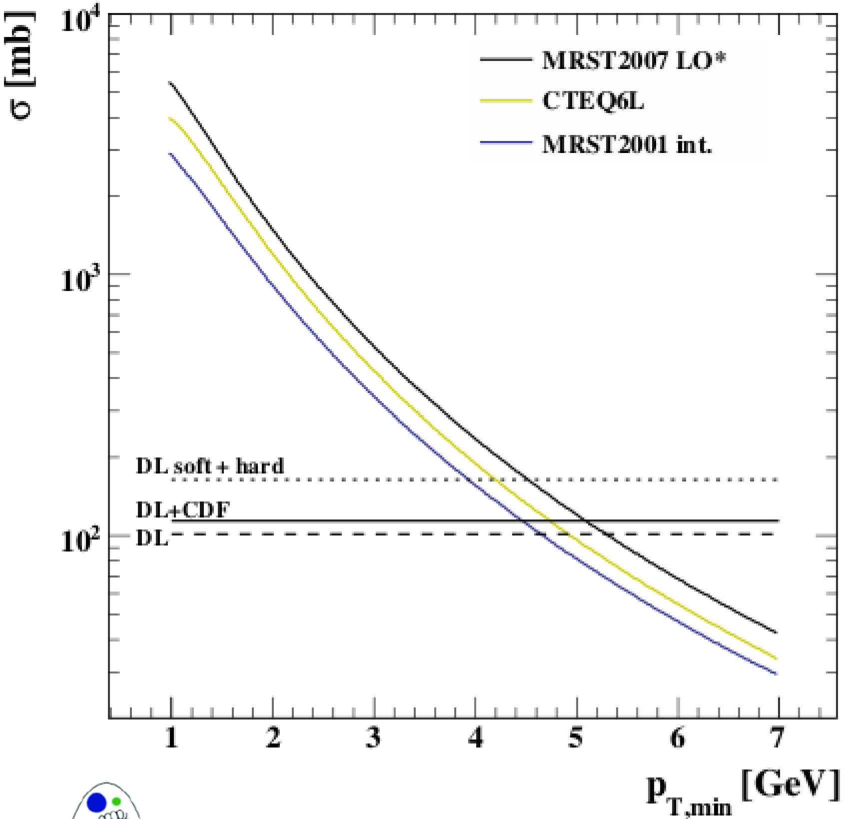

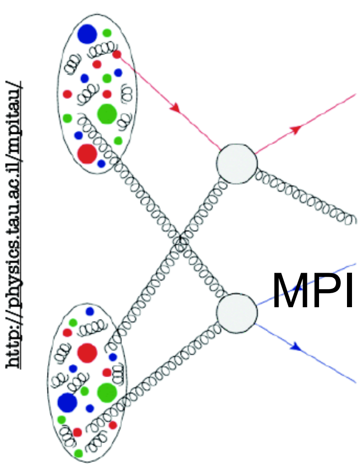

- In pp, the hard cross section exceeds the total cross section
- There must be multiple semi-hard collisions per pp event (MPI)
- Therefore there also must be more than Ncoll semi-hard scatterings in the addition to the hard process
- Implies (strong) correlation between hard process and bulk of particle production?
- Consequences for centrality determination?

Bias in number of hard scatters

ALICE, preliminary

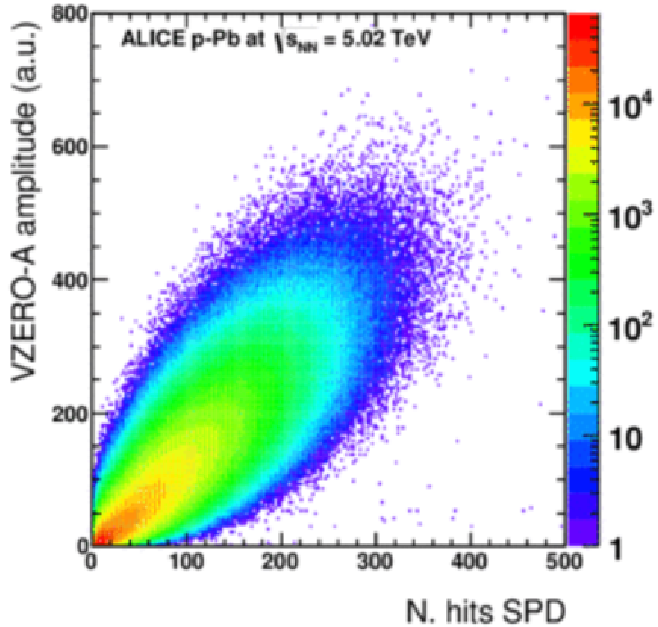

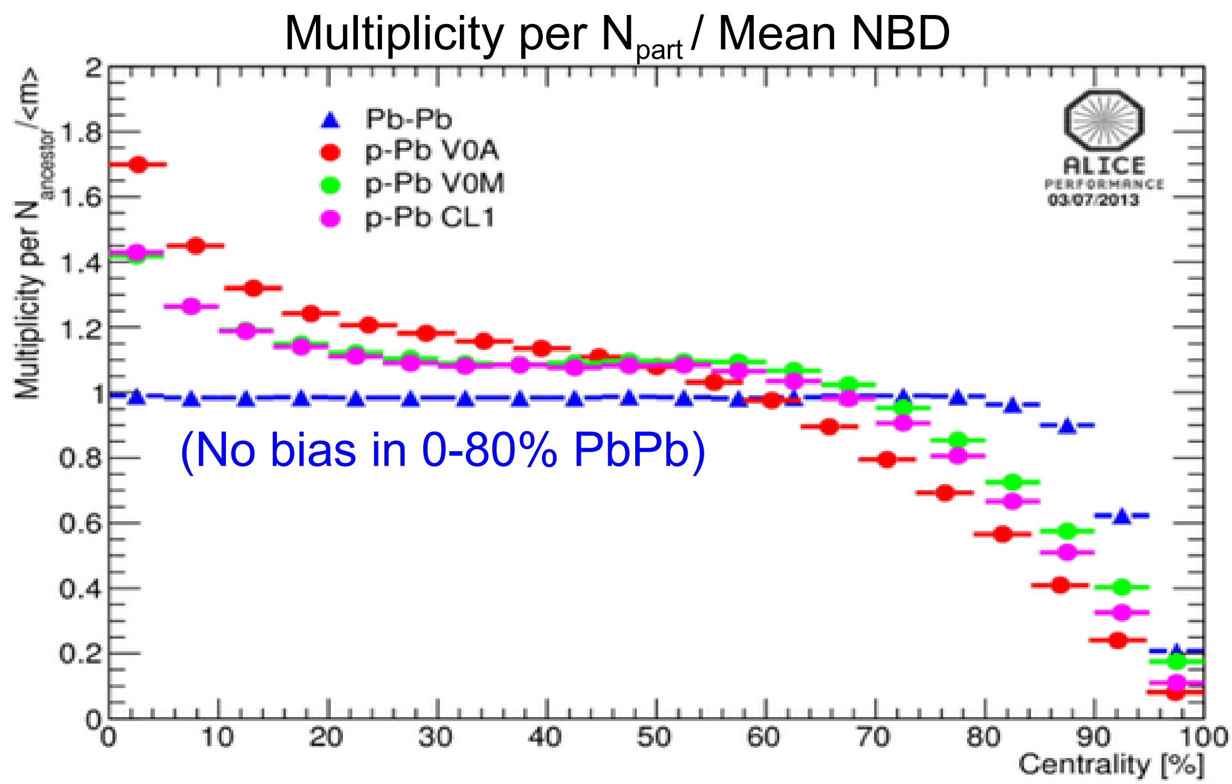

- Multiplicity fluctuations induce sizable bias on Mult/N_{part}
- All systems with fluctuations and dynamical limits show this
- Results in bias on the number of particle sources (hard scatterings)

Insights from models

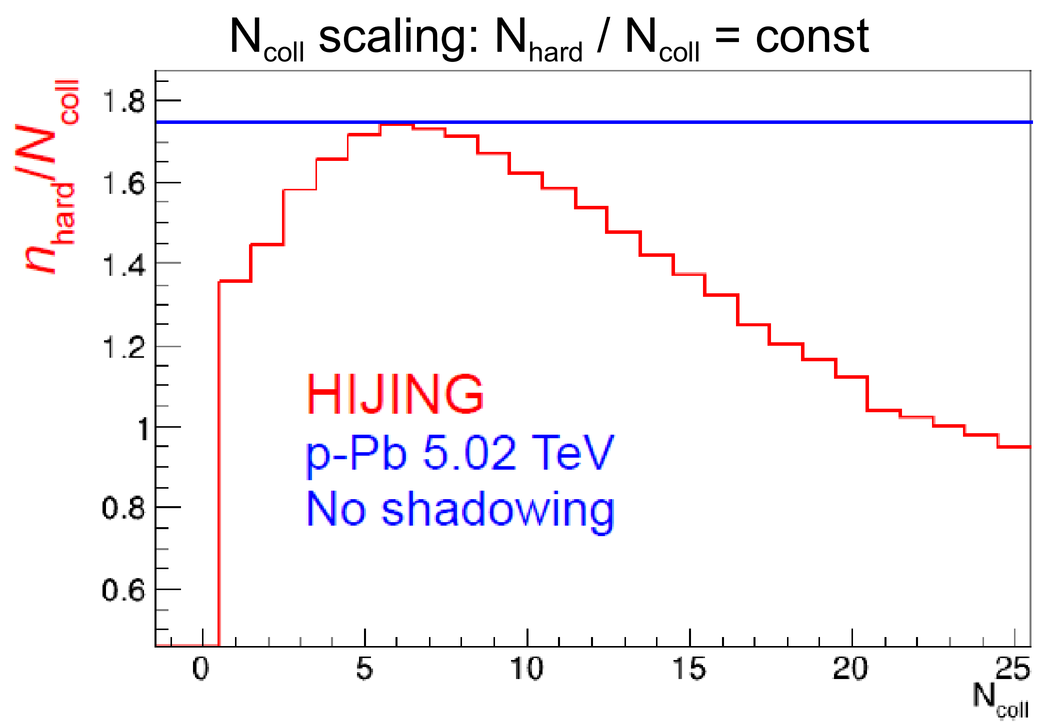

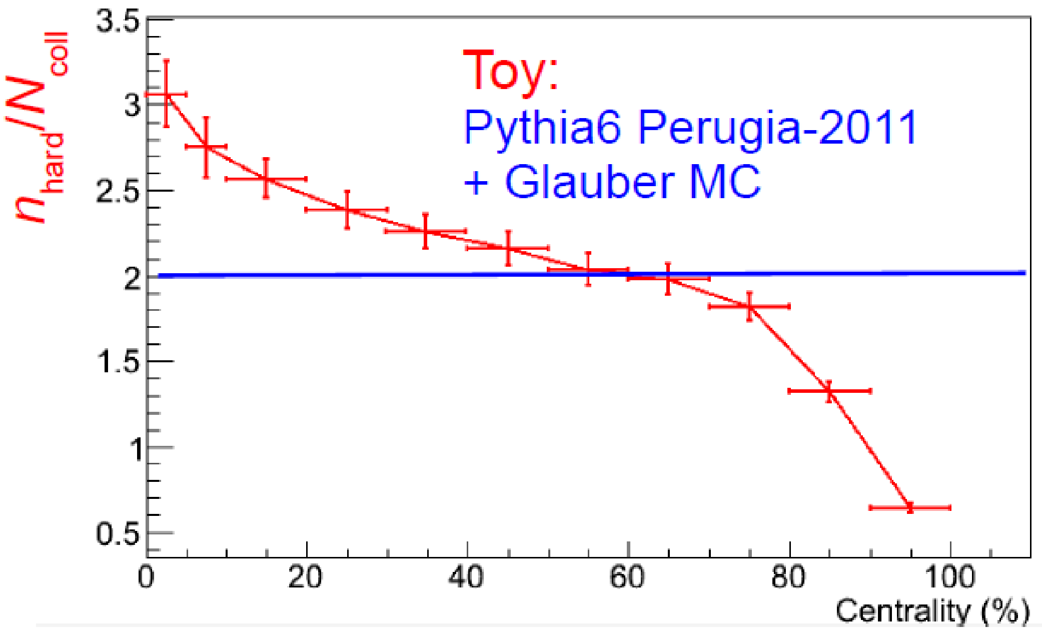

- Models based on MPI include intrinsically a fluctuating number of particles sources
- HIJING
  - studied vs Ncoll (ie no mulitplicity bias)
  - low Ncoll: Impact parameter between NN increases
  - high Ncoll: Energy conservation (breakdown of factorization)
- Toy model
  - Incoherent superposition of NN collisions (“Pythia6+Glauber”)
  - Vs centrality from mult in |η|<1.4 (ie only multplicity bias)
  - Strong deviation from Ncoll scaling at low and high centralites

Q_{pPb} (not R_{pPb})

- Qualitatively new elements
  - For a given centrality hard processes qualitatively scale with

    $$\langle N_{coll,cent}^{Glauber} \rangle \langle n_{hard} \rangle_{cent} / \langle n_{hard} \rangle_{pp}$$

  - Mean NN impact parameter increases in peripheral collisions
    - Expect softer than average collisions?
  - Also, veto for high-p_T processes in low multiplicity classes
- Alternative: Include (and indicate) bias in the definition

$$Q_{pPb,cent} = \langle N_{cent}^{Glauber} \rangle \frac{\langle dN^{pPb} / dp_T \rangle_{cent}}{dN^{pp} / dp_T}$$

Reminder:
R_{pPb} should be 1
in absence of
nuclear effects

Q_{pPb} (not R_{pPb})

ALICE, preliminary

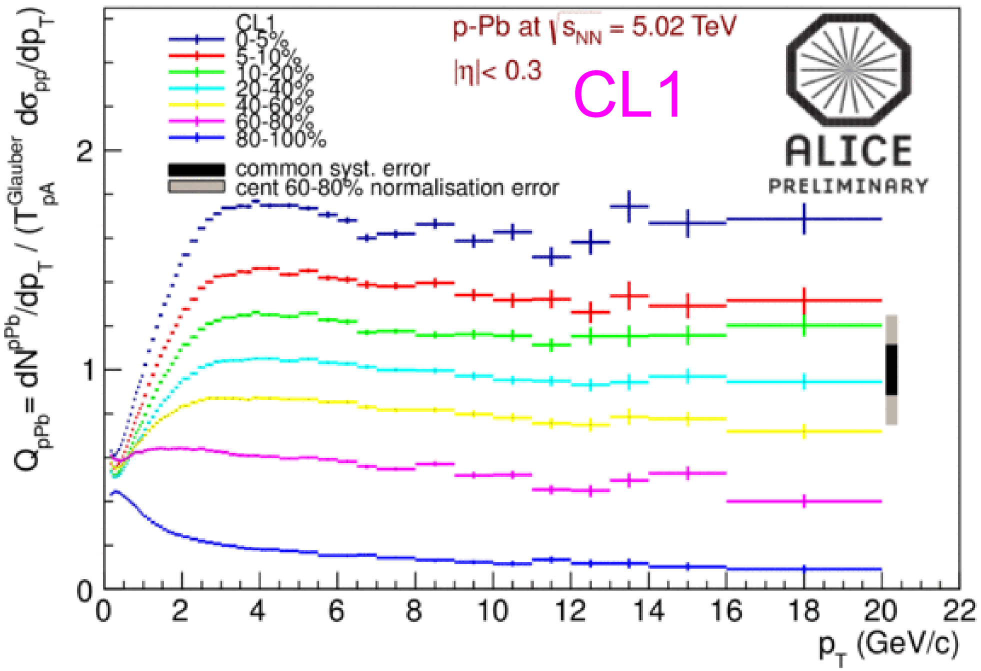

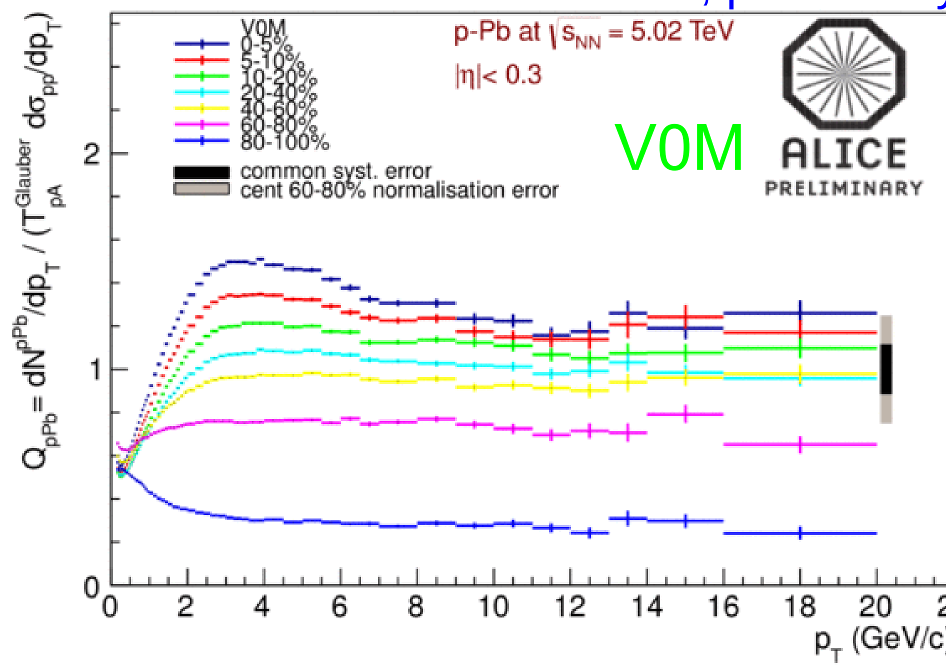

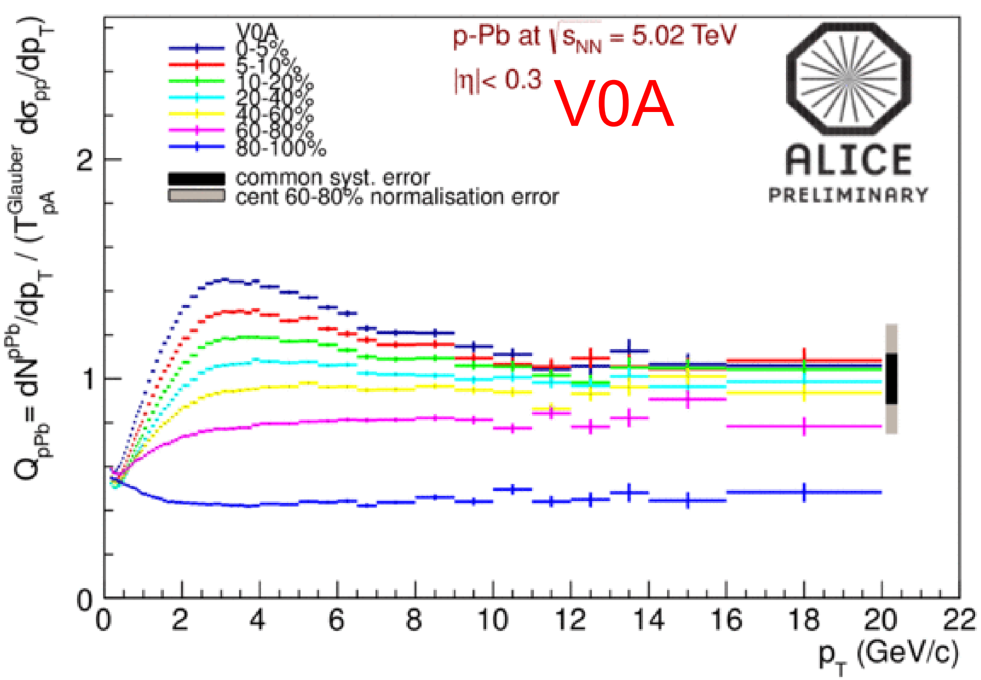

$$Q_{pPb,cent} = \langle N_{cent}^{Glauber} \rangle \frac{\langle dN^{pPb}/dp_T \rangle_{cent}}{dN^{pp}/dp_T}$$

Not a R_{pPb} measurement as not equals to 1 in absence of nuclear effects!!!

Spread reduces: CL1 → V0M → V0A

Jet veto present in 80-100% CL1, but not any longer in V0A

Q_{pPb} (not R_{pPb}) versus Pythia6+Glauber

ALICE, preliminary

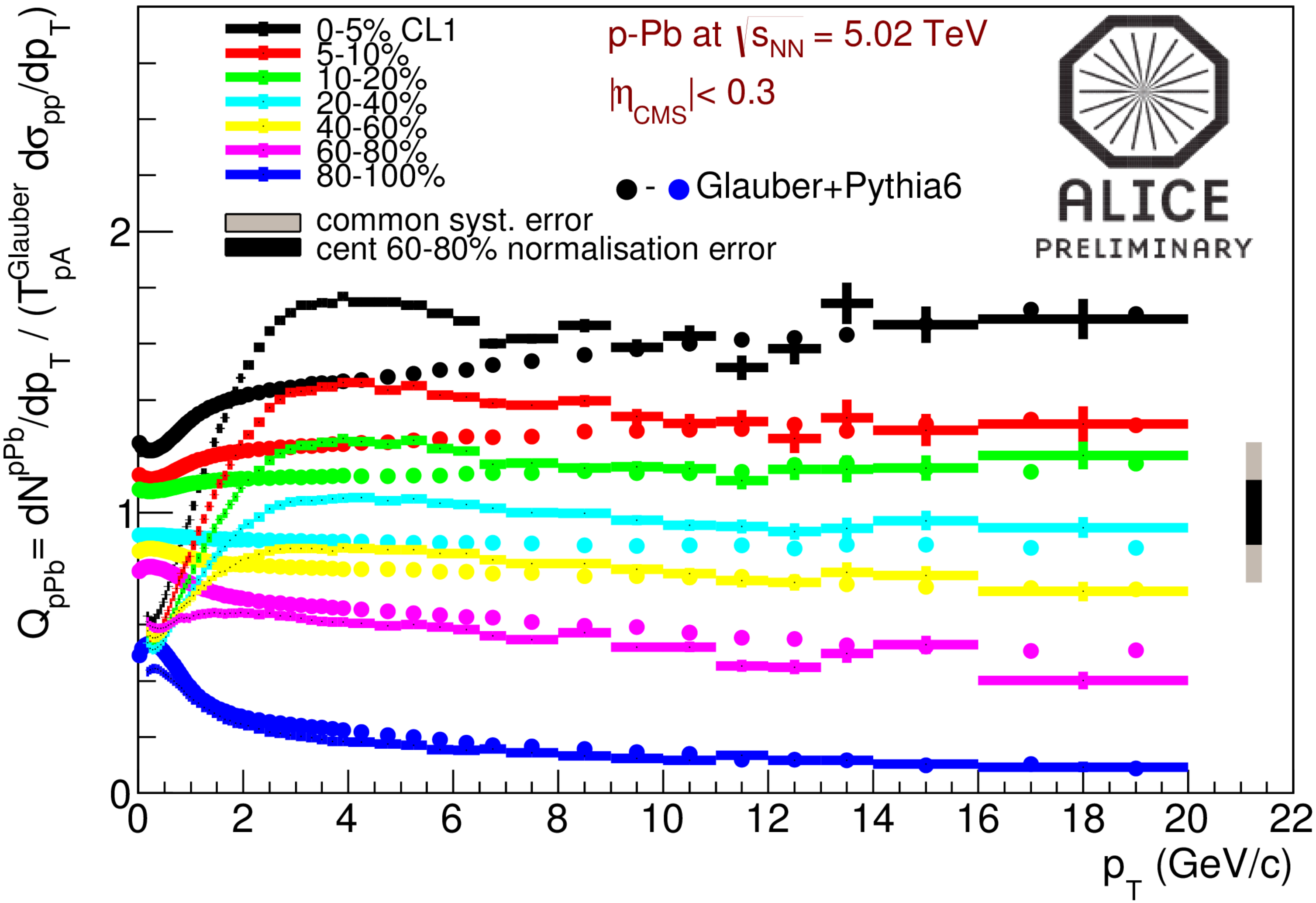

Data can be described (at high p_T, and for jet veto classes) with simple model based on incoherent superposition of pp collisions (Glauber+Pythia6)

Comparison of shapes (norm at 10 GeV) 136

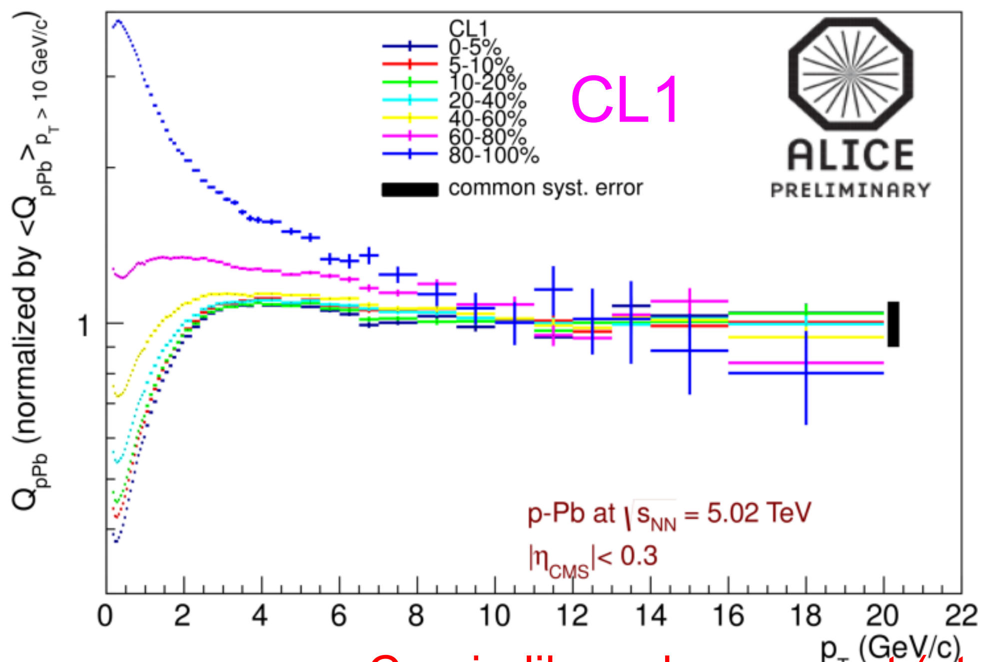

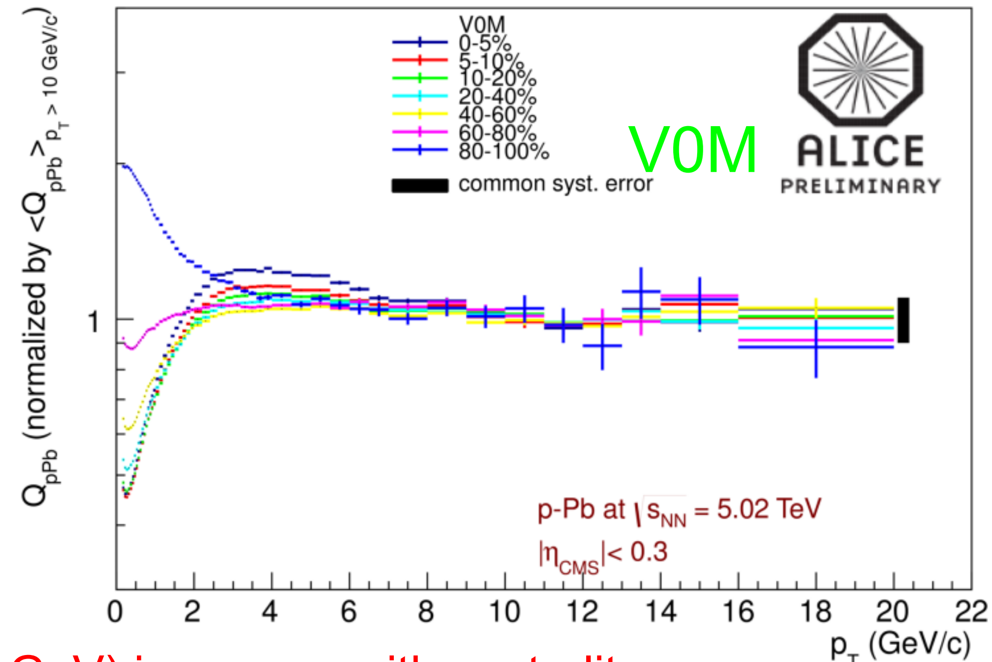

Cronin-like enhancement (at ~3 GeV) increases with centrality

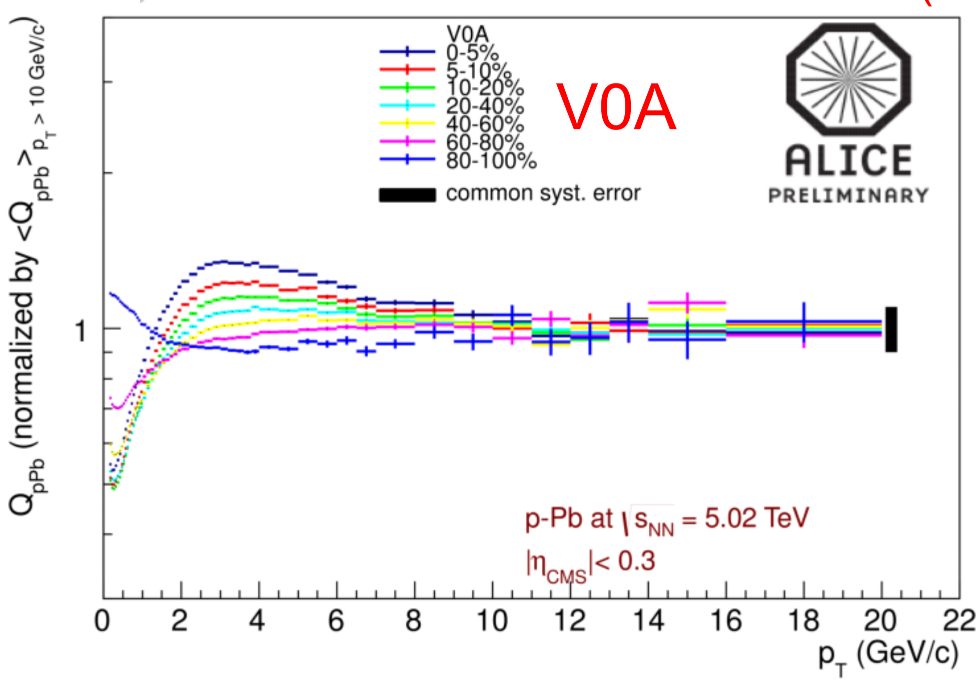

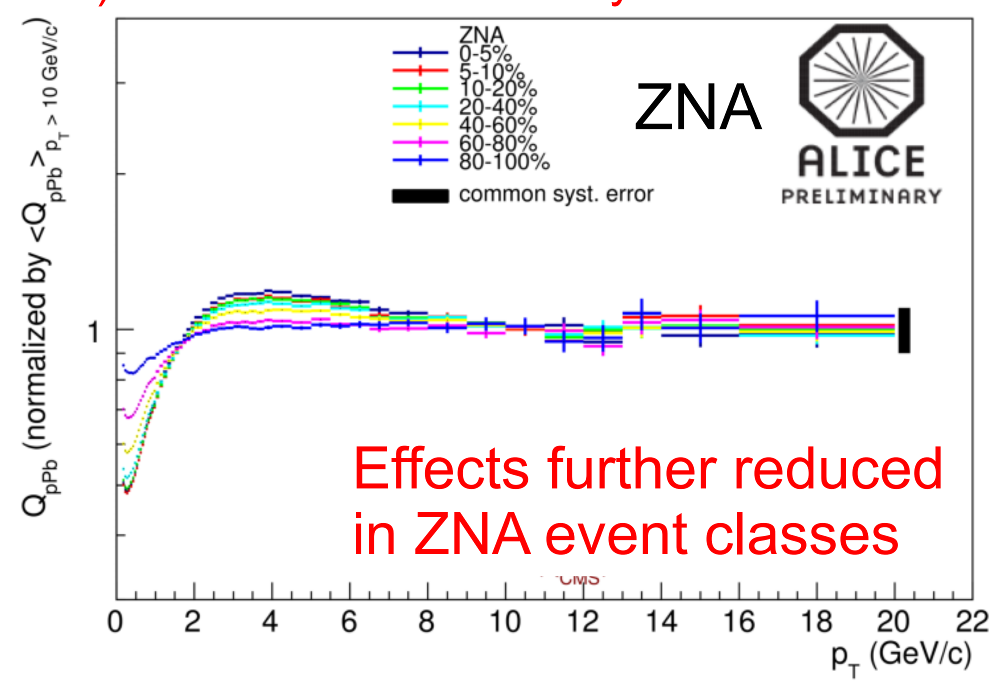

Effects further reduced in ZNA event classes

Bias from MPI versus fluctuations

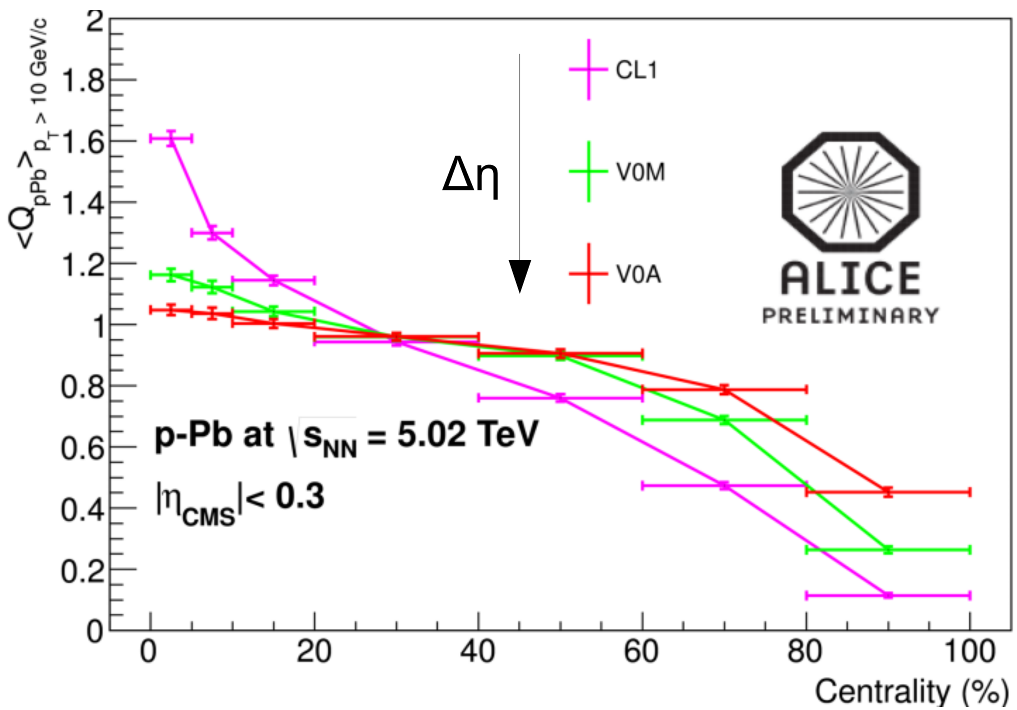

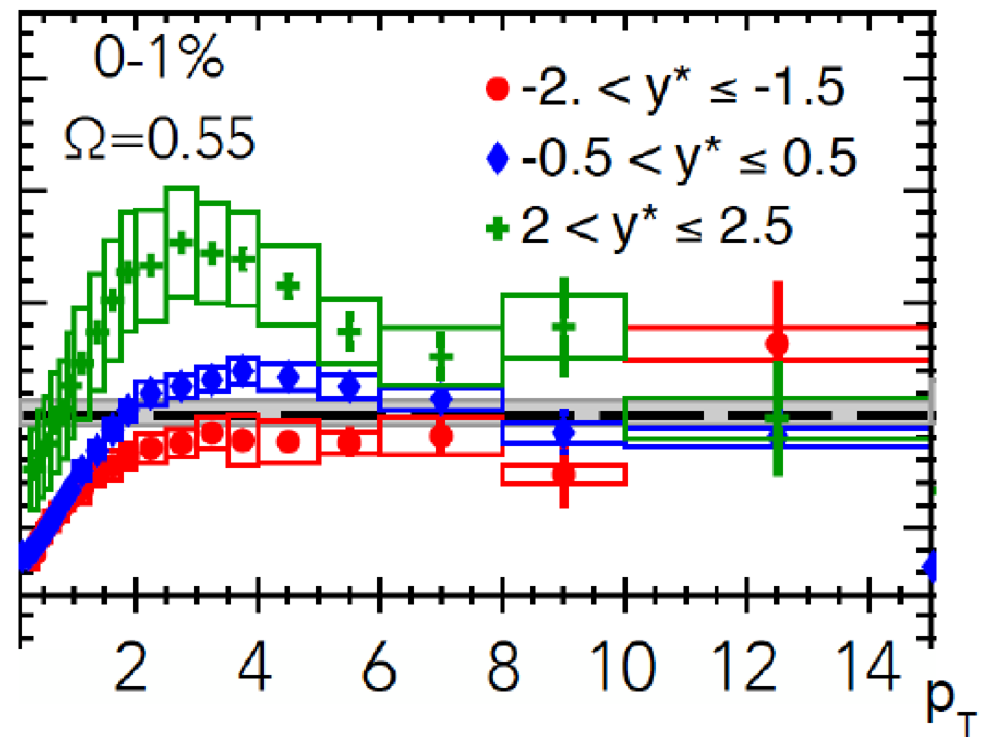

$$Q_{pPb,\,cent} = \langle N^{Glauber}_{cent} \rangle \frac{\langle dN^{pPb}/dp_T \rangle_{cent}}{dN^{pp}/dp_T}$$

$$R_{pPb,\,cent} = \langle N^{Geo}_{cent} \rangle \frac{\langle dN^{pPb}/dp_T \rangle_{cent}}{dN^{pp}/dp_T}$$

ALICE interpretation:
Biased not yet R_{pPb} measurement

ATLAS interpretation:
Centrality estimator in 3.2<η<4.9
Dep. on geometrical model

Fluctuations: Ω vs σ

From A. Morsch (HP13)

X.N. Wang and M. Gyulassy, nucl-th/9502021

$$T_N(b) = 2\frac{\chi_0(b,s)}{\sigma_{soft}}$$

$$d\,\sigma_{inelastic} = \pi\, db^2[1-\exp(-2\chi(b,s))] = \pi\, db^2[1-\exp(-(\sigma_{soft}+\sigma_{hard})T_N(b,s))]$$

$$\langle n_{\mathrm{hard}}\rangle(b_{\mathrm{NN}}) = \sigma_{\mathrm{hard}}\, T_{\mathrm{N}}(b_{\mathrm{NN}})$$

Counts fluctuate !

$$p_i(b_{\mathrm{NN}}) = \frac{\langle n_{\mathrm{hard}}\rangle^i}{i\,!}\exp(-\langle n_{\mathrm{hard}}\rangle)$$

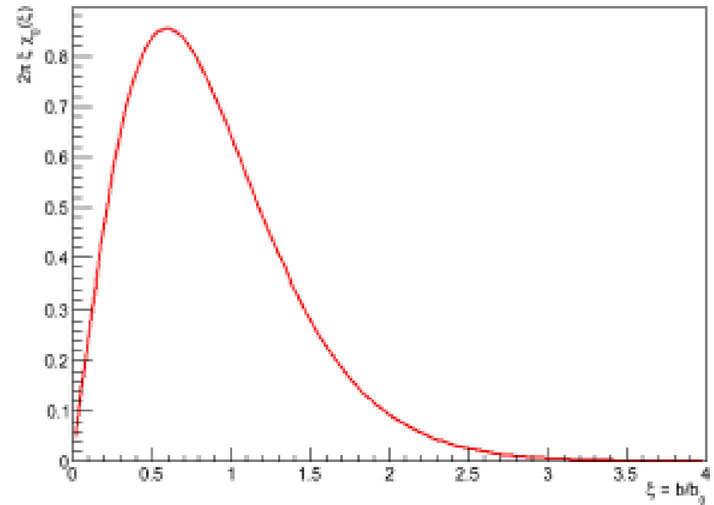

(similar approach used in PYTHIA)

Geometrical fluctuations described by overlap function (eikonal) T_N.

Cross-section itself does not fluctuate (since = *flux* (db^2) *x probability*).

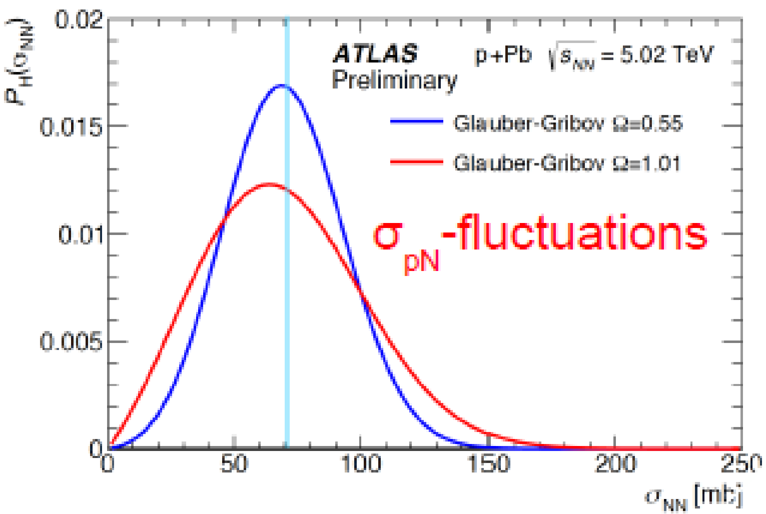

Only a question of terminology ?

At LHC $\sigma_{hard} >> \sigma_{tot}$

$\Omega \leftrightarrow \sigma_{hard}$??

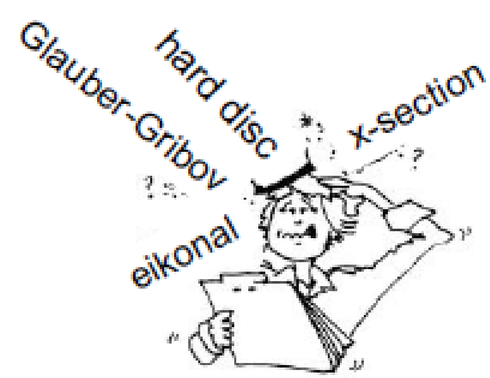

Scaling of particle production

- $\langle S \rangle_i / \langle S \rangle_{MB}$ vs $\langle dN/d\eta \rangle_i / \langle dN/d\eta \rangle_{MB} (-1<\eta_{lab}<0)$

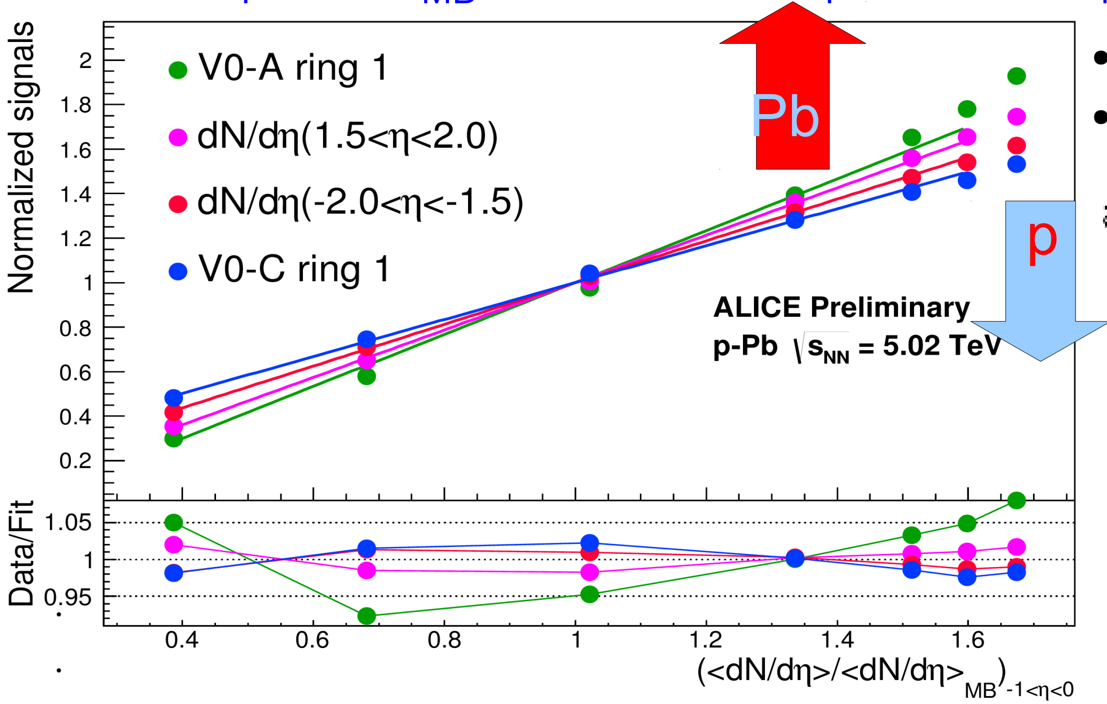

- PHOBOS d-Au: η→ 1.6*η (beam rapidity)
- Similar dependence except A-going dir.

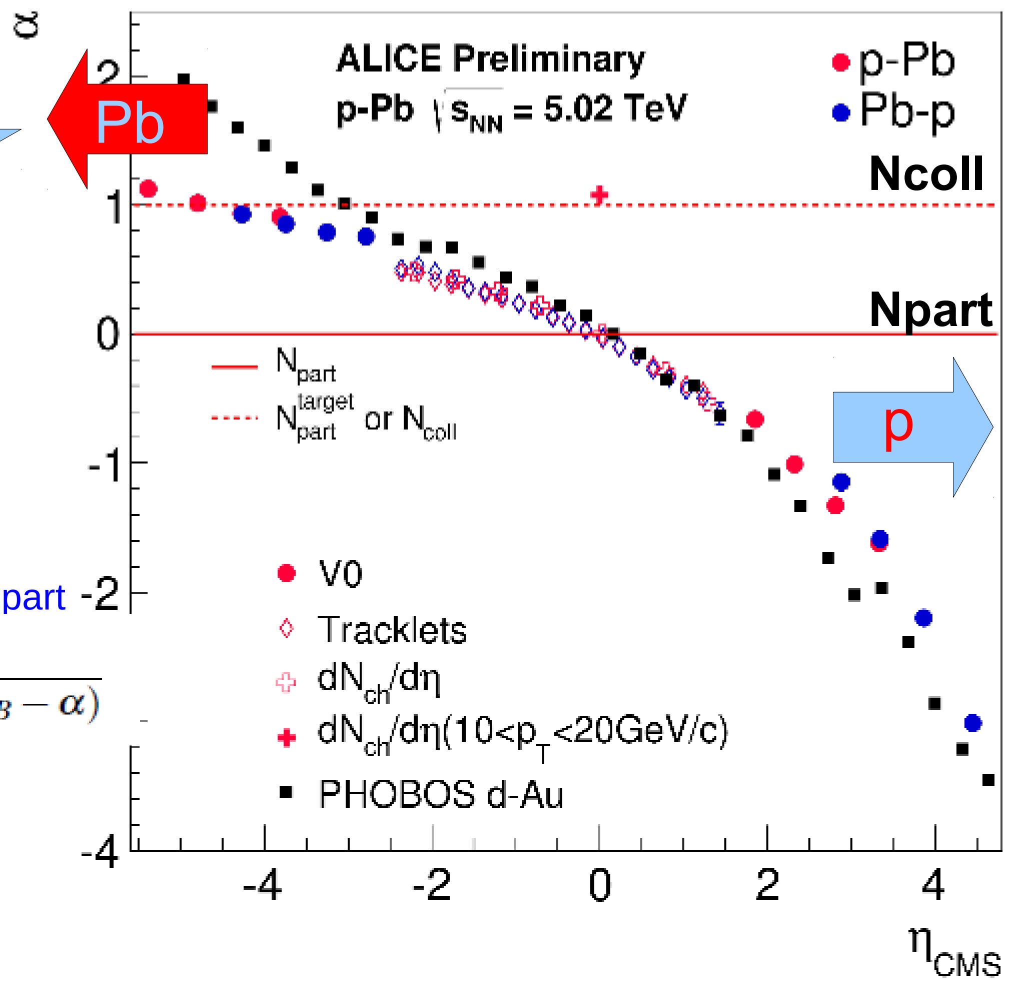

- Fit: assuming dN/dη scales with N_{part}

$$\frac{\langle S\rangle_i}{\langle S\rangle_{MB}} = \frac{\langle N_{part}\rangle_{MB}}{(\langle N_{part}\rangle_{MB}-\alpha)} \cdot \left(\frac{\langle dN/d\eta\rangle_i}{\langle dN/d\eta\rangle_{MB}}\right)_{-1<\eta<0} - \frac{\alpha}{(\langle N_{part}\rangle_{MB}-\alpha)}$$

α = 0 – perfect N_{part} scaling

α = 1 – perfect N_{coll} (or N_{part}^{target}) scaling

α has clear meaning (N_{part} vs N_{coll} scaling)

correlation between causally disconnected observables (eg: slow neutrons - multiplicity)

→ **connection to geometry.**

Hybrid Method

1) assumption: ZN insensitive to dynamical biases →slice events in ZN
2) assumption:
  a) Mid-rap dN/dη scales with N_{part}
  b) Pb-side dN/dη scales with N_{part}^{target} (= N_{coll} in pA)
  c) Yield at high-p_T scales with N_{coll}

$$\langle N_{\rm part}\rangle_i^{\rm mult} = \langle N_{\rm part}\rangle_{MB} \cdot \frac{\langle S\rangle_i}{\langle S\rangle_{MB}}$$

$$\langle N_{\rm coll}\rangle_i^{\rm mult} = \langle N_{\rm part}\rangle_i^{\rm mult} - 1$$

$$\langle N_{\rm coll}\rangle_i^{\rm Pb-side} = \langle N_{\rm coll}\rangle_{MB} \cdot \frac{\langle S\rangle_i}{\langle S\rangle_{MB}}$$

$$\langle N_{\rm coll}\rangle_i^{\rm high-p_T} = \langle N_{\rm coll}\rangle_{MB} \cdot \frac{\langle S\rangle_i}{\langle S\rangle_{MB}}$$

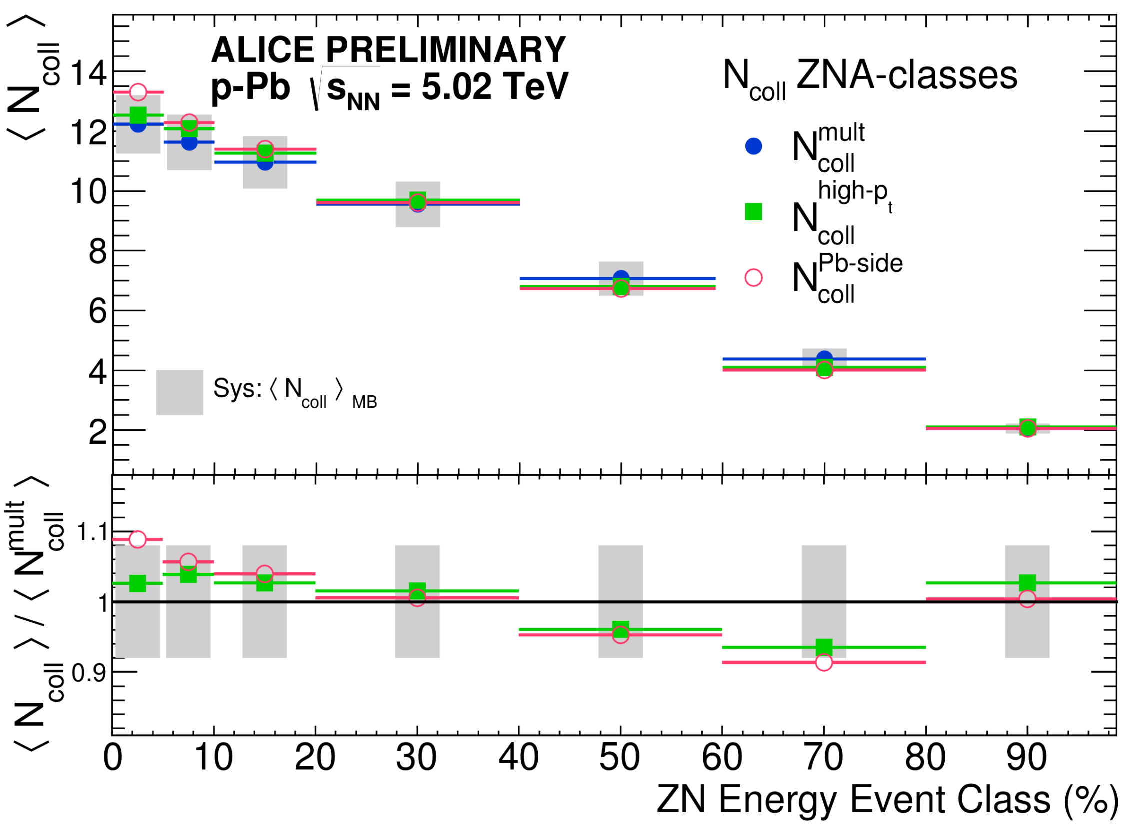

- All values within at most 10% → consistency of assumptions
- This does not yet prove the validity of any (or all) of these assumptions 2a),b),c)

Multiplicity vs Centrality

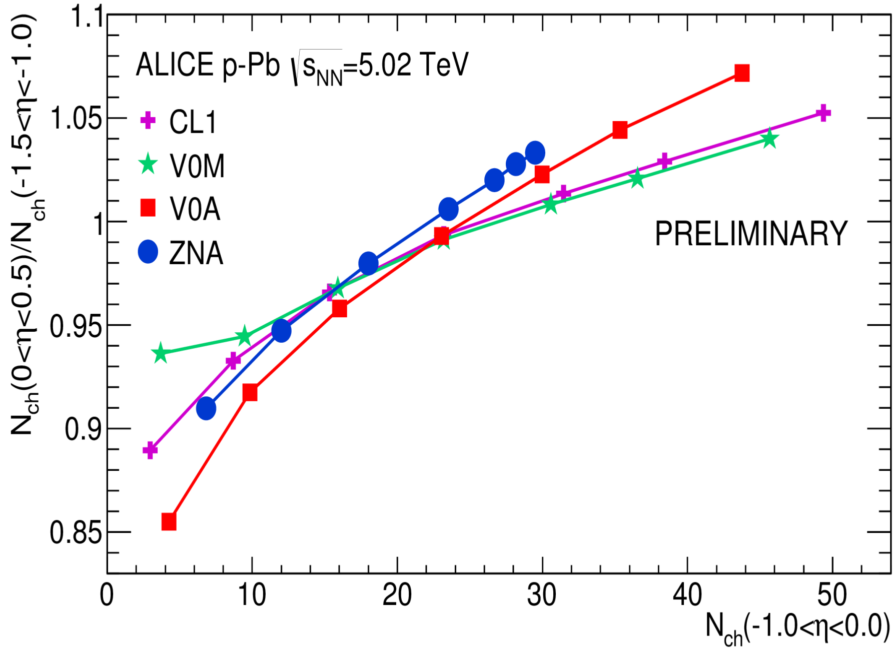

Asymmetry Evolution with N_{ch}

Increasing excess of particles in the direction of the Pb beam with respect to the proton-going direction.
Similar trend in common N_{ch}-range.

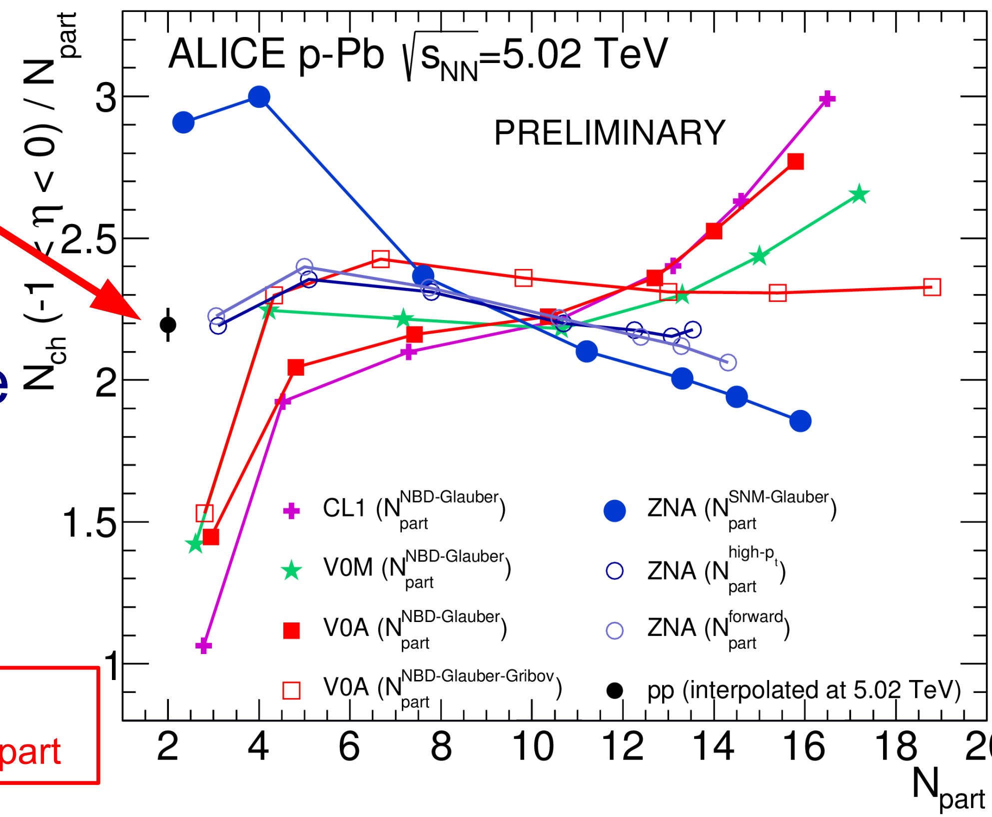

N_{ch}/N_{part} vs N_{part}

- CL1, V0M and V0A: increases more than linearly (multiplicity bias)
  - Not for Glauber-Gribov model
- ZNA: saturation above N_{part}~13

Hybrid: nearly perfect scaling with N_{part}